# High Order Finite Elements For Energy Harvesting Piezoelectric Beams

Roman Poya

Master Thesis

Civil & Computational Engineering Centre

Swansea University

Master of Science in Computational Mechanics
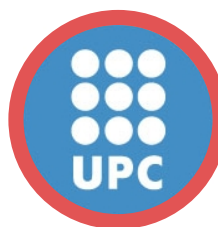
High Order Finite Elements for Energy Harvesting Piezoelectric Beams

Submitted in partial fulfillment of the requirements for the award of the degree of Master of Science

ROMAN POYA

Advisors:

DR. ANTONIO GIL & DR. PAUL LEDGER

MAY 31, 2013

A Word of Advice

This document is built with tooltip settings to provide its *less portable* format with pop-up features. While the portability of the document may have been compromised, the enhanced presentation style is for the reader's convenience. If you are reading the e-copy of this document, make sure that your pdf reader supports JavaScript. As of May 2013, only Adobe Reader and Adobe Acrobat have these capabilities. For Mac users, using OS 10.5.8 or later, Skim Reader can do the job. To get the most from reading this thesis, it is recommended to use one of these desktop publishing softwares.

ACKNOWLEDGEMENT

Abstract

Scavenging and harnessing electrical energy from alternative sources for powering electronic devices proves to be the sole credible way towards a significant reduction in worlds' electric consumption through self-sustainability. The present work focusses on building a sound thoeretical platform backed up by a reliable computational technique to perform device-level computations for energy harvesting piezoelectric beams. The point of departure is the enthalpy of the piezoelectric system which is supplemented with the kinetic energy and whose variational form is obtained through a Hellinger-Prange-Reissner mixed formulation. Consistent linearisation of this functional is performed to obtain the Euler-Lagrange equations. The kinematics of three-dimensional beam along with a quadratic electric potential distribution across the beam thickness and height, are embedded in the linearised equations and integration over the area is performed to obtain a set of partial differential equations in terms of stress and electric displacement resultants. High order Lagrangian basis and hierarchical Legendre basis functions are employed for finite element discretisation. The computational algorithm is first benchmarked with closed-form solutions which are reported here for the first time for this type of formulation. Finally, a number of static, modal and dynamic analyses are presented.

Contents

List of Figures

List of Tables

Mechanics of Piezoelectricity & Energy Harvesting

1. Introductory Remarks

In literary terms, piezoelectricity refers to electricity resulting from pressure. Piezoelectricity can be understood as an interaction between mechanical state and electrical state in crystalline materials with no inversion symmetry i.e. if they are not centrosymmetric. In general, when a piezoelectric material is mechanically strained, an electric polarisation proportional to strain is produced, which is called the direct effect. Similarly, an electric polarisation in the material yields proportional strain, called the reverse effect [16] [41]. A major application of piezoelectricity is in energy harvesting - exploiting the direct effect. Since the energy produced from piezoelectric materials is feeble enough to be utilised in large energy conversion devices, the industrial applications are tailored to a great extent toward consumer electronics. These include ambient vibration energy harvesters [16] [1], remote controls [11], life-long batteries, digital signal processors [12], shoe-mounted piezoelectrics [45] [39], backpack straps [20], short narrow sidewalks, noise-induced harvesters and many more.

Many of these energy harvesters are manufactured as thin films. From structural mechanics and mathematical modelling viewpoint this is an advantage in that it liberates us to carry out dimensional reduction from fully three-dimensional models to simplified three-dimensional membranes or beams.

It is the aim of present work to redress the problem of numerical modelling of energy harvesting linear piezoelectric beams by starting from the fundamental equations of continuum elasticity. To the best of our knowledge, such a sophisticated yet simple approach has not been attempted before. The merit of approaching the problem this way is that we can clearly see where are the strengths and limitations of piezoelectric beam theory, and the simplicity of the approach is that we still deal with linear small strain theory.

Akin to our work, what is found in the literature, is in the form of simplified approaches for single-degree-of-freedom systems and two-dimensional beams, which are often referred to as lumped-parameter and distributed-parameter approaches [16] [12] [4] [1]. In the lumped-parameter approach the piezoelectric device is modelled using a mass-spring-damper system coupled with a capacitor and a resistor [44] [12]. The lumped-parameter is an approximation limited to a single vibration mode and it lacks some important aspects of the coupled physical system, such as the dynamic mode shapes and accurate strain distribution as well as their effects on the electrical response [16]. The distributed-parameter approach on the other hand, is based on Euler-Bernoulli beam theory which neglects rotation of cross section, shear deformation and rotational inertia. Although convenient for thin piezoelectric beams,

distributed-parameter approach is mainly limited to two-dimensional beams [14]. A review of finite element modelling of piezoelectric beams is provided by Benjeddou [4]. Survey of energy harvesting with piezoelectric materials are also reported in [2] [16].

The main simplifying assumption in almost all of these approaches is the assumption of vanishing electric field in particular direction(s), depending on the polarisation [12] [5]. In piezoelectric beam literature, these are normally referred to as different modes of coupling and are denoted by d_{ij} where d is the piezoelectric coupling parameter and the subscript i and j is the notation for the poling direction and applied stress direction, respectively [34]. In this setting, a d_{31} mode implies coupling between transverse electric field and axial strain, and a d_{33} stands for coupling between axial electric field and axial strain [12]. Other electric field components are normally assumed to be zero. In the context of actuation, the two common coupling modes are shear actuation and extension actuation mechanisms [5], where in the former case the piezoelectric layer is sandwiched between two non-electro-active layers and the coupling is between shear strain and axial electric field and in the latter case, piezoelectric films are deposited on both side of a substrate and the actuation mechanism is driven by d_{31} mode of coupling. The piezoelectric effect is more pronounced when poling is along the longitudinal direction of the beam [46]. Fabrication of piezoelectric films which are polarised along the length or function in d_{33} mode is achieved by using an interdigitated electrode configuration (IDE) [12] [46], as shown in Fig. 5. An experimental comparison between various electrode configurations for energy harvesting piezoelectric beams is reported by Sodano [46]. A similar work on optimisation of interdigitated electrodes for piezoelectric actuators is also discussed in Bowen [7].
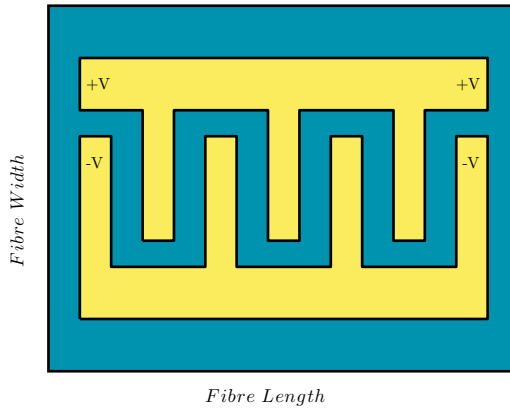
Figure 1: Plan View of an Interdigitated Electrode Configuration

Typically, piezoelectric materials are deposited either on one side (unimorph) or both sides (bimorph) of a substrate. The substrate is a non-electro-active platform which does not contribute to the electric output and merely serves as a mechanical supporting platform [16]. This can pose difficulties for integration of piezoelectric films with other microelectronic devices. Recently, there have been experimental reports on thick free-standing piezoelectric beams for energy harvesting [32] [31] [26] [33]. These are piezoelectric films which stand on their own and do not use a supporting platform and hence offer the advantage of minimising the movement constraints on them, thereby maximising output power [34]. For this reason, in our work, we consider the problem of free-standing piezoelectric energy harvesting beams.

On the mathematical modelling front, Benjeddou [5] attempts to build a unified beam finite elements for extension and shear actuation mechanisms in two-dimension, not the energy harvesting in particular, but rather the reverse effect. Tabesh [48] attempts to solve the problem of energy harvesting piezoelectric planar beams by employing Euler-Bernoulli approach with quadratic electric potential distribution across the height of the beam. In this paper, it is also shown that a linear electric potential assumption is not sufficient to describe the electrostatics of the model as it violates Gauss's law. It should be pointed out that many conventional models in the literature rely on linear electric potential assumption [12] [22]. This problem is caused due to a combination of assumptions on mechanical kinematics and electrostatics of piezoelectric beams. To illustrate this, let us consider the two fundamental equations utilised in coupled electromechanical problems.

$$\nabla \cdot \boldsymbol{\sigma} = \mathbf{0}$$
$$\nabla \cdot \vec{D} = 0$$

These are the differential form of linear momentum equation and Gauss's law, respectively, where $\boldsymbol{\sigma}$ is the elastic Cauchy stress tensor, $\vec{D}$ is the electric displacement vector and $\nabla \cdot (\cdot)$ is the divergence operator. For planar beams in $x - z$ plane the above equations can be written as,

$$\frac{\partial \sigma_{xx}}{\partial x} + \frac{\partial \sigma_{xz}}{\partial z} = 0$$
$$\frac{\partial D_x}{\partial x} + \frac{\partial D_z}{\partial z} = 0$$

where x lies along the longitudinal axis and z lies along the height of the beam. Let us now assume the electric potential ψ to have the following linear form.

$$\psi(x, z) = \phi(x) + z\beta(x)$$

Where ϕ is the electric potential at the centroid of the beam and β can be considered as the gradient of ϕ which characterises the variation of total electric potential ψ across the height. The displacement map of a planar beam is also given by,

$$u_1(x, z) = -z\theta(x)$$
$$u_3 = w(x)$$

where u_1 and u_3 are beam displacements in x and z directions, respectively. Also, w is the vertical displacement at the centroid and θ is the rotation. It is clear by now that we have adopted a Timoshenko approach for the kinematics of the beam and a similar mapping for electric potential. To show why Gauss's law is not satified for this model problem, let us rely on what is commonly assumed in the literature [5] [12] [22], i.e. let us assume a d_{31} coupling and postulate that the electric field $\vec{E}$ exists only in one direction, say z, then we have.

$$E_x = 0, \qquad\qquad E_z = -\frac{\partial \psi}{\partial z} = -\beta(x)$$

Without loss of generality, if we assume a cantilever beam with a point load, from elementary beam theory we know that θ is a quadratic function of x which implies σ_{xx} is linear

in x and z. From the equilibrium of linear momentum we can now observe that σ_{xz} should be quadratic in z and constant in x, which is not the case as shear stress σ_{xz} is constant. Certainly, this is the limitation of beam theory, be it Euler-Bernoulli approach or Timoshenko approach. However, in the case of Timoshenko approach that we have adopted in this work, a shear factor is introduced which makes the shear deformation consistent with a quadratic shear deformation on an average sense over the height. Now coming to Gauss's law, according to our prior discussion on coupling modes the electric displacement can be written as [5] [48],

$$D_x = \epsilon_{11} E_x + d_{15} \varepsilon_{xz}$$
$$D_z = \epsilon_{33} E_z + d_{31} \varepsilon_{xx}$$

where ϵ_{ij} is the second order dielectric tensor and ε_{ij} is the second order elastic strain tensor. Since similar to stresses, shear strain is quadratic in z and axial strain is linear in x and z, this implies that Gauss's law is also not satisfied, as the summation of quadratic function with a linear function never vanishes. Even if we assume a Timoshenko approach i.e. a constant shear stress across the height, Gauss's law is still not satified. However, in the context of beam theory, this problem can be rectified by assuming electric potential to be quadratic in z and at least linear in x, in which case Gauss's law can be imposed properly. Hence the common assumption of linear electric potential in z, is not valid [48]. As a further observation, from the expressions for electric displacement in x and z directions, we can clearly observe the coupling modes d_{15} and d_{31}, respectively, where in the first case axial electric field is coupled with shear strain and in the second case transverse electric field is coupled with axial strain. In piezoelectric beam literature, these coupling modes are taken into consideration once at a time and the other components of electric displacement are assumed to be zero.

Fundamental contribution to the field of energy harvesting beams comes from Erturk and Inman [16] [14] [15] [17] [13]. Their comprehensive analytical and experimental studies focus on building simplified techniques for piezoelectric energy harvesting cantilever beams. These include lumped-parameter and distributed-parameter energy harvesters, equivalent loading techniques, inclusion of tip mass for lowering frequency response and shape optimisation of beams for improved electricity output.

Literature on modelling of three-dimensional piezoelectric beams is scarce, specifically in the context of energy harvesting. While a two-dimensional approach is sufficient for bending energy harvesters, for capturing anistropic behaviour of materials it is not satisfactory. Moreover, energy harvesters which function under coupled bending-torsion scenarios [1] require a three-dimensional description. There are also actuators which function in torsional modes such as helical springs [40] [9].

While these approaches are straightforward and easy to follow for engineers, in the mechanics community in particular, there is not much evidence of investigation on piezoelectric energy harvesting beams, despite the fact that the literature on numerical modelling of piezoelectric plates and shells is plenty. A sophisticated approach with the elegance of deriving equations from continuum piezoelectricity, to variational formulation, finite element discretisation and the numerical issues involved therein, is missing in the literature. In this regard, among the few, one can refer to the work of Wanger and co-workers [9] [30] [29]. As in the case of beams, plates and shells shear locking is always suspected, modelling of

piezoelectric beams is also not imune from this numerical issue. Wagner [9] [29] reports a three-dimensional beam finite element with linear/nonlinear strain measures and hysteresis. To resolve the problem of locking, he adopts a six field mixed variational formulation, assuming a quadratic electric potential distribution along the area directions. The work is restricted to static analysis only and requires a preprocessing stage to compute the warping patterns by solving a two-dimensional boundary value problem, using a separate finite element discretisation. Another three-dimensional finite element formulation for piezoelectric beams is reported by Touratier [19]. Touratier's formulation is based on higher order shear deformation theory and trigonometric expansion of displacements, where for C^1 continuity a mixture of Hermite cubic basis functions, quadratic basis functions and linear functions are utilised for finite element discretisation. The warping of cross section is incorporated in the model by solving the three-dimensional equations of elasticity. As a result, each beam element has three nodes along the length with 27 degrees of freedom per element only for electric potential. Including the warping variables there are 21 mechanical degrees of freedom per element. The formulation does not suffer from locking and inconsistency in shear deformation, however the computational cost is increased due to the high number of unknowns for each element. The complexity of the model and usage of various bases, make it difficult for finite element implementation. The work is restricted to static analysis and hence cannot be used for the actual problems of energy harvesting. It should be noted, that from simple approaches used more frequently in the engineering community to such modelling techniques, is too long a jump. Along the same lines, Koutsawa [35] attempts to solve the problem of static piezoelectric beams by using higher oder displacement theories for beams. A much similar formulation to ours is that of Kushnir [36], with the difference that the former is on ferro-electricity and is restricted to two-dimension and static analysis only.

In this work the problem of three-dimensional linear piezoelectric beams under static and dynamic loading scenarios is considered. The kinematics of the beam adopts that of the first order shear deformation theory or Timoshenko approach and the electric potential is taken to be quadratic across the height and the thickness. Due to consistent usage of elastic, piezoelectric and dielectric tensors, strains and electric field are coupled in all the three directions, and there is no assumption on the electrostatics of the model. For avoiding shear locking and accurate analysis of the piezoelectric problem, we employ higher order as well as hierarchical bases in the form of Lagrange and Legendre family of approximating functions. The variational formulation is the so-called mixed Hellinger-Prange-Reissner formulation [41]. In light of [24] [25] we embed the postulated kinematics into the variational form of the problem and perfrom area integration to obtain a series of stress and electric displacement resultants. Some mathematical entities in the form of moment of electric displacements naturally arise. Further in the linearisation process we find the Euler-Lagrange equations of piezoelectric beams in the form of partial differential equations. We solve these equations analytically to benchmark the computational scheme. Due to similarity in mechanical and electrical kinematics, these equations show resemblence, which is in fact rooted in the beauty of modelling beams from the continuum mechanics viewpoint. The resulting finite element discretisation has 11 degrees of freedom per node in three-dimensional and 5 degrees of freedom per node in 2D. These are displacement, rotation, electric potential and the gradient and hessian of electric potential.

The structure of the thesis is as follows. In the next chapter, we introduce the kinematics of piezoelectric beams in $\mathbb{R}^3$ Euclidean space. This is succeeded with obtaining stress and electric displacement resultants for our problem, by performing area integration. Chapter 3. starts with the variational formulation of piezoelectric beams. Starting from the Lagrangian of the system and the mixed Hellinger-Prange-Reissner functional and using Hamilton's prinicple, we perform consistent linearisation and embed the obtained resultants into the linearised functional, which finally lead us to Euler-Lagrange equations. In chapter 4. the finite element discretisation strategy is presented. In chapter 5. we provide analytical solution for various coupling fashions depending on the nature of piezoelectricity and permitivity tensors. Finally, in chapter 6. a series of numerical simulations ranging from static to modal and dynamic analyses are reported. Many other aspects of the numerical scheme such as the choice of differernt basis functions, the role of different numerical integration schemes and the effect of static condensation for higher order elements are investigated. On its entirety, the following schematic diagram aptly represents all what is covered in this thesis.
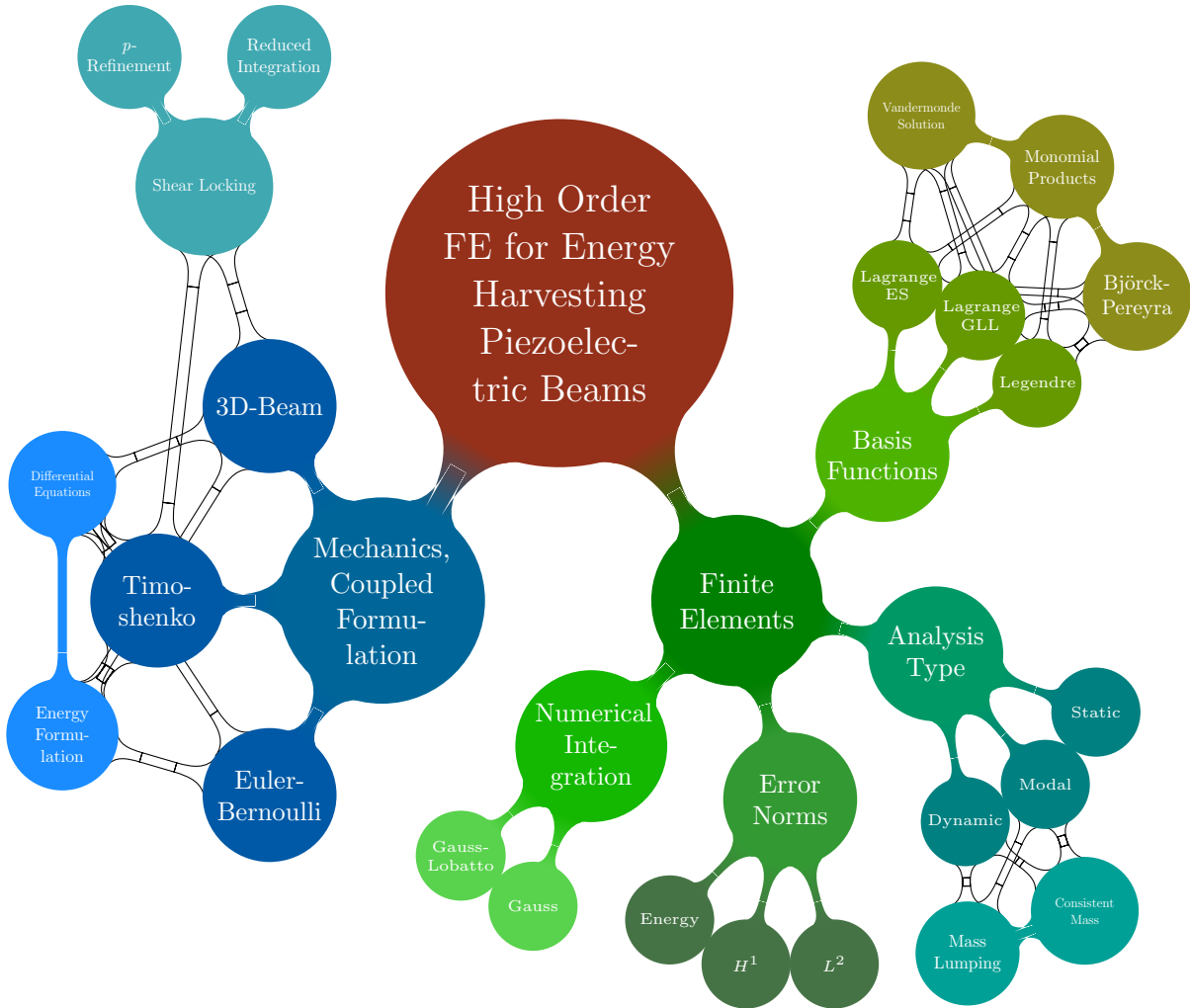
Figure 2: Scope of Work

Piezoelectricity of Three-Dimensional Beams

"Mechanics is the paradise of mathematical science because here we come to the fruits of mathematics."
Leonardo da Vinci

2. Kinematics & Electrostatics

2.1. Mechanical Kinematics

Consider motion of a beam in $\mathbb{R}^3$ Euclidean space as shown in Fig. 3. The beam in the undeformed configuration is completely characterised with three unit vectors $\vec{e}_1$, $\vec{e}_2$ and $\vec{e}_3$. For the sake of simplicity, $x_1 - x_2$ is taken as the plane on which the cross section lies and x_3 is the axis that coincides with the longitudinal axis of the beam. In the deformed configuration, the three vectors characterising the rotation of the cross section together with the deformation of point O are $\vec{c}_1$, $\vec{c}_2$ and $\vec{c}_3$, respectively.
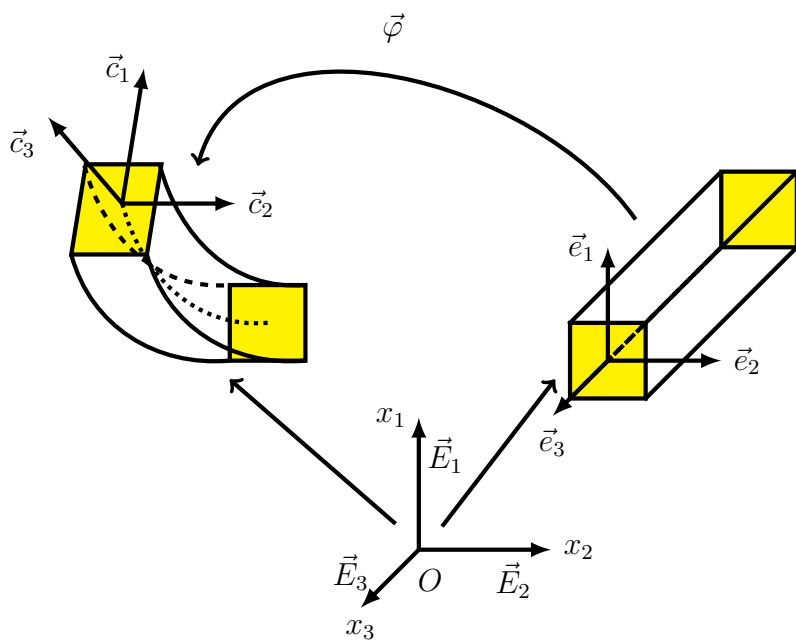
Figure 3: Motion of Beam in $\mathbb{R}^3$ Euclidean Space

7

The motion of beam from the undeformed configuration to deformed configuration is characterised by the mapping,

$$\vec{\varphi}(\vec{x}) = x_3 \vec{e}_3 + \vec{w}(x_3) + \mathbf{\Lambda}(x_3)\vec{p}(x_1, x_2) \tag{2.1}$$

where $\vec{p}(x_1, x_2) = x_1\vec{e}_1 + x_2\vec{e}_2$ is the position vector of a point within the cross-section. $\vec{w}(x_3)$ is the vector of displacements in three directions. For small rotations $\mathbf{\Lambda}\vec{p} \approx \vec{p} + \vec{\theta} \times \vec{p}$, where $\vec{\theta}$ is the rotation vector. We can now describe the deformation through the displacement map $\vec{u}(\vec{x})$.

$$\vec{u}(\vec{x}) = \vec{w}(x_3) + \vec{\theta}(x_3) \times \vec{p}(x_1, x_2) \tag{2.2}$$

Where the vectors $\vec{w} = w_i\vec{e}_i$ and $\vec{\theta} = \theta_i\vec{e}_i$ are collectively called the generalised beam displacements. If we write (2.2) explicitly we have,

$$u_1(x_1, x_2, x_3) = w_1(x_3) - x_2\theta_3(x_3)$$
$$u_2(x_1, x_2, x_3) = w_2(x_3) + x_1\theta_3(x_3)$$
$$u_3(x_1, x_2, x_3) = w_3(x_3) - x_1\theta_2(x_3) + x_2\theta_1(x_3)$$

which are the same equations also used in Hughes [25] for fomulating three-dimensional beam finite elements. The linearised strain tensor can now be computed as,

$$\varepsilon = \frac{1}{2}[\nabla\vec{u} + \nabla\vec{u}^T] \tag{2.3}$$

where the gradient of displacement $\nabla\vec{u}$ is given by.

$$\nabla\vec{u}(x) = \frac{\partial\vec{u}}{\partial x_i} \otimes \vec{e}_i \tag{2.4}$$

In (2.4) the Einstein's convention for repearted indices is assumed. Knowing that $\partial\vec{p}/\partial x_\alpha = \vec{e}_\alpha$ where $\alpha = 1, 2$, we have.

$$\nabla\vec{u}(x) = (\frac{d\vec{w}}{dx_3} + \frac{d\vec{\theta}}{dx_3} \times \vec{p}) \otimes \vec{e}_3 - \sum_{\alpha=1,2}(\vec{e}_\alpha \times \vec{\theta}) \otimes \vec{e}_\alpha \tag{2.5}$$

At this stage, it is important to note that,

$$\mathbf{\Psi} = (\vec{e}_i \times \vec{\theta}) \otimes \vec{e}_i = -(\vec{\theta} \times \vec{e}_i) \otimes \vec{e}_i = -[\vec{\theta}\times] \tag{2.6}$$

is the skew-symmetric tensor associated with the axial vector (i.e. rotation vector $\vec{\theta}$). Thus we can rewrite (2.5) in terms of $\mathbf{\Psi}$ as.

$$\nabla\vec{u}(x) = (\frac{d\vec{w}}{dx_3} + \vec{e}_3 \times \vec{\theta} + \frac{d\vec{\theta}}{dx_3} \times \vec{p}) \otimes \vec{e}_3 - \mathbf{\Psi} \tag{2.7}$$

The linearised strain tensor can now be computed [Note that $\mathbf{\Psi}^T + \mathbf{\Psi} = \mathbf{0}$],

$$\varepsilon = \frac{1}{2}\left[(\vec{\epsilon} + \vec{\kappa} \times \vec{p}) \otimes \vec{e}_3 + \vec{e}_3 \otimes (\vec{\epsilon} + \vec{\kappa} \times \vec{p})\right] \tag{2.8}$$

where,

$$\vec{\epsilon} = \frac{d\vec{w}}{dx_3} + \vec{e}_3 \times \vec{\theta} \tag{2.9}$$

$$\vec{\kappa} = \frac{d\vec{\theta}}{dx_3} \tag{2.10}$$

Equations (2.9) and (2.10) are called the strain resultants for the linear beam model. We can think of these two quantities characterising translational deformation and rotational deformation, respectively.

To obtain stresses and stress resultants let us consider linear isotropic case for the moment. The inclusion of anistropy is discussed later in this chapter once we are clear with the kinematics and electrostatics of our problem. Using the linear elastic constitutive equation, the Cauchy stress tensor $\boldsymbol{\sigma}^m$ is give by.

$$\boldsymbol{\sigma}^m = \lambda \mathrm{tr}(\boldsymbol{\varepsilon})\boldsymbol{I} + 2\mu\boldsymbol{\varepsilon} \tag{2.11}$$

A superscript m on Cauchy stress tensor stands for the mechanical contribution to the total stress tensor, which will be discussed in the stress resultants section, in a while. We are interested in the stress resultants (i.e. tractions) on a cross section with the normal $\vec{e}_3$ or $\vec{c}_3$, as there is no distinction between initial and deformed configuration in the small strain regime, therefore, from the Cauchy stress tensor $\boldsymbol{\sigma}^m$, we can proceed.

$$\vec{t}_{e_3} = \boldsymbol{\sigma}^m \vec{e}_3 = \lambda \mathrm{tr}(\boldsymbol{\varepsilon})\vec{e}_3 + 2\mu\boldsymbol{\varepsilon}\vec{e}_3 \tag{2.12}$$

Where $\boldsymbol{I}$ is the second order identity tensor, $\mathrm{tr}(\cdot)$ is the trace of second order tensor and λ and μ are Lame's constants. Substituting (2.8) in the above equation yields.

$$2\mu\boldsymbol{\varepsilon}\vec{e}_3 = \mu[\boldsymbol{I} + \vec{e}_3 \otimes \vec{e}_3](\vec{\epsilon} + \vec{\kappa} \times \vec{p})$$
$$\mathrm{tr}(\boldsymbol{\varepsilon}) = \vec{e}_3 \cdot (\vec{\epsilon} + \vec{\kappa} \times \vec{p})$$
$$\vec{t}_{e_3} = \left[\mu\boldsymbol{I} + (\lambda + \mu)\vec{e}_3 \otimes \vec{e}_3\right](\vec{\epsilon} + \vec{\kappa} \times \vec{p}) \tag{2.13}$$

2.2. Electrical Mapping

We postulate a similar mapping for electric potential ψ. While the scalar electric potential varies along the length of the beam, we assume the in-plane variation of electric potential as a sum of product of its gradient with the distance from neutral axis and product of its hessian with the square of the distance from neutral axis, where similar to generalised displacements, the gradient and hessian can be treated independently from the electric potential itself. In other words, we use the Taylor series expansion for electric potential up to quadratic term across the height and thickness. The electrostatics of three-dimensional beam is shown in Fig. 4.
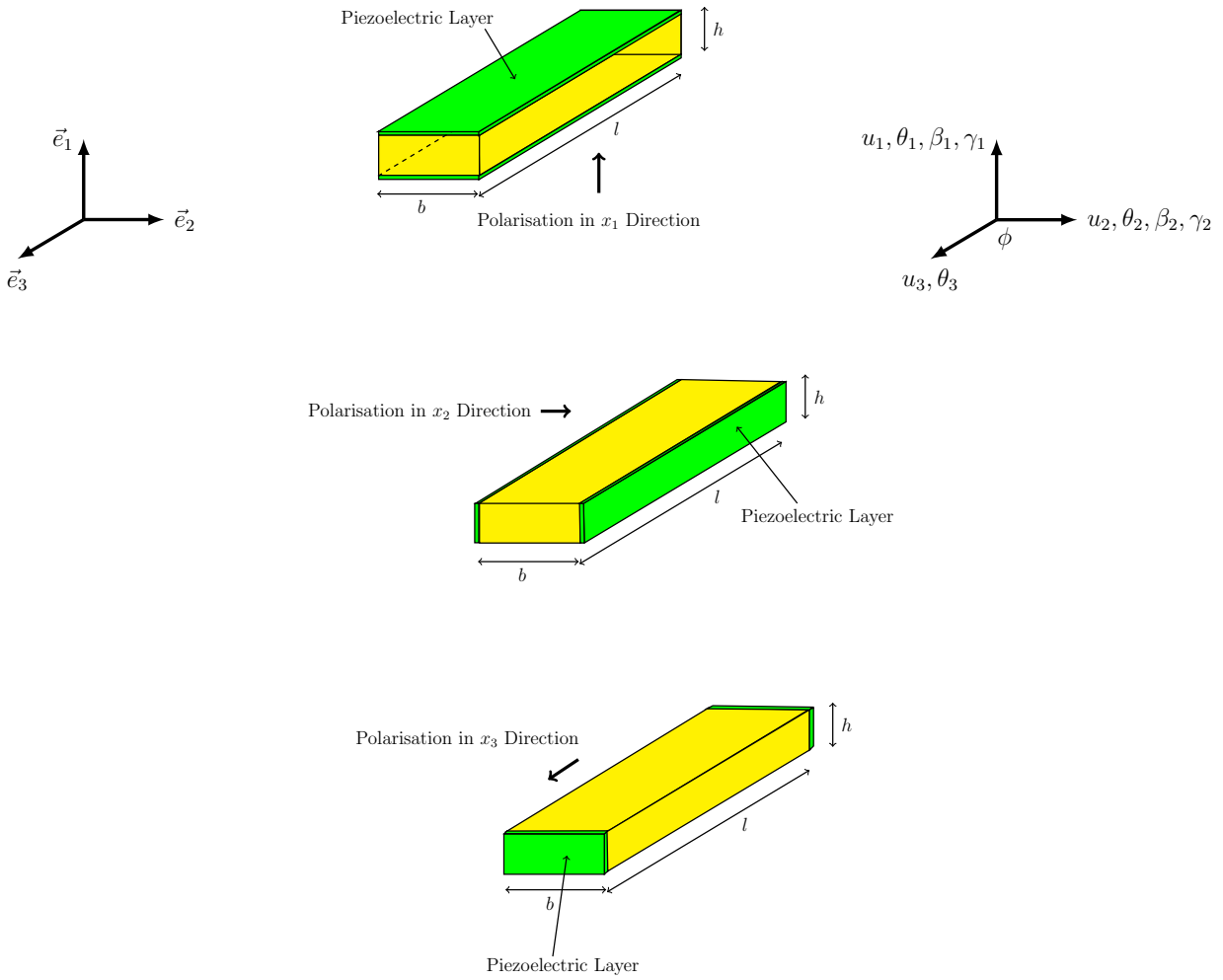
Figure 4: Electrostatics of Three-Dimensional Piezoelectric Beam

Hence we can write.

$$\psi(\vec{x}) = \phi(x_3) + \vec{\beta}(x_3) \cdot \vec{p}(x_1, x_2) + \frac{1}{2} \, \vec{p}(x_1, x_2) \cdot \boldsymbol{\gamma}(x_3) \vec{p}(x_1, x_2) \tag{2.14}$$

The scalar electric potential ϕ, the vector $\vec{\beta} = \beta_\zeta \vec{e}_\alpha = \beta_2 \vec{e}_1 + \beta_1 \vec{e}_2$ and the second order tensor

$\boldsymbol{\gamma} = \gamma_{\zeta\vartheta}\ \vec{e}_\zeta \otimes \vec{e}_\vartheta\ [\zeta, \vartheta = 2, 1]$ are the electrical variables of our problem. If we write (2.14) explicitly we have.

$$\psi(x_1, x_2, x_3) = \phi(x_3) + x_2\beta_1(x_3) + x_1\beta_2(x_3) + \frac{1}{2}x_2^2\gamma_{11}(x_3)$$
$$+ \frac{1}{2}x_1x_2\left(\gamma_{12}(x_3) + \gamma_{21}(x_3)\right) + \frac{1}{2}x_1^2\gamma_{22}(x_3)$$

Using summation over $\alpha = 1, 2$, the electric field vector is obtained by taking the gradient of electric potential,

$$\vec{E} = -\nabla\psi(\vec{x}) = -\left(\frac{d\phi}{dx_3} + \frac{d\vec{\beta}}{dx_3} \cdot \vec{p} + \frac{1}{2}\vec{p} \cdot \frac{d\boldsymbol{\gamma}}{dx_3}\vec{p}\right)\vec{e}_3 - \sum_{\alpha=1,2}\left(\vec{\beta} \cdot \vec{e}_\alpha + \frac{1}{2}\vec{e}_\alpha \cdot (\boldsymbol{\gamma} + \boldsymbol{\gamma}^T)\vec{p}\right)\vec{e}_\alpha$$

$$= -\frac{d\phi}{dx_3}(\vec{e}_3 \otimes \vec{e}_3)\vec{e}_3 - \sum_{\alpha=1,2}(\vec{e}_\alpha \otimes \vec{e}_\alpha)\vec{\beta} - (\vec{e}_3 \otimes \vec{p})\frac{d\vec{\beta}}{dx_3} - \mathcal{A}_1 : \boldsymbol{\gamma} - \mathcal{A}_2 : \frac{d\boldsymbol{\gamma}}{dx_3}$$

$$= -\boldsymbol{I}\vec{\epsilon^e} - (\vec{e}_3 \otimes \vec{p})\vec{\kappa^e} - \mathcal{A}_1 : \boldsymbol{\gamma} - \mathcal{A}_2 : \boldsymbol{\varsigma} \tag{2.15}$$

where,

$$\vec{\epsilon^e} = \frac{d\phi}{dx_3}\vec{e}_3 + \vec{\beta} \tag{2.16}$$

$$\vec{\kappa^e} = \frac{d\vec{\beta}}{dx_3} \tag{2.17}$$

$$\boldsymbol{\varsigma} = \frac{d\boldsymbol{\gamma}}{dx_3} \tag{2.18}$$

and $\mathcal{A}_1$ and $\mathcal{A}_2$ are third order tensors. They can be obtained more conveniently through indicial notation by employing summation over $[k, m, n = 1, 2]$, from the corresponding terms of (2.15).

$$\sum_{\alpha=1,2}\left(\frac{1}{2}\vec{e}_\alpha \cdot (\boldsymbol{\gamma} + \boldsymbol{\gamma}^T)\vec{p}\right)\vec{e}_\alpha = \sum_{\alpha=1,2}\left(\frac{1}{2}\vec{e}_\alpha \cdot \boldsymbol{\gamma}^s\vec{p}\right)\vec{e}_\alpha$$

$$= \sum_{\alpha=1,2}\vec{e}_{\alpha m}\gamma_{mn}^s\vec{p}_n\vec{e}_{\alpha k} = \sum_{\alpha=1,2}\vec{e}_{\alpha k}\vec{e}_{\alpha m}\vec{p}_n\gamma_{mn}^s = \sum_{\alpha=1,2}\vec{e}_\alpha \otimes \vec{e}_\alpha \otimes \vec{p} : \boldsymbol{\gamma}^s$$

Note that we have used the symmetric part of hessian, $\boldsymbol{\gamma}^s = \frac{1}{2}[\boldsymbol{\gamma} + \boldsymbol{\gamma}^T]$. Since in (2.15), we have used the hessian itself instead of its symmetric part, the above equation should then be modified as.

$$\sum_{\alpha=1,2}\vec{e}_\alpha \otimes \vec{e}_\alpha \otimes \vec{p} : \boldsymbol{\gamma}^s = \sum_{\alpha=1,2}\frac{1}{2}(\vec{e}_\alpha \otimes \vec{e}_\alpha \otimes \vec{p} + \vec{e}_\alpha \otimes \vec{p} \otimes \vec{e}_\alpha) : \boldsymbol{\gamma}$$

Hence $\mathcal{A}_1$ is.

$$\mathcal{A}_1 = \sum_{\alpha=1,2}\frac{1}{2}(\vec{e}_\alpha \otimes \vec{e}_\alpha \otimes \vec{p} + \vec{e}_\alpha \otimes \vec{p} \otimes \vec{e}_\alpha)$$

Similarly, to find $\mathcal{A}_2$ we write the corresponding terms of (2.15).

$$\frac{1}{2}\left(\vec{p}\cdot\frac{d\boldsymbol{\gamma}}{dx_3}\vec{p}\right)\vec{e}_3 = \frac{1}{2}\left(\vec{p}\cdot\boldsymbol{\varsigma}\vec{p}\right)\vec{e}_3 = \frac{1}{2}\vec{p}_m\varsigma_{mn}\vec{p}_n\vec{e}_{3_k} = \frac{1}{2}\vec{e}_{3_k}\vec{p}_m\vec{p}_n\varsigma_{mn} = \frac{1}{2}\left(\vec{e}_3\otimes\vec{p}\otimes\vec{p}\right):\boldsymbol{\varsigma}$$

Hence $\mathcal{A}_2$ is.

$$\mathcal{A}_2 = \frac{1}{2}\left(\vec{e}_3\otimes\vec{p}\otimes\vec{p}\right)$$

The explicit forms of these tensors are given in Appendix 1.1.6. To have removed the ambiguity of notations for the reader, the explicit form of electric field intensity vector is.

$$\vec{E} = -\left\{\begin{array}{c}\beta_2 + x_1\gamma_{22} + \frac{1}{2}x_2(\gamma_{12}+\gamma_{21})\\ \beta_1 + x_2\gamma_{11} + \frac{1}{2}x_1(\gamma_{12}+\gamma_{21})\\ \phi_{,3} + x_2\beta_{1,3} + x_1\beta_{2,3} + \frac{1}{2}x_2^2\gamma_{11,3} + \frac{1}{2}x_1x_2(\gamma_{12,3}+\gamma_{21,3}) + \frac{1}{2}x_1^2\gamma_{22,3}\end{array}\right\} \tag{2.19}$$

The electric displacement can now be written as,

$$\vec{D}^e = \boldsymbol{\epsilon}\vec{E} \tag{2.20}$$

where $\boldsymbol{\epsilon}$ is the second order dielectric tensor.

Remark 1. To maintain a correspondence between mechanical and electrical variables, the components of gradient and hessian of electric potential are arranged in a reverse order, i.e.

$$\vec{\beta} = \left\{\begin{array}{c}\beta_2\\\beta_1\end{array}\right\}, \qquad\qquad \boldsymbol{\gamma} = \begin{bmatrix}\gamma_{22} & \gamma_{21}\\\gamma_{12} & \gamma_{11}\end{bmatrix}$$

This is because the displacements of the beam are obtained through a cross product of $\vec{\theta}$ with $\vec{p}$ and the total electric potential ψ is calculated through a scalar product of gradient and hessian with $\vec{p}$, which will certainly produce incosistent notations, unless we rearrange the components. We follow this arrangement throughout our formulation.

Remark 2. Gradient and hessian of electric potential do not have a third component, since unlike displacements, electric potential is a scalar and its in-plane variation can be fully described with only two components.

2.3.   Stress Resultants

The stress tensor in the theory of piezoelectricity evolves naturally from consistent linearisation of the enthalpy density of the system, as discussed in chapter 3. The symmetric stress tensor is as an algebraic summation of mechanical and electrical components. The components may not necessarily be symmetric (although in this case they are). The total stress tensor can be written in the following form, using vectorial and indicial notations.

$$\boldsymbol{\sigma} = \boldsymbol{\sigma}^m + \boldsymbol{\sigma}^e = \lambda \mathrm{tr}(\boldsymbol{\varepsilon})\boldsymbol{I} + 2\mu\boldsymbol{\varepsilon} - \mathcal{P}^{T^\star}\vec{E}$$

$$\sigma_{ij} = \lambda\varepsilon_{kk}\delta_{ij} + 2\mu\varepsilon_{ij} - \mathcal{P}_{kij}E_k \tag{2.21}$$

$$\tag{2.22}$$

Where $\mathcal{P}$ is the third order piezoelectric tensor and a superscript e on $\boldsymbol{\sigma}$ indicates stress tensor arising from electrical contribution. The traction resulting from this tensor can now be obtained.

$$\boldsymbol{\sigma}^e\vec{e}_3 = -\mathcal{P}^{T^\star}\vec{E}\vec{e}_3 = \mathcal{P}^{T^\star}\left[\boldsymbol{I}\vec{\epsilon^e} + (\vec{e}_3 \otimes \vec{p})\vec{\kappa^e} + \mathcal{A}_1 : \boldsymbol{\gamma} + \mathcal{A}_2 : \boldsymbol{\varsigma}\right]\vec{e}_3 \tag{2.23}$$

The third order tensor $\mathcal{P}^{T^\star}$ is what we will refer to as the double transpose of the piezoelectric tensor, since it involves an even permutation of indices [cf. Appendix 1 for a detailed investigation of third order tensors and their representation rules on a space of matrices which are strictly obeyed throughout this thesis]. While the mechanical part of traction force $\boldsymbol{\sigma}^m\vec{e}_3$ is straightforward to understand, in that it involves only vectors and second order tensors, the process of simplifying the electrical component is not as trivial. To understand this, let us calculate each of these components separately and then sum them up.

$$\boldsymbol{\sigma}^m\vec{e}_3 = \left[\mu\boldsymbol{I} + (\lambda + \mu)\vec{e}_3 \otimes \vec{e}_3\right](\vec{\epsilon} + \vec{\kappa} \times \vec{p}) = \boldsymbol{\Xi}\vec{\epsilon} + \boldsymbol{\Xi}[\vec{p}\times]^T\vec{\kappa} \tag{2.24}$$

Where the second order tensor $\boldsymbol{\Xi}$ contains material properties,

$$\boldsymbol{\Xi} = \mu\boldsymbol{I} + (\lambda + \mu)\vec{e}_3 \otimes \vec{e}_3$$

For the electrical component let us use indicial notation, and replace $\vec{e}_3$ with vector $\vec{a}$, and $\vec{E}$ with vector $\vec{b}$, for generality. The summation is now over $[i, j, k, l, m, n, p, q, r, s = 1, 2, 3]$.

$$\boldsymbol{\sigma}^e\vec{a} = -\mathcal{P}^{T^\star}\vec{b}\vec{a} = \mathcal{P}^{T^\star}\left[\boldsymbol{I}\vec{\epsilon^e} + (\vec{a} \otimes \vec{p})\vec{\kappa^e} + \mathcal{A}_1 : \boldsymbol{\gamma} + \mathcal{A}_2 : \boldsymbol{\varsigma}\right]\vec{a}$$

$$\sigma_{ij}^e a_i\ \vec{e}_j = -\mathcal{P}_{ijk}b_i a_k\ \vec{e}_j = \mathcal{P}_{ijk}\left[\delta_{il}\epsilon_l^e + a_i p_m k_m^e + \mathcal{A}_{1_{ipq}}\gamma_{pq} + \mathcal{A}_{2_{irs}}\varsigma_{rs}\right]a_k\ \vec{e}_j$$

$$= \mathcal{P}_{ijk}\left[a_k\delta_{il}\epsilon_l^e + a_k a_i p_m k_m^e + a_k\mathcal{A}_{1_{ipq}}\gamma_{pq} + a_k\mathcal{A}_{2_{irs}}\varsigma_{rs}\right]\vec{e}_j \tag{2.25}$$

In (2.25), vector $\vec{e}_j$ characterises the traction vector in the jth direction. It is crucial to point out, that since $\mathcal{A}_1$ and $\mathcal{A}_2$ contain the terms x_α and x_α^2, respectively, by considering the axis of the beam to coincide with the coordinate axis x_3 and be the principal direction, after integration $\mathcal{A}_1$ vanishes, while $\mathcal{A}_2$ only gives rise to principal second moments of area i.e. I_{11} and I_{22} which characterise third order derivatives ς_{11} and ς_{22}, respectively. This liberates us

to eliminate the two off-diagonal variables of $\boldsymbol{\gamma}$ and $\boldsymbol{\varsigma}$, and reintroduce these quantities in vector form as.

$$\vec{\gamma} = \begin{Bmatrix} \gamma_2 \\ \gamma_1 \end{Bmatrix}, \qquad\qquad \vec{\varsigma} = \begin{Bmatrix} \varsigma_2 \\ \varsigma_1 \end{Bmatrix} \qquad (2.26)$$

By following this simplification, we should also note that the third order derivative $\vec{\varsigma}$ can no longer be pre and post multiplied with $\vec{p}$ and instead we need to introduce another vector $\vec{s}$ containing the squares of distance from neutral axis in the area directions, i.e. $\vec{s} = x_\alpha^2 \vec{e}_\alpha$. This vector will be utilised more frequently later on. The two third order tensors in (2.25) will be now reduced to second order tensors $\boldsymbol{A}_1$ and $\boldsymbol{A}_2$, which can be obtained in the same manner that we obtained their third order counterparts.

$$\boldsymbol{A}_1 = \sum_{\alpha=1,2} x_\alpha\, \vec{e}_\alpha \otimes \vec{e}_\alpha$$

$$\boldsymbol{A}_2 = \frac{1}{2}\, \vec{e}_3 \otimes \vec{s}$$

Expression (2.25) now takes the form,

$$\sigma_{ij}^e a_i\, \vec{e}_j = \mathcal{P}_{ijk}\left[a_k \delta_{il}\epsilon_l^e + a_k a_i p_m k_m^e + a_k A_{1_{iq}}\gamma_q + a_k A_{2_{is}}\varsigma_s \right]\, \vec{e}_j$$

$$= \mathcal{P}_{ijk}\left[\mathcal{A}_{kil}^3 \epsilon_l^e + \mathcal{A}_{kim}^4 k_m^e + \mathcal{A}_{kiq}^1 \gamma_q + \mathcal{A}_{kis}^2 \varsigma_s \right]\, \vec{e}_j \qquad (2.27)$$

where the newly emerged third order tensors $\mathcal{A}^1, \mathcal{A}^2, \mathcal{A}^3$ and $\mathcal{A}^4$ are.

$$\begin{array}{llll}
\mathcal{A}_{kiq}^1 = a_k A_{1_{iq}}, & \mathcal{A}_{kis}^2 = a_k A_{2_{is}}, & \mathcal{A}_{kil}^3 = a_k \delta_{il}, & \mathcal{A}_{kim}^4 = a_k a_i p_m \\
\mathcal{A}^1 = \vec{a} \otimes \boldsymbol{A}_1, & \mathcal{A}^2 = \vec{a} \otimes \boldsymbol{A}_2, & \mathcal{A}^3 = \vec{a} \otimes \boldsymbol{I}, & \mathcal{A}^4 = \vec{a} \otimes \vec{a} \otimes \vec{p}
\end{array}$$

Knowing that $\vec{a}$ is in fact $\vec{e}_3$, we substitute back,

$$\mathcal{A}^1 = \vec{e}_3 \otimes \boldsymbol{A}_1, \qquad \mathcal{A}^2 = \vec{e}_3 \otimes \boldsymbol{A}_2, \qquad \mathcal{A}^3 = \vec{e}_3 \otimes \boldsymbol{I}, \qquad \mathcal{A}^4 = \vec{e}_3 \otimes \vec{e}_3 \otimes \vec{p} \qquad (2.28)$$

and by manipulating (2.27) we obtain.

$$\sigma_{i3}^e \vec{e}_3 = \mathcal{P}_{3ki}\left[\mathcal{A}_{kil}^3 \epsilon_l^e + \mathcal{A}_{kim}^4 k_m^e + \mathcal{A}_{kiq}^1 \gamma_q + \mathcal{A}_{kis}^2 \varsigma_s \right]\, \vec{e}_3$$

$$\boldsymbol{\sigma}^e \vec{e}_3 = \mathcal{P}^{T^\star} : \left[\mathcal{A}^3 \vec{\epsilon}^e + \mathcal{A}^4 \vec{k}^e + \mathcal{A}^1 \vec{\gamma} + \mathcal{A}^2 \vec{\varsigma} \right] \qquad (2.29)$$

The first stress resultant can now be computed as,

$$\vec{Q} = \int_A \boldsymbol{\sigma} \vec{e}_3\, \mathrm{d}A = \int_A \left(\boldsymbol{\Xi}\vec{\epsilon} + \boldsymbol{\Xi}[\vec{p}\times]^T \vec{\kappa} \right)\, \mathrm{d}A$$

$$+ \mathcal{P}^{T^\star} : \left\{ \int_A \left[\mathcal{A}^3 \vec{\epsilon}^e + \mathcal{A}^4 \vec{k}^e + \mathcal{A}^1 \vec{\gamma} + \mathcal{A}^2 \vec{\varsigma} \right] \mathrm{d}A \right\}$$

$$= \mathbf{A}^m \vec{\epsilon} + \mathbf{S}^m \vec{\kappa} + \mathbf{A}_1^e \vec{\epsilon}^e + \mathbf{S}_1^e \vec{\kappa}^e + \mathbf{S}_2^e \vec{\gamma} + \mathbf{I}_1^e \vec{\varsigma} \qquad (2.30)$$

where

$$\mathbf{A}^m = \int_A \mathbf{\Xi} \, \mathrm{d}A \qquad \mathbf{S}^m = \int_A \mathbf{\Xi}[\vec{p}\times]^T \, \mathrm{d}A \qquad \mathbf{A}_1^e = \int_A \mathcal{P}^{T^\star} : \mathcal{A}^3 \, \mathrm{d}A$$

$$\mathbf{S}_1^e = \int_A \mathcal{P}^{T^\star} : \mathcal{A}^4 \, \mathrm{d}A \qquad \mathbf{S}_2^e = \int_A \mathcal{P}^{T^\star} : \mathcal{A}^1 \, \mathrm{d}A \qquad \mathbf{I}_1^e = \int_A \mathcal{P}^{T^\star} : \mathcal{A}^2 \, \mathrm{d}A$$

We employ the rules laid out at Appendix 1.1.6. for generating third order tensors. The explicit forms these tensors can be found in 1.1.6. In a similar fashion we now calculate the stress resultant of angular momentum,

$$\begin{aligned}
\vec{p} \times \boldsymbol{\sigma}\vec{e}_3 &= [\vec{p}\times]\left[\mu\boldsymbol{I} + (\lambda+\mu)\vec{e}_3 \otimes \vec{e}_3\right](\vec{\epsilon} + \vec{\kappa} \times \vec{p}) \\
&\quad + [\vec{p}\times]\mathcal{P}^{T^\star}\left[\boldsymbol{I}\vec{\epsilon^e} + (\vec{e}_3 \otimes \vec{p})\vec{\kappa^e} + \mathcal{A}_1 : \boldsymbol{\gamma} + \mathcal{A}_2 : \boldsymbol{\varsigma}\right]\vec{e}_3 \\
&= \left([\vec{p}\times]\mathbf{\Xi}\vec{\epsilon} + [\vec{p}\times]\mathbf{\Xi}[\vec{p}\times]^T\vec{\kappa}\right) \\
&\quad + [\vec{p}\times]\mathcal{P}^{T^\star}\left[\boldsymbol{I}\vec{\epsilon^e} + (\vec{e}_3 \otimes \vec{p})\vec{\kappa^e} + \mathcal{A}_1 : \boldsymbol{\gamma} + \mathcal{A}_2 : \boldsymbol{\varsigma}\right]\vec{e}_3 \qquad (2.31)
\end{aligned}$$

where $[\vec{p}\times]\mathcal{P}$ is a third order tensor, containing geometric and piezoelectric material parameters. Performing integration as before we find the second stress resultant as,

$$\begin{aligned}
\vec{M} &= \int_A \vec{p} \times \boldsymbol{\sigma}\vec{e}_3 \, \mathrm{d}A = \int_A \left([\vec{p}\times]\mathbf{\Xi}\vec{\epsilon} + [\vec{p}\times]\mathbf{\Xi}[\vec{p}\times]^T\vec{\kappa}\right) \mathrm{d}A \\
&\quad + \int_A [\vec{p}\times]\mathcal{P}^{T^\star} : \left[\mathcal{A}^3\vec{\epsilon^e} + \mathcal{A}^4\vec{k^e} + \mathcal{A}^1\vec{\gamma} + \mathcal{A}^2\vec{\varsigma}\right]\mathrm{d}A \\
&= \int_A \left([\vec{p}\times]\mathbf{\Xi}\vec{\epsilon} + [\vec{p}\times]\mathbf{\Xi}[\vec{p}\times]^T\vec{\kappa}\right) \mathrm{d}A \\
&= \mathbf{S}^T\vec{\epsilon} + \mathbf{I}^m\vec{\kappa} + \mathbf{S}_3^e\vec{\epsilon^e} + \mathbf{I}_2^e\vec{\kappa^e} + \mathbf{I}_3^e\vec{\gamma} + \mathbf{G}_1^e\vec{\varsigma} \qquad (2.32)
\end{aligned}$$

where

$$\mathbf{I}^m = \int_A [\vec{p}\times]\mathbf{\Xi}[\vec{p}\times]^T \, \mathrm{d}A \qquad \mathbf{S}_3^e = \int_A [\vec{p}\times]\mathcal{P}^{T^\star} : \mathcal{A}^3 \, \mathrm{d}A \qquad \mathbf{I}_2^e = \int_A [\vec{p}\times]\mathcal{P}^{T^\star} : \mathcal{A}^4 \, \mathrm{d}A$$

$$\mathbf{I}_3^e = \int_A [\vec{p}\times]\mathcal{P}^{T^\star} : \mathcal{A}^1 \, \mathrm{d}A \qquad \mathbf{G}_1^e = \int_A [\vec{p}\times]\mathcal{P}^{T^\star} : \mathcal{A}^2 \, \mathrm{d}A$$

Once again, computing second stress resultant can be best understood using indicial notation with summation convention employed. [1]

---

[1] $\mathcal{P}\vec{v}\vec{u} = \mathcal{P}_{jkl}(\vec{e}_j \otimes \vec{e}_k \otimes \vec{e}_l)v_m\vec{e}_m u_n\vec{e}_n = \mathcal{P}_{jkl}v_m(\vec{e}_j \otimes \vec{e}_k)\delta_{lm}u_n\vec{e}_n = \mathcal{P}_{jkl}v_l u_n\delta_{kn}\vec{e}_j$
$= \mathcal{P}_{jkl}u_k v_l\vec{e}_j = \mathcal{P} : (\vec{u} \otimes \vec{v})$
$\vec{p} \times \mathcal{P}\vec{v}\vec{u} = [\vec{p}\times]\mathcal{P}\vec{v}\vec{u} = p_{mn}(\vec{e}_m \otimes \vec{e}_n)\mathcal{P}_{jkl}u_k v_l\vec{e}_j = p_{mj}\mathcal{P}_{jkl}u_k v_l\vec{e}_m = [\vec{p}\times]\mathcal{P} : (\vec{u} \otimes \vec{v})$
$\vec{p} \times \mathcal{P}^{T^\star}\vec{v}\vec{u} = [\vec{p}\times]\mathcal{P}^{T^\star}\vec{v}\vec{u} = p_{mn}(\vec{e}_m \otimes \vec{e}_n)\mathcal{P}_{ljk}v_l u_k\vec{e}_j = p_{mj}\mathcal{P}_{ljk}u_k v_l\vec{e}_m$
$= p_{mj}\mathcal{P}_{jkl}u_k v_l\vec{e}_m = [\vec{p}\times]\mathcal{P}^{T^\star} : (\vec{u} \otimes \vec{v})$
Which indicates, pre-multiplying the second order tensor $[\vec{p}\times]$ with each horizontal slice of the third order piezoelectric tensor $\mathcal{P}$ and then performing double contraction with tensor $(\vec{u} \otimes \vec{v})$.

$$\vec{p} \times \boldsymbol{\sigma}^e \vec{a} = -[\vec{p}\times]\mathcal{P}^{T^\star}\vec{b}\vec{a} = [\vec{p}\times]\mathcal{P}^{T^\star}\left[\boldsymbol{I}\epsilon^{\vec{e}} + (\vec{a}\otimes\vec{p})\kappa^{\vec{e}} + \mathcal{A}_1 : \boldsymbol{\gamma} + \mathcal{A}_2 : \boldsymbol{\varsigma}\right]\vec{a}$$

$$p_{tj}\sigma_{ij}^e a_i \ \vec{e}_t = -p_{tj}\mathcal{P}_{itk}b_i a_k \ \vec{e}_t = \mathcal{C}_{itk}\left[\delta_{il}\epsilon_l^e + a_i p_m k_m^e + \mathcal{A}_{1_{ipq}}\gamma_{pq} + \mathcal{A}_{2_{irs}}\varsigma_{rs}\right]a_k \ \vec{e}_t$$

$$= \mathcal{C}_{itk}\left[a_k\delta_{il}\epsilon_l^e + a_k a_i p_m k_m^e + a_k\mathcal{A}_{1_{ipq}}\gamma_{pq} + a_k\mathcal{A}_{2_{irs}}\varsigma_{rs}\right]\ \vec{e}_t$$

$$= \mathcal{C}_{itk}\left[a_k\delta_{il}\epsilon_l^e + a_k a_i p_m k_m^e + a_k A_{1_{iq}}\gamma_q + a_k A_{2_{is}}\varsigma_s\right]\ \vec{e}_t$$

$$= \mathcal{C}_{itk}\left[\mathcal{A}_{kil}^3\epsilon_l^e + \mathcal{A}_{kim}^4 k_m^e + \mathcal{A}_{kiq}^1\gamma_q + \mathcal{A}_{kis}^2\varsigma_s\right]\ \vec{e}_t$$

$$= \mathcal{C}_{tki}\left[\mathcal{A}_{kil}^3\epsilon_l^e + \mathcal{A}_{kim}^4 k_m^e + \mathcal{A}_{kiq}^1\gamma_q + \mathcal{A}_{kis}^2\varsigma_s\right]\ \vec{e}_t$$

$$\vec{p} \times \boldsymbol{\sigma}^e \vec{e}_3 = \mathcal{C}^{T^\star} : \left[\mathcal{A}^3\vec{\epsilon^e} + \mathcal{A}^4\vec{k^e} + \mathcal{A}^1\vec{\gamma} + \mathcal{A}^2\vec{\varsigma}\right] \tag{2.33}$$

In the above derivation, for convenience we have used $\mathcal{C}^{T^\star} = [\vec{p}\times]\mathcal{P}^{T^\star}$. Let us now consider the electric displacement vector, which also naturally evolves from consistent linearisation of enthalpy density, as an algebraic summation of mechanical and electrical components.

$$\vec{D} = \vec{D}^e + \vec{D}^m = \boldsymbol{\epsilon}\vec{E} + \mathcal{P} : \boldsymbol{\varepsilon}$$

$$= -\boldsymbol{\epsilon}\left[\boldsymbol{I}\epsilon^{\vec{e}} + (\vec{e}_3\otimes\vec{p})\kappa^{\vec{e}} + \mathcal{A}_1 : \boldsymbol{\gamma} + \mathcal{A}_2 : \boldsymbol{\varsigma}\right]$$

$$+ \frac{1}{2}\mathcal{P} : \left[(\vec{\epsilon} + \vec{\kappa}\times\vec{p})\otimes\vec{e}_3 + \vec{e}_3\otimes(\vec{\epsilon} + \vec{\kappa}\times\vec{p})\right]$$

$$= -\boldsymbol{\epsilon}\left[\boldsymbol{I}\epsilon^{\vec{e}} + (\vec{e}_3\otimes\vec{p})\kappa^{\vec{e}} + \boldsymbol{A}_1\vec{\gamma} + \boldsymbol{A}_2\vec{\varsigma}\right]$$

$$+ \frac{1}{2}\left[\vec{e}_3\mathcal{P}^{T^\star}\vec{\epsilon} + \vec{e}_3\mathcal{P}^{T^\star}[\vec{p}\times]^T\vec{\kappa} + \vec{e}_3\mathcal{P}^{T}\vec{\epsilon} - \vec{e}_3\mathcal{P}^{T}[\vec{p}\times]^T\vec{\kappa}\right]$$

$$= -\boldsymbol{\epsilon}\left[\boldsymbol{I}\epsilon^{\vec{e}} + (\vec{e}_3\otimes\vec{p})\kappa^{\vec{e}} + \boldsymbol{A}_1\vec{\gamma} + \boldsymbol{A}_2\vec{\varsigma}\right] + \boldsymbol{A}_3\vec{\epsilon} + \boldsymbol{A}_4\vec{\kappa} \tag{2.34}$$

Where the second order tensors $\boldsymbol{A}_3$ and $\boldsymbol{A}_4$ are.

$$\boldsymbol{A}_3 = \frac{1}{2}\vec{e}_3\left(\mathcal{P}^{T^\star} + \mathcal{P}^T\right), \qquad\qquad \boldsymbol{A}_4 = \frac{1}{2}\vec{e}_3\left(\mathcal{P}^{T^\star} + \mathcal{P}^T\right)[\vec{p}\times]^T$$

By integrating (2.34) over the area we obtain the resultant of first electric displacement resultant.

$$\vec{Q}^e = \int_A \vec{D}\ \mathrm{d}A = \int_A\left\{-\boldsymbol{\epsilon}\left[\boldsymbol{I}\epsilon^{\vec{e}} + (\vec{e}_3\otimes\vec{p})\kappa^{\vec{e}} + \boldsymbol{A}_1\vec{\gamma} + \boldsymbol{A}_2\vec{\varsigma}\right] + \boldsymbol{A}_3\vec{\epsilon} + \boldsymbol{A}_4\vec{\kappa}\right\}\mathrm{d}A$$

$$= -\mathbf{A}_2^e\epsilon^{\vec{e}} - \mathbf{S}_4^e\kappa^{\vec{e}} - \mathbf{S}_5^e\vec{\gamma} - \mathbf{I}_4^e\vec{\varsigma} + \mathbf{A}_1^{e^T}\vec{\epsilon} + \mathbf{S}_3^{e^T}\vec{\kappa} \tag{2.35}$$

where.

$$\mathbf{A}_2^e = \int_A \boldsymbol{\epsilon} \; \mathrm{d}A, \qquad\qquad \mathbf{S}_4^e = \int_A \boldsymbol{\epsilon} \left(\vec{e}_3 \otimes \vec{p} \right) \mathrm{d}A$$

$$\mathbf{S}_5^e = \int_A \boldsymbol{\epsilon} \boldsymbol{A}_1 \; \mathrm{d}A, \qquad\qquad \mathbf{I}_4^e = \int_A \boldsymbol{\epsilon} \boldsymbol{A}_2 \; \mathrm{d}A$$

Anistropic Case

The incorporation of anistropic linear elasticity into our formulation is now relatively straightforward, in that we only have to modify *mechanical* stress resultants, i.e.

$$\boldsymbol{\sigma} = \boldsymbol{\sigma}^m + \boldsymbol{\sigma}^e = \mathbb{C} : \varepsilon - \mathcal{P}^{T^\star} \vec{E}$$

$$\boldsymbol{\sigma}\vec{e}_3 = (\mathbb{C} : \varepsilon)\vec{e}_3 - \mathcal{P}^{T^\star}\vec{E}\vec{e}_3 = \mathcal{C}^1 : \varepsilon - \mathcal{P}^{T^\star}\vec{E}\vec{e}_3$$

where $\mathcal{C}^1$ is the third order tensor produced from the action of $\mathbb{C}$ over $\vec{e}_3$.
To illustrate this; due to symmetry of strain tensor we can write.

$$\boldsymbol{\sigma}^m\vec{e}_3 = \mathbb{C} : \left[(\vec{\epsilon} + \vec{\kappa} \times \vec{p}) \otimes \vec{e}_3 \right] \vec{e}_3$$

Performing a general tensor analysis on fourth, second and first order tensors we have.

$$\sigma_{ij}^m e_j = \mathrm{C}_{ijkl} \left[(a_k + P_{km}b_m)d_l \right] e_j = e_j \mathrm{C}_{jikl} \left[(a_k + P_{km}b_m)d_l \right]$$
$$= \mathrm{C}_{ikl}^1 (a_k + P_{km}b_m)d_l = d_l \mathrm{C}_{lik}^1 a_k + d_l \mathrm{C}_{lik}^1 P_{km}b_m$$

Substituting for corresponding tensors we obtain,

$$\boldsymbol{\sigma}^m\vec{e}_3 = \vec{e}_3 \, \mathcal{C}^{1^{T^\star}} \vec{\epsilon} + \vec{e}_3 \, \mathcal{C}^{1^{T^\star}} [\vec{p}\times]^T \vec{\kappa}$$

Comparing the isotropic and anistropic cases, we identify that $\boldsymbol{\Xi}$ tensor is now replaced with $\vec{e}_3 \, \mathcal{C}^{1^{T^\star}}$. For convenience, we use the same symbol for anistropic case and write.

$$\boldsymbol{\sigma}^m\vec{e}_3 = \boldsymbol{\Xi}\vec{\epsilon} + \boldsymbol{\Xi}[\vec{p}\times]^T \vec{\kappa}$$

The stress resultants then take the same form.

$$\vec{Q} = \mathbf{A}^m\vec{\epsilon} + \mathbf{S}^m\vec{\kappa}, \qquad\qquad \vec{M} = \mathbf{S}^{m^T}\vec{\epsilon} + \mathbf{I}^m\vec{\kappa}$$

Where similar to isotropic case, the above-mentioned tensors are.

$$\mathbf{A}^m = \int_A \boldsymbol{\Xi} \; \mathrm{d}A, \qquad \mathbf{S}^m = \int_A \boldsymbol{\Xi}[\vec{p}\times]^T \; \mathrm{d}A, \qquad \mathbf{I}^m = \int_A [\vec{p}\times]\boldsymbol{\Xi}[\vec{p}\times]^T \; \mathrm{d}A$$

The explicit forms of these tensors are given in 1.1.6. If origin of the coordinates in the cross sectional plane is taken as centroid of the section then tensors $\mathbf{S}, \mathbf{S}_1^e, \mathbf{S}_2^e, \mathbf{S}_3^e, \mathbf{S}_4^e, \mathbf{S}_5^e, \mathcal{S}_6^e$ and $\mathbf{G}$ vanish, and further if axes are taken to coincide with the principal axes of the cross

section then tensor $\mathbf{I}$ becomes diagonal and tensor $\mathbf{I}_2^e$ and $\mathbf{I}_3^e$ only give rise to principal second moments of area and hence the stress resultants become

$$\vec{Q} = \mathbf{A}^m \vec{\epsilon} + \mathbf{A}_1^e \vec{\epsilon^e} + \mathbf{I}_1^e \vec{\varsigma} \tag{2.36}$$

$$\vec{M} = \mathbf{I}^m \vec{\kappa} + \mathbf{I}_2^e \vec{\kappa^e} + \mathbf{I}_3^e \vec{\gamma} \tag{2.37}$$

$$\vec{Q^e} = \mathbf{A}_1^{e^T} \vec{\epsilon} - \mathbf{A}_2^e \vec{\epsilon^e} - \mathbf{I}_4^e \vec{\varsigma} \tag{2.38}$$

2.4. Governing Equations of Three-Dimensional Piezoelectric Beams

To reduce the problem of continuum linear piezoelectricity to three-dimensional beam model, the equilibrium of linear momentum, the equilibrium of angular momentum and Gauss's law, should be satisfied in an average sense over the cross sectional area of the beam. If we integrate the governing equations of continuum piezoelectro-elastictiy over the cross sectional area of the beam, we end up with the governing equations of three-dimensional beams. Consider the linear momentum,

$$\int_A (\text{div}\boldsymbol{\sigma} + \vec{b}) \; \mathrm{d}A = \mathbf{0}$$

$$\int_A (\text{div}\boldsymbol{\sigma} + \vec{b}) \; \mathrm{d}A = \int_A \left(\frac{\partial \boldsymbol{\sigma} \vec{e}_3}{\partial x_3} + \sum_{\alpha=1,2} \frac{\partial \boldsymbol{\sigma} \vec{e}_\alpha}{\partial x_\alpha} + \vec{b} \right) \mathrm{d}A$$

$$= \frac{\partial}{\partial x_3} \int_A \boldsymbol{\sigma} \vec{e}_3 \; \mathrm{d}A + \int_A \sum_{\alpha=1,2} \frac{\partial \boldsymbol{\sigma} \vec{e}_\alpha}{\partial x_\alpha} \; \mathrm{d}A + \int_A \vec{b} \; \mathrm{d}A$$

$$= \frac{\partial \vec{Q}}{\partial x_3} + \int_\Gamma \boldsymbol{\sigma} \vec{n}_\Gamma \; \mathrm{d}s + \int_A \vec{b} \; \mathrm{d}A = \mathbf{0} \tag{2.39}$$

where, as computed in the earlier section, $\vec{Q}$ is the traction force vector acting on the cross section, $\vec{n}_\Gamma$ is the unit outward normal to the boundary of the cross section Γ, as shown in Fig. 5, $\vec{b}$ is the vector of body forces and div is the divergence operator. One can observe the similitude of (2.39) with the linear momentum of continuum linear elasticity, where the last two terms here indicate the traction force vector and the body force vector, respectively.

$$\vec{q} = \int_A \vec{b} \; \mathrm{d}A + \int_\Gamma \vec{t}_\Gamma \; \mathrm{d}s \tag{2.40}$$
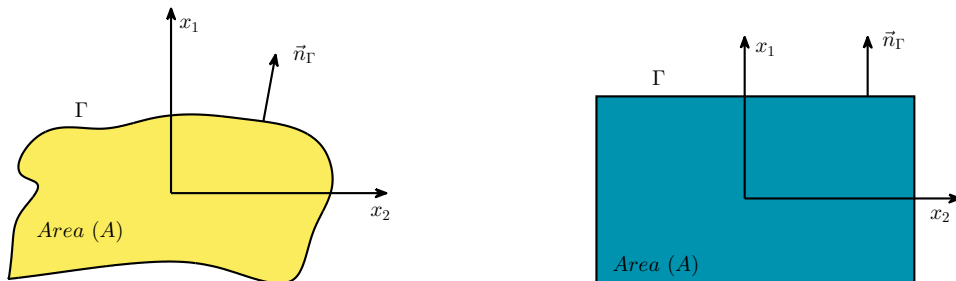
Figure 5: Cross Section of Arbitrary and Prismatic Beams

For angular momentum we have.

$$\int_A \vec{p} \times (\text{div}\boldsymbol{\sigma} + \vec{b}) \; \mathrm{d}A = \mathbf{0}$$

$$\int_A \vec{p} \times (\text{div}\boldsymbol{\sigma} + \vec{b}) \; \mathrm{d}A = \int_A \vec{p} \times \left(\frac{\partial \boldsymbol{\sigma}\vec{e}_3}{\partial x_3} + \sum_{\alpha=1,2} \frac{\partial \boldsymbol{\sigma}\vec{e}_\alpha}{\partial x_\alpha} + \vec{b} \right) \; \mathrm{d}A$$

$$= \frac{\partial}{\partial x_3} \int_A \vec{p} \times \boldsymbol{\sigma}\vec{e}_3 \; \mathrm{d}A + \int_A \sum_{\alpha=1,2} \vec{p} \times \frac{\partial \boldsymbol{\sigma}\vec{e}_\alpha}{\partial x_\alpha} \; \mathrm{d}A + \int_A \vec{p} \times \vec{b} \; \mathrm{d}A \quad (2.41)$$

The second integrand in the above equation can be written as.

$$\sum_{\alpha=1,2} \frac{\partial}{\partial x_\alpha} \left(\vec{p} \times \boldsymbol{\sigma}\vec{e}_\alpha \right) = \sum_{\alpha=1,2} \vec{p} \times \frac{\partial \boldsymbol{\sigma}\vec{e}_\alpha}{\partial x_\alpha} + \sum_{\alpha=1,2} \frac{\partial \vec{p}}{\partial x_\alpha} \times \boldsymbol{\sigma}\vec{e}_\alpha \quad (2.42)$$

Considering that the equilibrium of angular momentum in continuum level implies,

$$\vec{e}_i \times \boldsymbol{\sigma}\vec{e}_i = \vec{e}_3 \times \boldsymbol{\sigma}\vec{e}_3 + \sum_{\alpha=1,2} \vec{e}_\alpha \times \boldsymbol{\sigma}\vec{e}_\alpha = \mathbf{0} \quad (2.43)$$

and noting that $\partial\vec{p}/\partial x_\alpha = \vec{e}_\alpha$, we obtain.

$$\sum_{\alpha=1,2} \vec{p} \times \frac{\partial \boldsymbol{\sigma}\vec{e}_\alpha}{\partial x_\alpha} = \sum_{\alpha=1,2} \frac{\partial}{\partial x_\alpha} \left(\vec{p} \times \boldsymbol{\sigma}\vec{e}_\alpha \right) + \vec{e}_3 \times \boldsymbol{\sigma}\vec{e}_3 \quad (2.44)$$

Hence (2.41) takes the form.

$$\frac{\partial}{\partial x_3} \int_A \vec{p} \times \boldsymbol{\sigma}\vec{e}_3 \; \mathrm{d}A + \int_A \sum_{\alpha=1,2} \frac{\partial}{\partial x_\alpha} \left(\vec{p} \times \boldsymbol{\sigma}\vec{e}_\alpha \right) \; \mathrm{d}A + \int_A (\vec{e}_3 \times \boldsymbol{\sigma}\vec{e}_3) \mathrm{d}A + \int_A \vec{p} \times \vec{b} \; \mathrm{d}A$$

$$= \frac{\partial \vec{M}}{\partial x_3} + \int_\Gamma \vec{p} \times \boldsymbol{\sigma}\vec{n}_\Gamma \; \mathrm{d}s + \vec{e}_3 \times \vec{Q} + \int_A \vec{p} \times \vec{b} \; \mathrm{d}A = \mathbf{0} \quad (2.45)$$

If we make a comparison between (2.45) and the balance of angular momentum of continuum elasticity, we identify the appearance of an additional term $\vec{e}_3 \times \vec{Q}$ which in fact arises by using the continuum balance of angular momentum itself and corresponds to the moment of traction force vector. The second term and last term correspond to applied moments per unit length i.e.

$$\vec{m} = \int_A \vec{p} \times \vec{b} \; \mathrm{d}A + \int_\Gamma \vec{p} \times \vec{t}_\Gamma \; \mathrm{d}s \quad (2.46)$$

and the first moment of traction force being $\vec{M}$.

$$\vec{M} = \int_A \vec{p} \times \boldsymbol{\sigma}\vec{e}_3 \; \mathrm{d}A = \int_A \vec{p} \times \vec{t}_{e_3} \; \mathrm{d}A \quad (2.47)$$

Similarly, we can evaluate the integral form of Gauss's law over the cross sectional area.

$$\int_A (\mathrm{div}\vec{D} - q^e)\mathrm{d}A = 0$$

$$\int_A (\mathrm{div}\vec{D} - q^e)\mathrm{d}A = \int_A \left(\frac{\partial D_3}{\partial x_3} + \sum_{\alpha=1,2} \frac{\partial D_\alpha}{\partial x_\alpha}\right)\mathrm{d}A - \int_A q^e\,\mathrm{d}A$$

$$= \frac{\partial}{\partial x_3}\int_A D_3\,\mathrm{d}A + \int_A \sum_{\alpha=1,2}\frac{\partial D_\alpha}{\partial x_\alpha}\,\mathrm{d}A - \int_A q^e\,\mathrm{d}A$$

$$= \frac{\partial Q_3^e}{\partial x_3} + \int_\Gamma \sum_{\alpha=1,2} D_\alpha\vec{n}_{\Gamma_\alpha}\,\mathrm{d}s - \int_A q^e\,\mathrm{d}A = 0 \qquad (2.48)$$

Here, $\vec{Q}^e$ as evaulated in the previous section, denotes the resultant of electric displacement. In the context of electrical terminologies, Q_3^e can be interpreted as the amount of free charge required to balance the bounded charge over the sections area, had it been a free surface [36]. Similar to the other two resultant forces $\vec{q}$ and $\vec{m}$, the last two terms in (2.48) correspond to electric displacement through the perimeter of beam cross section and the specified free surface charge, respectively.

$$r = \int_\Gamma \sum_{\alpha=1,2} D_\alpha\vec{n}_{\Gamma_\alpha}\,\mathrm{d}s - \int_A q^e\,\mathrm{d}A \qquad (2.49)$$

As we will see in chapter 3. we need the first moment and the second moment of electric displacement, both of which can be treated mainly as mathematical entities. These quantities arise naturally from the variational form of Gauss's law, in that, while evaluating $\delta W^e = \int_V D_i \delta E_i \mathrm{d}\Omega$, once we substitute for electric field E_i, expressions like $\vec{p}D_3$ and $\vec{s}D_\alpha$ emerge, which need to be first integrated over the cross section. After integration, these quantities yield moments of electric displacement. To obtain the expression for first moment and second moment of free charge $\vec{Q}^e$, we need the integrand of (2.48) multiplied with vector $\vec{p}$ and square of this vector which we have denoted as $\vec{s} = x_\alpha^2 \vec{e}_\alpha$. As mentioned earlier, the emergence of $\vec{s}$ is due to the disappearance of off-diagonal components in $\boldsymbol{\gamma}$, and in fact the equivalent form of electric potential is now written as,

$$\psi = \phi + \vec{\beta}\cdot\vec{p} + \frac{1}{2}\vec{\gamma}\cdot\vec{s} \qquad (2.50)$$

where $\vec{\gamma}$ is given by (2.26). The modified electric field now becomes.

$$\vec{E} = -\nabla\psi(\vec{x}) = -\left(\frac{d\phi}{dx_3} + \frac{d\vec{\beta}}{dx_3}\cdot\vec{p} + \frac{1}{2}\frac{d\vec{\gamma}}{dx_3}\cdot\vec{s}\right)\vec{e}_3 - \sum_{\alpha=1,2}\left(\vec{\beta}\cdot\vec{e}_\alpha + x_\alpha\vec{e}_\alpha\cdot\vec{\gamma}\right)\vec{e}_\alpha \qquad (2.51)$$

Having noted the modified form of electric potential and electric field, we can now proceed

with obtaining the moment resultants,

$$\int_A \vec{p}(\operatorname{div}\vec{D} - q^e)\mathrm{d}A = \mathbf{0}$$

$$\int_A \vec{p}(\operatorname{div}\vec{D} - q^e)\mathrm{d}A = \int_A \vec{p}\left(\frac{\partial D_3}{\partial x_3} + \sum_{\alpha=1,2}\frac{\partial D_\alpha}{\partial x_\alpha}\right)\mathrm{d}A - \int_A \vec{p}q^e \ \mathrm{d}A$$

$$= \int_A \frac{\partial(\vec{p}D_3)}{\partial x_3} \ \mathrm{d}A + \int_A \sum_{\alpha=1,2}\vec{p}\frac{\partial D_\alpha}{\partial x_\alpha} \ \mathrm{d}A - \int_A \vec{p}q^e \ \mathrm{d}A$$

$$= \frac{\partial}{\partial x_3}\int_A \vec{p}D_3 \ \mathrm{d}A + \int_A \sum_{\alpha=1,2}\frac{\partial(\vec{p}D_\alpha)}{\partial x_\alpha} \ \mathrm{d}A - \int_A \sum_{\alpha=1,2}D_\alpha\vec{e}_\alpha \ \mathrm{d}A - \int_A \vec{p}q^e \ \mathrm{d}A$$

$$= \frac{\partial\vec{M}^e}{\partial x_3} + \int_\Gamma \sum_{\alpha=1,2}\vec{p}D_\alpha\vec{n}_{\Gamma_\alpha}\vec{e}_\alpha \ \mathrm{d}s - \sum_{\alpha=1,2}Q^e_\alpha - \int_A \vec{p}q^e \ \mathrm{d}A = \mathbf{0} \qquad (2.52)$$

where $\vec{M}^e$ is the moment resulting from the 3rd component of electric displacement (after integration). The second and fourth terms in the above equation can be mathematically characterised as moments of applied electric displacement and free charge, respectively. While we can clearly observe the similarity between moment resultant arising from mechanical kinematics (2.32) and moment resultant arising from electrostatics (2.52), the latter comprises of an additional term Q^e_α (which is in fact not a moment, but the two components of resultant electric displacement). The moments of applied electric displacement and free charge, can be denoted by m^e.

$$\vec{M}^e = \int_A \vec{p}D_3 \ \mathrm{d}A \qquad (2.53)$$

$$\vec{m}^e = \int_\Gamma \sum_{\alpha=1,2}\vec{p}D_\alpha\vec{n}_{\Gamma_\alpha}\vec{e}_\alpha \ \mathrm{d}s - \int_A \vec{p}q^e \ \mathrm{d}A \qquad (2.54)$$

Similar to (2.52), we can find the second moment of electric displacement and applied charges.

$$\int_A \vec{s}(\operatorname{div}\vec{D} - q^e)\mathrm{d}A = \mathbf{0}$$

$$\int_A \vec{s}(\operatorname{div}\vec{D} - q^e)\mathrm{d}A = \int_A \vec{s}\left(\frac{\partial D_3}{\partial x_3} + \sum_{\alpha=1,2}\frac{\partial D_\alpha}{\partial x_\alpha}\right)\mathrm{d}A - \int_A \vec{s}q^e \ \mathrm{d}A$$

$$= \int_A \frac{\partial(\vec{s}D_3)}{\partial x_3} \ \mathrm{d}A + \int_A \sum_{\alpha=1,2}\vec{s}\frac{\partial D_\alpha}{\partial x_\alpha} \ \mathrm{d}A - \int_A \vec{s}q^e \ \mathrm{d}A$$

$$= \frac{\partial}{\partial x_3}\int_A \vec{s}D_3 \ \mathrm{d}A + \int_A \sum_{\alpha=1,2}\frac{\partial(\vec{s}D_\alpha)}{\partial x_\alpha} \ \mathrm{d}A$$

$$- \int_A 2\sum_{\alpha=1,2}x_\alpha D_\alpha\vec{e}_\alpha \ \mathrm{d}A - \int_A \vec{s}q^e \ \mathrm{d}A$$

$$= \frac{\partial\vec{O}^e}{\partial x_3} + \int_\Gamma \sum_{\alpha=1,2}\vec{s}D_\alpha\vec{n}_{\Gamma_\alpha}\vec{e}_\alpha \ \mathrm{d}s - \vec{M}^e_1 - \int_A \vec{s}q^e \ \mathrm{d}A = \mathbf{0} \qquad (2.55)$$

21

Where the second moment of electric displacement and free charge are,

$$\vec{O}^e = \int_A \vec{s} D_3 \ \mathrm{d}A \tag{2.56}$$

$$\vec{o}^e = \int_\Gamma \sum_{\alpha=1,2} \vec{s} D_\alpha \vec{n}_{\Gamma_\alpha} \vec{e}_\alpha \ \mathrm{d}s - \int_A \vec{s} q^e \ \mathrm{d}A \tag{2.57}$$

respectively. We can observe the emergence of an extra moment $\vec{M}_1^e$, which eventually also enters into the variational form of the problem.

$$\vec{M}_1^e = 2 \int_A \sum_{\alpha=1,2} x_\alpha D_\alpha \vec{e}_\alpha \ \mathrm{d}A$$

By now, we have obtained the governing differential equations of piezoelectric three-dimensional beams in terms of stress and electric displacement resultants. For the static case, when stress resultants are not time-dependent, these are ordinary differential equations of the following form.

$$\frac{d\vec{Q}}{dx_3} + \vec{q} = 0 \tag{2.58}$$

$$\frac{d\vec{M}}{dx_3} + \vec{e}_3 \times \vec{Q} + \vec{m} = 0 \tag{2.59}$$

$$\frac{dQ_3^e}{dx_3} + r = 0 \tag{2.60}$$

$$\frac{d\vec{M}^e}{dx_3} - Q_\alpha^e + \vec{m}^e = 0 \tag{2.61}$$

$$\frac{d\vec{O}^e}{dx_3} - \vec{M}_1^e + \vec{o}^e = 0 \tag{2.62}$$

Equations (2.58), (2.59), (2.60), (2.61) and (2.62) constitute a set of first order differential equation in one dimension. If the above set of equations are satisfied then the continuum balance equations are also satisfied in an average sense over the cross section.

Mixed Variational Formulation

"This field is fun; it is fun more than fun."
T. J. R. Hughes

3. Variational Formulation

This chapter is devoted to variational formulation for three-dimensional piezoelectric beams. The point of departure is the Lagrangian of the system, which contains kinetic energy, enthalpy density and the external potential energy of the conservative system. Starting from the continuum level, let Ω be the configuration occupied by the piezoelectric solid, $\Omega \subset \mathbb{R}^3$, as shown in Fig. 6. The configuration is characterised by the mechanical displacement field $\vec{u} : \Omega \to \mathbb{R}^3$ and electric potential $\psi : \Omega \to \mathbb{R}^1$. If we consider two material points with their position vectors as $\vec{X_1}$ and $\vec{X_2}$, then associated with them, we have the infinitesimal strain tensor $\boldsymbol{\varepsilon} : \Omega \to \mathbb{R}^{3\times3}_{sym}$, where $\mathbb{R}^{3\times3}_{sym}$ represents the space of symmetric tensors, as well as electric field $\vec{E} : \Omega \to \mathbb{R}^3$, as defined in the previous chapter.
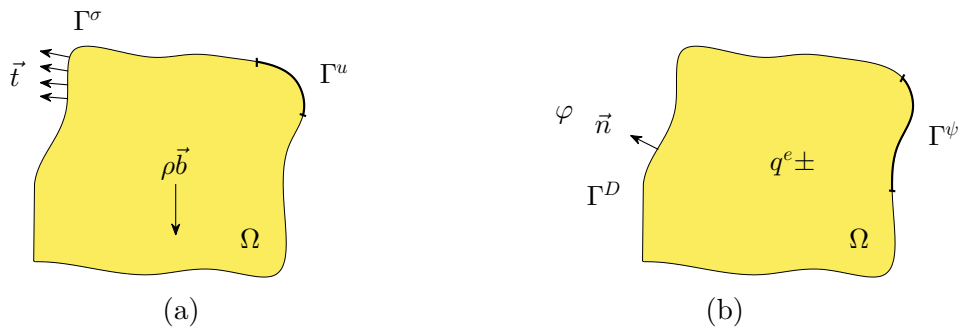
Figure 6: Decompostion of (a) Mechanical Boundary $\Gamma = \Gamma^\sigma \cup \Gamma^u$ & $\Gamma^\sigma \cap \Gamma^u = \emptyset$ and (b) Electrical Boundary $\Gamma = \Gamma^D \cup \Gamma^\psi$ & $\Gamma^D \cap \Gamma^\psi = \emptyset$

The enthalpy density of the piezoelectric system under small deformation regime can be written as [50] [4],

$$H(\boldsymbol{\varepsilon}, \vec{E}) = \frac{1}{2}\,\boldsymbol{\varepsilon} : \mathbb{C} : \boldsymbol{\varepsilon} - \vec{E} \cdot \mathcal{P} : \boldsymbol{\varepsilon} - \frac{1}{2}\,\vec{E} \cdot \boldsymbol{\epsilon}\vec{E}$$

where $\mathbb{C} : \Omega \to \mathbb{R}^{3\times3\times3\times3}_{sym}$ is the 4th order elasticity tensor, $\mathcal{P} : \Omega \to \mathbb{R}^{3\times3\times3}_{sym}$ the 3rd order piezoelectric tensor and $\boldsymbol{\epsilon} : \Omega \to \mathbb{R}^{3\times3}_{sym}$ the 2nd order dielectric tensor. Also, a dot indicates

scalar product and a colon implies double contraction. The Lagrangian of the system $\mathcal{L}$, can now be written as [50],

$$\mathcal{L}(\vec{u}, \vec{\dot{u}}, \psi) = \mathcal{K}(\vec{\dot{u}}) - \Pi_{int}(\vec{u}, \psi) - \Pi_{ext}(\vec{u}, \psi)$$

where the kinetic, internal potential and external potential energies of the system are,

$$\mathcal{K} = \int_{\Omega_t} \frac{1}{2} \rho \, \vec{\dot{u}} \cdot \vec{\dot{u}} \, \mathrm{d}V \tag{3.1}$$

$$\Pi_{int} = \int_{\Omega_t} H \, \mathrm{d}V \tag{3.2}$$

$$\Pi_{ext} = \int_{\Omega_t} \left(\vec{b}\vec{u} - q^e \psi \right) \mathrm{d}V + \int_{\Gamma_t^\sigma} \vec{t} \, \mathrm{d}A - \int_{\Gamma_t^D} \varphi \, \mathrm{d}A \tag{3.3}$$

respectively. In the above expressions, $\vec{\dot{u}} = D\vec{u}/Dt$ is the material velocity (or local velocity, since there is no distinction between the two in small deformation regime), $\vec{b}$ is the vector of body forces, $\vec{t}$ is the applied mechanical traction, q^e is the total electric charge density, φ is the applied surface charge and ρ is the density of material. Ω_t represents the volume occupied by the body at time t and similarly at a given time t, Γ_t^σ and Γ_t^D represent the boundaries where mechanical traction and surface charge are applied, respectively, see Fig. 6. The action integral I, can now be defined as the integral of the Lagrangian over the time interval $[t_1, t_2]$. For simplicity, we assume $t_1 = 0$.

$$I = \int_{t_1}^{t_2} \mathcal{L}(\vec{u}, \vec{\dot{u}}, \psi) \, \mathrm{d}t \tag{3.4}$$

Hamilton's principle states that the deformation satisfying the equations of motion and the electrical mapping satisfying the equations of electrostatics, can be obtained by making the action integral stationary with respect to all possible mappings which are compatible with the boundary conditions [38] [42]. To this end, we perform directional derivatives, for variation of displacements $\vec{\delta u}$ and variation of electric potential $\delta\psi$, respectively. The directional derivative, assuming a perturbation of displacements $\vec{\underline{u}} = \vec{u} + \zeta\vec{\delta u}$, where ζ is small and $\vec{\delta u}$ is a differentiable function satisfying $\vec{\delta u}(t_1) = \vec{\delta u}(t_2) = \mathbf{0}$, yields.

$$\frac{\mathrm{d}I}{\mathrm{d}\zeta} = \frac{\mathrm{d}}{\mathrm{d}\zeta} \int_{t_1}^{t_2} \mathcal{L}(\vec{\underline{u}}, \vec{\dot{\underline{u}}}, \psi) \, \mathrm{d}t = \int_{t_1}^{t_2} \frac{\mathrm{d}\mathcal{L}}{\mathrm{d}\zeta} \, \mathrm{d}t$$

$$= \int_{t_1}^{t_2} \left(\frac{\mathrm{d}\vec{\underline{u}}}{\mathrm{d}\zeta} \cdot \frac{\partial\mathcal{L}}{\partial\vec{\underline{u}}} + \frac{\mathrm{d}\vec{\dot{\underline{u}}}}{\mathrm{d}\zeta} \cdot \frac{\partial\mathcal{L}}{\partial\vec{\dot{\underline{u}}}} + \frac{\mathrm{d}\psi}{\mathrm{d}\zeta} \frac{\partial\mathcal{L}}{\partial\psi} \right) \mathrm{d}t = \int_{t_1}^{t_2} \left(\vec{\delta u} \cdot \frac{\partial\mathcal{L}}{\partial\vec{\underline{u}}} + \vec{\dot{\delta u}} \cdot \frac{\partial\mathcal{L}}{\partial\vec{\dot{\underline{u}}}} \right) \mathrm{d}t$$

When $\zeta = 0$, we have $\vec{\underline{u}} = \vec{u}$ and the action integral has an extermum so that.

$$\left. \frac{\mathrm{d}I}{\mathrm{d}\zeta} \right|_{\zeta=0} = 0$$

$$\left. \frac{\mathrm{d}I}{\mathrm{d}\zeta} \right|_{\zeta=0} = \int_{t_1}^{t_2} \left(\vec{\delta u} \cdot \frac{\partial\mathcal{L}}{\partial\vec{u}} + \vec{\dot{\delta u}} \cdot \frac{\partial\mathcal{L}}{\partial\vec{\dot{u}}} \right) \mathrm{d}t$$

$$= \int_{t_1}^{t_2} \left(\frac{\partial\mathcal{L}}{\partial\vec{u}} - \frac{\mathrm{d}}{\mathrm{d}t} \frac{\partial\mathcal{L}}{\partial\vec{\dot{u}}} \right) \cdot \vec{\delta u} \, \mathrm{d}t + \left[\vec{\delta u} \cdot \frac{\partial\mathcal{L}}{\partial\vec{\dot{u}}} \right]_{t_1}^{t_2} = 0$$

In arriving to the last expression, we have used integration by part. Knowing that the boundary term in the above expression vanishes, and using the fundamental lemma of variational calculus, we obtain the Euler-Lagrange equation of our dynamical system.

$$\frac{\partial \mathcal{L}}{\partial \vec{u}} - \frac{\mathrm{d}}{\mathrm{d}t}\frac{\partial \mathcal{L}}{\partial \dot{\vec{u}}} = \mathbf{0} \tag{3.5}$$

Similarly, by perturbing the electric field through a variation $\underline{\psi} = \psi + \zeta\delta\psi$, where $\delta\psi$ is a differentiable function such that, $\delta\psi(t_1) = \delta\psi(t_2) = 0$, we obtain.

$$\left.\frac{\mathrm{d}I}{\mathrm{d}\zeta}\right|_{\zeta=0} = \int_{t_1}^{t_2} \frac{\partial \mathcal{L}}{\partial \psi}\,\delta\psi\,\mathrm{d}t = 0$$

Applying the fundamental lemma of variational calculus, we obtain the electrostatic equation of our system.

$$\frac{\partial \mathcal{L}}{\partial \psi} = 0 \tag{3.6}$$

From the second term of of (3.5), we can now obtain the linearised form of kinetic energy.

$$\frac{\mathrm{d}}{\mathrm{d}t}\frac{\partial \mathcal{L}}{\partial \dot{\vec{u}}} = \frac{\mathrm{d}}{\mathrm{d}t}\frac{\partial \mathcal{K}}{\partial \dot{\vec{u}}} = \frac{\mathrm{d}}{\mathrm{d}t}\int_{\Omega_t} \frac{1}{2}\rho\,\dot{\vec{u}}\cdot\dot{\vec{u}}\,\mathrm{d}V$$

$$= \frac{\mathrm{d}}{\mathrm{d}t}\int_{\Omega_t} \rho\dot{\vec{u}}\,\mathrm{d}V = \int_{\Omega_t} \rho\frac{\mathrm{d}^2\vec{u}}{\mathrm{d}t^2}\,\mathrm{d}V = \int_{\Omega_t} \rho\frac{D^2\vec{u}}{Dt^2}\,\mathrm{d}V \tag{3.7}$$

It should be noted that in small deformation regime, no distniction is made between spatial and material volumes, and hence the time derivative outside a volume integral can be moved inside. We now need to obtain the linearised forms of elastostatics and electrostatics of the piezoelectric system. This can be achieved from the principle of virtual wok, as Hamilton's principle also reduces to principle of virtual work for static problems.

$$\frac{\partial \mathcal{L}}{\partial \vec{u}} = \mathbf{0}, \qquad\qquad \frac{\partial \mathcal{L}}{\partial \psi} = 0$$

To this end, the virtual internal potential energy at any time instant can be found.

$$\delta\Pi_{int} = \int_{\Omega_t}\left(\frac{1}{2}\boldsymbol{\varepsilon}:\mathbb{C}:\boldsymbol{\varepsilon} - \vec{E}\cdot\mathcal{P}:\boldsymbol{\varepsilon} - \frac{1}{2}\vec{E}\cdot\boldsymbol{\epsilon}\vec{E}\right)\mathrm{d}V$$

$$= \int_{\Omega_t}\left(\boldsymbol{\varepsilon}:\mathbb{C}:\delta\boldsymbol{\varepsilon} - \vec{E}\cdot\mathcal{P}:\delta\boldsymbol{\varepsilon} - \delta\vec{E}\cdot\mathcal{P}:\boldsymbol{\varepsilon} - \delta\vec{E}\cdot\boldsymbol{\epsilon}\vec{E}\right)\mathrm{d}V$$

$$= \int_{\Omega_t}\left(\boldsymbol{\sigma}^m:\nabla^s\delta\vec{u} + \boldsymbol{\sigma}^e:\nabla^s\delta\vec{u} + \nabla\delta\psi\cdot\vec{D}^m + \nabla\delta\psi\cdot\vec{D}^e\right)\mathrm{d}V$$

$$= \int_{\Omega_t}\left(\boldsymbol{\sigma}:\nabla^s\delta\vec{u} + \vec{D}\cdot\nabla\delta\psi\right)\mathrm{d}V$$

$$= \int_{\Omega_t}\mathrm{div}(\boldsymbol{\sigma}\delta\vec{u})\,\mathrm{d}V - \int_{\Omega_t}\mathrm{div}\boldsymbol{\sigma}\cdot\delta\vec{u}\,\mathrm{d}V + \int_{\Omega_t}\mathrm{div}(\delta\psi\vec{D})\,\mathrm{d}V - \int_{\Omega_t}\delta\psi\,\mathrm{div}\vec{D}\,\mathrm{d}V$$

$$= \int_{\Gamma_t^\sigma}\delta\vec{u}\cdot\boldsymbol{\sigma}\vec{n}\,\mathrm{d}A + \int_{\Gamma_t^D}\delta\psi\vec{D}\cdot\vec{n}\,\mathrm{d}A - \int_{\Omega_t}\mathrm{div}\boldsymbol{\sigma}\cdot\delta\vec{u}\,\mathrm{d}V - \int_{\Omega_t}\delta\psi\,\mathrm{div}\vec{D}\,\mathrm{d}V \tag{3.8}$$

Finally, the variation of external forces yields.

$$\delta\Pi_{ext} = \int_{\Omega_t} \left(\vec{b}\cdot\vec{\delta u} - q^e \delta\psi \right) dV + \int_{\Gamma_t^\sigma} \vec{t}\cdot\vec{\delta u}\ dA - \int_{\Gamma_t^D} \varphi\delta\psi\ dA \tag{3.9}$$

Summing (3.7)-(3.9), we obtain.

$$\int_{\Omega_t} (\mathrm{div}\boldsymbol{\sigma} + \vec{b} - \rho\frac{D^2\vec{u}}{Dt^2})\cdot\vec{\delta u}\ dV + \int_{\Omega_t} (\mathrm{div}\vec{D} - q^e)\ \delta\psi\ dV$$
$$+ \int_{\Gamma_t^\sigma} (\boldsymbol{\sigma}\vec{n} - \vec{t})\cdot\vec{\delta u}\ dA + \int_{\Gamma_t^D} (\vec{D}\cdot\vec{n} - \varphi)\delta\psi\ dA = 0 \tag{3.10}$$

The Euler-Lagrange equations can now be written.

$$\begin{array}{ll}
\rho\dfrac{D^2\vec{u}}{Dt^2} = \mathrm{div}\boldsymbol{\sigma} + \vec{b} & \text{in } \Omega \times [0,t] \\[2mm]
\mathrm{div}\vec{D} = q^e & \text{in } \Omega \times [0,t] \\[2mm]
\vec{u} = \vec{\bar{u}} & \text{on } \Gamma^u \times [0,t] \\[2mm]
\psi = \bar{\psi} & \text{on } \Gamma^\psi \times [0,t] \\[2mm]
\boldsymbol{\sigma}\vec{n} = \vec{t} & \text{on } \Gamma^\sigma \times [0,t] \\[2mm]
\vec{D}\cdot\vec{n} = \varphi & \text{on } \Gamma^D \times [0,t] \\[2mm]
\vec{u}(t) = \mathbf{0} \quad \vec{\dot{u}}(t) = \mathbf{0} & \text{at } \Omega \times t = 0
\end{array}$$

From the governing equations, we observe that the coupled electromechanical boundary value problem consists of Cauchy equilibrium equations coupled with the equations of electrostatics. In order to embed the beam kinematics into the variational form of the problem we just obtained, let us first consider the static equilibrium equation. For simplicity we drop the subscript t on volume Ω.

$$\int_\Omega (\mathrm{div}\boldsymbol{\sigma} + \vec{b})\cdot\vec{\delta u}\ dV = \int_\Omega \left(\frac{\partial\boldsymbol{\sigma}\vec{e}_3}{\partial x_3} + \sum_{\alpha=1,2} \frac{\partial\boldsymbol{\sigma}\vec{e}_\alpha}{\partial x_\alpha} \right)\cdot\vec{\delta u}\ dV + \int_\Omega \vec{b}\cdot\vec{\delta u}\ dV$$

$$= \int_\Omega \frac{\partial\boldsymbol{\sigma}\vec{e}_3}{\partial x_3}\cdot\vec{\delta u}\ dV + \int_\Omega \sum_{\alpha=1,2} \frac{\partial\boldsymbol{\sigma}\vec{e}_\alpha}{\partial x_\alpha}\cdot\vec{\delta u}\ dV + \int_\Omega \vec{b}\cdot\vec{\delta u}\ dV$$

$$= \int_A \int_l \frac{\partial(\boldsymbol{\sigma}\vec{e}_3\cdot\vec{\delta u})}{\partial x_3}\ dx_3 dA - \int_l \int_A \frac{\partial\vec{\delta u}}{\partial x_3}\cdot\boldsymbol{\sigma}\vec{e}_3\ dA dx_3$$

$$+ \int_l \int_A \sum_{\alpha=1,2} \frac{\partial(\boldsymbol{\sigma}\vec{e}_\alpha\cdot\vec{\delta u})}{\partial x_\alpha}\ dA dx_3 - \int_l \int_A \sum_{\alpha=1,2} \frac{\partial\vec{\delta u}}{\partial x_\alpha}\cdot\boldsymbol{\sigma}\vec{e}_\alpha\ dA dx_3$$

$$+ \int_l \int_A \vec{b}\cdot\vec{\delta u}\ dA dx_3 = \int_A (\boldsymbol{\sigma}\vec{n_{e_3}}\cdot\vec{\delta u}|_{\Gamma^m})\ dA$$

$$- \int_l \int_A \left(\frac{\partial\vec{\delta u}}{\partial x_3}\cdot\boldsymbol{\sigma}\vec{e}_3 + \sum_{\alpha=1,2} \frac{\partial\vec{\delta u}}{\partial x_\alpha}\cdot\boldsymbol{\sigma}\vec{e}_\alpha \right) dA dx_3$$

$$+ \int_l \left(\int_\Gamma (\boldsymbol{\sigma}\vec{n_\Gamma}\cdot\vec{\delta u})\ ds \right) dx_3 + \int_l \int_A \vec{b}\cdot\vec{\delta u}\ dA dx_3 \tag{3.11}$$

It is worth pausing here evaluating the terms that we have arrived at in (3.11). The integral in the second last line of (3.11) contributes to the internal virtual work of piezoelectric system and the remaining terms give rise to external virtual work of *mechanical* forces i.e. we assume that electric contribution does not play a role in generating traction forces. We now embed the kinematics of piezoelectric beam model in the second last line of (3.11) to find an expression for internal virtual work.

$$
\begin{aligned}
\delta W_{int}^m &= \int_l \int_A \left(\frac{\partial \vec{\delta u}}{\partial x_3} \cdot \boldsymbol{\sigma} \vec{e}_3 + \sum_{\alpha=1,2} \frac{\partial \vec{\delta u}}{\partial x_\alpha} \cdot \boldsymbol{\sigma} \vec{e}_\alpha \right) \mathrm{d}A \mathrm{d}x_3 \\
&= \int_l \frac{d\vec{\delta w}}{dx_3} \cdot \left(\int_A \boldsymbol{\sigma} \vec{e}_3 \, \mathrm{d}A \right) \mathrm{d}x_3 + \int_\Omega \left(\frac{d\vec{\delta \theta}}{dx_3} \times \vec{p} \right) \cdot \boldsymbol{\sigma} \vec{e}_3 \, \mathrm{d}V \\
&\quad - \int_l \left(\vec{e}_\alpha \times \vec{\delta \theta} \right) \cdot \left(\int_A \boldsymbol{\sigma} \vec{e}_\alpha \, \mathrm{d}A \right) \mathrm{d}x_3 \\
&= \int_l \left(\frac{d\vec{\delta w}}{dx_3} + \vec{e}_3 \times \vec{\delta \theta} \right) \cdot \left(\int_A \boldsymbol{\sigma} \vec{e}_3 \, \mathrm{d}A \right) \mathrm{d}x_3 + \int_\Omega \left(\frac{d\vec{\delta \theta}}{dx_3} \times \vec{p} \right) \cdot \boldsymbol{\sigma} \vec{e}_3 \, \mathrm{d}V \\
&= \int_l \left(\frac{d\vec{\delta w}}{dx_3} + \vec{e}_3 \times \vec{\delta \theta} \right) \cdot \left(\int_A \boldsymbol{\sigma} \vec{e}_3 \, \mathrm{d}A \right) \mathrm{d}x_3 + \int_l \frac{d\vec{\delta \theta}}{dx_3} \cdot \left(\int_A \vec{p} \times \boldsymbol{\sigma} \vec{e}_3 \, \mathrm{d}A \right) \mathrm{d}x_3 \\
&= \int_l \left(\vec{Q} \cdot \vec{\delta \epsilon} + \vec{M} \cdot \vec{\delta \kappa} \right) \mathrm{d}x_3 \tag{3.12}
\end{aligned}
$$

For external virtual work of mechanical forces, from (3.11) we proceed.

$$
\begin{aligned}
\delta W_{ext}^m &= \int_A \left(\boldsymbol{\sigma} \vec{n}_{e_3} \cdot \vec{\delta u}|_{\Gamma^m} \right) \mathrm{d}A + \int_l \left(\int_\Gamma (\boldsymbol{\sigma} \vec{n}_\Gamma \cdot \vec{\delta u}) \, \mathrm{d}s \right) \mathrm{d}x_3 + \int_l \int_A \vec{b} \cdot \vec{\delta u} \, \mathrm{d}A \mathrm{d}x_3 \\
&= \left[\int_A (\vec{\delta w} + \vec{\delta \theta} \times \vec{p}) \cdot \boldsymbol{\sigma} \vec{n}_{e_3} \, \mathrm{d}A \right]_{\Gamma^m} + \int_l \int_\Gamma \left[\vec{\delta w} + \vec{\delta \theta} \times \vec{p} \right] \cdot \left(\boldsymbol{\sigma} \vec{n}_\Gamma \, \mathrm{d}s \right) \mathrm{d}x_3 \\
&\quad + \int_l \int_A \left[\vec{\delta w} + \vec{\delta \theta} \times \vec{p} \right] \cdot \vec{b} \, \mathrm{d}A \, \mathrm{d}x_3 = (\vec{\delta w} \cdot \vec{q_0})|_{\Gamma^m} + (\vec{\delta \theta} \cdot \vec{m_0})|_{\Gamma^m} \\
&\quad + \int_l \vec{\delta w} \cdot \left(\int_A \vec{b} \, \mathrm{d}A + \int_\Gamma \vec{t}_\Gamma \, \mathrm{d}s \right) \mathrm{d}x_3 + \int_l \vec{\delta \theta} \cdot \left(\int_A \vec{p} \times \vec{b} \, \mathrm{d}A + \int_\Gamma \vec{p} \times \vec{t}_\Gamma \, \mathrm{d}s \right) \mathrm{d}x_3 \tag{3.13}
\end{aligned}
$$

Thus, the external virtual work in terms of specified traction and distributed forces becomes.

$$
\delta W_{ext}^m = (\vec{\delta w} \cdot \vec{q_0})|_{\Gamma^m} + (\vec{\delta \theta} \cdot \vec{m_0})|_{\Gamma^m} + \int_l \vec{\delta w} \cdot \vec{q} \, \mathrm{d}x_3 + \int_l \vec{\delta \theta} \cdot \vec{m} \, \mathrm{d}x_3 \tag{3.14}
$$

The first two terms in (3.14) correspond to applied point forces and applied point moments. These are equivalent to traction boundary conditions of continuum elasticity, in that they are prescribed at specific region of the beam and thus their boundary is termed as Γ^m, where superscript m stands for mechanical. The last two terms in this equation correspond to distributed load and distributed moment along the length of the beam which are equivalent to the body forces of continuum elasticity. While distributed loads are quite common in beam theory, distributed moments are not normally applied as they cannot be interpreted physically.

For the virtual work of inertial forces, we have.

$$\delta W_{iner} = \frac{D^2}{Dt^2} \int_\Omega \rho \vec{u} \cdot \vec{\delta u} \, dV = \frac{D^2}{Dt^2} \int_\Omega \rho \left[\vec{w} + \vec{\theta} \times \vec{p} \right] \cdot \left[\vec{\delta w} + \vec{\delta \theta} \times \vec{p} \right] dV$$

$$= \frac{D^2}{Dt^2} \int_\Omega \rho \vec{\delta w} \cdot \left[\vec{w} + \vec{\theta} \times \vec{p} \right] dV + \frac{D^2}{Dt^2} \int_\Omega \rho \left[\vec{\delta \theta} \times \vec{p} \right] \cdot \left[\vec{w} + \vec{\theta} \times \vec{p} \right] dV$$

$$= \frac{D^2}{Dt^2} \left\{ \int_\Omega \rho \vec{\delta w} \cdot \left[\vec{w} + [\vec{p}\times]^T \vec{\theta} \right] dV + \int_\Omega \rho \vec{\delta \theta} [\vec{p}\times] \cdot \left[\vec{w} + [\vec{p}\times]^T \vec{\theta} \right] dV \right\} \quad (3.15)$$

Once again, by integrating over the cross section area, the one-dimensional expression is obtained.

$$\delta W_{iner} = \frac{D^2}{Dt^2} \left\{ \int_l \vec{\delta w} \cdot \left(\int_A \rho \boldsymbol{I} \, dA \right) \vec{w} \, dx_3 + \int_l \vec{\delta w} \cdot \left(\int_A \rho [\vec{p}\times]^T dA \right) \vec{\theta} \, dx_3 \right.$$

$$\left. + \int_l \vec{\delta \theta} \cdot \left(\int_A \rho [\vec{p}\times] dA \right) \vec{w} \, dx_3 + \int_l \vec{\delta \theta} \cdot \left(\int_A \rho [\vec{p}\times][\vec{p}\times]^T dA \right) \vec{\theta} \, dx_3 \right\} \quad (3.16)$$

As before, substituting the terms inside the brackets with their corresponding tensors, where the subscript D now is chosen to stand for dynamic version of the tensors, we can write.

$$\delta W_{iner} = \frac{D^2}{Dt^2} \left\{ \int_l \vec{\delta w} \cdot \mathbf{A}_D \vec{w} \, dx_3 + \int_l \vec{\delta w} \cdot \mathbf{S}_D \vec{\theta} \, dx_3 \right.$$

$$\left. + \int_l \vec{\delta \theta} \cdot \mathbf{S}_D^T \vec{w} \, dx_3 + \int_l \vec{\delta \theta} \cdot \mathbf{I}_D \vec{\theta} \, dx_3 \right\} \quad (3.17)$$

As discussed before if origin of the coordinates is chosen as centroid of the section then first moment of area vanishes and we obtain

$$\delta W_{iner} = \frac{D^2}{Dt^2} \left\{ \int_l \vec{\delta w} \cdot \mathbf{A}_D \vec{w} \, dx_3 + \int_l \vec{\delta \theta} \cdot \mathbf{I}_D \vec{\theta} \, dx_3 \right\} \quad (3.18)$$

In the context of dynamic analysis, the first integral in (3.18) is the translational inertia and the second the rotary inertia. The semi-discrete weak form of the dynamic beam problem can finally be stated as

$$\delta W_{iner} + \delta W_{int}^m - \delta W_{ext}^m = \frac{D^2}{Dt^2} \left\{ \int_l \vec{\delta w} \cdot \mathbf{A}_D \vec{w} \, dx_3 + \int_l \vec{\delta \theta} \cdot \mathbf{I}_D \vec{\theta} \, dx_3 \right\} + \int_l \left(\vec{Q} \cdot \vec{\delta \epsilon} + \vec{M} \cdot \vec{\delta \kappa} \right) dx_3$$

$$- \left[\int_l \vec{\delta w} \cdot \vec{q} \, dx_3 + \int_l \vec{\delta \theta} \cdot \vec{m} \, dx_3 + (\vec{\delta w} \cdot \vec{q}_0) \Big|_{\Gamma^m} + (\vec{\delta \theta} \cdot \vec{m}_0) \Big|_{\Gamma^m} \right] = 0 \quad (3.19)$$

Eventually, as observed from (3.10), the integral form of Gauss's law contributes to the virtual work.

$$\delta W^e = \int_V (\mathrm{div}\vec{D} - q^e)\delta\psi \ \mathrm{d}\Omega = \int_V \mathrm{div}\vec{D}\delta\psi \ \mathrm{d}\Omega - \int_V q^e\delta\psi \ \mathrm{d}\Omega$$

$$= \int_V \mathrm{div}(\vec{D}\delta\psi) \ \mathrm{d}\Omega - \int_V \vec{D}\nabla\delta\psi \ \mathrm{d}\Omega - \int_V q^e\delta\psi \ \mathrm{d}\Omega$$

$$= \int_A \int_l \frac{\partial(D_3\delta\psi)}{\partial x_3} \ \mathrm{d}x_3\mathrm{d}A + \int_l \int_A \sum_{\alpha=1,2} \frac{\partial(D_\alpha\delta\psi)}{\partial x_\alpha} \ \mathrm{d}A\mathrm{d}x_3 - \int_V \vec{D}\nabla\delta\psi \ \mathrm{d}\Omega - \int_V q^e\delta\psi \ \mathrm{d}\Omega$$

$$(3.20)$$

At this stage we can clearly identify the weak forms associated with internal and boundary terms of our electrostatic problem. Similar to its mechanical counterpart, we treat the internal and the boundary terms separately, starting with the former.

$$\delta W_{int}^e = \int_V \vec{D}\nabla\delta\psi \ \mathrm{d}\Omega = \int_V \left(D_3\frac{\partial\delta\psi}{\partial x_3} + \sum_{\alpha=1,2} D_\alpha\frac{\partial\delta\psi}{\partial x_\alpha} \right)\mathrm{d}\Omega$$

$$= \int_V \left(\frac{d\delta\phi}{dx_3} + \frac{d\vec{\delta\beta}}{dx_3}\cdot\vec{p} + \frac{1}{2}\frac{d\vec{\delta\gamma}}{dx_3}\cdot\vec{s} \right)D_3 \ \mathrm{d}\Omega + \int_V \sum_{\alpha=1,2} \left(\vec{e}_\alpha\cdot\delta\vec{\beta} + \vec{e}_\alpha\cdot x_\alpha\delta\vec{\gamma} \right)D_\alpha \ \mathrm{d}\Omega$$

$$= \int_l \frac{d\delta\phi}{dx_3}\left(\int_A D_3 \ \mathrm{d}A \right)\mathrm{d}x_3 + \int_l \frac{d\vec{\delta\beta}}{dx_3}\cdot\left(\int_A \vec{p}D_3 \ \mathrm{d}A \right)\mathrm{d}x_3 + \frac{1}{2}\int_l \frac{d\vec{\delta\gamma}}{dx_3}\cdot\left(\int_A \vec{s}D_3 \ \mathrm{d}A \right)\mathrm{d}x_3$$

$$+ \int_l \delta\vec{\beta}\cdot\left(\int_A \sum_{\alpha=1,2} D_\alpha \ \mathrm{d}A \right)\mathrm{d}x_3 + \int_l \delta\vec{\gamma}\cdot\left(\int_A \sum_{\alpha=1,2} x_\alpha D_\alpha \ \mathrm{d}A \right)\mathrm{d}x_3$$

$$= \int_l \left(\frac{d\delta\phi}{dx_3}\vec{e}_3 + \delta\vec{\beta} \right)\cdot\left(\int_A \vec{D} \ \mathrm{d}A \right)\mathrm{d}x_3 + \int_l \frac{d\vec{\delta\beta}}{dx_3}\cdot\left(\int_A \vec{p}D_3 \ \mathrm{d}A \right)\mathrm{d}x_3$$

$$+ \int_l \frac{d\vec{\delta\gamma}}{dx_3}\cdot\left(\frac{1}{2}\int_A \vec{s}D_3 \ \mathrm{d}A \right)\mathrm{d}x_3 + \int_l \delta\vec{\gamma}\cdot\left(\int_A \sum_{\alpha=1,2} x_\alpha D_\alpha \ \mathrm{d}A \right)\mathrm{d}x_3$$

$$= \int_l \left(\vec{Q}^e\cdot\delta\vec{\epsilon}^e + \vec{M}^e\cdot\delta\vec{\kappa}^e + \vec{M}_1^e\cdot\delta\vec{\gamma} + \vec{O}^e\cdot\delta\vec{\varsigma} \right) \ \mathrm{d}x_3 \qquad (3.21)$$

Remark 3. In the first line of (3.21), the expressions $\vec{D}$ and $\nabla\delta\psi$ are both assoicated with orthonomral bases $\vec{e}_i$, where $i = 1, 2, 3$ which after carrying out inner product produce unity $||\vec{e}_i|| = \vec{e}_i\cdot\vec{e}_i = 1$ and hence they are taken away a priori.

Remark 4. In the second line we have substituted for values of $\frac{\partial\delta\psi}{\partial x_3}$ and $\frac{\partial\delta\psi}{\partial x_\alpha}$.

Remark 5. Critical to our later investigation is the emergence of factor $\frac{1}{2}$ which is embedded into the definition of $\vec{O}^e$ and $\vec{M}_1^e$. The analytical solutions reported in chapter 5. make use of this modification.

Remark 6. If we draw an analogy between the internal virtual work arising from Cauchy momentum equations and the one from Gauss's law, despite the clear similarity, in the above expression $\vec{Q}^e$ is the resultant of electric displacement in all direction and not like the stress resultant $\vec{Q}$ which only consists of the tractions in $\vec{e}_3$ direction. The equilibrium of angular momentum plays a key role here, in that it eliminates the stress resultants of the other two directions, as can be verified from (3.11) by utilising (2.43).

The emergence of extra terms in (3.21) is due to the second order electric potential assumption across the area directions. These terms would vanish, had we assumed a linear electric potential across the thickness and height of the beam. This issue is addressed in the upcoming section. As we will see later, from a finite element implementation point of view, it is much more elegant to evaluate the remaining electric displacement resultants ($\vec{M}^e$, $\vec{M}_1^e$ and $\vec{O}^e$) in a similar form to $\vec{Q}^e$ i.e. separate kinematical variables in vector form and the constitutive parameters in tensor form. To this end, we can redo (3.21) with a view to find the explicit forms of these electric displacement resultants. In fact, the electric displacement resultants arise naturally in the desired form if we directly substitute for the values of $\vec{D}$ and $\nabla\delta\psi$ in the first line of (3.21). While it is equally possible to evaluate these resultants from (3.21), what is followed here is only for the purpose of a convenient presentation.

$$
\begin{aligned}
\delta W_{int}^e &= \int_V \vec{D}\nabla\delta\psi \ \mathrm{d}\Omega \\[4pt]
&= -\int_V \left\{ \boldsymbol{\epsilon}\left[\boldsymbol{I}\vec{\epsilon}^e + (\vec{e}_3\otimes\vec{p})\vec{\kappa}^e + \boldsymbol{A}_1\vec{\gamma} + \boldsymbol{A}_2\vec{\varsigma} \right] - \boldsymbol{A}_3\vec{\epsilon} - \boldsymbol{A}_4\vec{\kappa} \right\} \\[4pt]
&\quad \cdot \left\{ \boldsymbol{I}\delta\vec{\epsilon}^e + (\vec{e}_3\otimes\vec{p})\delta\vec{\kappa}^e + \boldsymbol{A}_1\delta\vec{\gamma} + \boldsymbol{A}_2\delta\vec{\varsigma} \right\}\mathrm{d}\Omega \\[4pt]
&= -\int_l\int_A \delta\vec{\epsilon}^e\left\{ \boldsymbol{\epsilon}\left[\boldsymbol{I}\vec{\epsilon}^e + (\vec{e}_3\otimes\vec{p})\vec{\kappa}^e + \boldsymbol{A}_1\vec{\gamma} + \boldsymbol{A}_2\vec{\varsigma} \right] - \boldsymbol{A}_3\vec{\epsilon} - \boldsymbol{A}_4\vec{\kappa} \right\}\mathrm{d}A\mathrm{d}x_3 \\[4pt]
&\quad - \int_l\int_A \delta\vec{\kappa}^e(\vec{p}\otimes\vec{e}_3)\left\{ \boldsymbol{\epsilon}\left[\boldsymbol{I}\vec{\epsilon}^e + (\vec{e}_3\otimes\vec{p})\vec{\kappa}^e + \boldsymbol{A}_1\vec{\gamma} + \boldsymbol{A}_2\vec{\varsigma} \right] - \boldsymbol{A}_3\vec{\epsilon} - \boldsymbol{A}_4\vec{\kappa} \right\}\mathrm{d}A\mathrm{d}x_3 \\[4pt]
&\quad - \int_l\int_A \delta\vec{\gamma}\boldsymbol{A}_1^T\left\{ \boldsymbol{\epsilon}\left[\boldsymbol{I}\vec{\epsilon}^e + (\vec{e}_3\otimes\vec{p})\vec{\kappa}^e + \boldsymbol{A}_1\vec{\gamma} + \boldsymbol{A}_2\vec{\varsigma} \right] - \boldsymbol{A}_3\vec{\epsilon} - \boldsymbol{A}_4\vec{\kappa} \right\}\mathrm{d}A\mathrm{d}x_3 \\[4pt]
&\quad - \int_l\int_A \delta\vec{\varsigma}\boldsymbol{A}_2^T\left\{ \boldsymbol{\epsilon}\left[\boldsymbol{I}\vec{\epsilon}^e + (\vec{e}_3\otimes\vec{p})\vec{\kappa}^e + \boldsymbol{A}_1\vec{\gamma} + \boldsymbol{A}_2\vec{\varsigma} \right] - \boldsymbol{A}_3\vec{\epsilon} - \boldsymbol{A}_4\vec{\kappa} \right\}\mathrm{d}A\mathrm{d}x_3 \\[4pt]
&= \int_l \delta\vec{\epsilon}^e\cdot\vec{Q}^e \ \mathrm{d}x_3 + \int_l \delta\vec{\kappa}^e\cdot\left[\mathbf{S}_4^{e^T}\vec{\epsilon}^e + \mathbf{I}_5^e\vec{\kappa}^e + \mathbf{I}_6^e\vec{\gamma} + \mathbf{G}_2^e\vec{\varsigma} - \mathbf{S}_1^{e^T}\vec{\epsilon} - \mathbf{I}_2^{e^T}\vec{\kappa} \right] \ \mathrm{d}x_3 \\[4pt]
&\quad + \int_l \delta\vec{\gamma}\cdot\left[\mathbf{S}_5^{e^T}\vec{\epsilon}^e + \mathbf{I}_6^{e^T}\vec{\kappa}^e + \mathbf{I}_7^e\vec{\gamma} + \mathbf{G}_3^e\vec{\varsigma} - \mathbf{S}_2^{e^T}\vec{\epsilon} - \mathbf{I}_3^{e^T}\vec{\kappa} \right] \ \mathrm{d}x_3 \\[4pt]
&\quad + \int_l \delta\vec{\varsigma}\cdot\left[\mathbf{I}_4^{e^T}\vec{\epsilon}^e + \mathbf{G}_2^{e^T}\vec{\kappa}^e + \mathbf{G}_3^{e^T}\vec{\gamma} + \mathbf{J}^e\vec{\varsigma} - \mathbf{I}_1^{e^T}\vec{\epsilon} - \mathbf{G}_1^{e^T}\vec{\kappa} \right] \ \mathrm{d}x_3 \\[4pt]
&= \int_l \left(\delta\vec{\epsilon}^e\cdot\vec{Q}^e + \delta\vec{\kappa}^e\cdot\vec{M}^e + \delta\vec{\gamma}^e\cdot\vec{M}_1^e + \delta\vec{\varsigma}\cdot\vec{O}^e \right) \ \mathrm{d}x_3
\end{aligned}
\tag{3.22}
$$

where.

$$
-\vec{M}^e = \mathbf{S}_4^{e^T}\vec{\epsilon}^e + \mathbf{I}_5^e\vec{\kappa}^e + \mathbf{I}_6^e\vec{\gamma} + \mathbf{G}_2^e\vec{\varsigma} - \mathbf{S}_1^{e^T}\vec{\epsilon} - \mathbf{I}_2^{e^T}\vec{\kappa} \tag{3.23}
$$

$$
-\vec{M}_1^e = \mathbf{S}_5^{e^T}\vec{\epsilon}^e + \mathbf{I}_6^{e^T}\vec{\kappa}^e + \mathbf{I}_7^e\vec{\gamma} + \mathbf{G}_3^e\vec{\varsigma} - \mathbf{S}_2^{e^T}\vec{\epsilon} - \mathbf{I}_3^{e^T}\vec{\kappa} \tag{3.24}
$$

$$
-\vec{O}^e = \mathbf{I}_4^{e^T}\vec{\epsilon}^e + \mathbf{G}_2^{e^T}\vec{\kappa}^e + \mathbf{G}_3^{e^T}\vec{\gamma} + \mathbf{J}^e\vec{\varsigma} - \mathbf{I}_1^{e^T}\vec{\epsilon} - \mathbf{G}_1^{e^T}\vec{\kappa} \tag{3.25}
$$

In the above expressions $\mathbf{G}_i^e$ are all second order tensors with their entries being third moments of area. Similarly, the only second order tensor $\mathbf{J}$ contains of fourth moments of area.

While it is mathematically possible to define higher order moments of area, it is difficult to intrepret these entities physically [for a detailed discussion on this see for instance [27]]. The explicit form of these tensors are given in 1.1.6. From above expressions we can conjecture the final computational cost that this formulation entails when finite elements are employed. If the material and geometric properties remain unchanged along the length of the beam, then we can compute all these constitutive tensors only once. Also, by choosing coordinate axis x_3 to coincide with the principal axis of the beam, first and third moments of area vanish and the reduced moment resultants become.

$$\vec{M^e} = \mathbf{I}_2^{e^T}\vec{\kappa} - \mathbf{I}_5^e\vec{\kappa^e} - \mathbf{I}_6^e\vec{\gamma} \tag{3.26}$$

$$\vec{M_1^e} = \mathbf{I}_3^{e^T}\vec{\kappa} - \mathbf{I}_6^{e^T}\vec{\kappa^e} - \mathbf{I}_7^e\vec{\gamma} \tag{3.27}$$

$$\vec{O^e} = \mathbf{I}_1^{e^T}\vec{\epsilon} - \mathbf{I}_4^{e^T}\vec{\epsilon^e} - \mathbf{J}^e\vec{\varsigma} \tag{3.28}$$

We are now left with the weak form of boundary terms. Proceeding from the last line of (3.20) we have.

$$
\begin{aligned}
\delta W_{ext}^e &= \int_A \int_l \frac{\partial(D_3\delta\psi)}{\partial x_3}\,\mathrm{d}x\mathrm{d}A + \int_l \int_A \sum_{\alpha=1,2}\frac{\partial(D_\alpha\delta\psi)}{\partial x_\alpha}\,\mathrm{d}A\mathrm{d}x - \int_V q^e\delta\psi\,\mathrm{d}\Omega \\
&= \int_A \left(D_3\delta\psi\right)\Big|_{\Gamma^\psi}\mathrm{d}A + \int_l\int_\Gamma \sum_{\alpha=1,2}D_\alpha\vec{n}_{\Gamma_\alpha}\delta\psi\,\mathrm{d}s\mathrm{d}x_3 - \int_l\int_A q^e\delta\psi\mathrm{d}A\mathrm{d}x_3 \\
&= \int_A D_3\left(\delta\phi + \vec{p}\cdot\delta\vec{\beta} + \frac{1}{2}\vec{s}\cdot\delta\vec{\gamma}\right)\Big|_{\Gamma^\psi}\mathrm{d}A + \int_l \delta\phi\left(\int_\Gamma \sum_{\alpha=1,2}D_\alpha\vec{n}_{\Gamma_\alpha}\,\mathrm{d}s - \int_A q^e\,\mathrm{d}A\right)\mathrm{d}x_3 \\
&\quad + \int_l \delta\vec{\beta}\cdot\left(\int_\Gamma \sum_{\alpha=1,2}\vec{p}D_\alpha\vec{n}_{\Gamma_\alpha}\vec{e}_\alpha\,\mathrm{d}s - \int_A \vec{p}q^e\,\mathrm{d}A\right)\mathrm{d}x_3 \\
&\quad + \int_l \delta\vec{\gamma}\cdot\frac{1}{2}\left(\int_\Gamma \sum_{\alpha=1,2}\vec{s}D_\alpha\vec{n}_{\Gamma_\alpha}\vec{e}_\alpha\,\mathrm{d}s - \int_A \vec{s}q^e\,\mathrm{d}A\right)\mathrm{d}x_3 \\
&= (\delta\phi r_0)\Big|_{\Gamma^e} + (\delta\vec{\beta}\cdot\vec{m_0^e})\Big|_{\Gamma^e} + (\delta\vec{\gamma}\cdot\vec{o_0^e})\Big|_{\Gamma^e} \\
&\quad + \int_l \delta\phi r\,\mathrm{d}x_3 + \int_l \delta\vec{\beta}\cdot\vec{m^e}\,\mathrm{d}x_3 + \int_l \delta\vec{\gamma}\cdot\vec{o^e}\,\mathrm{d}x_3
\end{aligned}
\tag{3.29}
$$

Where r_0 is the resultant free charge which is applied as Neumann boundary condition in our boundary value problem and $\vec{m_0^e}$ and $\vec{o_0^e}$ are specified first and second moments of such resultant, respectively. These quantities are similar to specified point forces and moments. The quantities inside the integral are the distributed counterparts of the earlier boundary conditions i.e. distributed free charge over the lateral surface of the beam and its first and second moments, respectively. The region Γ^e corresponds to "points" where resultant free charge and/or its moments is applied, where a superscript e stands for electrical. The virtual

work of piezoelectric system is now complete and can be summed up as.

$$
\begin{aligned}
\delta W &= \delta W_{iner} + \delta W_{int}^m + \delta W_{int}^e - \delta W_{ext}^m - \delta W_{ext}^e \\
&= \frac{D^2}{Dt^2}\left\{ \int_l \delta\vec{w} \cdot \mathbf{A}_D \vec{w} \, \mathrm{d}x_3 + \int_l \delta\vec{\theta} \cdot \mathbf{I}_D \vec{\theta} \, \mathrm{d}x_3 \right\} \\
&\quad + \int_l \left(\vec{Q} \cdot \delta\vec{\epsilon} + \vec{M} \cdot \delta\vec{\kappa} + \vec{Q}^e \cdot \delta\vec{\epsilon}^e + \vec{M}^e \cdot \delta\vec{\kappa}^e + \vec{M}_1^e \cdot \delta\vec{\gamma} + \vec{O}^e \cdot \delta\vec{\varsigma} \right) \mathrm{d}x_3 \\
&\quad - \left[\int_l \delta\vec{w} \cdot \vec{q} \, \mathrm{d}x_3 + \int_l \delta\vec{\theta} \cdot \vec{m} \, \mathrm{d}x_3 + \int_l \delta\phi r \, \mathrm{d}x_3 + \int_l \delta\vec{\beta} \cdot \vec{m}^e \, \mathrm{d}x_3 + \int_l \delta\vec{\gamma} \cdot \vec{o}^e \, \mathrm{d}x_3 \right] \\
&\quad - \left[(\delta\vec{w} \cdot \vec{q}_0)\Big|_{\Gamma^m} + (\delta\vec{\theta} \cdot \vec{m}_0)\Big|_{\Gamma^m} + (\delta\phi r_0)\Big|_{\Gamma^e} + (\delta\vec{\beta} \cdot \vec{m}_0^e)\Big|_{\Gamma^e} + (\delta\vec{\gamma} \cdot \vec{o}_0^e)\Big|_{\Gamma^e} \right] = 0 \quad (3.30)
\end{aligned}
$$

Expression (3.30) completely describes the virtual work of our piezoelectric three-dimensional beam model. If we refer back to where we started i.e. (3.10), we identify that the last two terms in this expression have not entered in our virtual work expression, namely the variation of traction forces and the variational form of applied surface charges, both of which are area integrals. This is because the equivalent form of these expressions naturally arise while reducing the three dimensional boundary value problem to the one dimensional boundary value problem of beams.

3.1.   The Choice of Linear Electric Potential

The similitude between piezoelectric beam and a purely mechanical beam is more pronounced if we assume a linear electric potential across the area directions. Although as explained in chapter 1. this assumption violates Gauss's law [48] [9] and will not be pursued in this work, the piezoelectric beam formulated in the earlier sections is best understood with this assumption and in fact it is fascinating to observe that we have not deviated ourselves much to reformulate the problem. The corresponding equations and expressions evolving from the choice of linear electric potential can be deduced from what we have presented so far. To this view, let us reconsider the electric potential but upto linear term this time.

$$
\psi(\vec{x}) = \phi(x_3) + \vec{p}(x_1, x_2) \cdot \vec{\beta}(x_3) \tag{3.31}
$$

The electric field vector emerging from the gradient of this potential becomes,

$$
\begin{aligned}
\vec{E} = -\nabla\psi(\vec{x}) &= -\left(\frac{d\phi}{dx_3} + \frac{d\vec{\beta}}{dx_3} \cdot \vec{p} \right)\vec{e}_3 - \sum_{\alpha=1,2} \left(\vec{e}_\alpha \cdot \vec{\beta} \right)\vec{e}_\alpha \\
&= -\left[\frac{d\phi}{dx_3}(\vec{e}_3 \otimes \vec{e}_3)\vec{e}_3 + \sum_{\alpha=1,2} \vec{\beta}(\vec{e}_\alpha \otimes \vec{e}_\alpha) \right] - \left[(\vec{e}_3 \otimes \vec{p})\frac{d\vec{\beta}}{dx_3} \right] \\
&= -\boldsymbol{I}\vec{\epsilon}^e - (\vec{e}_3 \otimes \vec{p})\vec{\kappa}^e \tag{3.32}
\end{aligned}
$$

where $\vec{\epsilon}^e$ and $\vec{\kappa}^e$ are given by (2.16) and (2.17). If we now evaluate stress resultants based on our new electrical kinematics assuming the coordinate axis x_3 to coincide with the principal

axis of the beam, we find.

$$\vec{Q} = \mathbf{A}^m\vec{\epsilon} + \mathbf{A}_1^e\vec{\epsilon^e} \tag{3.33}$$

$$\vec{Q^e} = \mathbf{A}_1^{e^T}\vec{\epsilon} - \mathbf{A}_2^e\vec{\epsilon^e} \tag{3.34}$$

$$\vec{M} = \mathbf{I}^m\vec{\kappa} + \mathbf{I}_2^e\vec{\kappa^e} \tag{3.35}$$

$$\vec{M^e} = \mathbf{I}_2^{e^T}\vec{\kappa} - \mathbf{I}_5^e\vec{\kappa^e} \tag{3.36}$$

In the above expressions only terms having $\vec{\gamma}$ and $\vec{\varsigma}$ have disappeared and the remaining constitutive matrices are exactly the same as before. At this stage, we can clearly identify the similarity between electromechanical and mechanical stress resultants. Certainly, the coupled formulation also seems more elegant this way, in that, each resultant is a function of both mechanical kinematics and its electrical counterpart, either translational ones or rotational ones but not both. Finally, the virtual work expression based on linear electrical potential assumption takes the form.

$$\begin{aligned}
\delta W = {}& \delta W_{iner} + \delta W_{int}^m + \delta W_{int}^e - \delta W_{ext}^m - \delta W_{ext}^e \\
= {}& \frac{D^2}{Dt^2}\left\{ \int_l \delta\vec{w} \cdot \mathbf{A}_D\vec{w}\,\mathrm{d}x_3 + \int_l \delta\vec{\theta} \cdot \mathbf{I}_D\vec{\theta}\,\mathrm{d}x_3 \right\} \\
& + \int_l \left(\vec{Q} \cdot \delta\vec{\epsilon} + \vec{M} \cdot \delta\vec{\kappa} + \vec{Q^e} \cdot \delta\vec{\epsilon^e} + \vec{M^e} \cdot \delta\vec{\kappa^e} \right)\,\mathrm{d}x_3 \\
& - \left[\int_l \delta\vec{w} \cdot \vec{q}\,\mathrm{d}x_3 + \int_l \delta\vec{\theta} \cdot \vec{m}\,\mathrm{d}x_3 + \int_l \delta\phi r\,\mathrm{d}x_3 + \int_l \delta\vec{\beta} \cdot \vec{m^e}\,\mathrm{d}x_3 \right] \\
& - \left[(\delta\vec{w} \cdot \vec{q_0})\Big|_{\Gamma^m} + (\delta\vec{\theta} \cdot \vec{m_0})\Big|_{\Gamma^m} + (\delta\phi r_0)\Big|_{\Gamma^e} + (\delta\vec{\beta} \cdot \vec{m_0^e})\Big|_{\Gamma^e} \right] = 0 \tag{3.37}
\end{aligned}$$

Higher Order Finite Elements

"Students and research visitors to Swansea were frequently roped in to act as crew,
but all competitive instincts during a race would be quickly abandoned if
a particularly interesting finite element discussion arose."
D. R. J. Owen on O. C. Zienkiewicz

4.   The Finite Element Discretisation

The finite element equations of three-dimensional beam model can be obtained directly from (3.30) of chapter 3. The weak form of the problem can now be stated as:

Find $[\vec{w}, \vec{\theta}, \phi, \vec{\beta}, \vec{\gamma}] \in \vec{U}$ such that

$$
\frac{D^2}{Dt^2}\left\{ \int_l \delta\vec{w} \cdot \mathbf{A}_D \vec{w} \, dx_3 + \int_l \delta\vec{\theta} \cdot \mathbf{I}_D \vec{\theta} \, dx_3 \right\}
$$

$$
+ \int_l \left(\vec{Q} \cdot \delta\vec{\epsilon} + \vec{M} \cdot \delta\vec{\kappa} + \vec{Q}^e \cdot \delta\vec{\epsilon}^e + \vec{M}^e \cdot \delta\vec{\kappa}^e + \vec{M}^e_1 \cdot \delta\vec{\gamma} + \vec{O}^e \cdot \delta\vec{\varsigma} \right) dx_3
$$

$$
- \left[\int_l \delta\vec{w} \cdot \vec{q} \, dx_3 + \int_l \delta\vec{\theta} \cdot \vec{m} \, dx_3 + \int_l \delta\phi r \, dx_3 + \int_l \delta\vec{\beta} \cdot \vec{m}^e \, dx_3 + \int_l \delta\vec{\gamma} \cdot \vec{o}^e \, dx_3 \right]
$$

$$
- \left[(\delta\vec{w} \cdot \vec{q}_0)\Big|_{\Gamma^m} + (\delta\vec{\theta} \cdot \vec{m}_0)\Big|_{\Gamma^m} + (\delta\phi r_0)\Big|_{\Gamma^e} \right.
$$

$$
\left. + (\delta\vec{\beta} \cdot \vec{m}^e_0)\Big|_{\Gamma^e} + (\delta\vec{\gamma} \cdot \vec{o}^e_0)\Big|_{\Gamma^e} \right] = 0 \qquad \forall \quad [\delta\vec{w}, \delta\vec{\theta}, \delta\phi, \delta\vec{\beta}, \delta\vec{\gamma}] \in \vec{U}_0 \qquad (4.1)
$$

where,

$$
\vec{U} = \left\{ \vec{u} \in \left(\boldsymbol{H^1} \right)^{11} \mid \vec{u} = \vec{u}_D \quad \text{on} \quad \partial\Omega_D \right\} \tag{4.2}
$$

$$
\vec{U}_0 = \left\{ \delta\vec{u} \in \left(\boldsymbol{H^1} \right)^{11} \mid \delta\vec{u} = \boldsymbol{0} \quad \text{on} \quad \partial\Omega_D \right\} \tag{4.3}
$$

where $\partial\Omega_D$ now represents the boundary where all Dirichlet boundary conditions are applied and $\boldsymbol{H^1}$ is the standard vectorial Sobolev space with a superscript 11 standing for number unknowns. If we introduce the $\boldsymbol{H^1}$-conforming set of interpolating functions as,

$$
\vec{X}_{hp} = \left\{ N_1, \, N_2, \, N_3, \, N_4, ..., N_n \right\} \subset \boldsymbol{H^1}
$$

where n stands for number of nodes per element, then, with a slight abuse of notation, describing the discretised variables with the same symbols, the semi-discrete weak form of the problem can be stated as:

Find $[\vec{w}, \vec{\theta}, \phi, \vec{\beta}, \vec{\gamma}] \in \vec{U} \cap \vec{Y}_{hp}$ such that,

$$
\frac{D^2}{Dt^2} \left\{ \int_l \delta\vec{w} \cdot \mathbf{A}_D \vec{w} \, dx_3 + \int_l \delta\vec{\theta} \cdot \mathbf{I}_D \vec{\theta} \, dx_3 \right\}
$$

$$
+ \int_l \left(\vec{Q} \cdot \delta\vec{\epsilon} + \vec{M} \cdot \delta\vec{\kappa} + \vec{Q}^e \cdot \delta\vec{\epsilon}^e + \vec{M}^e \cdot \delta\vec{\kappa}^e + \vec{M}_1^e \cdot \delta\vec{\gamma} + \vec{O}^e \cdot \delta\vec{\varsigma} \right) dx_3
$$

$$
- \left[\int_l \delta\vec{w} \cdot \vec{q} \, dx_3 + \int_l \delta\vec{\theta} \cdot \vec{m} \, dx_3 + \int_l \delta\phi r \, dx_3 + \int_l \delta\vec{\beta} \cdot \vec{m}^e \, dx_3 + \int_l \delta\vec{\gamma} \cdot \vec{o}^e \, dx_3 \right]
$$

$$
- \left[(\delta\vec{w} \cdot \vec{q}_0) \Big|_{\Gamma^m} + (\delta\vec{\theta} \cdot \vec{m}_0) \Big|_{\Gamma^m} + (\delta\phi r_0) \Big|_{\Gamma^e} \right.
$$

$$
\left. + (\delta\vec{\beta} \cdot \vec{m}_0^e) \Big|_{\Gamma^e} + (\delta\vec{\gamma} \cdot \vec{o}_0^e) \Big|_{\Gamma^e} \right] = \mathbf{0} \qquad \forall \ [\delta\vec{w}, \delta\vec{\theta}, \delta\phi, \delta\vec{\beta}, \delta\vec{\gamma}] \in \vec{U}_0 \cap \vec{Y}_{hp} \qquad (4.4)
$$

where,

$$
\vec{Y}_{hp} = \left\{ \vec{u} \mid \vec{u} \in \left(\vec{X}_{hp} \right)^{11} \right\} \qquad (4.5)
$$

From above it is evident that we use the same basis for all the nodal unknowns i.e. equal polynomial degree interpolation for mechanical translations and rotations as well as for electric potentials and their gradients and hessians,

$$
w_k = \sum_{i=1}^{n} N^i w_k^i \qquad\qquad \theta_k = \sum_{i=1}^{n} N^i \theta_k^i \qquad (4.6)
$$

$$
\phi = \sum_{i=1}^{n} N^i \phi^i \qquad \beta_j = \sum_{i=1}^{n} N^i \beta_j^i \qquad \gamma_j = \sum_{i=1}^{n} N^i \gamma_j^i \qquad (4.7)
$$

where $k = 1, 2, 3$ represents the direction of mechanical nodal variables and $j = 1, 2$ represents the direction of nodal electric potential gradient and hessian. We utilise both higher order Lagrangian and hierarchical Legendre basis functions and examine the relative performance of each. The primary unkowns of a 2-noded beam (i.e. when linear basis functions are employed) are.

$$
\vec{w} = [w_1, w_2, w_3, w_4, w_5, w_6]^T \qquad (4.8)
$$

$$
\vec{\theta} = [\theta_1, \theta_2, \theta_3, \theta_4, \theta_5, \theta_6]^T \qquad (4.9)
$$

$$
\vec{\psi} = [\beta_2, \beta_1, \phi_1, \gamma_2, \gamma_1, \beta_4, \beta_3, \phi_2, \gamma_4, \gamma_3]^T \qquad (4.10)
$$

The finite element matrices arising from the semi-discrete virtual work of inertial, internal and external forces, correspond to the following integrands, respectively.

$$
[\vec{\delta w} \quad \vec{\delta \theta}]
\begin{bmatrix}
\mathbf{A}_D & \mathbf{S}_D \\
\mathbf{S}_D^T & \mathbf{I}_D
\end{bmatrix}
\begin{bmatrix}
\vec{w} \\
\vec{\theta}
\end{bmatrix}
\tag{4.11}
$$

$$
[\vec{\delta \epsilon} \ \vec{\delta \kappa} \ \vec{\delta \epsilon^e} \ \vec{\delta \kappa^e} \ \vec{\delta \gamma} \ \vec{\delta \varsigma}]
\begin{bmatrix}
\mathbf{A}^m & \mathbf{S}^m & \mathbf{A}_1^e & \mathbf{S}_1^e & \mathbf{S}_2^e & \mathbf{I}_1^e \\
 & \mathbf{I}^m & \mathbf{S}_3^e & \mathbf{I}_2^e & \mathbf{I}_3^e & \mathbf{G}_1^e \\
 & & -\mathbf{A}_2^e & -\mathbf{S}_4^e & -\mathbf{S}_5^e & -\mathbf{I}_4^e \\
 & & & -\mathbf{I}_5^e & -\mathbf{I}_6^e & -\mathbf{G}_2^e \\
 & & & & -\mathbf{I}_7^e & -\mathbf{G}_3^e \\
 sym & & & & & -\mathbf{J}
\end{bmatrix}
\begin{bmatrix}
\vec{\epsilon} \\
\vec{\kappa} \\
\vec{\epsilon^e} \\
\vec{\kappa^e} \\
\vec{\gamma} \\
\vec{\varsigma}
\end{bmatrix}
\tag{4.12}
$$

$$
[\vec{\delta w} \ \vec{\delta \theta} \ \delta \phi \ \vec{\delta \beta} \ \vec{\delta \gamma}]
\begin{bmatrix}
\vec{q} \\
\vec{m} \\
r \\
\vec{m^e} \\
\vec{o^e}
\end{bmatrix}
\tag{4.13}
$$

$$
\left\{ [\vec{\delta w} \ \vec{\delta \theta} \ \delta \phi \ \vec{\delta \beta} \ \vec{\delta \gamma}]
\begin{bmatrix}
\vec{q_0} \\
\vec{m_0} \\
r_0 \\
\vec{m_0^e} \\
\vec{o_0^e}
\end{bmatrix}
\right\} \Bigg|_{\Gamma^m \cup \Gamma^e}
\tag{4.14}
$$

If we were to look at (4.12) with an eye on the explicit form of matrices presented in 1.1.6. then vectors $\vec{\kappa^e}$, $\vec{\gamma}$ and $\vec{\varsigma}$ should have three components with their third component being zero and hence the 18×18 matrix in this equation which we will shortly call it H, would have some zero elments corresponding to these entries [which can be verified from 1.1.6.]. In fact the H matrix has three rows and columns with zero entries which can be eliminated at this level. This will give the desired 15×15 coupled electromechanical constitutive matrix. To continue building the semi-discrete finite element equations let us group some quantities

and name them.

$$\boldsymbol{H}_D = \begin{bmatrix} \mathbf{A}_D & \mathbf{S}_D \\ \mathbf{S}_D^T & \mathbf{I}_D \end{bmatrix} \tag{4.15}$$

$$\boldsymbol{H} = \begin{bmatrix} \mathbf{A}^m & \mathbf{S}^m & \mathbf{A}_1^e & \mathbf{S}_1^e & \mathbf{S}_2^e & \mathbf{I}_1^e \\ & \mathbf{I}^m & \mathbf{S}_3^e & \mathbf{I}_2^e & \mathbf{I}_3^e & \mathbf{G}_1^e \\ & & -\mathbf{A}_2^e & -\mathbf{S}_4^e & -\mathbf{S}_5^e & -\mathbf{I}_4^e \\ & & & -\mathbf{I}_5^e & -\mathbf{I}_6^e & -\mathbf{G}_2^e \\ & & & & -\mathbf{I}_7^e & -\mathbf{G}_3^e \\ sym & & & & & -\mathbf{J} \end{bmatrix} \tag{4.16}$$

$$\vec{v}_b = \begin{bmatrix} \vec{q} \\ \vec{m} \\ r \\ \vec{m}^e \\ \vec{o}^e \end{bmatrix} \tag{4.17}$$

$$\vec{v}_t = \begin{bmatrix} \vec{q}_0 \\ \vec{m}_0 \\ r_0 \\ \vec{m}_0^e \\ \vec{o}_0^e \end{bmatrix} \tag{4.18}$$

The zero component of vectors $\vec{\kappa}^e$, $\vec{\gamma}$ and $\vec{\zeta}$ are now excluded and $\boldsymbol{H}$ is a 15×15 matrix. The finite element matrices can now be written as,

$$\boldsymbol{M}^e = \frac{l_e}{2} \int_{l_e} \boldsymbol{N}_D^T \boldsymbol{H}_D \boldsymbol{N}_D \ \mathrm{d}x_3 \tag{4.19}$$

$$\boldsymbol{K}^e = \frac{l_e}{2} \int_{l_e} \boldsymbol{B}^T \boldsymbol{H} \boldsymbol{B} \ \mathrm{d}x_3 \tag{4.20}$$

$$\vec{F}_b^e = \frac{l_e}{2} \int_{l_e} \boldsymbol{N}^T \vec{v}_b \ \mathrm{d}x_3 \tag{4.21}$$

$$\vec{F}_t^e = \left[\boldsymbol{N}^T \vec{v}_t \right]_{\Gamma^m \cup \Gamma^e} \tag{4.22}$$

where

$$\boldsymbol{N}_D = \underbrace{\begin{bmatrix} N_1 & 0 & 0 & 0 & 0 & 0 & N_2 & 0 & 0 & 0 & 0 & 0 \\ 0 & N_1 & 0 & 0 & 0 & 0 & 0 & N_2 & 0 & 0 & 0 & 0 \\ 0 & 0 & N_1 & 0 & 0 & 0 & 0 & 0 & N_2 & 0 & 0 & 0 \\ 0 & 0 & 0 & N_1 & 0 & 0 & 0 & 0 & 0 & N_2 & 0 & 0 \\ 0 & 0 & 0 & 0 & N_1 & 0 & 0 & 0 & 0 & 0 & N_2 & 0 \\ 0 & 0 & 0 & 0 & 0 & N_1 & 0 & 0 & 0 & 0 & 0 & N_2 \end{bmatrix}}_{6 \times 12} \tag{4.23}$$

and $\boldsymbol{B}$ and $\boldsymbol{N}$ are given by (4.24) and (4.25), respectively.

$$\boldsymbol{B} = \begin{bmatrix}
\frac{dN_1}{d\zeta}\frac{2}{l_e} & 0 & 0 & 0 & 0 & 0 & 0 & 0 & 0 & 0 & 0 & 0 & 0 & 0 & 0 & 0 & 0 & 0 & 0 & 0 & 0 & 0 \\
0 & \frac{dN_1}{d\zeta}\frac{2}{l_e} & 0 & 0 & 0 & 0 & 0 & 0 & 0 & 0 & 0 & 0 & 0 & 0 & 0 & 0 & 0 & 0 & 0 & 0 & 0 & 0 \\
0 & 0 & \frac{dN_1}{d\zeta}\frac{2}{l_e} & 0 & 0 & 0 & 0 & 0 & 0 & 0 & 0 & 0 & 0 & 0 & 0 & 0 & 0 & 0 & 0 & 0 & 0 & 0 \\
0 & N_1 & 0 & 0 & \frac{dN_1}{d\zeta}\frac{2}{l_e} & 0 & 0 & 0 & 0 & 0 & 0 & 0 & 0 & 0 & 0 & 0 & 0 & 0 & 0 & 0 & 0 & 0 \\
-N_1 & 0 & 0 & 0 & \frac{dN_1}{d\zeta}\frac{2}{l_e} & 0 & 0 & 0 & 0 & 0 & 0 & 0 & 0 & 0 & 0 & 0 & 0 & 0 & 0 & 0 & 0 & 0 \\
& & & & & \frac{dN_1}{d\zeta}\frac{2}{l_e} & & & & & & & & & & & & & & & & \\
N_1 & 0 & 0 & \frac{dN_1}{d\zeta}\frac{2}{l_e} & 0 & & & & & & & & & & & & & & & & & \\
0 & N_1 & 0 & 0 & \frac{dN_1}{d\zeta}\frac{2}{l_e} & 0 & & & & & & & & & & & & & & & & \\
& & & \frac{dN_1}{d\zeta}\frac{2}{l_e} & & & & & & & & & & & & & & & & & & \\
0 & 0 & N_1 & 0 & 0 & \frac{dN_1}{d\zeta}\frac{2}{l_e} & 0 & & & & & & & & & & & & & & & \\
\end{bmatrix}_{15\times 22}$$

$$(4.24)$$

$$
\boldsymbol{N} =
\begin{bmatrix}
N_1 & 0 & 0 & 0 & 0 & 0 & 0 & 0 & 0 & 0 & 0 & N_2 & 0 & 0 & 0 & 0 & 0 & 0 & 0 & 0 & 0 & 0 \\
0 & N_1 & 0 & 0 & 0 & 0 & 0 & 0 & 0 & 0 & 0 & 0 & N_2 & 0 & 0 & 0 & 0 & 0 & 0 & 0 & 0 & 0 \\
0 & 0 & N_1 & 0 & 0 & 0 & 0 & 0 & 0 & 0 & 0 & 0 & 0 & N_2 & 0 & 0 & 0 & 0 & 0 & 0 & 0 & 0 \\
0 & 0 & 0 & N_1 & 0 & 0 & 0 & 0 & 0 & 0 & 0 & 0 & 0 & 0 & N_2 & 0 & 0 & 0 & 0 & 0 & 0 & 0 \\
0 & 0 & 0 & 0 & N_1 & 0 & 0 & 0 & 0 & 0 & 0 & 0 & 0 & 0 & 0 & N_2 & 0 & 0 & 0 & 0 & 0 & 0 \\
0 & 0 & 0 & 0 & 0 & N_1 & 0 & 0 & 0 & 0 & 0 & 0 & 0 & 0 & 0 & 0 & N_2 & 0 & 0 & 0 & 0 & 0 \\
0 & 0 & 0 & 0 & 0 & 0 & N_1 & 0 & 0 & 0 & 0 & 0 & 0 & 0 & 0 & 0 & 0 & N_2 & 0 & 0 & 0 & 0 \\
0 & 0 & 0 & 0 & 0 & 0 & 0 & N_1 & 0 & 0 & 0 & 0 & 0 & 0 & 0 & 0 & 0 & 0 & N_2 & 0 & 0 & 0 \\
0 & 0 & 0 & 0 & 0 & 0 & 0 & 0 & N_1 & 0 & 0 & 0 & 0 & 0 & 0 & 0 & 0 & 0 & 0 & N_2 & 0 & 0 \\
0 & 0 & 0 & 0 & 0 & 0 & 0 & 0 & 0 & N_1 & 0 & 0 & 0 & 0 & 0 & 0 & 0 & 0 & 0 & 0 & N_2 & 0 \\
0 & 0 & 0 & 0 & 0 & 0 & 0 & 0 & 0 & 0 & N_1 & 0 & 0 & 0 & 0 & 0 & 0 & 0 & 0 & 0 & 0 & N_2
\end{bmatrix}_{11\times22}
\tag{4.25}
$$

Analytical Solution of Planar Piezoelectric Beams

> *"Although I am a computational mechanician, but I often say:*
> *A good closed form solution is worth a thousand of computations."*
> *Ted Belytschko*

5. Analytical Solution of Planar Piezoelectric Beams

5.1. Governing Equations of Planar Piezoelectric Beam

In this chapter, we solve the two-dimensional piezoelectric beam problem outlined in the earlier chapters, analytically. If we consider the hessian of electric potential γ, i.e. a quadratic distribtution of electric potential across the thickness, then the system of equations consists of five ordinary differential equations (2.58)-(2.62), where the unknown variables are stress and electric displacement resultants. Knowing that,

$$\vec{Q} = \mathbf{A}\vec{\epsilon} + \mathbf{A}_1^e \vec{\epsilon^e} + \mathbf{I}_1^e \vec{\varsigma}$$

$$\vec{M} = \mathbf{I}\vec{\kappa} + \mathbf{I}_2^e \vec{\kappa^e} + \mathbf{I}_3^e \vec{\gamma}$$

$$\vec{Q^e} = \mathbf{A}_1^{e^T} \vec{\epsilon} - \mathbf{A}_2^e \vec{\epsilon^e} - \mathbf{I}_4^e \vec{\varsigma}$$

$$\vec{M^e} = \mathbf{I}_2^{e^T} \vec{\kappa} - \mathbf{I}_5^e \vec{\kappa^e} - \mathbf{I}_6^e \vec{\gamma}$$

$$\vec{M_1^e} = \mathbf{I}_3^{e^T} \vec{\kappa} - \mathbf{I}_6^{e^T} \vec{\kappa^e} - \mathbf{I}_7^e \vec{\gamma}$$

$$\vec{O^e} = \mathbf{I}_1^{e^T} \vec{\epsilon} - \mathbf{I}_4^{e^T} \vec{\epsilon^e} - \mathbf{J}^e \vec{\varsigma}$$

and that distributed moments are merely mathematical entities, referring to Appendix 1 for the explicit forms of the above tensors and noting that.

$$\vec{\epsilon} = \begin{Bmatrix} \frac{dw_1}{dx_3} - \theta_2 \\ \frac{dw_2}{dx_3} + \theta_1 \\ \frac{dw_3}{dx_3} \end{Bmatrix} \quad \vec{\kappa} = \begin{Bmatrix} \frac{d\theta_1}{dx_3} \\ \frac{d\theta_2}{dx_3} \\ \frac{d\theta_3}{dx_3} \end{Bmatrix} \quad \vec{\epsilon^e} = \begin{Bmatrix} \beta_2 \\ \beta_1 \\ \frac{d\phi}{dx_3} \end{Bmatrix} \quad \vec{\kappa^e} = \begin{Bmatrix} \frac{d\beta_2}{dx_3} \\ \frac{d\beta_1}{dx_3} \\ 0 \end{Bmatrix} \quad \vec{\gamma} = \begin{Bmatrix} \gamma_2 \\ \gamma_1 \\ 0 \end{Bmatrix} \quad \vec{\varsigma} = \begin{Bmatrix} \frac{d\gamma_2}{dx_3} \\ \frac{d\gamma_1}{dx_3} \\ 0 \end{Bmatrix}$$

We obtain the following system of differential equations corresponding to each of the above differential equations.

$$
\frac{d}{dx_3}\begin{bmatrix} \mu Ak_s & 0 & 0 \\ & \mu Ak_s & 0 \\ sym & & (2\mu+\lambda)A \end{bmatrix}\begin{pmatrix} \frac{dw_1}{dx_3}-\theta_2 \\ \frac{dw_2}{dx_3}+\theta_1 \\ \frac{dw_3}{dx_3} \end{pmatrix} + \frac{d}{dx_3}A\begin{bmatrix} P_{113} & P_{213} & P_{313} \\ P_{123} & P_{223} & P_{323} \\ P_{133} & P_{233} & P_{333} \end{bmatrix}\begin{pmatrix} \beta_2 \\ \beta_1 \\ \frac{d\phi}{dx_3} \end{pmatrix}
$$

$$
+ \frac{d}{dx_3}\frac{1}{2}\begin{bmatrix} P_{313}I_{11} & P_{313}I_{22} & 0 \\ P_{323}I_{11} & P_{323}I_{22} & 0 \\ P_{333}I_{11} & P_{333}I_{22} & 0 \end{bmatrix}\begin{pmatrix} \frac{d\gamma_2}{dx_3} \\ \frac{d\gamma_1}{dx_3} \\ 0 \end{pmatrix} + \begin{pmatrix} q_1 \\ q_2 \\ q_3 \end{pmatrix} = \begin{pmatrix} 0 \\ 0 \\ 0 \end{pmatrix} \quad (5.1)
$$

$$
\frac{d}{dx_3}\begin{bmatrix} (2\mu+\lambda)I_{22} & 0 & 0 \\ & (2\mu+\lambda)I_{11} & 0 \\ sym & & \mu J \end{bmatrix}\begin{pmatrix} \frac{d\theta_1}{dx_3} \\ \frac{d\theta_2}{dx_3} \\ \frac{d\theta_3}{dx_3} \end{pmatrix} + \frac{d}{dx_3}\begin{bmatrix} 0 & P_{333}I_{22} & 0 \\ -P_{333}I_{11} & 0 & 0 \\ P_{323}I_{11} & -P_{313}I_{22} & 0 \end{bmatrix}\begin{pmatrix} \frac{d\beta_2}{dx_3} \\ \frac{d\beta_1}{dx_3} \\ 0 \end{pmatrix}
$$

$$
\frac{d}{dx_3}\begin{bmatrix} 0 & P_{233}I_{22} & 0 \\ -P_{133}I_{11} & 0 & 0 \\ P_{123}I_{11} & -P_{213}I_{22} & 0 \end{bmatrix}\begin{pmatrix} \gamma_2 \\ \gamma_1 \\ 0 \end{pmatrix} + \vec{e_3}\times\vec{Q} = \begin{pmatrix} 0 \\ 0 \\ 0 \end{pmatrix} \quad (5.2)
$$

$$
\left(\frac{d}{dx_3}A\begin{bmatrix} P_{113} & P_{123} & P_{133} \\ P_{213} & P_{223} & P_{233} \\ P_{313} & P_{323} & P_{333} \end{bmatrix}\begin{pmatrix} \frac{dw_1}{dx_3}-\theta_2 \\ \frac{dw_2}{dx_3}+\theta_1 \\ \frac{dw_3}{dx_3} \end{pmatrix} - \frac{d}{dx_3}A\begin{bmatrix} \epsilon_{11} & \epsilon_{12} & \epsilon_{13} \\ & \epsilon_{22} & \epsilon_{23} \\ sym & & \epsilon_{33} \end{bmatrix}\begin{pmatrix} \beta_2 \\ \beta_1 \\ \frac{d\phi}{dx_3} \end{pmatrix}\right.
$$

$$
\left. - \frac{d}{dx_3}\frac{1}{2}\begin{bmatrix} \epsilon_{13}I_{11} & \epsilon_{13}I_{22} & 0 \\ \epsilon_{23}I_{11} & \epsilon_{23}I_{22} & 0 \\ \epsilon_{33}I_{11} & \epsilon_{33}I_{22} & 0 \end{bmatrix}\begin{pmatrix} \frac{d\gamma_2}{dx_3} \\ \frac{d\gamma_1}{dx_3} \\ 0 \end{pmatrix} + \begin{pmatrix} 0 \\ 0 \\ r \end{pmatrix} = \begin{pmatrix} 0 \\ 0 \\ 0 \end{pmatrix}\right)_3 \quad (5.3)
$$

$$
\frac{d}{dx_3}\begin{bmatrix} 0 & -P_{333}I_{11} & P_{323}I_{11} \\ P_{333}I_{22} & 0 & -P_{313}I_{22} \\ 0 & 0 & 0 \end{bmatrix}\begin{pmatrix} \frac{d\theta_1}{dx_3} \\ \frac{d\theta_2}{dx_3} \\ \frac{d\theta_3}{dx_3} \end{pmatrix} - \frac{d}{dx_3}\begin{bmatrix} \epsilon_{33}I_{11} & 0 & 0 \\ & \epsilon_{33}I_{22} & 0 \\ sym & & 0 \end{bmatrix}\begin{pmatrix} \frac{d\beta_2}{dx_3} \\ \frac{d\beta_1}{dx_3} \\ 0 \end{pmatrix}
$$

$$
- \frac{d}{dx_3}\begin{bmatrix} \epsilon_{31}I_{11} & 0 & 0 \\ & \epsilon_{32}I_{22} & 0 \\ sym & & 0 \end{bmatrix}\begin{pmatrix} \gamma_2 \\ \gamma_1 \\ 0 \end{pmatrix} - Q_\alpha^e = \begin{pmatrix} 0 \\ 0 \\ 0 \end{pmatrix} \quad (5.4)
$$

$$\frac{d}{dx_3}\frac{1}{2}\begin{bmatrix} P_{313}I_{11} & P_{323}I_{11} & P_{333}I_{11} \\ P_{313}I_{22} & P_{323}I_{22} & P_{333}I_{22} \\ 0 & 0 & 0 \end{bmatrix}\begin{pmatrix} \frac{dw_1}{dx_3}-\theta_2 \\ \frac{dw_2}{dx_3}+\theta_1 \\ \frac{dw_3}{dx_3} \end{pmatrix} - \frac{d}{dx_3}\frac{1}{2}\begin{bmatrix} \epsilon_{13}I_{11} & \epsilon_{23}I_{11} & \epsilon_{33}I_{11} \\ \epsilon_{13}I_{22} & \epsilon_{23}I_{22} & \epsilon_{33}I_{22} \\ 0 & 0 & 0 \end{bmatrix}\begin{pmatrix} \beta_2 \\ \beta_1 \\ \frac{d\phi}{dx_3} \end{pmatrix}$$

$$-\frac{d}{dx_3}\frac{1}{4}\begin{bmatrix} \epsilon_{33}J_{1111} & \epsilon_{33}J_{1122} & 0 \\ \epsilon_{33}J_{2211} & \epsilon_{33}J_{2222} & 0 \\ 0 & 0 & 0 \end{bmatrix}\begin{pmatrix} \frac{d\gamma_2}{dx_3} \\ \frac{d\gamma_1}{dx_3} \\ 0 \end{pmatrix} - \begin{bmatrix} 0 & -P_{133}I_{11} & P_{123}I_{11} \\ P_{233}I_{22} & 0 & -P_{213}I_{22} \\ 0 & 0 & 0 \end{bmatrix}\begin{pmatrix} \frac{d\theta_1}{dx_3} \\ \frac{d\theta_2}{dx_3} \\ \frac{d\theta_3}{dx_3} \end{pmatrix}$$

$$+\begin{bmatrix} \epsilon_{31}I_{11} & 0 & 0 \\ 0 & \epsilon_{32}I_{22} & 0 \\ 0 & 0 & 0 \end{bmatrix}\begin{pmatrix} \frac{d\beta_2}{dx_3} \\ \frac{d\beta_1}{dx_3} \\ 0 \end{pmatrix} + \begin{bmatrix} \epsilon_{11}I_{11} & 0 & 0 \\ 0 & \epsilon_{22}I_{22} & 0 \\ 0 & 0 & 0 \end{bmatrix}\begin{pmatrix} \gamma_2 \\ \gamma_1 \\ 0 \end{pmatrix} = \begin{pmatrix} 0 \\ 0 \\ 0 \end{pmatrix}$$

$$(5.5)$$

A few remarks are in order.

Remark 7. In (5.2) and (5.4) the expressions $\vec{e_3}\times\vec{Q}$ and Q_α^e are the stress and electric displacement resultants, as given in (5.1) and (5.3), respectively (certainly without the outer derivatives).

Remark 8. The brackets and subscript 3 in equation (5.3) implies that we only need the third component of this vector i.e. $\frac{dQ_3^e}{dx_3}+r$. The other two components of Q_α^e are used in moment resultants as mentioned earlier.

Remark 9. In the theory of beams it is a common practice to tune the Young's modulus $E=2\mu+\lambda$. Note that the shear coefficient for a piezoelectric beam needs to be calculated separately due to the emergence of coupled shear stresses which are one order higher in electric part compared to the mechanical part. In many of the examples we will assume this factor as unity. A purely mechanical shear factor is also admissible because the electric part does not need any corrections as it uses higher order terms of the Taylor series.

In order to solve the two-dimensional piezoelectric beam problem analytically, we chose the x_1-x_3 plane and reduce the number of unknown variables to the ones corresponding to this plane. Assuming no axial displacements and rotation about x_3 axis, we have,

$$\begin{aligned} w_1 &= w, & w_2 &= 0, & w_3 &= 0 \\ \theta_2 &= \theta, & \theta_1 &= 0, & \theta_3 &= 0 \\ \phi &= \phi \\ \beta_2 &= \beta, & \beta_1 &= 0 \\ \gamma_2 &= \gamma, & \gamma_1 &= 0 \\ x_3 &= x, & I_{11} &= I, & I_{22} &= 0 \\ & & J_{1111} &= J \end{aligned}$$

With these simplification, taking the first row of (5.1), second row of (5.2), third row of (5.3), first row of (5.4) and first row of (5.5) we obtain the generic governing equations of piezoelectric beam.

42

$$\frac{d}{dx}\left(\mu A k_s(\frac{dw}{dx} - \theta)\right) + \frac{d}{dx}\left(A(P_{113}\beta + P_{313}\frac{d\phi}{dx}) + \frac{1}{2}P_{313}I\frac{d\gamma}{dx}\right) + q_1 = 0$$

$$\frac{d}{dx}\left(EI\frac{d\theta}{dx}\right) - \frac{d}{dx}\left(P_{333}I\frac{d\beta}{dx}\right) - P_{133}I\frac{d\gamma}{dx} + \mu A k_s(\frac{dw}{dx} - \theta)$$
$$+ A(P_{113}\beta + P_{313}\frac{d\phi}{dx}) + \frac{1}{2}P_{313}I\frac{d\gamma}{dx} = 0$$

$$\frac{d}{dx}\left(P_{313}A(\frac{dw}{dx} - \theta)\right) - \frac{d}{dx}\left(A(\epsilon_{13}\beta + \epsilon_{33}\frac{d\phi}{dx}) + \frac{1}{2}\epsilon_{33}I\frac{d\gamma}{dx}\right) + r = 0$$

$$\frac{d}{dx}\left(P_{333}I\frac{d\theta}{dx}\right) + \frac{d}{dx}\left(\epsilon_{33}I\frac{d\beta}{dx}\right) + \epsilon_{13}I\frac{d\gamma}{dx} + P_{113}A k_s(\frac{dw}{dx} - \theta)$$
$$- A(\epsilon_{11}\beta + \epsilon_{13}\frac{d\phi}{dx}) - \frac{1}{2}\epsilon_{13}I\frac{d\gamma}{dx} = 0$$

$$\frac{d}{dx}\left[\frac{1}{2}P_{313}I(\frac{dw}{dx} - \theta) - \frac{1}{2}I(\epsilon_{13}\beta + \epsilon_{33}\frac{d\phi}{dx}) - \frac{1}{4}\epsilon_{33}J\frac{d\gamma}{dx}\right] + I\left(P_{133}\frac{d\theta}{dx} + \epsilon_{13}\frac{d\beta}{dx} + \epsilon_{11}\gamma\right) = 0$$

Together with the appropriate boundary conditions the piezoelectric beam problem is completely closed with the above set of equations.

Our aim is to solve for a cantilever energy harvesting piezoelectric beam purely under the action of mechanical loads. To this end, we simplify the above five equations by equating $r = 0$ and integrating the third equation inside the box. Note that we also set the constant appearing after integration to zero, since that represents a point electric charge (counterpart of point load). Similarly, in the first equation, we set $q_1 = 0$ and perform integration. The constant of integration gives rise to point load P acting at the free end of the cantilever beam. In practice, the beam energy harvesters are normally excited with a point load rather than with a distributed load. Assuming that all material and geometric properties remain constant throughout the beam length, we can take out the coefficients and simplify,

$$a_1(\frac{dw}{dx} - \theta) + a_2\beta + a_3\frac{d\phi}{dx} + \frac{1}{2}a_{12}\frac{d\gamma}{dx} = P \qquad (5.6)$$

$$a_4\frac{d^2\theta}{dx^2} - a_5\frac{d^2\beta}{dx^2} - a_{13}\frac{d\gamma}{dx} + a_1(\frac{dw}{dx} - \theta) + a_2\beta + a_3\frac{d\phi}{dx} + \frac{1}{2}a_{12}\frac{d\gamma}{dx} = 0 \qquad (5.7)$$

$$a_6(\frac{dw}{dx} - \theta) - a_7\beta - a_8\frac{d\phi}{dx} - \frac{1}{2}a_9\frac{d\gamma}{dx} = 0 \qquad (5.8)$$

$$a_5\frac{d^2\theta}{dx^2} + a_9\frac{d^2\beta}{dx^2} + a_{14}\frac{d\gamma}{dx} + a_2(\frac{dw}{dx} - \theta) - a_{10}\beta - a_{11}\frac{d\phi}{dx} - \frac{1}{2}a_{14}\frac{d\gamma}{dx} = 0 \qquad (5.9)$$

$$\frac{d}{dx}\left[\frac{1}{2}a_{12}(\frac{dw}{dx} - \theta) - \frac{1}{2}(a_{14}\beta + a_9\frac{d\phi}{dx}) - \frac{1}{4}a_{15}\frac{d\gamma}{dx}\right] + a_{13}\frac{d\theta}{dx} + a_{14}\frac{d\beta}{dx} + a_{16}\gamma = 0 \qquad (5.10)$$

which are the five governing equations of a cantilever piezoelectric beam under the action of point load at the free end. The set of equations is closed by the following ten boundary

conditions,

$$w(x = 0) = 0 \qquad (5.11)$$
$$\theta(x = 0) = 0 \qquad (5.12)$$
$$\phi(x = 0) = 0 \qquad (5.13)$$
$$\beta(x = 0) = 0 \qquad (5.14)$$
$$\gamma(x = 0) = 0 \qquad (5.15)$$

$$Q(x = l) = \left[a_1(\frac{dw}{dx} - \theta) + a_2\beta + a_3\frac{d\phi}{dx} + \frac{1}{2}a_{12}\frac{d\gamma}{dx} \right]_{x=l} = P \qquad (5.16)$$

$$M(x = l) = \left[a_4\frac{d\theta}{dx} - a_5\frac{d\beta}{dx} - a_{13}\gamma \right]_{x=l} = 0 \qquad (5.17)$$

$$Q^e(x = l) = \left[a_6(\frac{dw}{dx} - \theta) - a_7\beta - a_8\frac{d\phi}{dx} - \frac{1}{2}a_9\frac{d\gamma}{dx} \right]_{x=l} = 0 \qquad (5.18)$$

$$M^e(x = l) = \left[a_5\frac{d\theta}{dx} + a_9\frac{d\beta}{dx} + a_{14}\gamma \right]_{x=l} = 0 \qquad (5.19)$$

$$O^e(x = l) = \left[a_{12}(\frac{dw}{dx} - \theta) - \frac{1}{2}(a_{14}\beta + a_9\frac{d\phi}{dx}) - \frac{1}{4}a_{15}\frac{d\gamma}{dx} \right]_{x=l} = 0 \qquad (5.20)$$

where.

$a_1 = \mu A k_s$	$a_2 = P_{113}A k_s$	$a_3 = P_{313}A k_s$	$a_4 = EI$
$a_5 = P_{333}I$	$a_6 = P_{313}A$	$a_7 = \epsilon_{13}A$	$a_8 = \epsilon_{33}A$
$a_9 = \epsilon_{33}I$	$a_{10} = \epsilon_{11}A k_s$	$a_{11} = \epsilon_{13}A k_s$	$a_{12} = P_{313}I$
$a_{13} = P_{133}I$	$a_{14} = \epsilon_{13}I$	$a_{15} = \epsilon_{33}J$	$a_{16} = \epsilon_{11}I$

Note that the two boundary conditions (5.16) and (5.18) are already present in the governing equations. From the theory of beams and plates we know that Neumann boundary conditions are normally given in the governing equations themselves in the form of shear force and bending moment. In this problem we postulate a similar Dirichlet and Neumann boundary conditions for electric kinematics i.e. all the electric variables are zero at the fixed end and their resultant derivatives are specified at the free end in coupled fashion. This is also shown in Fig. 7.

To solve the above set of equations we proceed as follows. From (5.6) and (5.9) we can eliminate $\frac{dw}{dx} - \theta$ and find $\frac{d\phi}{dx}$ in terms of other variables i.e.

$$\frac{dw}{dx} - \theta = \frac{P}{a_1} - \frac{a_2}{a_1}\beta - \frac{a_3}{a_1}\frac{d\phi}{dx} - \frac{1}{2}\frac{a_{12}}{a_1}\frac{d\gamma}{dx} \qquad (5.21)$$

$$\frac{d\phi}{dx} = \frac{a_6}{a_1 b_2}P - \frac{b_1}{b_2}\beta - \frac{b_9}{b_2}\frac{d\gamma}{dx} \qquad (5.22)$$

where,

$$b_1 = \frac{a_2 a_6}{a_1} + a_7, \qquad b_2 = \frac{a_3 a_6}{a_1} + a_8, \qquad b_9 = \frac{1}{2}(\frac{a_{12}a_6}{a_1} + a_9)$$

Substituting (5.21) in (5.9), we eliminate $\frac{dw}{dx} - \theta$ from this equation as well,

$$a_5\frac{d^2\theta}{dx^2} + a_9\frac{d^2\beta}{dx^2} - b_{10}\frac{d\gamma}{dx} - b_3\beta - b_4\frac{d\phi}{dx} + \frac{a_2}{a_1}P = 0 \tag{5.23}$$

where.

$$b_3 = \frac{a_2^2}{a_1} + a_{10}, \qquad b_4 = \frac{a_2 a_3}{a_1} + a_{11}, \qquad b_{10} = \frac{1}{2}(\frac{a_{12}a_2}{a_1} - a_{14})$$

Substituting (5.22) in (5.23), we obtain.

$$a_5\frac{d^2\theta}{dx^2} + a_9\frac{d^2\beta}{dx^2} + b_{11}\frac{d\gamma}{dx} - b_5\beta + b_6P = 0 \tag{5.24}$$

$$b_5 = b_3 - \frac{b_1 b_9}{b_2}, \qquad b_6 = \frac{a_2}{a_1} - \frac{a_6 b_4}{a_1 b_2}, \qquad b_{11} = \frac{b_4 b_9}{b_2} - b_{10}$$

Similarly, we can eliminate $\frac{dw}{dx} - \theta$ and $\frac{d\phi}{dx}$ from (5.23),

$$a_{13}\frac{d\theta}{dx} + b_{15}\frac{d\beta}{dx} + b_{16}\frac{d^2\gamma}{dx^2} + a_{16}\gamma = 0 \tag{5.25}$$

where.

$$b_{15} = -b_{10} + \frac{b_1 b_{13}}{b_2}, \qquad\qquad b_{16} = \frac{b_{13}b_9}{b_2} - b_{14}$$

$$b_{13} = \frac{1}{2}(\frac{a_3 a_{12}}{a_1} + a_9) \qquad\qquad b_{14} = \frac{1}{4}\frac{a_{12}^2}{a_1} + \frac{1}{4}a_{15}$$

With these modifications we now have a system of three equations with three variables.

$$\begin{cases} a_4\frac{d^2\theta}{dx^2} - a_5\frac{d^2\beta}{dx^2} - a_{13}\frac{d\gamma}{dx} + P = 0 \\ a_5\frac{d^2\theta}{dx^2} + a_9\frac{d^2\beta}{dx^2} + b_{11}\frac{d\gamma}{dx} - b_5\beta + b_6P = 0 \\ a_{13}\frac{d\theta}{dx} + b_{15}\frac{d\beta}{dx} + b_{16}\frac{d^2\gamma}{dx^2} + a_{16}\gamma = 0 \end{cases}$$

These three coupled equations are in terms of rotations; if we can emancipate from maths to say so. At this stage, it is necessary to mention that not all cases of piezoelectric cantilever beam yield the above set of equations. Many piezoelectric materials have an inordinate number of zero entries in their piezoelectric and permitivity tensors, and this significantly affects the coupled nature of the governing equations. In this work, the aforementioned three equations are categorised into three main cases namely, the fully coupled case, the case when permitivity tensor is diagonal and $P_{133} = 0$ and the case when only the solution with a first order electric potential is sought for. While the first case is mathematically important to solve, in practice very few piezoelectric materials give rise to such a coupling. The most notable piezoelectric materials like PZT-5H, PZT-5A, Quartz and many more have diagonal permitivity tensors meaning that in our case $\epsilon_{33} = 0$ and this as we will see changes the nature of electromechanical coupling significantly. The last case considered is when our approximation of electric potential is up to first order. This is an elegant case which provides us with an insight into a simpler way of coupling and whose solution can be compared with many other numerical models in the literature. We solve for all these three cases starting from the last case and working our way backwards.

5.2.   Piezoelectric Beam with First Order Electric Potential

Considering a linear electric potential across the beam thickness, one ends up with only two coupled equations in terms of θ and β which are,

$$a_4 \frac{d^2\theta}{dx^2} - a_5 \frac{d^2\beta}{dx^2} + P = 0 \tag{5.26}$$

$$a_5 \frac{d^2\theta}{dx^2} + a_9 \frac{d^2\beta}{dx^2} - b_5\beta + b_6 P = 0 \tag{5.27}$$

with the following boundary conditions.

$$\theta(x=0) = 0 \qquad\qquad \beta(x=0) = 0$$

$$\left[a_4 \frac{d\theta}{dx} - a_5 \frac{d\beta}{dx}\right]_{x=l} = 0 \qquad\qquad \left[a_5 \frac{d\theta}{dx} + a_9 \frac{d\beta}{dx}\right]_{x=l} = 0$$

Certainly the last two coupled boundary conditions can be written in uncoupled form as

$$\left[\frac{d\theta}{dx}\right]_{x=l} = 0 \qquad\qquad \left[\frac{d\beta}{dx}\right]_{x=l} = 0$$

Integrating (5.26) twice and applying the boundary conditions for θ we obtain.

$$\theta = \frac{a_5}{a_4}\beta - \frac{P}{2EI}x^2 + \frac{PL}{EI}x \tag{5.28}$$

Substituting (5.28) in (5.27) we obtain a non-homogeneous second order ordinary differential equation in terms of β,

$$b_7 \frac{d^2\beta}{dx^2} - b_5\beta + b_8 P = 0 \tag{5.29}$$

where.

$$b_7 = \frac{a_5^2}{a_4} + a_9, \qquad\qquad b_8 = b_6 - \frac{a_5}{a_4}$$

The complete solution to (5.29) is given by,

$$\beta = c_3 e^{kx} + c_4 e^{-kx} + \frac{b_8}{b_5}P \tag{5.30}$$

where $k = \sqrt{\frac{b_5}{b_7}}$ and the coefficients c_i are found after applying the boundary condition as.

$$c_3 = -\frac{b_8}{b_5}\left[\frac{1}{1 + e^{2kl}}\right]P \qquad\qquad c_4 = -\frac{b_8}{b_5}\left[\frac{e^{2kl}}{1 + e^{2kl}}\right]P$$

All the remaining variables (θ, w and ϕ) can be found by back substitution.

$$\beta = -\frac{b_8}{b_5}\left[\frac{1}{1 + e^{2kl}}\right]P\left(e^{kx} + e^{2kl}e^{-kx}\right) + \frac{b_8}{b_5}P \tag{5.31}$$

$$\theta = \frac{a_5}{a_4}\beta - \frac{P}{2EI}x^2 + \frac{PL}{EI}x \tag{5.32}$$

$$\phi = \left(\frac{a_6}{a_1 b_2} - \frac{b_1 b_8}{b_2 b_5}\right)Px + \frac{b_1}{b_2 k}\left[\frac{1}{1 + e^{2kl}}\right]P\left(e^{kx} - e^{2kl}e^{-kx}\right)$$
$$+ \frac{b_1}{b_2}\left[\frac{1}{1 + e^{2kl}}\right]P\left(1 - e^{2kl}\right) \tag{5.33}$$

$$w = \left(\frac{\lambda_3}{E} - \frac{a_2}{a_1}\right)\left[\frac{1}{k}\left[\frac{1}{1 + e^{2kl}}\right]P\left(e^{kx} - e^{2kl}e^{-kx}\right) + \frac{b_8}{b_5}Px\right] - \frac{a_3}{a_1}\phi$$
$$- \frac{P}{6EI}x^3 + \frac{PL}{2EI}x^2 + \frac{P}{\mu A k_s}x - \frac{1}{k}\left(\frac{a_5}{a_4} - \frac{a_2}{a_1}\right)\left[\frac{1}{1 + e^{2kl}}\right]P\left(1 - e^{2kl}\right) \tag{5.34}$$

5.3. Piezoelectric Beam with Diagonal Permitivity Tensor

An important and simple way to solve for all the variables for a piezoelectric beam with quadratic electric potential assumption arises for materials with diagonal permitivity tensor and $P_{133} = 0$, certainly when poled along the longitudinal direction.

$$a_4\frac{d^2\theta}{dx^2} - a_5\frac{d^2\beta}{dx^2} + P = 0 \tag{5.35}$$

$$a_5\frac{d^2\theta}{dx^2} + a_9\frac{d^2\beta}{dx^2} - b_5\beta + b_6 P = 0 \tag{5.36}$$

$$b_{15}\frac{d\beta}{dx} + b_{16}\frac{d^2\gamma}{dx^2} + a_{16}\gamma = 0 \tag{5.37}$$

with the following boudnary conditions.

$$\theta(x = 0) = 0 \qquad\qquad \left[a_4\frac{d\theta}{dx} - a_5\frac{d\beta}{dx}\right]_{x=l} = 0$$

$$\beta(x = 0) = 0 \qquad\qquad \left[a_5\frac{d\theta}{dx} + a_9\frac{d\beta}{dx}\right]_{x=l} = 0$$

$$\gamma(x = l) = 0 \qquad \left[\frac{1}{2}a_{12}(\frac{dw}{dx} - \theta) - \frac{1}{2}a_9\frac{d\phi}{dx} - \frac{1}{4}a_{15}\frac{d\gamma}{dx}\right]_{x=l} = 0$$

The first two equations are the same as before (together with their boundary conditions), so we do not need to solve for θ and β once again. The expression for γ can then be obtained by solving the third equation,

$$\gamma = \frac{m_1 m_2\sinh\left(\sqrt{m_1}x\right) + \sqrt{m_1}m_3\cosh\left(l\sqrt{m_1} - \sqrt{m_1}x\right) - \sqrt{m_1}m_4\cosh\left(l\sqrt{m_1} - \sqrt{m_1}x\right)}{\sqrt{m_1}\cosh\left(l\sqrt{m_1}\right)(m_1 - k^2)}$$
$$+ \frac{-k^2 m_2\sinh\left(\sqrt{m_1}x\right) + k m_3\sinh\left(\sqrt{m_1}x\right)e^{kl} + km_4\sinh\left(\sqrt{m_1}x\right)e^{-kl}}{\sqrt{m_1}\cosh\left(l\sqrt{m_1}\right)(m_1 - k^2)}$$
$$- \frac{\sqrt{m_1}m_3\,e^{kx} - \sqrt{m_1}m_4\,e^{-kx}}{\sqrt{m_1}(m_1 - k^2)} \tag{5.38}$$

where,

$$m_1 = \frac{a_{16}}{b_{16}}, \qquad\qquad m_2 = \left[\frac{b_{23}}{b_{16}}\beta - \frac{b_{24}}{b_{16n}}P\right]_{x=L}$$

$$m_3 = \frac{b_8 b_{15}}{b_5 b_{16}}\left(\frac{Pk}{1+e^{2kL}}\right), \qquad m_4 = \frac{b_8 b_{15}}{b_5 b_{16}}\left(\frac{Pke^{2kL}}{1+e^{2kL}}\right) = m_3 e^{2kL}$$

The two remaining variables (ϕ and w) can be found by substiting the values of known θ, β and γ in (5.22) and (5.21), respectively.

5.4. The Fully Coupled Case

Assuming no piezoelectric or dielectric constants to be zero, we need to solve the three equations in their original form. The three equations can be reduced to two equations in terms of β and γ as follows,

$$b_7\frac{d^2\beta}{dx^2} - b_5\beta + b_{17}\frac{d\gamma}{dx} + b_8 P = 0 \tag{5.39}$$

$$b_{16}\frac{d^2\gamma}{dx^2} + b_{19}\gamma + b_{18}\frac{d\beta}{dx} - b_{20}Px + a_{13}c_1 = 0 \tag{5.40}$$

with the following boundary condition,

$$\beta(x=0) = 0 \qquad\qquad \left[b_7\frac{d\beta}{dx} + b_{21}\gamma\right]_{x=l} = 0$$

$$\gamma(x=l) = 0 \qquad\qquad \left[b_{23}\beta - b_{16}\frac{d\gamma}{dx} - b_{24}P\right]_{x=l} = 0$$

where c_1 is a yet to be determined constant and the remaining constants being.

$$b_{17} = b_{11} + \frac{a_5 a_{13}}{a_4}, \qquad b_{18} = \frac{a_{13}a_5}{a_4} + b_{15}, \qquad b_{19} = \frac{a_{13}^2}{a_4} + a_{16}$$

$$b_{20} = -\frac{a_{13}}{a_4} \qquad b_{21} = \frac{a_{13}a_5}{a_4} + a_{14}, \qquad b_{22} = \frac{1}{2}a_{14} + \frac{a_{12}a_2}{a_1}$$

$$b_{23} = b_{22} - \frac{b_1}{b_2}, \qquad b_{24} = \frac{a_{12}}{a_1} - \frac{b_{13}a_6}{a_1 b_2}$$

In order to solve the above coupled equations we use the matrix method and proceed as.

$$y_1 = \beta, \qquad\qquad y_2 = \gamma$$

$$y_3 = \frac{d\beta}{dx} = y_1', \qquad\qquad y_3 = \frac{d\gamma}{dx} = y_2',$$

This leads us to the following system of equations,

$$\begin{Bmatrix} y_1' \\ y_2' \\ y_3' \\ y_4' \end{Bmatrix} = \begin{bmatrix} 0 & 0 & 1 & 0 \\ 0 & 0 & 0 & 1 \\ -n_1 & 0 & 0 & -n_2 \\ 0 & -n_3 & -n_4 & 0 \end{bmatrix} \begin{Bmatrix} y_1 \\ y_2 \\ y_3 \\ y_4 \end{Bmatrix} - \begin{Bmatrix} 0 \\ 0 \\ f_1 \\ f_2 x + f_3 \end{Bmatrix} \tag{5.41}$$

where.

$$n_1 = -\frac{b_5}{b_7}, \qquad\qquad n_2 = \frac{b_{17}}{b_7}, \qquad\qquad n_3 = \frac{b_{19}}{b_{16}}$$

$$n_4 = \frac{b_{18}}{b_{16}}, \qquad\qquad f_1 = \frac{b_8}{b_7}P, \qquad\qquad f_2 = -\frac{b_{20}}{b_{16}}P$$

$$f_3 = \frac{a_{13}c_1}{b_{16}}$$

The homogeneous solution to this problem is obtained by finding the eigenvalues and eigenvectors of the matrix above and has the following form,

$$\vec{y}_c = c_2\vec{x_1}e^{\lambda_1 x} + c_3\vec{x_2}e^{\lambda_2 x} + c_4\vec{x_1}e^{\lambda_2 x} + c_5\vec{x_1}e^{\lambda_4 x}$$

where c_2, c_3, c_4 and c_5 are constants, $\vec{x}_i$ the eigenvectors and λ_i the eigenvalues. Since the particular solution involves linear terms we will need to use fundamental matrix $\boldsymbol{\Phi}$, which is essentially the matrix with columns as $\vec{x}_i e^{\lambda_x}$. The particular solution is then,

$$\vec{y}_p = \boldsymbol{\Phi}\int \boldsymbol{\Phi}^{-1}f(x)\mathrm{d}x$$

where $f(x)$ is the source vector. To find the constants the boundary conditions are applied as.

$$\begin{Bmatrix} y_1 \\ y_2 \end{Bmatrix} = \begin{Bmatrix} 0 \\ 0 \end{Bmatrix} \qquad\qquad \begin{bmatrix} 0 & n_5 & 1 & 0 \\ n_6 & 0 & 0 & 1 \end{bmatrix}\vec{y} = \begin{Bmatrix} 0 \\ -n_7 \end{Bmatrix}$$

This leaves us with a 4×4 system whose solution is the vector containing constants. Note that,

$$n_1 = \frac{b_{21}}{b_7}, \qquad\qquad n_6 = -\frac{b_{23}}{b_{16}}, \qquad\qquad n_7 = \frac{b_{24}}{b_{16}}P$$

The solution is quite lengthy and is not reported here.

Numerical Simulations

"First, solve the problem. Then, write the code."
John Johnson

6. Representative Numerical Examples

6.1. Static Analysis

6.1.1. Energy Harvesting with Cantilever Piezoelectric Beams

The numerical examples presented in this section are primarily tailored towards simulation of fabric-type harvesters and fibre-based sensors, which are essentially single layer piezoelectric sheets with no substrate material, polarised along the length, more commonly referred to as interdigitated electrode configuration (IDE) [46] [21] [36] [12]. To this end, we begin with the analysis of a cantilever piezoelectric beam with an applied point load at the free end. The analytical solution for this problem in the setting of the present formulation, was reported in the previous section. Fig. 7 shows a cantilever beam polarised along the length with an end load acting at the free end. Much of our numerical examples will follow similar geometrical configuration, unless explicitly stated.
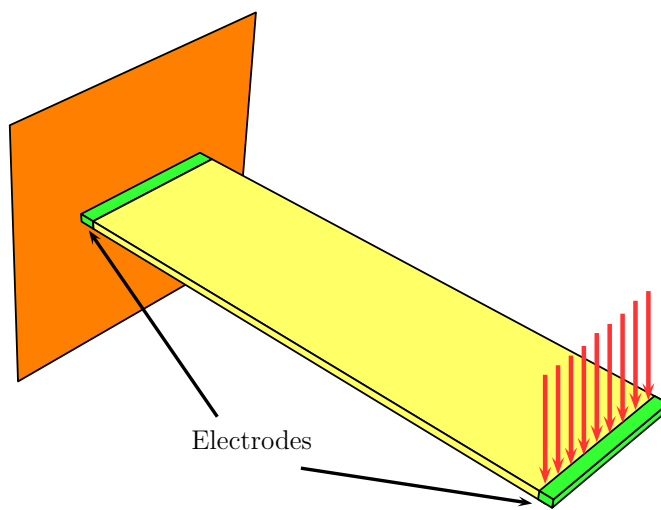
Figure 7: Piezoelectric cantilever beam polarised along the length

According to [50] and [5], the material properties for PZT-5H when polarised along the length is given by:

$$
\left\{ \begin{matrix} \lambda \\ \mu \end{matrix} \right\} = \left\{ \begin{matrix} 7.95 \times 10^{10} \\ 2.33 \times 10^{10} \end{matrix} \right\} \frac{N}{m^2}, \quad P = \begin{bmatrix} 0 & 0 & -6.5 \\ 0 & 0 & -6.5 \\ 0 & 0 & 23.3 \\ 0 & 17 & 0 \\ 17 & 0 & 0 \\ 0 & 0 & 0 \end{bmatrix} \frac{C}{m^2}, \quad \epsilon = \begin{bmatrix} 1.505 & 0 & 0 \\ & 1.505 & 0 \\ & & 1.3 \end{bmatrix} 10^{-8} \frac{C}{Vm}
$$

The h, p and hp convergence of all variables are obtained with the finite elements outlined in chapter 4. and are plotted in the following figures. Length of the beam is taken as 100mm and height as 1mm. The point load at the free end is $0.1N$ for this case. Legendre bases with Gauss quadrature integration rules are employed in the following analysis. We emphasise on numerical integration since two types of quadrature have been implemented, Gauss quadrature and Gauss Lobatto quadrature and shortly we will see the comparative performance of each.
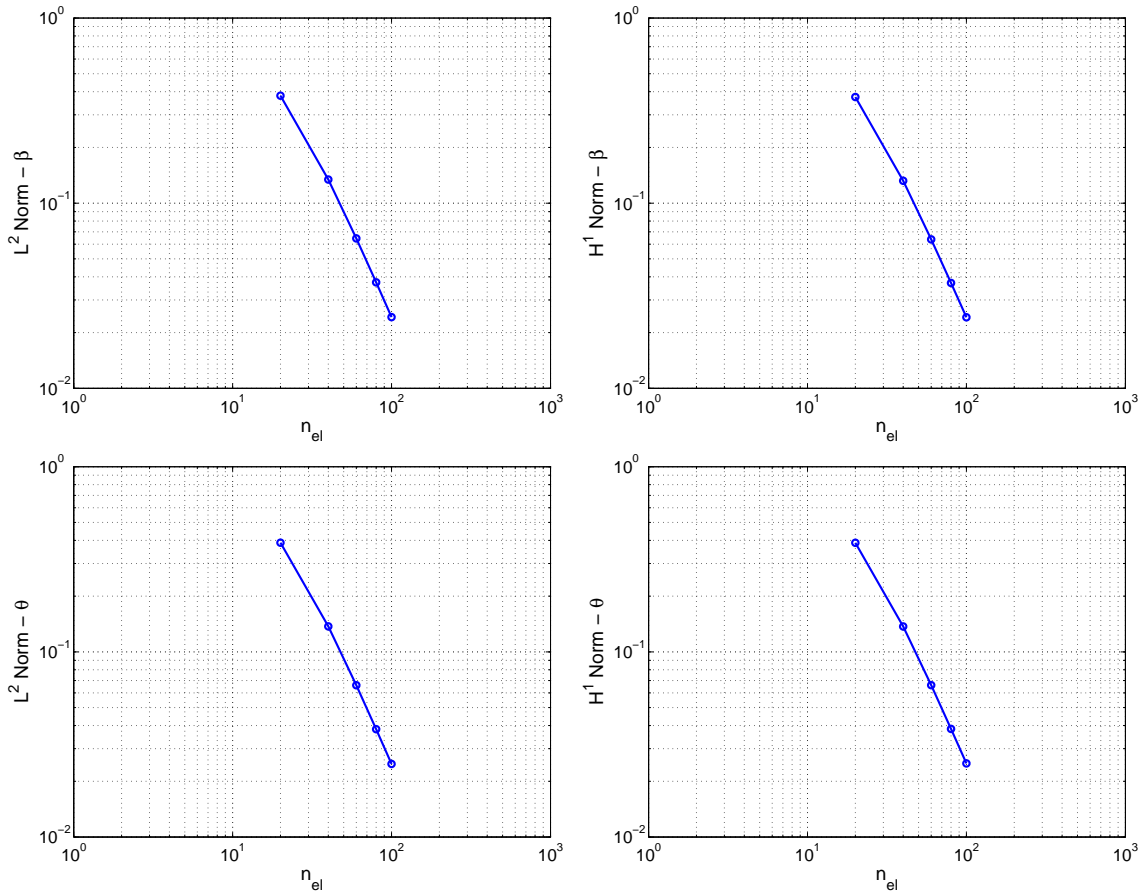
Figure 8: L^2 and H^1 Norm for: Top- Electric Potential Gradient β; Bottom- Mechanical Rotation θ for $p = 1$
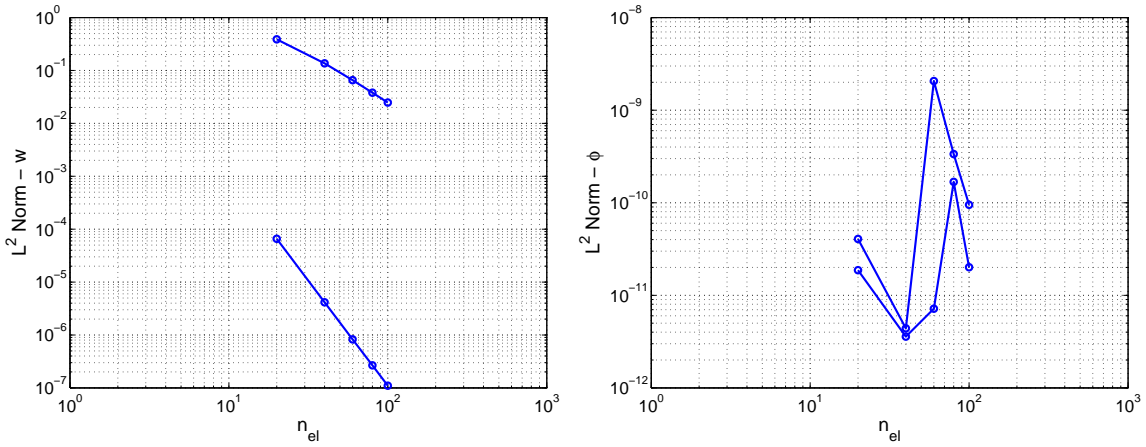
Figure 9: L^2 Norm for: L- Displacemnt w; R- Central Electric Potential ϕ for $p = 1, 2$
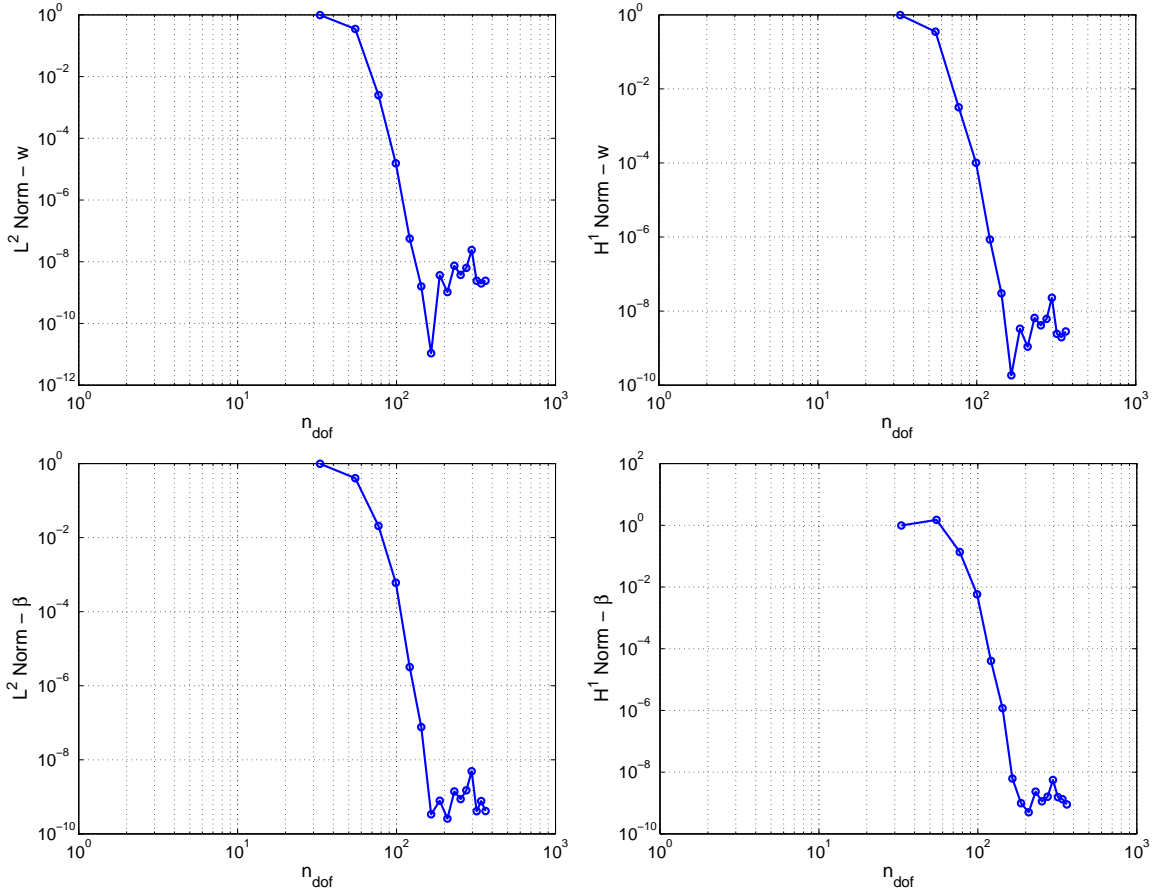
Figure 10: p convergence of L^2 and H^1 norms for T - displacements w; B - β

Let us now consider the case where the permitivity tensor is diagonal. To verify the computational scheme with the analytical solution, we first plot each variable vs number of elements, shown in Fig. 11. Note that red circles represent analytical solution and the blue lines the numerical one. Important to this analysis is the importance of coupled Neumann boundary conditions.
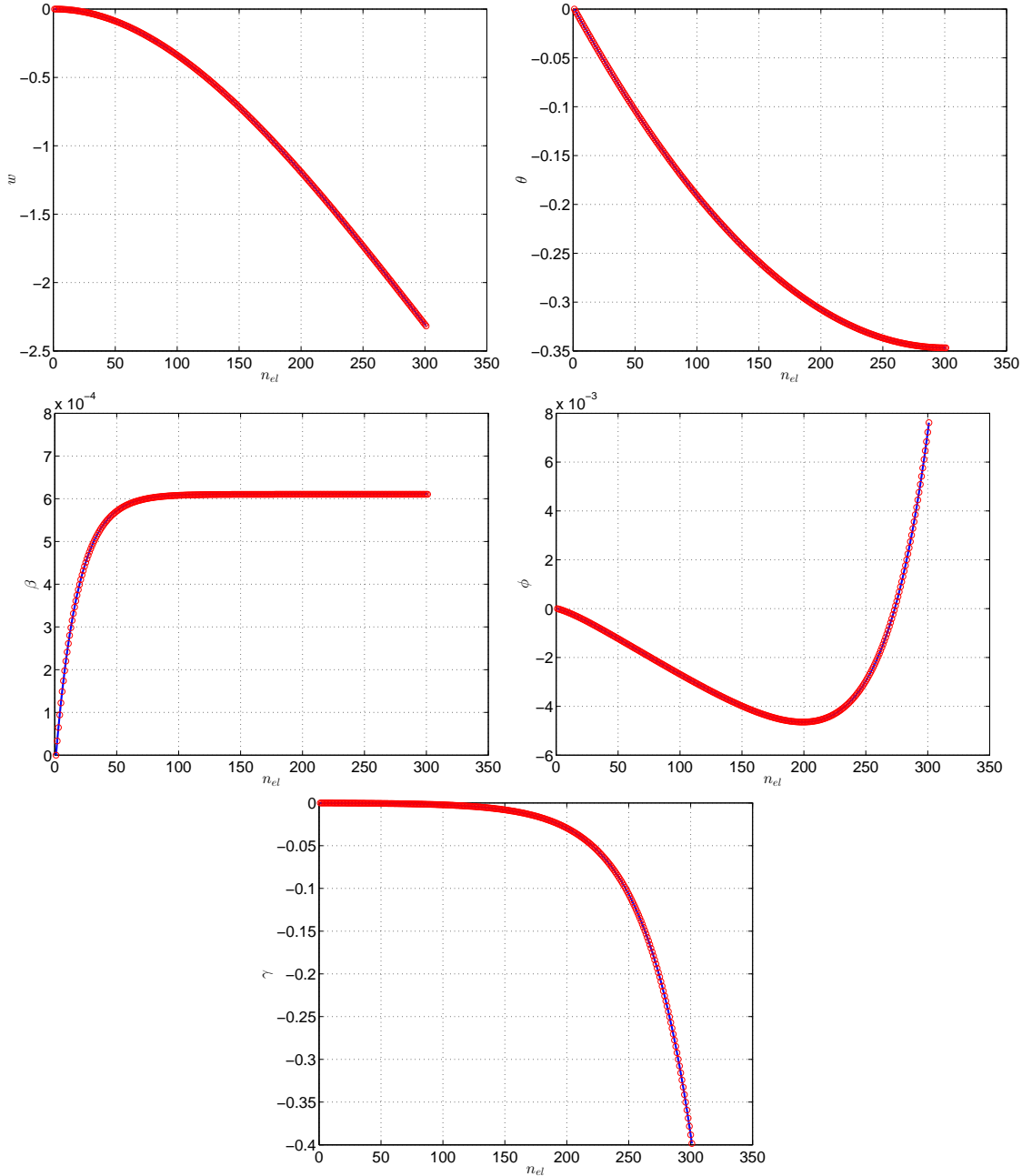
Figure 11: Comparison of Numerical and Analytical solutions

As can be verified from the analytical problem presented in chapter 5. the boundary condition is now such that one needs to explicity modify the right hand side vector. The Neumann boundary condition for γ translates into a moment term added to the right hand side vector by the amount $b_{23}\beta - b_{24}P$. Numerical solution of these cases are treated here as a two-step procedure. First we solve the system with first order electric assumption ignoring

γ, since β and θ are decoupled from the rest of variables and then we modify the right hand side and solve the system with γ. It should be emphasised that this problem occurs only in the case of piezoelectric beams with diagonal permitivity tensors and $P_{133} = 0$, due to the natural way, boundary conditions evolve, and this has to be treated automatically in the computational scheme. All other cases are imune from this issue. Also note that to have non-zero γ and ϕ, we need to have non-zero P_{313} which is assumed to be $20C/m^2$ for this analysis. The point-wise h-convergence for all the variables including the hessian γ is shown in the following, where blue lines represent linear bases and red lines quadratric bases.
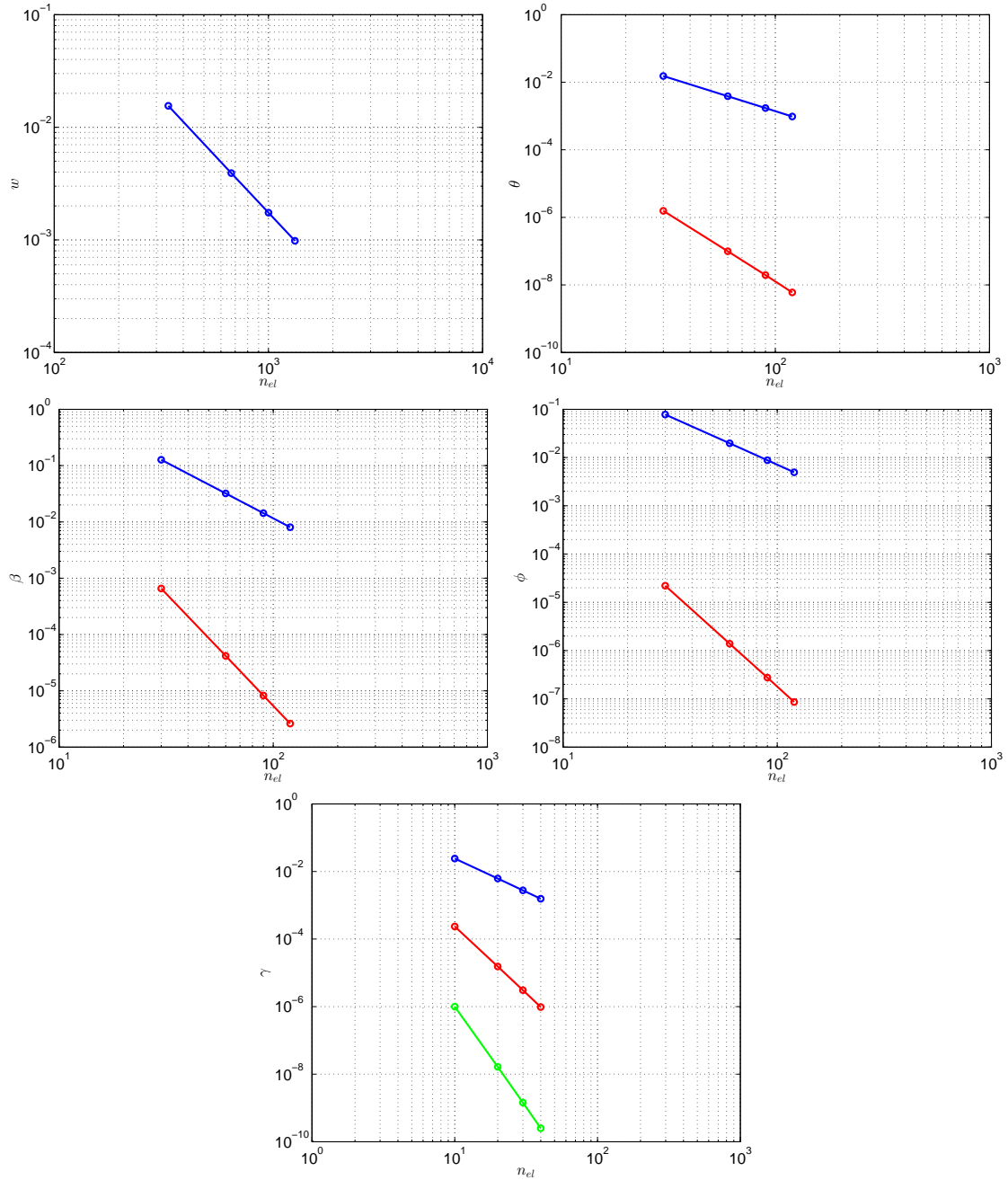
Figure 12: h convergence for diagonal permitivity case

In order to verify the numerical solution with the analytical one for the fully coupled case, we assume a piezoelectric material which has non-zero material data wherever required. The following data have been assumed [units omitted]:

$$\left\{\begin{matrix}\lambda\\\mu\end{matrix}\right\} = \left\{\begin{matrix}7.95\\2.33\end{matrix}\right\}, \quad \mathcal{P} = \begin{bmatrix}0 & 0 & -6.5\\0 & 0 & -6.5\\20 & 0 & 23.3\\0 & 0 & 0\\0 & 17 & 20\\17 & 0 & 0\end{bmatrix}, \quad \boldsymbol{\epsilon} = \begin{bmatrix}1.505 & 0 & 1\\ & 1.505 & 0\\ & & 1.3\end{bmatrix}$$
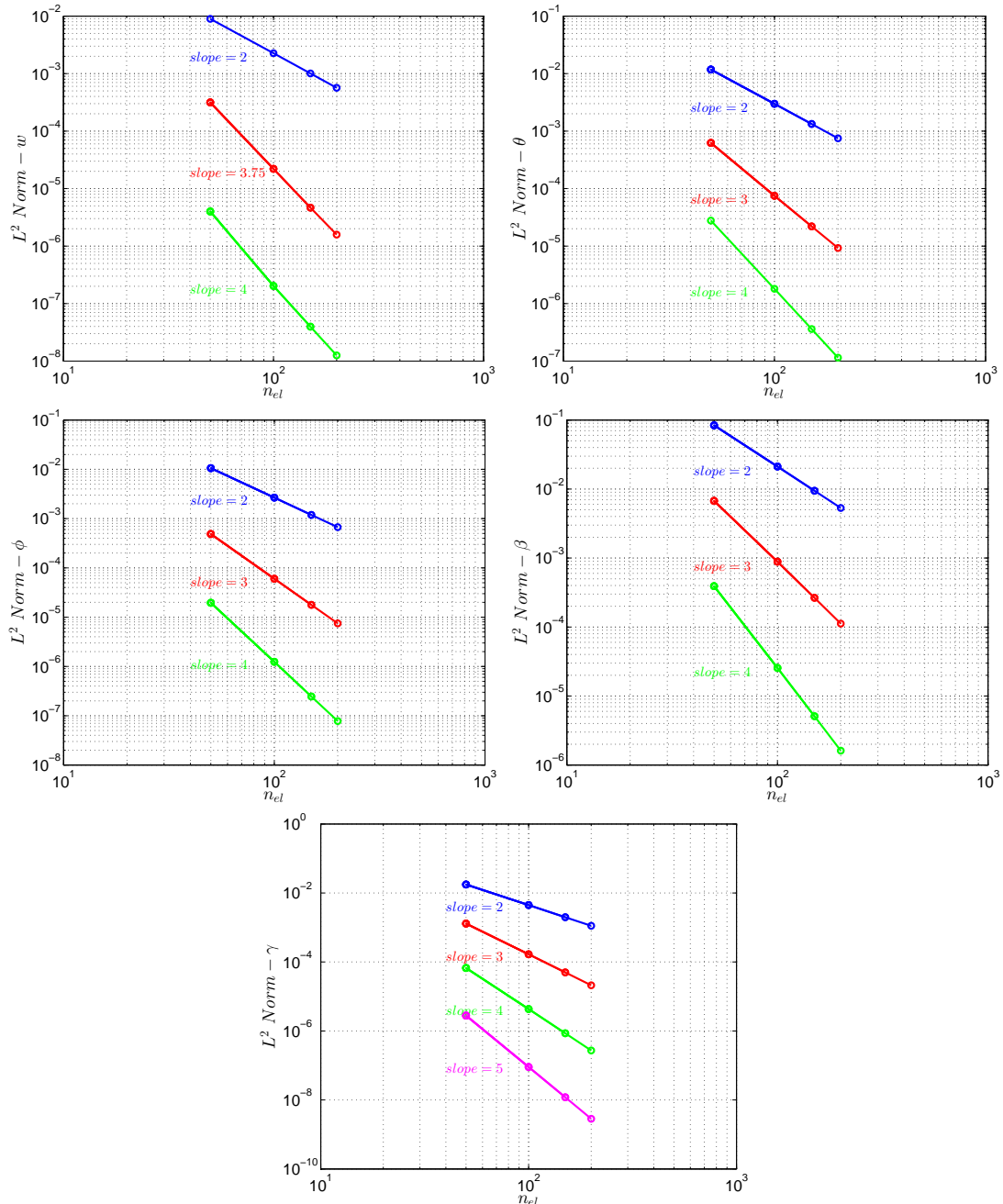
Figure 13: h-convergence of L^2 Norm for each Variable - w, θ, ϕ, β, γ

The gemetric properties are taken as $L = 10$, $h = 1$ for this example. The following plots show the h-convergence of H^1 norm. The convergence of energy norm is also plotted at last. It should be noted that blue lines represent linear basis functions, red quadratic basis, green cubic basis, magenta quartic basis, cyan quintic basis and yellow sextic basis. The convergence of H^1 norm and L^2 norm, completely comply with theoritical predictions.
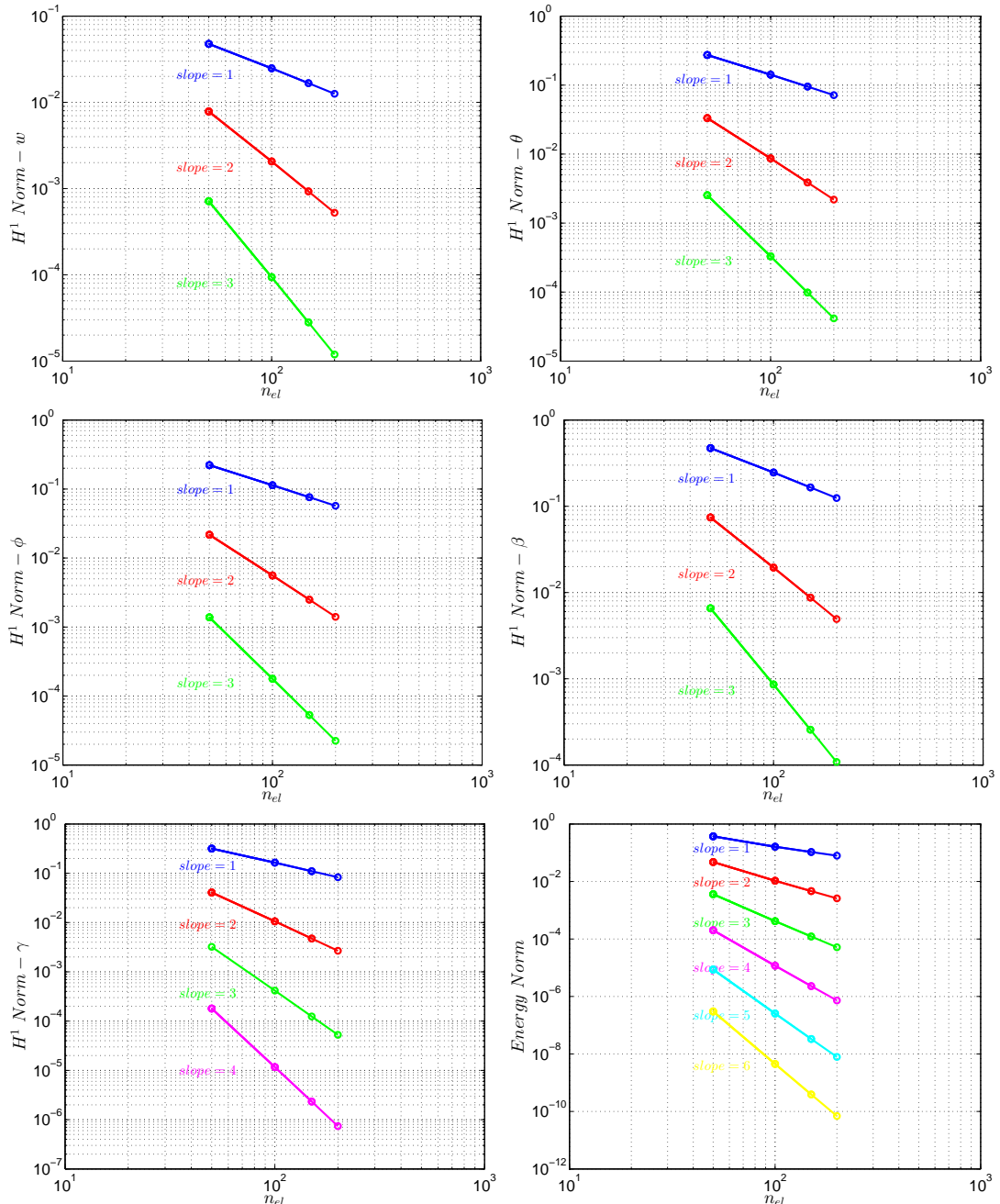
Figure 14: h-convergence of H^1 and Energy norms

56
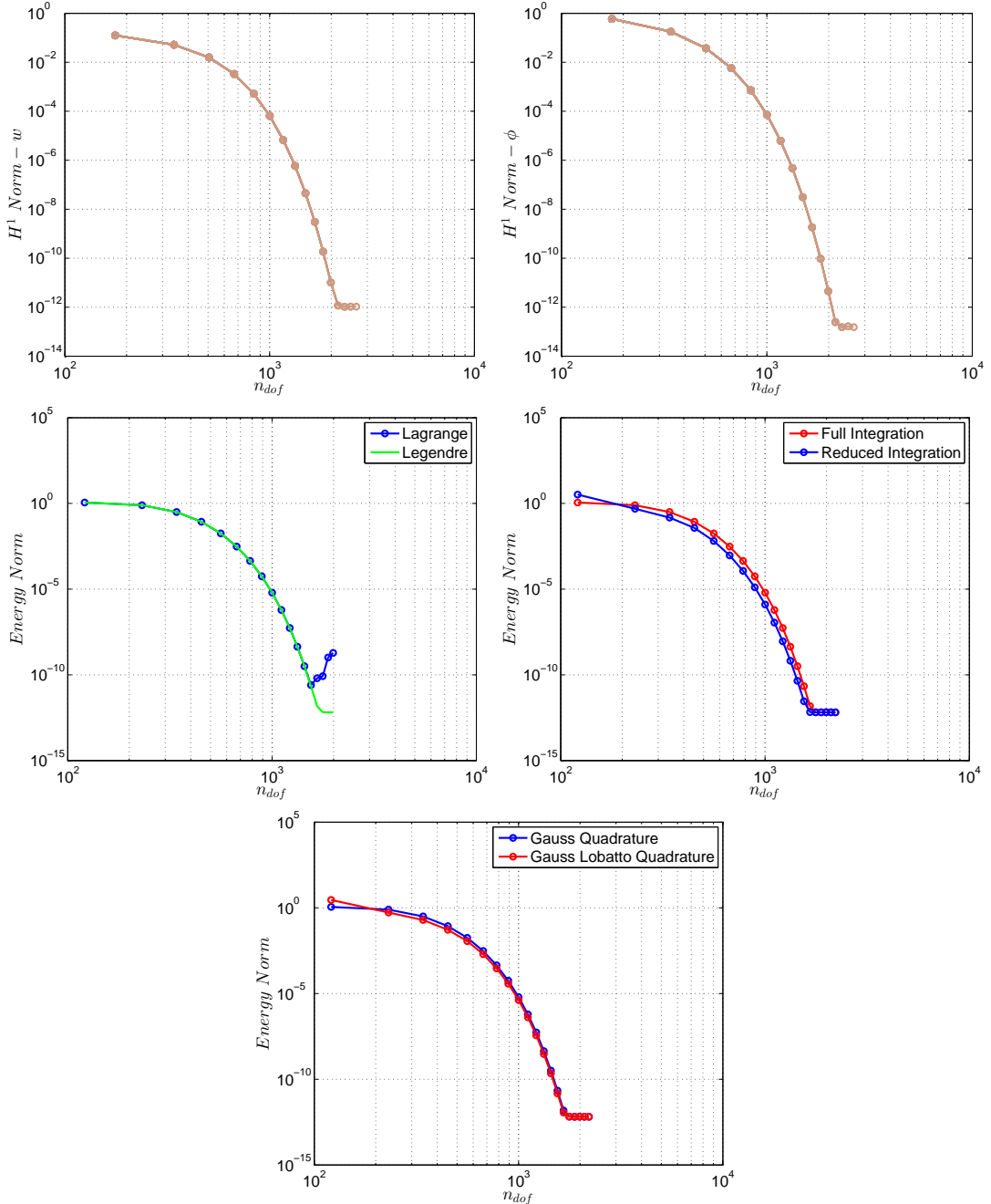
Figure 15: p-Convergence of H^1 and Energy Norms

Since the analytical solution is extremely lengthy and involves many trigonometric, hyperbolic and exponential functions, the accuracy achieved in any computing environemnt is limited due to evaluation of these functions and the numerical solution on the other hand completely justifies this arguement. In fact one can conjecture that the numerical scheme is giving superior results compared to those of analytical.

6.1.2. Energy Harvesting with PZT-5H

We now perform a realistic numerical simulations of energy harvesting with a cantilever beam of PZT-5H in 2D. Since our model is essentially that of Timoshenko which is more suited for thick beams, the dimensions are taken as $h = 1mm$ and $L = 10mm$. The material properties are.

$$\begin{Bmatrix} \lambda \\ \mu \end{Bmatrix} = \begin{Bmatrix} 7.95 \times 10^{10} \\ 2.3 \times 10^{10} \end{Bmatrix} \frac{N}{m^2}, \quad \mathcal{P} = \begin{bmatrix} 0 & 0 & -6.5 \\ 0 & 0 & -6.5 \\ 0 & 0 & 23.3 \\ 0 & 17 & 0 \\ 17 & 0 & 0 \\ 0 & 0 & 0 \end{bmatrix} \frac{C}{m^2}, \quad \boldsymbol{\epsilon} = \begin{bmatrix} 1.505 & 0 & 0 \\ & 1.505 & 0 \\ & & 1.3 \end{bmatrix} 10^{-8} \frac{C}{Vm}$$

As common in the theory of beams, in the post-processing stage we recover stress resultants instead of stresses and strains. Since in our formulation electric displacement resultants also naturally arise, hence its plausible to compute these quantities as well at this stage. However, since these quantities are the internal counterparts of external *"forces i.e. Neumann boundary conditions"*, and in practice such boundary conditions are not imposed, they should be zero. In finite element computations these are the recovered quantities which are certainly not as accurate as the primary variables. This issue can be identified from the following figures.
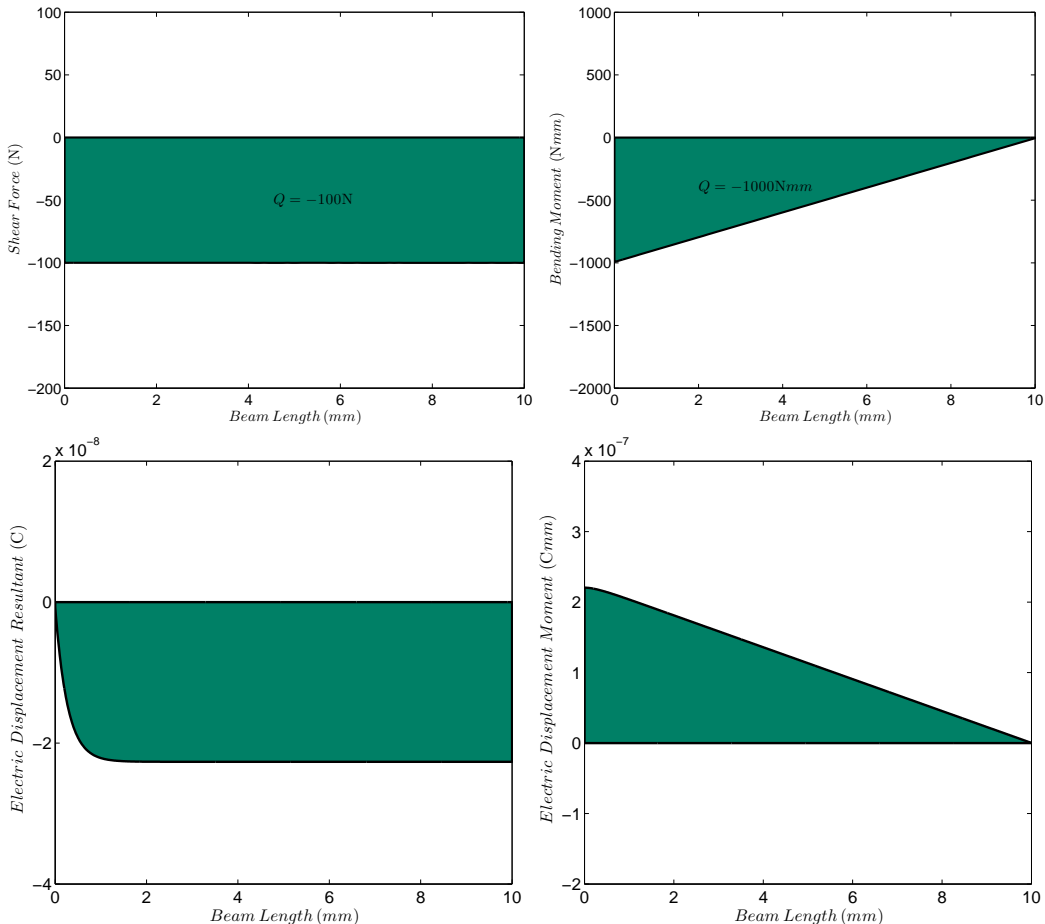

Figure 16: Stress and Electric Displacement Resultants
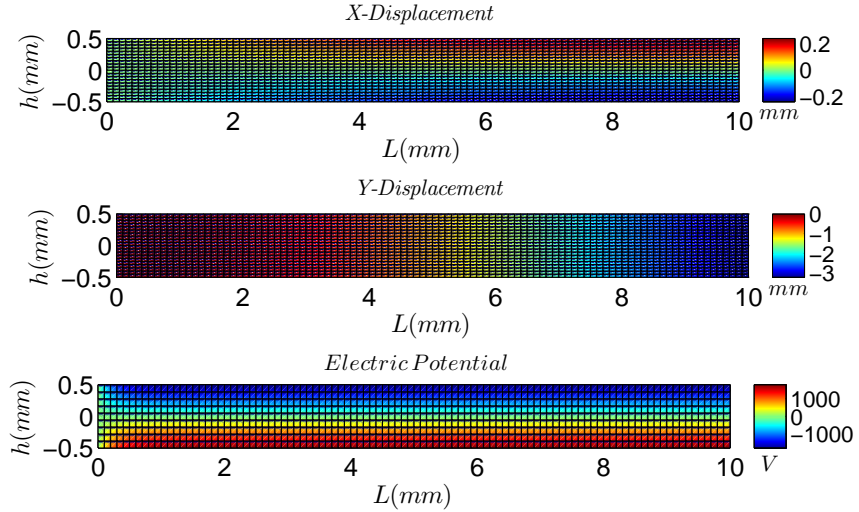
Figure 17: Displacements and Electric Potential (Isotropic Case) on Initial Configuration

It is interesting that the inclusion of anistropy does not affect the results in a significant way for PZT-5H. To include anistropy, we have to use the full elasticity tensor, which for PZT-5H is given by [50].

$$
\mathbb{C} = \begin{bmatrix}
12.6 & 7.95 & 8.41 & 0 & 0 & 0 \\
 & 12.6 & 8.41 & 0 & 0 & 0 \\
 & & 11.7 & 0 & 0 & 0 \\
 & & & 2.3 & 0 & 0 \\
 & & & & 2.3 & 0 \\
sym & & & & & 2.33
\end{bmatrix} \times 10^{10} \frac{N}{m^2}
$$

Looking at the colorbars in Fig. 17 and Fig. 19, one can observe that the differences in the results for isotropic and anistropic cases is in fact small. For a quantitive comparison, Fig. 18 shows the variation of each variable along the length of the beam.
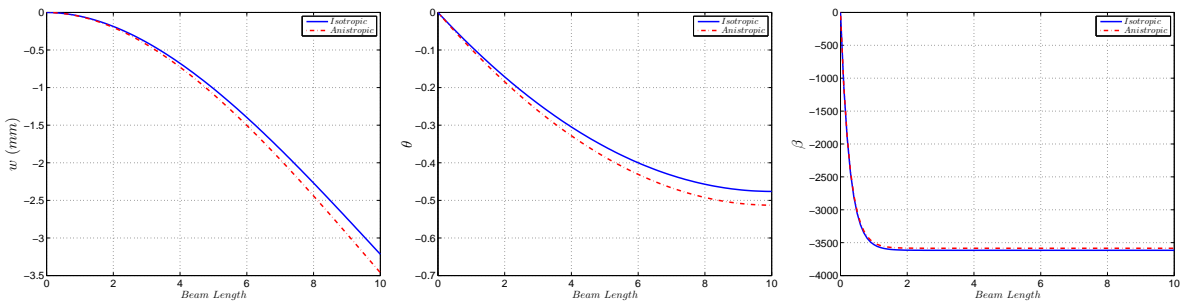
Figure 18: Comparison Between Isotropic & Anistropic Cases for w, θ & β

This is because PZT-5H is a transverse isotropic material which has nonzero off-diagonal entries in its elastic constitutive tensor, and as a matter of fact only two of these elements are accessed in the current example namely C_{33} and C_{55} which are in fact the replacements for Young's modulus and shear modulus in the isotropic case, respectively. Since $C_{55} = \mu$ and C_{33} is a bit less than the Young's modulus hence the stiffness of the system is decreased and as a result the displacements and consequently the electric potential are increased. It should

59

however be noted that the resemblence in final outputs between isotropic and anistropic states is specific to PZT-5H and may also be observed in materials with cubic symmetry, transverse isotropy and orthotropy. The plots in Fig. 18 correspond to the only non-zero variables in this case, since the problem is mechanically driven and all electrostatic boundary conditions are zero.
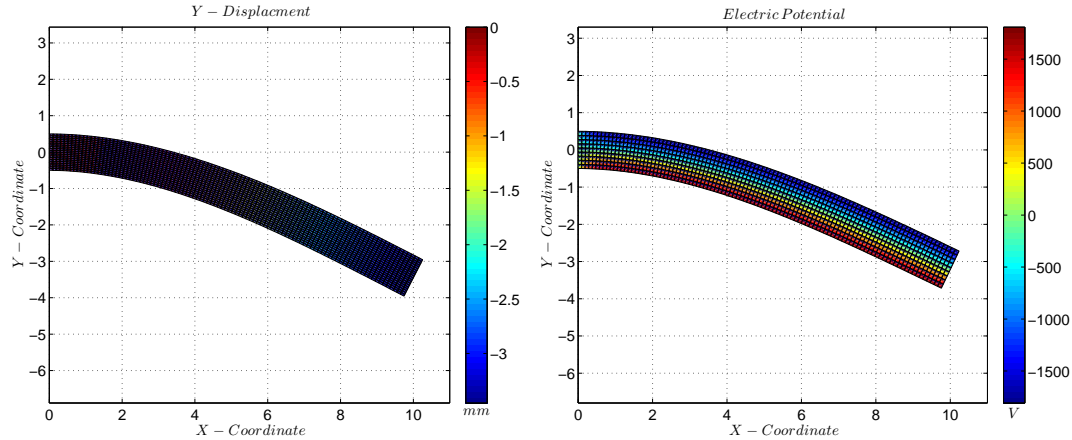

Figure 19: Displacements and Electric Potential (Anistropic Case) on Deformed Configuration

6.1.3. Cantilever with Uniformly Distributed Load

We now analyse an anisotropic PZT-5H cantilever beam under the action of uniformly distributed load. A load of $5\text{N}/mm^2$ is applied on the beam, and the geometric properties of the beam are kept the same as before. To remove locking phenomena we adopt a higher polynomial degree interpolation, since with linear bases, one has to use at least more than 200 elements. The resulting displacements and electric potential are shown in a two-dimensional format.
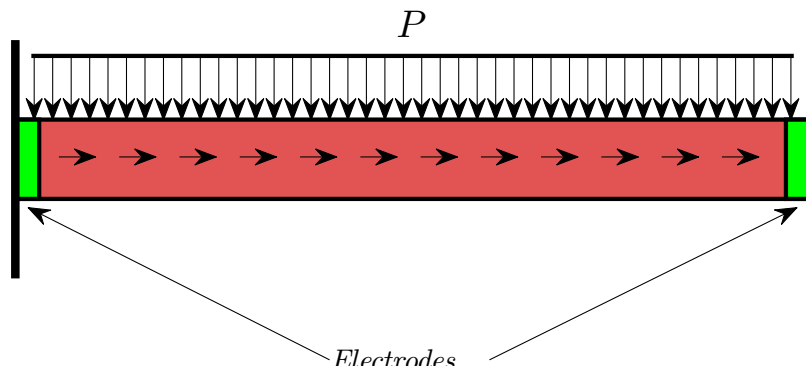

Figure 20: Piezoelectric Cantilever Beam with Uniformly Distributed Load
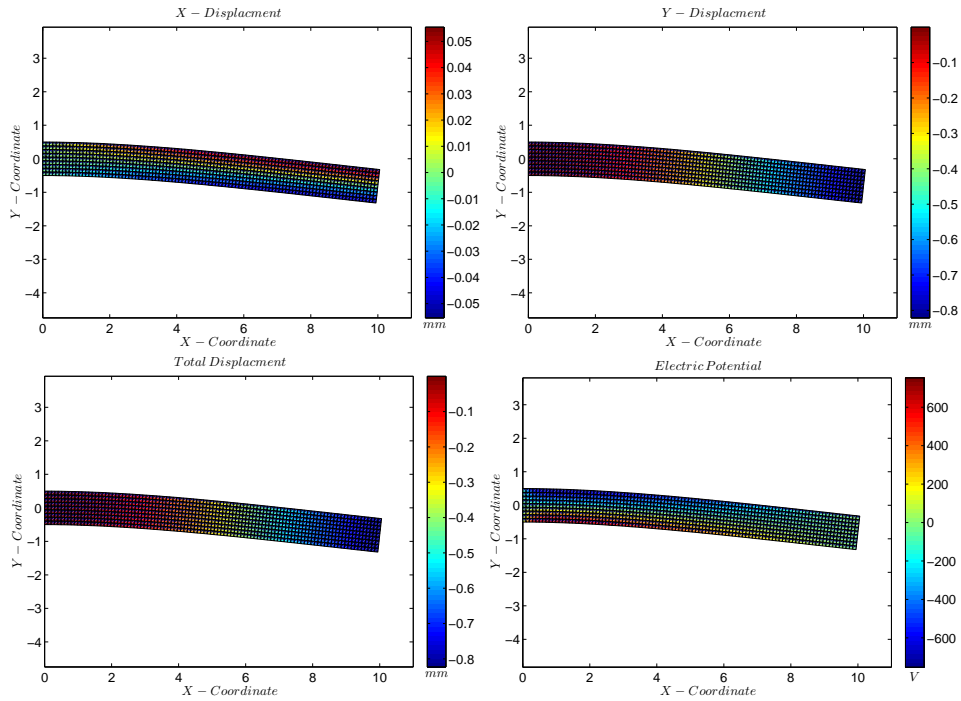
Figure 21: Displacements and Electric Potential on Deformed Configuration

Also, the stress and electric displacement resultants are.
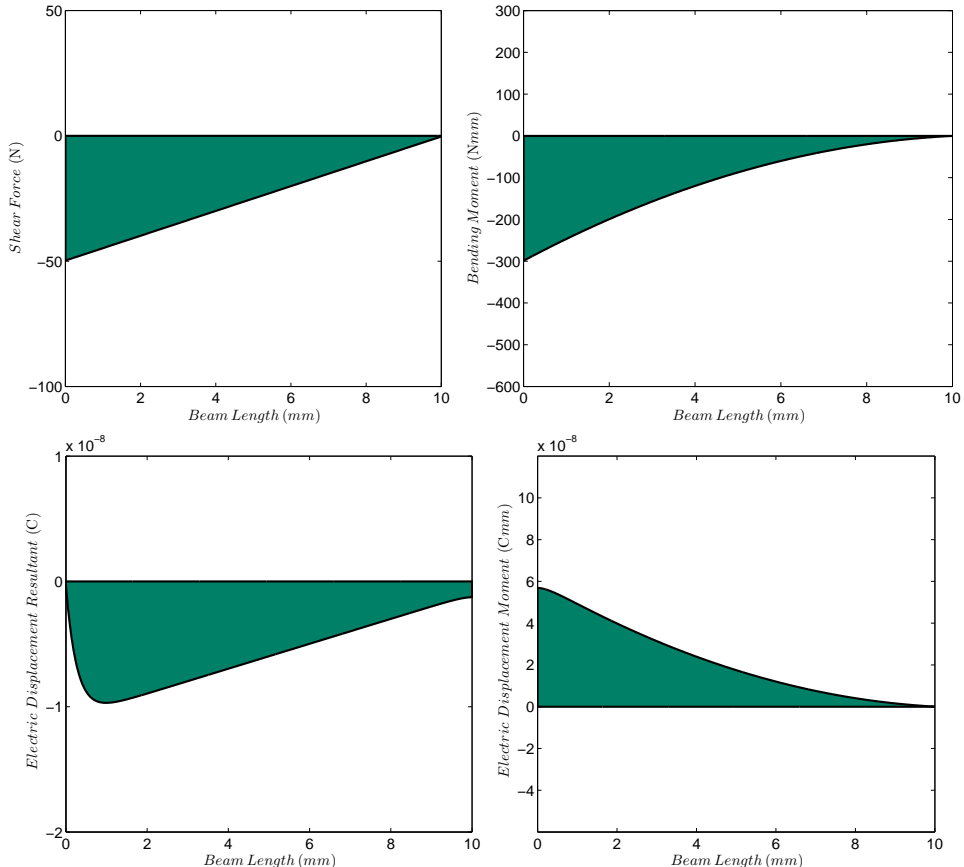
Figure 22: Stress and Electric Displacement Resultants

61

6.2. Modal Analysis

Exciting piezoelectric structures to specific frequencies is crucial in energy harvesting. Many piezoelectric beams function in low frequency range and if they are designed to harvest from ambient vibration, then the lowest frequency of the beam should be adjusted to the natural frequency of ambient structures. For our later investigation, it is essential to perform some eigenvalue analysis. To start off, we benchmark the problem again with the analytical results to assure the reliability of computational scheme. The analytical solution is given in Appendix 3 for simply supported and cantilever planar Timoshenko beams. In the current scenario the mass of piezoelectric structure remains that of Timoshenko and its stiffness is obtained through static condensation which we here call it *"equivalent stiffness"*. It is in fact advantageous to benchmark our eigenvalue problem with Timoshenko model as the inclusion of piezoelectricity shifts the eigenspectrum by a small amount; and this is the case for a major class of piezoelectric materials. This argument is followed by the Fig. 23.
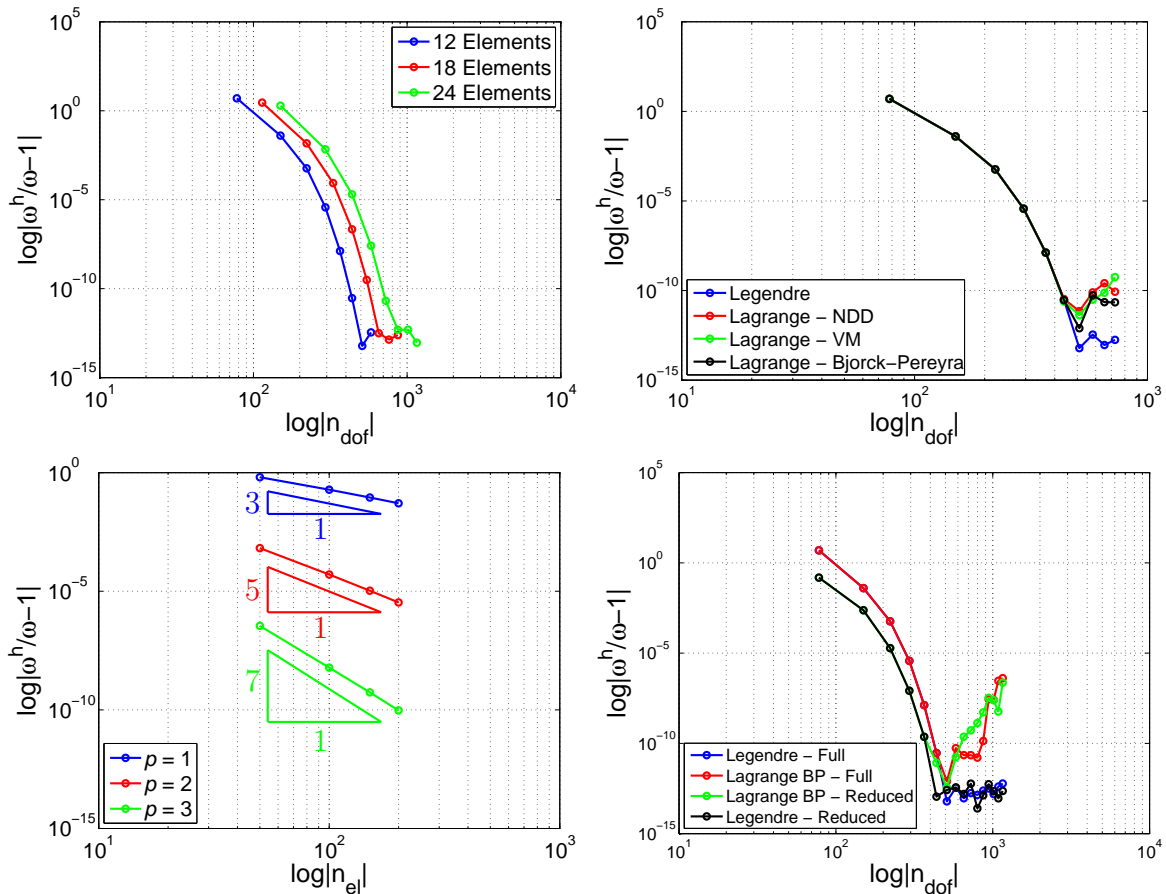

Figure 23: *hp* Convergence of 4th Eigenfrequency for Simply Supported Beam

Note that in Fig. 23 [bottom-right one] a uniformly reduced integration is not performed for Legendre basis functions [2], and thus it may not correspond to a mixed formulation, mathematically, as in the case of Lagrangian basis with uniformly reduced integration and so their comparison [Lagrange and Legendre] is perhaps not plausible.

---

[2]Since Legendre basis functions are hierarchical, implementing a uniformly reduced integration becomes difficult, as each element of the stiffness matrix will have a different polynomial degree.

Cantilever case is considered next. Fig. 24 follows the argument.
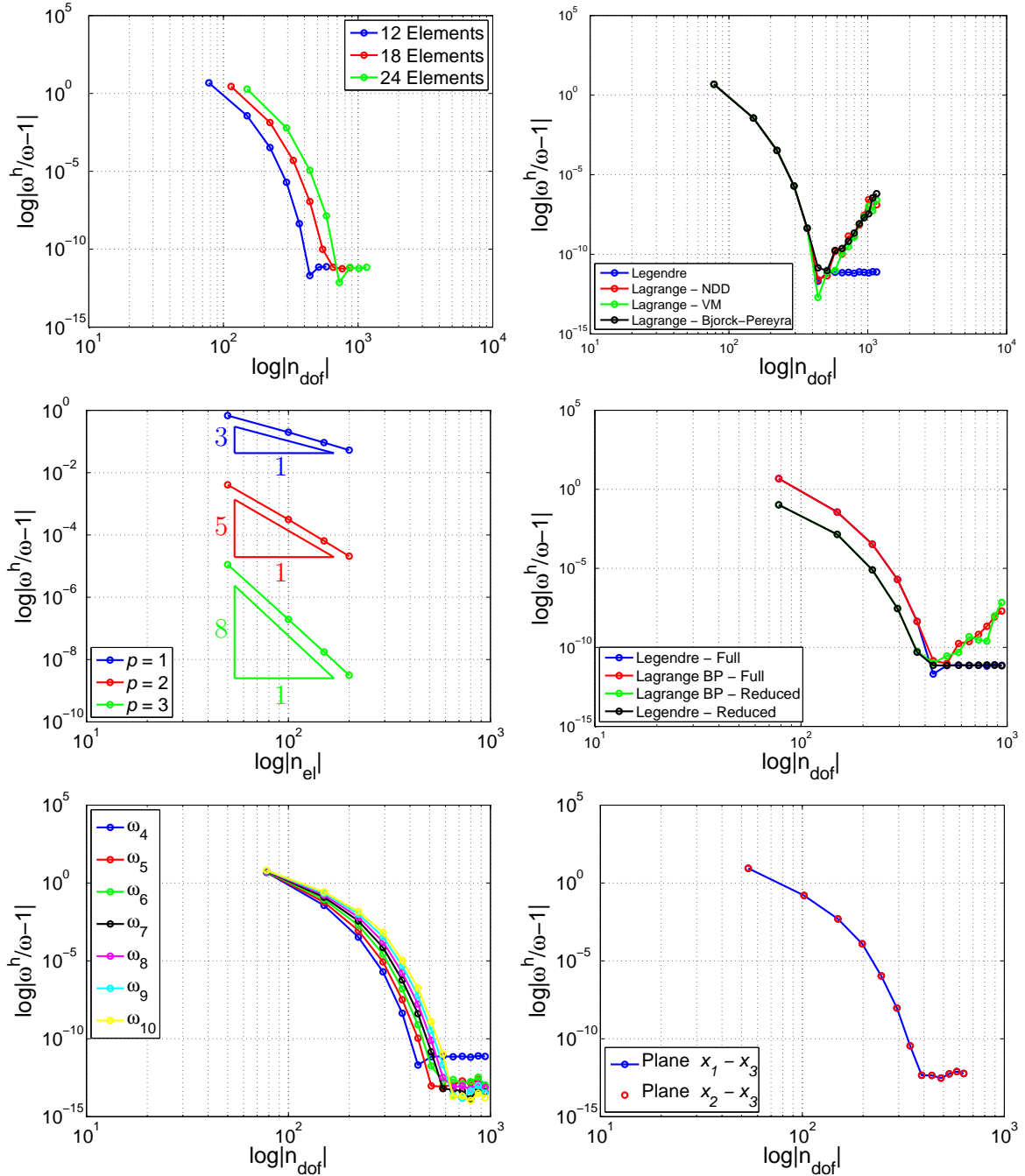
Figure 24: *hp* Convergence of 4th Eigenfrequency for Cantilever Beam

As mentioned earlier, the deformation in the plane $x_1 - x_3$ and the plane $x_2 - x_3$ are identical for purely mechanical beams, which is well captured by the numerical scheme as shown in Fig. 24 [bottom-right]. In this analysis 5th frequency of the planes are compared. Note that in this analysis material properties are assumed as $\lambda = 0$, $\mu = \frac{1}{2}10^6$ and $\rho = 500$ and the remaining results all correspond to those of plane $x_1 - x_3$.

63

Now that we have benchmarked our scheme, we perform modal analysis for a thin anistropic PZT-5H cantilever beam with $L = 30mm$, $b = 10mm$ and $h = 1mm$. Normalised eigenmodes and eigen-frequencies are shown below. The magnitude in the colorbar indicates normalised absolute magnitude of total deformation.
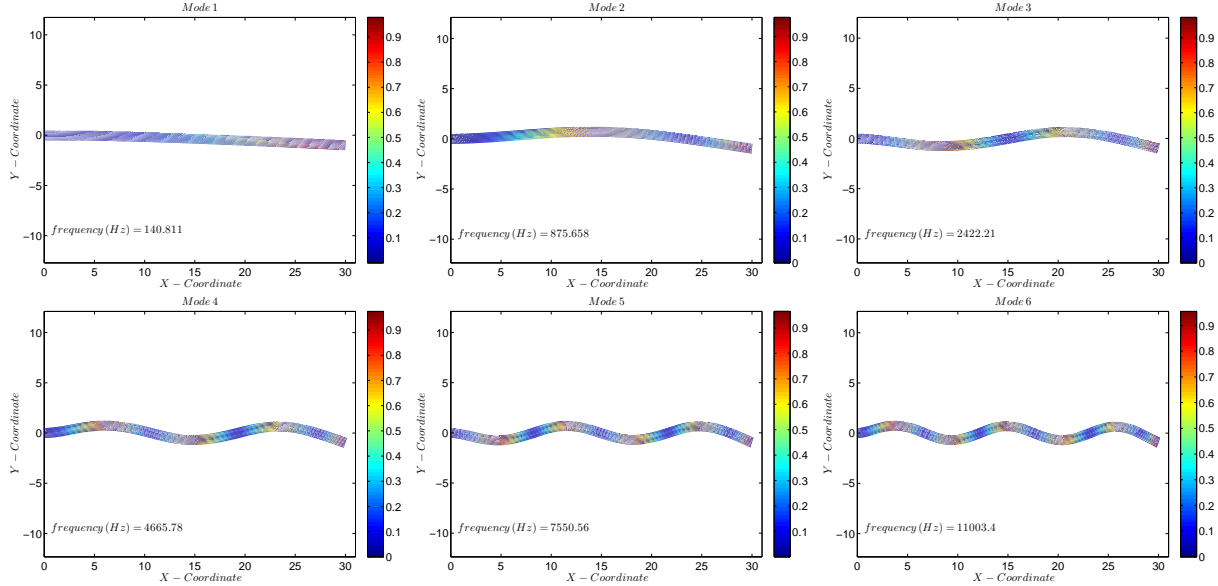

Figure 25: Normalised Eigen Modes and Frequencies of PZT-5H - Coupled Equivalent Stiffness
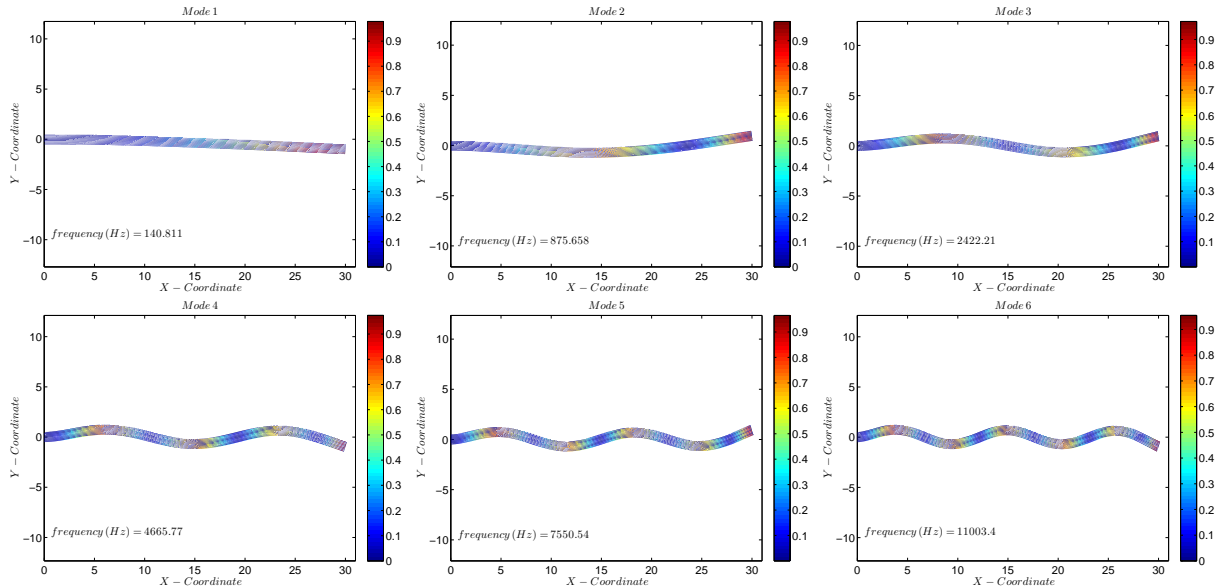
Figure 26: Normalised Eigen Modes and Frequencies of PZT-5H - Purely Mechanical Stiffness

One can observe that eigenvalues and normalised eigenvectors for mechanical stiffness and equivalent stiffness have remained the same. To evaluate this more precisely, let us dig a bit deeper. Table Table 1 lists the natural frequencies in each case for up to ω_{10}.

Table 1: Natural Frequencies

| Mode	ω_m	ω_p	$\frac{\omega_m - \omega_p}{\omega_m}$
1	140.81149134	140.81149451	2.25613409e-08
2	875.65766700	875.65805424	4.42223200e-07
3	2422.20896950	2422.21145393	1.02568804e-06
4	4665.76977219	4665.77830766	1.82938086e-06
5	7550.54225521	7550.56336363	2.79561643e-06
6	11003.36779600	11003.41050281	3.88124838e-06
7	14950.01035772	14950.08575128	5.04304395e-06
8	19318.97869416	19319.09929792	6.24276081e-06
9	24044.52728908	24044.70637895	7.44825923e-06
10	29068.14324649	29068.39421358	8.63375018e-06
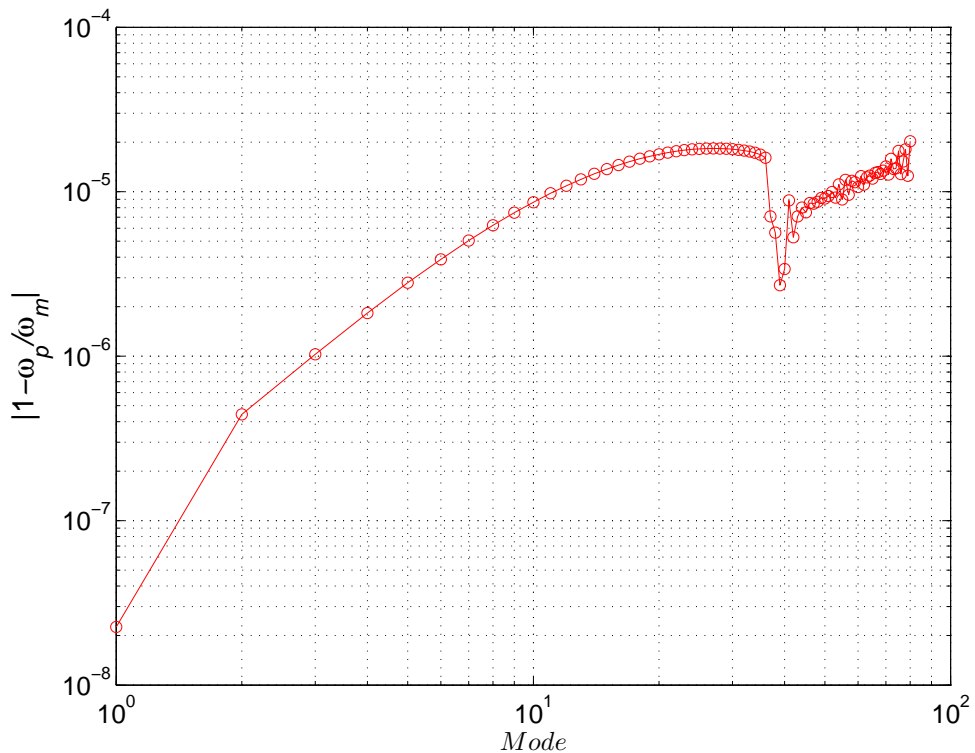
Figure 27: Absolute Relative Difference in Frequency Response between Mechanical Stiffness and Equivalent Piezoelectric Stiffness

It should be noted that higher order frequencies are normally not accurate in finite elements [25] and the results above should be looked upon with suspicion. However from Table 1 one can observe a minute shift in frequencies. Since the piezoelectric and dielectric parameters are way smaller than the mechanical ones, these results may differ from material to material.

6.3. Dynamic Analysis

In this section, we perform dynamic analysis on cantilever piezoelectric beams. Since we have utilised higher order basis functions, the computational cost of dynamic problems for larger systems will be reduced substantially if we perform static condensation for interior degrees of freedom. To perform static condensation in a dynamic scenario is not that straightforward. To show how static condensation is performed for problems involving inertial terms, consider the HHT-α method which is one of the most generic methods in the family implicit dynamic integrators for structural problems, with integration parameters α, δ and γ [cf. Appendix 4 for procedural details of direct time integrators utilised in this work].

$$\boldsymbol{M}\ddot{\vec{u}}_{i+1} + (1+\gamma)\boldsymbol{K}\vec{u}_{i+1} - \gamma\boldsymbol{K}\vec{u}_i = (1+\gamma)\vec{F}_{i+1} - \gamma\vec{F}_i \tag{6.1}$$

$$\dot{\vec{u}}_{i+1} = \dot{\vec{u}}_i + \Delta t\left[(1-\delta)\ddot{\vec{u}}_i + \delta\ddot{\vec{u}}_{i+1}\right] \tag{6.2}$$

$$\vec{u}_{i+1} = \vec{u}_i + \Delta t\dot{\vec{u}}_i + \Delta t^2\left[(\frac{1}{2}-\alpha)\ddot{\vec{u}}_i + \alpha\ddot{\vec{u}}_{i+1}\right] \tag{6.3}$$

While carrying out static condensation on global matrices, the above equations can be rewritten in the following form.

$$\begin{bmatrix}\boldsymbol{M}_{aa} & \boldsymbol{M}_{ab} \\ \boldsymbol{M}_{ba} & \boldsymbol{M}_{bb}\end{bmatrix}\begin{Bmatrix}\ddot{\vec{u}}^a_{i+1} \\ \ddot{\vec{u}}^b_{i+1}\end{Bmatrix} + (1+\gamma)\begin{bmatrix}\boldsymbol{K}_{aa} & \boldsymbol{K}_{ab} \\ \boldsymbol{K}_{ba} & \boldsymbol{K}_{bb}\end{bmatrix}\begin{Bmatrix}\vec{u}^a_{i+1} \\ \vec{u}^b_{i+1}\end{Bmatrix} - \gamma\begin{bmatrix}\boldsymbol{K}_{aa} & \boldsymbol{K}_{ab} \\ \boldsymbol{K}_{ba} & \boldsymbol{K}_{bb}\end{bmatrix}\begin{Bmatrix}\vec{u}^a_i \\ \vec{u}^b_i\end{Bmatrix}$$

$$= (1+\gamma)\begin{Bmatrix}\vec{F}^a_{i+1} \\ \vec{F}^b_{i+1}\end{Bmatrix} - \gamma\begin{Bmatrix}\vec{F}^a_i \\ \vec{F}^b_i\end{Bmatrix} \tag{6.4}$$

$$\begin{Bmatrix}\dot{\vec{u}}^a_{i+1} \\ \dot{\vec{u}}^b_{i+1}\end{Bmatrix} = \begin{Bmatrix}\dot{\vec{u}}^a_i \\ \dot{\vec{u}}^b_i\end{Bmatrix} + \Delta t\left[(1-\delta)\begin{Bmatrix}\ddot{\vec{u}}^a_i \\ \ddot{\vec{u}}^b_i\end{Bmatrix} + \delta\begin{Bmatrix}\ddot{\vec{u}}^a_{i+1} \\ \ddot{\vec{u}}^b_{i+1}\end{Bmatrix}\right] \tag{6.5}$$

$$\begin{Bmatrix}\vec{u}^a_{i+1} \\ \vec{u}^b_{i+1}\end{Bmatrix} = \begin{Bmatrix}\vec{u}^a_i \\ \vec{u}^b_i\end{Bmatrix} + \Delta t\begin{Bmatrix}\dot{\vec{u}}^a_i \\ \dot{\vec{u}}^b_i\end{Bmatrix} + \Delta t^2\left[(\frac{1}{2}-\alpha)\begin{Bmatrix}\ddot{\vec{u}}^a_i \\ \ddot{\vec{u}}^b_i\end{Bmatrix} + \alpha\begin{Bmatrix}\ddot{\vec{u}}^a_{i+1} \\ \ddot{\vec{u}}^b_{i+1}\end{Bmatrix}\right] \tag{6.6}$$

From (6.6) we have.

$$\begin{Bmatrix}\ddot{\vec{u}}^a_{i+1} \\ \ddot{\vec{u}}^b_{i+1}\end{Bmatrix} = \frac{1}{\Delta t^2\alpha}\left[\begin{Bmatrix}\vec{u}^a_{i+1} \\ \vec{u}^b_{i+1}\end{Bmatrix} - \begin{Bmatrix}\vec{u}^a_i \\ \vec{u}^b_i\end{Bmatrix}\right] - \frac{1}{\Delta t\alpha}\begin{Bmatrix}\dot{\vec{u}}^a_i \\ \dot{\vec{u}}^b_i\end{Bmatrix} + (1-\frac{1}{2\alpha})\begin{Bmatrix}\ddot{\vec{u}}^a_i \\ \ddot{\vec{u}}^b_i\end{Bmatrix} \tag{6.7}$$

Substituting (6.7) in (6.4), and condensing out $\vec{u}^b_{i+1}$, after lengthy algebra we obtain,

$$\left[\tilde{\boldsymbol{K}}_{aa} - \tilde{\boldsymbol{K}}_{ab}\tilde{\boldsymbol{K}}^{-1}_{bb}\tilde{\boldsymbol{K}}_{ba}\right]\vec{u}^a_{i+1} = (1+\gamma)\left[\vec{F}^a_{i+1} - \tilde{\boldsymbol{K}}_{ab}\tilde{\boldsymbol{K}}^{-1}_{bb}\vec{F}^b_{i+1}\right]$$

$$-\gamma\left[\vec{F}^a_i - \tilde{\boldsymbol{K}}_{ab}\tilde{\boldsymbol{K}}^{-1}_{bb}\vec{F}^b_i\right] + \left[\hat{\boldsymbol{K}}_{aa} - \tilde{\boldsymbol{K}}_{ab}\tilde{\boldsymbol{K}}^{-1}_{bb}\hat{\boldsymbol{K}}_{ba}\right]\vec{u}^a_i + \left[\hat{\boldsymbol{K}}_{ab} - \tilde{\boldsymbol{K}}_{ab}\tilde{\boldsymbol{K}}^{-1}_{bb}\hat{\boldsymbol{K}}_{bb}\right]\vec{u}^b_i$$

$$+ \frac{1}{\Delta t\alpha}\left[\boldsymbol{M}_{aa} - \tilde{\boldsymbol{K}}_{ab}\tilde{\boldsymbol{K}}^{-1}_{bb}\boldsymbol{M}_{ba}\right]\dot{\vec{u}}^a_i + \frac{1}{\Delta t\alpha}\left[\boldsymbol{M}_{ab} - \tilde{\boldsymbol{K}}_{ab}\tilde{\boldsymbol{K}}^{-1}_{bb}\boldsymbol{M}_{bb}\right]\dot{\vec{u}}^b_i$$

$$- (1-\frac{1}{2\alpha})\left[\boldsymbol{M}_{aa} - \tilde{\boldsymbol{K}}_{ab}\tilde{\boldsymbol{K}}^{-1}_{bb}\boldsymbol{M}_{ba}\right]\ddot{\vec{u}}^a_i - (1-\frac{1}{2\alpha})\left[\boldsymbol{M}_{aa} - \tilde{\boldsymbol{K}}_{ab}\tilde{\boldsymbol{K}}^{-1}_{bb}\boldsymbol{M}_{bb}\right]\ddot{\vec{u}}^b_i \tag{6.8}$$

where,

$$\tilde{\boldsymbol{K}}_{mn} = (1 + \gamma)\boldsymbol{K}_{mn} + \frac{1}{\Delta t^2 \alpha} \boldsymbol{M}_{mn} \tag{6.9}$$

$$\hat{\boldsymbol{K}}_{mn} = \gamma \boldsymbol{K}_{mn} + \frac{1}{\Delta t^2 \alpha} \boldsymbol{M}_{mn} \tag{6.10}$$

for any $m, n = a, b$. Once the exterior degrees of freedom $\vec{u}_{i+1}^a$ are computed, the interior degrees of freedom $\vec{u}_{i+1}^b$ can be computed as.

$$\tilde{\boldsymbol{K}}_{bb}\vec{u}_{i+1}^b = \hat{\boldsymbol{K}}_{bb}\vec{u}_i^b - \tilde{\boldsymbol{K}}_{ba}\vec{u}_{i+1}^a + \hat{\boldsymbol{K}}_{ba}\vec{u}_i^a + \boldsymbol{M}_{bb}\left[\frac{1}{\Delta t\alpha}\dot{\vec{u}}_i^b - (1 - \frac{1}{2\alpha})\ddot{\vec{u}}_i^b\right]$$
$$+ \boldsymbol{M}_{ba}\left[\frac{1}{\Delta t\alpha}\dot{\vec{u}}_i^a - (1 - \frac{1}{2\alpha})\ddot{\vec{u}}_i^a\right] + (1 + \gamma)\vec{F}_{i+1}^b - \gamma\vec{F}_{i+1}^b \tag{6.11}$$

The algorithm is summarised in the following.

---

1. Build Stiffness $\boldsymbol{K}$ and Mass $\boldsymbol{M}$ Matrices.

2. Split the matrices into exterior and interior parts $\boldsymbol{K}_{mn}$ and $\boldsymbol{M}_{mn}$, $[m, n = a, b]$

3. Build modified *stiffness* matrices $\tilde{\boldsymbol{K}}_{mn}$ and $\hat{\boldsymbol{K}}_{mn}$, $[m, n = a, b]$

4. Initiate nodal displacements $\vec{u}_0$, nodal velocities $\dot{\vec{u}}_0$ and nodal forces vectors $\vec{F}_0$

5. Choose Δt, *nstep*, α, δ and γ.

6. For each time step compute the nodal quantities

   (a) Compute nodal displacements of exterior DoF's $\vec{u}_{i+1}^a$ from (6.8)

   (b) Compute nodal displacements of interior DoF's $\vec{u}_{i+1}^b$ from (6.11)

   (c) Compute nodal accelerations

   $$\left\{\begin{matrix} \ddot{\vec{u}}_{i+1}^a \\ \ddot{\vec{u}}_{i+1}^b \end{matrix}\right\} = \frac{1}{\Delta t^2 \alpha}\left[\left\{\begin{matrix} \vec{u}_{i+1}^a \\ \vec{u}_{i+1}^b \end{matrix}\right\} - \left\{\begin{matrix} \vec{u}_i^a \\ \vec{u}_i^b \end{matrix}\right\}\right] - \frac{1}{\Delta t\alpha}\left\{\begin{matrix} \dot{\vec{u}}_i^a \\ \dot{\vec{u}}_i^b \end{matrix}\right\} + (1 - \frac{1}{2\alpha})\left\{\begin{matrix} \ddot{\vec{u}}_i^a \\ \ddot{\vec{u}}_i^b \end{matrix}\right\}$$

   (d) Compute nodal velocities :

   $$\left\{\begin{matrix} \dot{\vec{u}}_{i+1}^a \\ \dot{\vec{u}}_{i+1}^b \end{matrix}\right\} = \left\{\begin{matrix} \dot{\vec{u}}_i^a \\ \dot{\vec{u}}_i^b \end{matrix}\right\} + \Delta t\left[(1 - \delta)\left\{\begin{matrix} \ddot{\vec{u}}_i^a \\ \ddot{\vec{u}}_i^b \end{matrix}\right\} + \delta\left\{\begin{matrix} \ddot{\vec{u}}_{i+1}^a \\ \ddot{\vec{u}}_{i+1}^b \end{matrix}\right\}\right]$$

Before starting with the dynamics of piezoelectric beams, we first examine the performance of the developed methodology with the same geometry and material parameters used for modal analysis. The following plots compare dynamical results for the choice of static condensation and different polynomial bases - p.
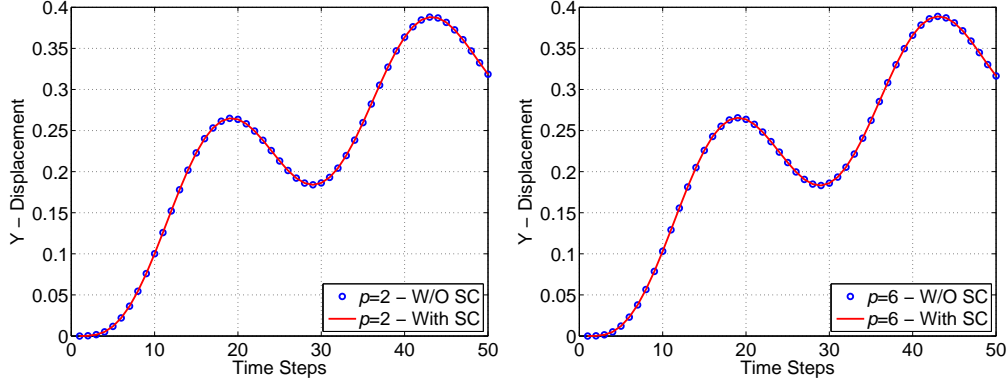

Figure 28: HHT-α integrator with & without static condensation
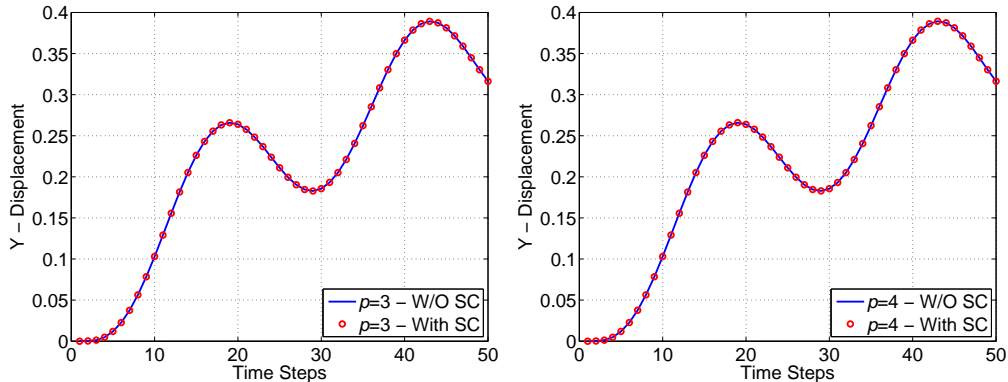
Figure 29: Newmark's Method with & without static condensation
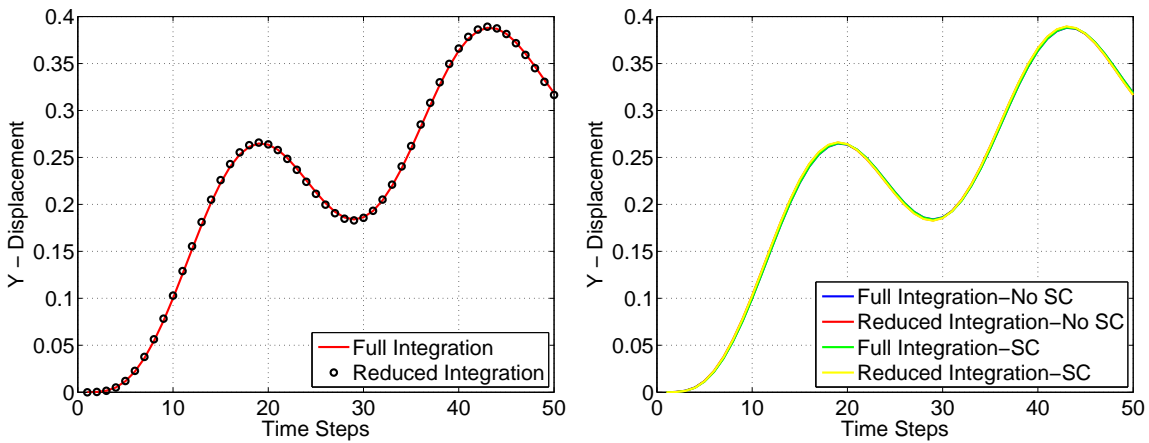
Figure 30: The choice of full & reduced integration for stiffness matrix; Left - HHT-α Method, Right - Newmark's Method

As the first example of energy harvesting via vibration, we analyse a thick cantilever beam of anistropic PZT-5H under the action of sinusoidal point load $P = 100 \sin x$, $x = 0, 4\pi$. The dimensions are $L = 10mm$ and $h = 1mm$.
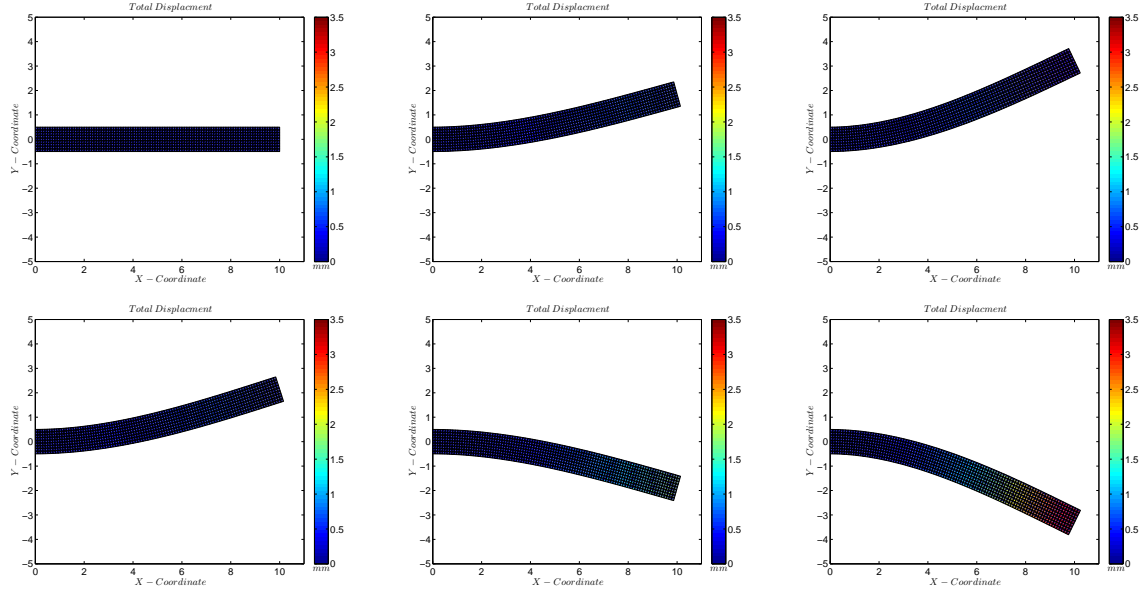

Figure 31: Total Displacements at Various Time-Steps

6.3.1. An Ambient Vibration Energy Harvester Undergoing Coupled Bending-Torsion

In this section we analyse a fully three-dimensional piezoelectric energy harvesting beam undergoing coupled bending torsion vibration. As reported by [1], coupled bending-torsion harvesters can function on broader frequency ranges and are advantageous in improving efficiency of energy harvesting. To this effect, we analyse a fibre of AT-cut Quartz with dimensions as follows,

Table 2: Beam Dimensions

Material	Length (mm)	Height (mm)	Width (mm)
AT-cut Quartz	40	0.9	12

and material properties as [50].

$$\rho = 2649\frac{kg}{m^3}, \qquad \mathbb{C} = \begin{bmatrix} 86.74 & -8.25 & 27.15 & -3.66 & 0 & 0 \\ & 129.77 & -7.42 & 5.7 & 0 & 0 \\ & & 102.83 & 9.92 & 0 & 0 \\ & & & 38.61 & 0 & 0 \\ & & & & 68.81 & 2.53 \\ sym & & & & & 29.01 \end{bmatrix} \times 10^9 \frac{N}{m^2}$$

$$\mathcal{P} = \begin{bmatrix} 0.171 & 0 & 0 \\ -0.152 & 0 & 0 \\ -0.0187 & 0 & 0 \\ 0.067 & 0 & 0 \\ 0 & 0.108 & -0.0761 \\ 0 & -0.095 & 0.067 \end{bmatrix} \frac{C}{m^2}, \quad \boldsymbol{\epsilon} = \begin{bmatrix} 39.21 & 0 & 0 \\ & 39.82 & 0.86 \\ sym & & 40.42 \end{bmatrix} \times 10^{-12} \frac{C}{Vm}$$

To start with, we first compute the first six natrual frequencies of the beam. The dimensions of the beam are chosen such that one of these modes (sixth mode) correspond to twisting. In the next step, we perform a static analysis and compare the results obtained with first order and second order electrical potential assumption across the thickness. For computing natrual frequencies, we employ 5th order Lagrange basis functions using 50 elements. As observed in the modal analysis section, higher order bases produce robust results up to computer precision. The first six natural frequencies are listed in Table 3.

Table 3: Natural Frequencies of Bending-Torsion Fibre (Hz)

1	2	3	4	5	6
112.4549400	703.7163505	1412.3115348	1965.8138759	3839.1405538	6321.4888954

The mode shapes corresponding to these frequencies are shown in the Fig. 32. Note that for the purpose of plotting the interior degrees of freedom are condensed out and the colors in the plot which essentially show the absolute magnitude of deformation are magnified by a scale of 50.
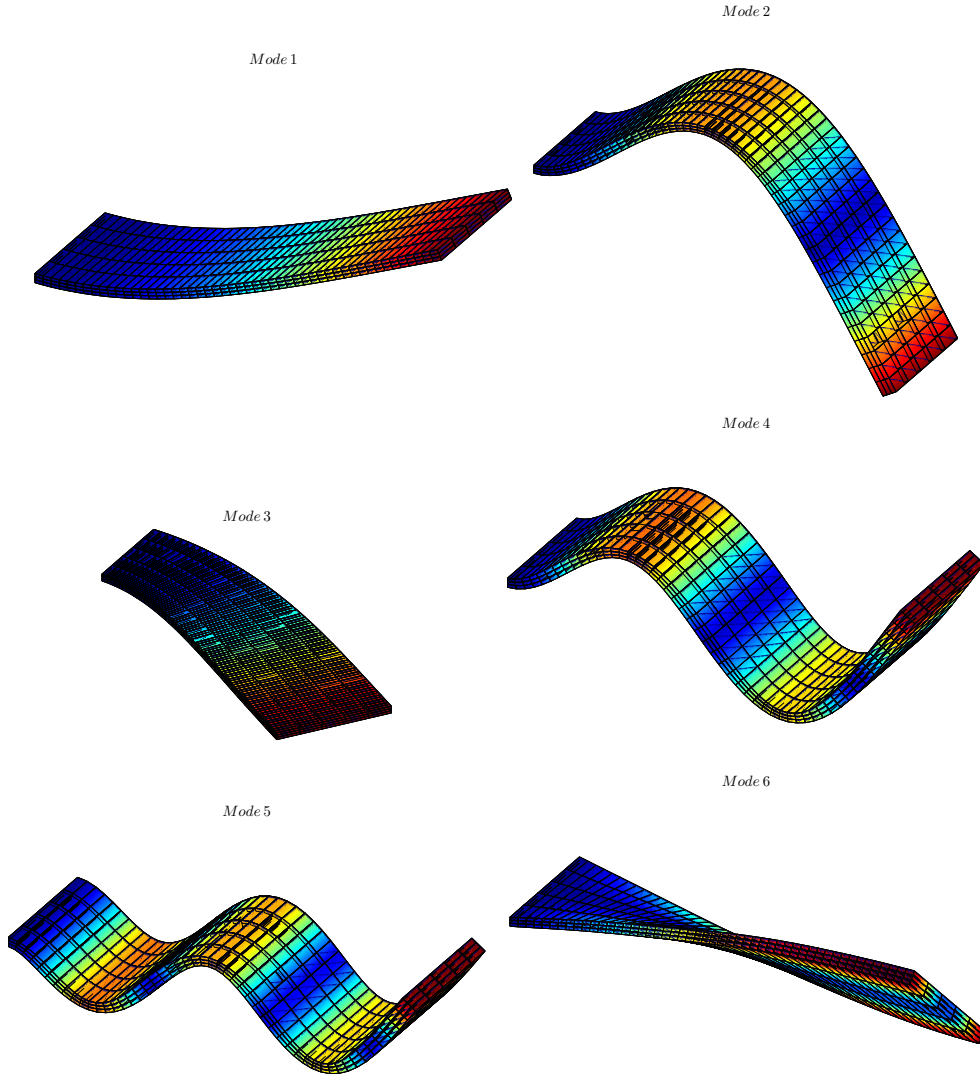
Figure 32: First Six Modes of Bending-Torsion Fibre

This problem is completely coupled in nature. Unlike the common three-dimensional mechanical beam problems in which displacements and rotations in one direction do not affect those of the other directions, here due to the usage of full material tensors the electrical potential counterparts of rotations i.e. electric potential gradients and hessians β_α and γ_α are coupled in all directions although mechanical variables are still decoupled. This is the sophistication of this formulation which although still using the simple mechanics of beams we can replicate the linear piezoelectric behaviour reliably. As pointed out in first section the available piezoelectric beam models in the literature are extremely simplified, a good number of which rely on the assumption that electric field/electric displacement vanish in some specified direction(s) [4] [12]. At the end, depending on the level of simplification, a lot is taken away from the actual physics of the problem. We categorise the static analysis into three cases, bending only, torsion only and coupled bending torsion. The loading scenarios are listed in the following table, where a negative sign indicates downward loading and a positive moment stands for clockwise rotation.

Table 4: Loading Scenarios for Bending-Torsion Harvester

Cases/ Load	End Point Load (N)	End Twisting Moment (Nmm)
Case 1 - Bending	-5	0
Case 2 - Torsion	0	150
Case 3 - Bending-Torsion	-5	150

The electric potential is plotted in the following figures on the deformed mesh. Note that while the potential produced between end electrodes can be high for sensor application, our aim here is to find optimum electric output for energy harvesting purposes.
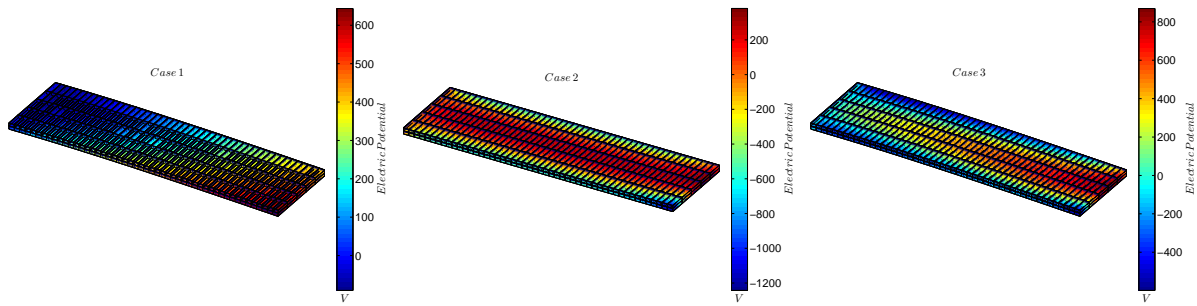

Figure 33: Voltage Output for Three Loading Cases

One important aspect that we would like to shed some light upon is the inclusion of quadratic term in electric potential. To show how the results vary from a linear case to quadratic case, we first show the variation of each variable over the length of the beam. These are shown in the following figures for the coupled bending-torsion case.
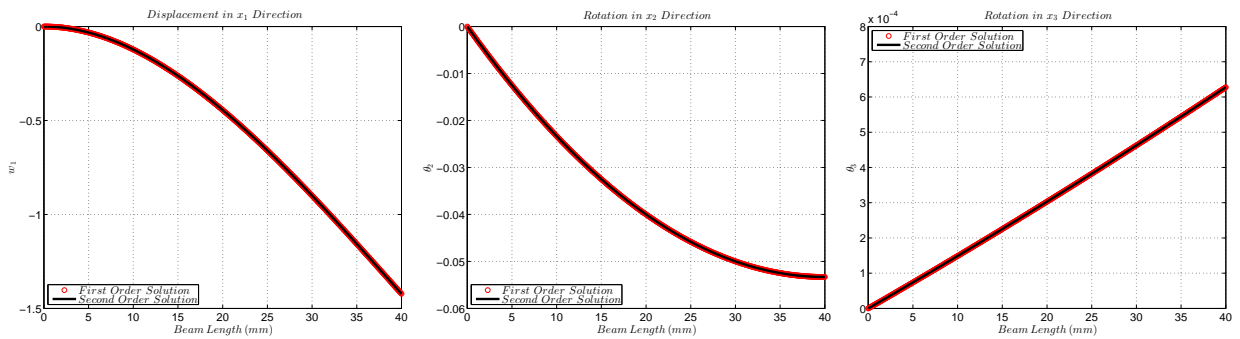

Figure 34: Variation of Mechanical Variables over the Length

All the remaining variables which are not shown are zero in this case. This includes gradient of electric potential in x_2 direction β_2.

72
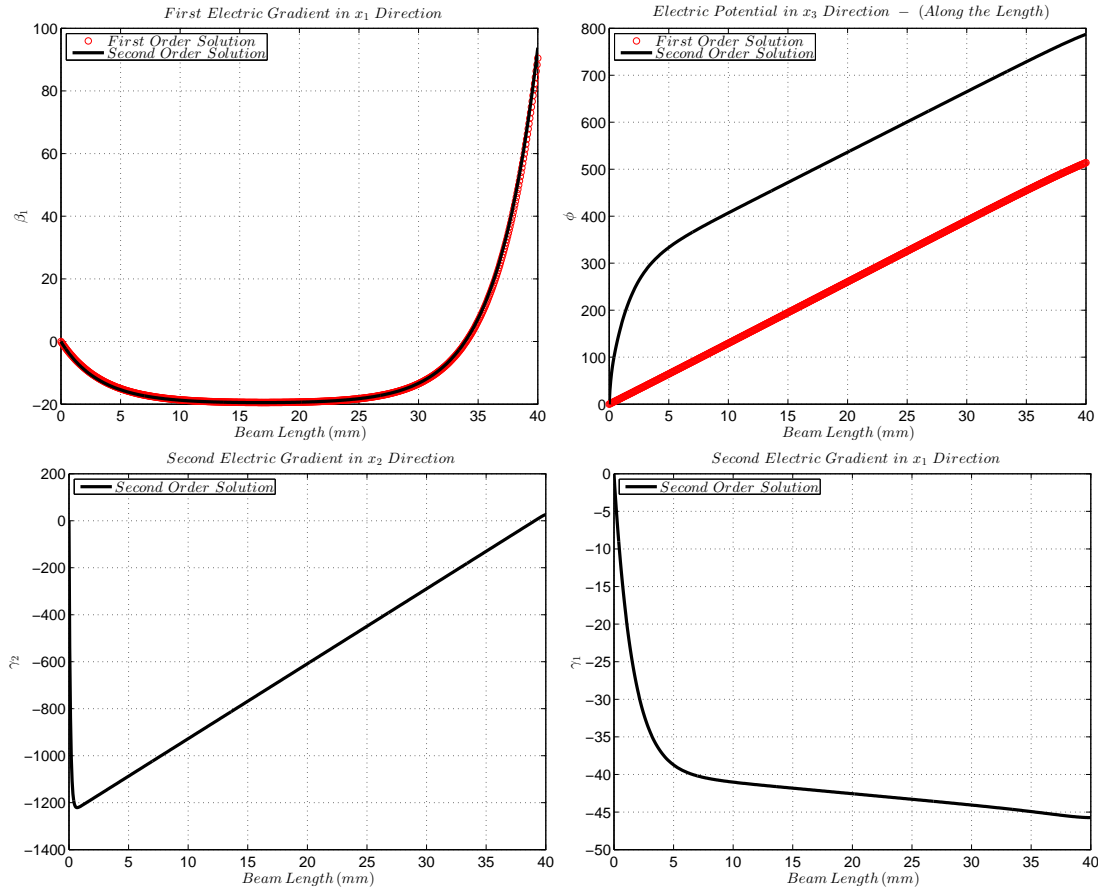
Figure 35: Variation of Electrical Variables over the Length

If we keep the hessians of electric potential γ_1, γ_2 aside, all the remaining variables are the same for first order solution and second order solution, apart from the electric potential ϕ. Due to the nature of coupling one can observe from Fig. 35 that there is a shift in electric potential. With this information if we plot the variation of total electric potential ψ on the right end cross section and compare its variation through-the-height and through-the-thickness for both cases, we will have.
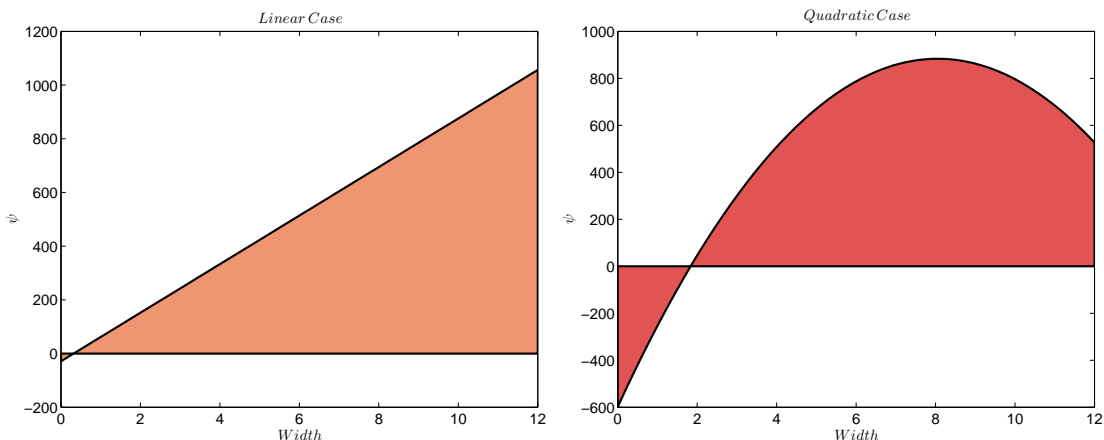

Figure 36: Variation of Electric Potential Across the Width

73
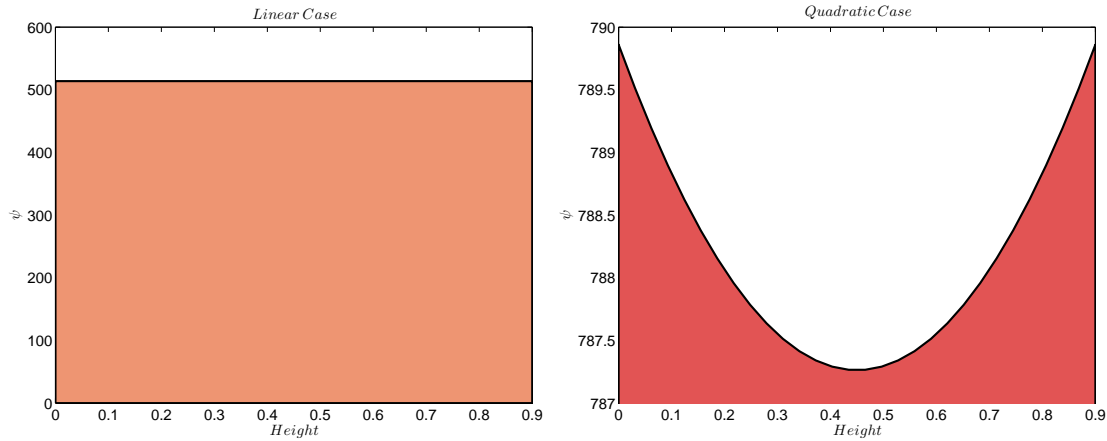
Figure 37: Variation of Electric Potential Across the Height

Observe that the variation of total electric potential across the height is constant in linear case, due to β_2 being zero. Also in the quadratic case, contribution of hessian γ_2 is small through the height. These discrepancies in the results are expected as the coupling in both cases differ substantially.

Earlier in this section, we caught sight of stress and electric displacement resultants for cantilever beams under the action of point loads and uniformly distributed loads. It is certain that these quantities are composition of electrical and mechanical contributions. Also the moment of electric displacement resultants in these plots correspond to $\vec{M}^e$ and not the sum of $\vec{M}^e$ and $\vec{M}_1^e$. Since the D_3 component of electric displacement produces a separate moment $\vec{M}^e$ from those of its other components D_α - which give rise to $\vec{M}_1^e$ moment, then the total first moment of electric displacement should be realised as a summation of these two quantities. Also the second moment of electric displacement $\vec{O}^e$ was not plotted earlier. This is due to fact that all electric displacement resultant quantities are associated with Neumann boundary conditions, exactly in the same manner that recovered shear force and bending moment are associated with the external load and moment - Neumann boundary conditions. Since we impose zero Neumann boundary condition for electric displacement resultants, they should vanish. In the following figures all these resultants for the case of coupled bending-torsion beam are clearly decomposed into their electrical and mechanical contributions.
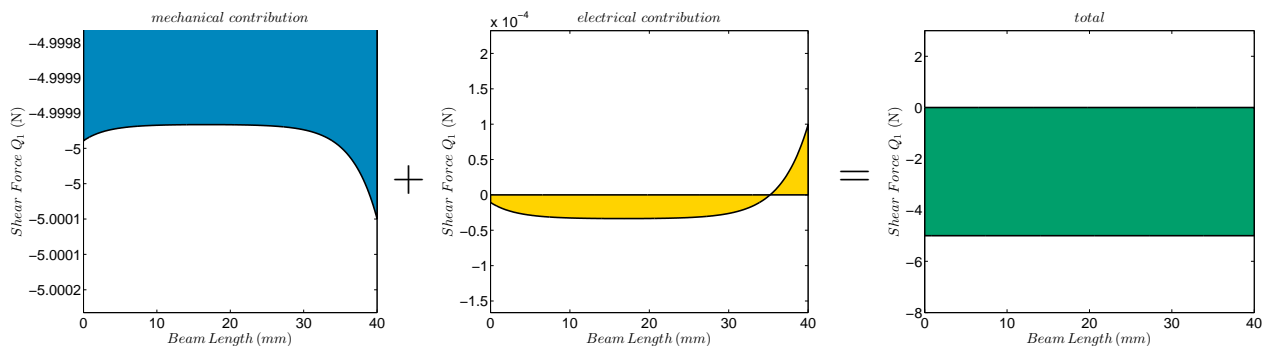

Figure 38: Shear Force of Coupled Bending-Torsion Fibre

74
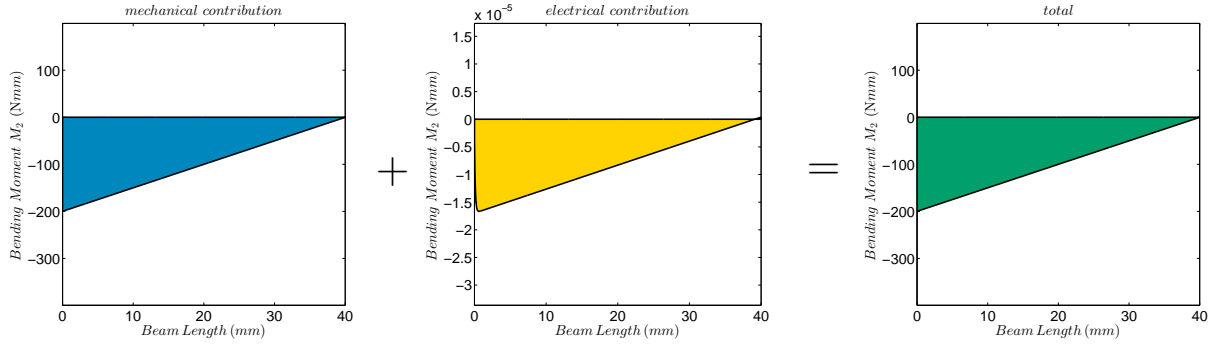
Figure 39: Bending Moment of Coupled Bending-Torsion Fibre
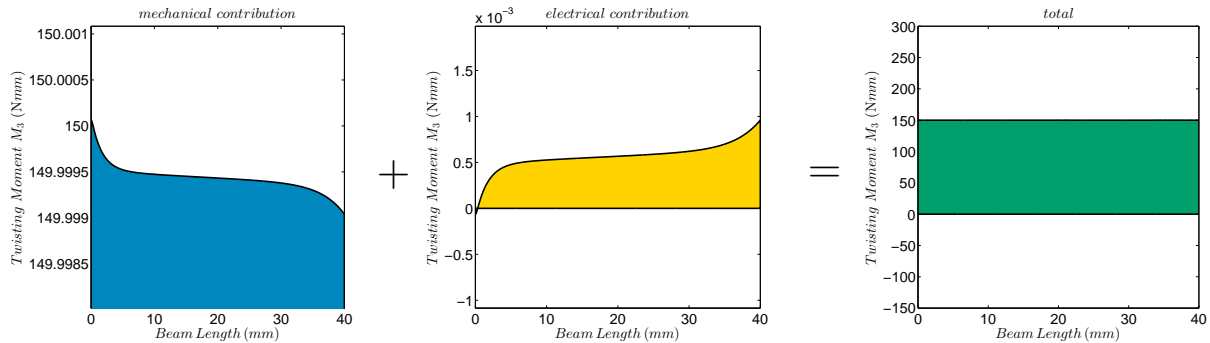
Figure 40: Torque of Coupled Bending-Torsion Fibre
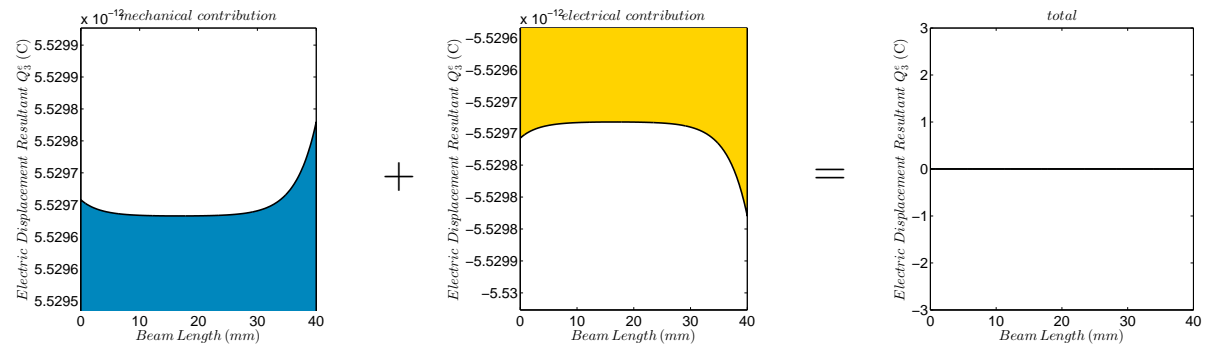
Figure 41: Electric Displacement Resultant of Coupled Bending-Torsion Fibre

Finally, we perform dynamic analysis under tip load or tip twisting moment with frequencies of applied vibration being those of natural frequencies of the beam computed earlier i.e. we excite the beam at resonant frequencies. We perform the analysis with various damping coefficients for the system. Classical damping with various coefficients are used. The dynamic problem is solved with Newmark's method using 50 elements and quadratic Lagrange basis functions with Gauss-Lobbato points. A dynamic load of $P = P_0 \sin(\omega t)$ is applied on the fibre, where ω is the frequency of vibration, P_0 the amplitude of vibration chosen as 100 here and t is time chosen as 60 seconds for the analysis. Fig. 42 and Fig. 43 show the loading pattern and the end displacement for the case when beam is excited at first natural frequency. Load is applied in the first 30 seconds and the timestep size is chosen as 1/150.
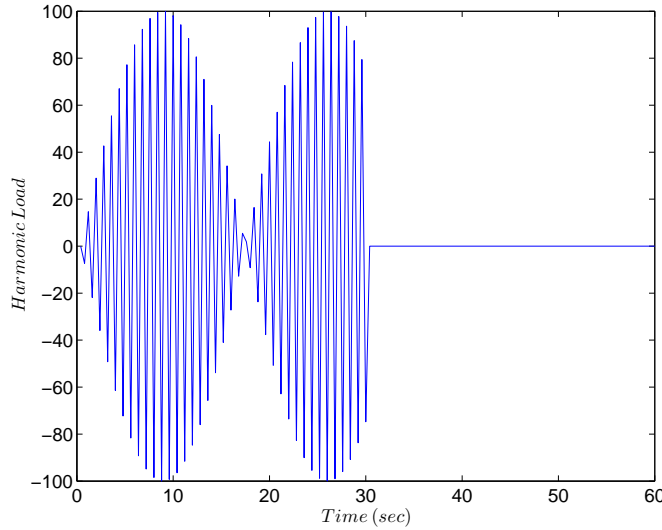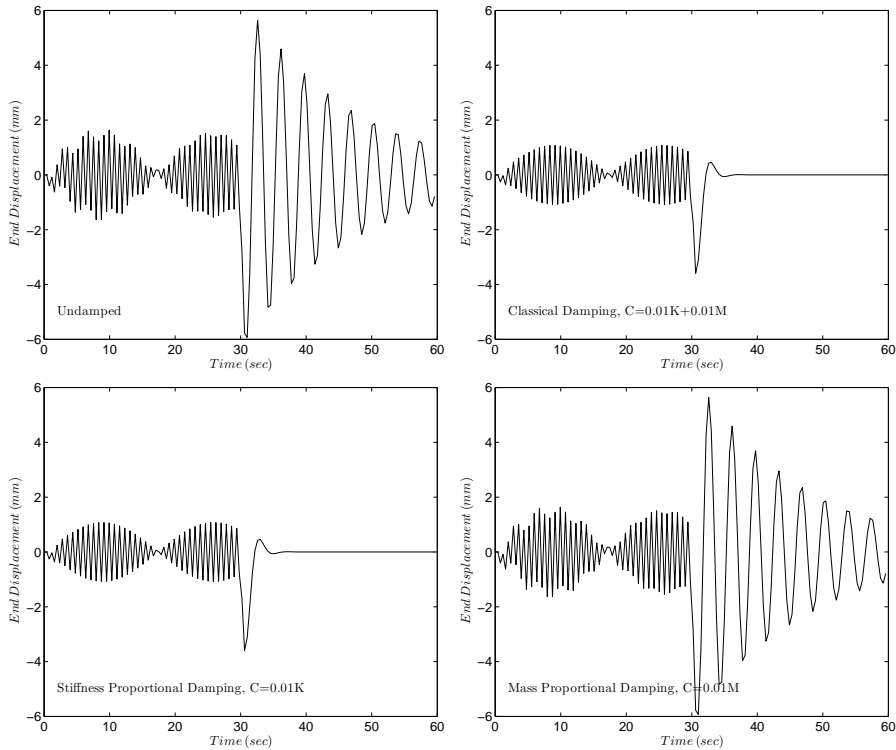
Figure 42: Harmonic Vibration with Resonant Frequency

Figure 43: End Displacement with Various Damping Coefficients Excited near 1$^{\text{st}}$ Natural Frequency

Since the elastic properties of the system is orders of magnitude larger than the density the major contribution in damping comes from stiffness. As can be observed that excitations damp out quickly for the case of stiffness proportional damping.To wrap up, we compute the absolute maximum power harvested for six lowest natural frequency excitations. The power can be computed from the variational form of Gauss's law, which is presented in section 4.

The instantaneous electrical power can be computed as.

$$P_w = \frac{dW_{int}^e}{dt} = \int_l \left(\dot{\vec{\epsilon}}^e \cdot \vec{Q}^e + \dot{\vec{\kappa}}^e \cdot \vec{M}^e + \dot{\vec{\gamma}}^e \cdot \vec{M}_1^e + \dot{\vec{\varsigma}} \cdot \vec{O}^e \right) \mathrm{d}x_3 \tag{6.12}$$

In the finite element context one needs to compute the electrical power at each time step by carrying out the normal post-processing used in stress recovery i.e. numerical integration to compute the desired quantity at Gauss points and then looping over elements. The harvested power for 60 seconds (full excitation cycle) and 30 seconds (half excitation cycle) for damped and undamped system is shown in the following figures.
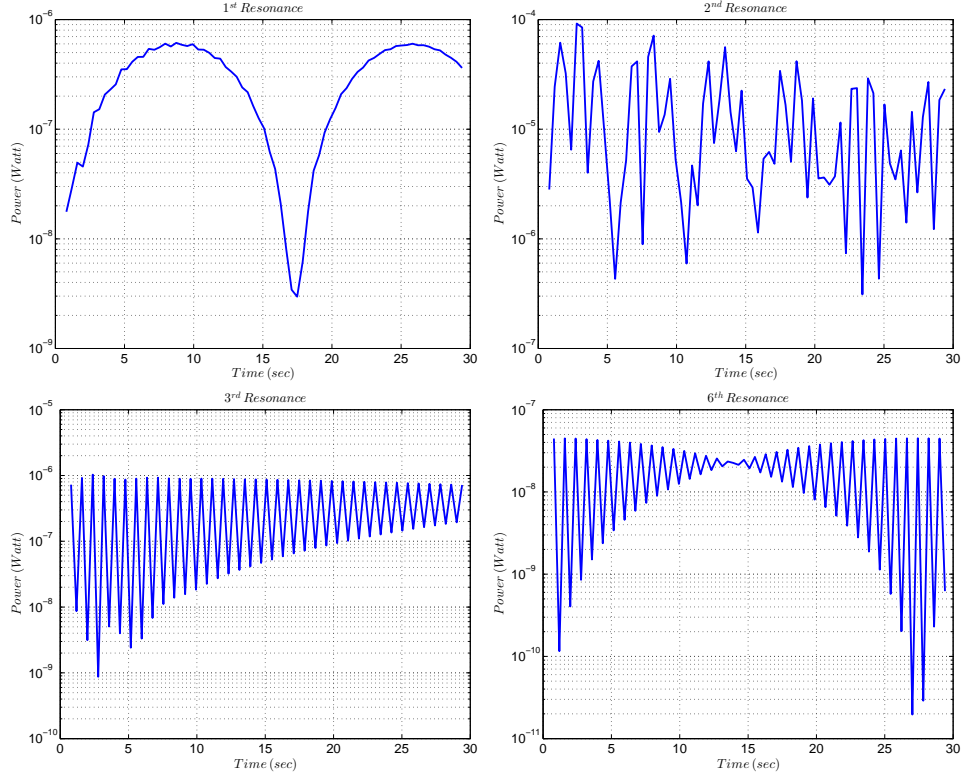
Figure 44: Harvested Power at Resonance Frequencies - Half Excitation Cycle - Undamped
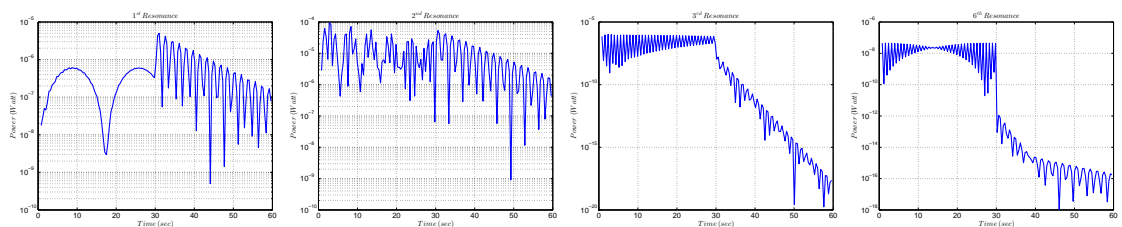
Figure 45: Harvested Power at Resonance Frequencies - Full Excitation Cycle - Undamped
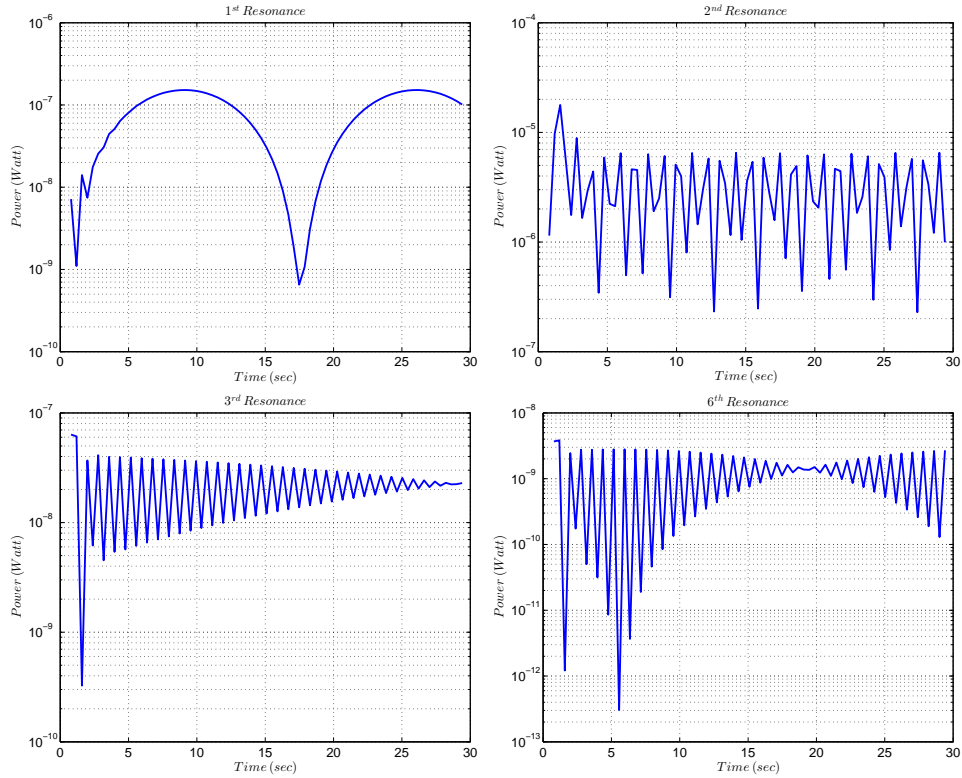
Figure 46: Harvested Power at Resonance Frequencies - Half Excitation Cycle - Damped
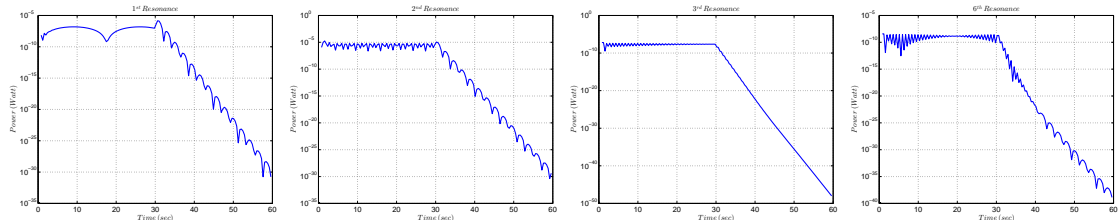
Figure 47: Harvested Power at Resonance Frequencies - Full Excitation Cycle - Damped

It should be noted that this maximum power corresponds to an instantaneous power where it is assumed that the electrodes are not attached to an external resistor. As observed the maximum power is associated with the second resonance frequency. This is partly because the amplitude of applied harmonic loads is kept the same for all loading cases but the loads are applied in compliance with eigen modes of the system, i.e. in each case the fibre is loaded in such a way that the deformed configuration is that of its corresponding modes.

Concluding Remarks

*"The important thing in science is not so much to obtain
new facts as to discover new ways of think about them."*
William Henry Bragg

7. Conclusion

In this work, a three dimensional linear piezoelectric beam formulation and its subsequent finite element implementation has been presented. The mechanical kinematics of the beam is that of Timoshenko i.e. the cross sectional planes remain plane but not necessarily normal to the mid-surface. The electric potential distribution is quadratic across the height and thickness of the beam. Unlike many available models [4] [12] [1], there is no assumption of vanishing electric field in particular directions and thus strains and electric field are coupled in all three directions. Starting from the enthalpy density of the piezoelectric system, supplemented by kinetic and external potential energies [50], and utilising Hamilton's principle, consistent linearisation of the mixed functional has been performed and the kinematics of the piezoelectric beam have been then embedded in the linearised form of the problem to obtain the Euler-Lagrange equations in the form of partial differential equations. These equations have been then solved analytically for planar beams to provide a benchmark for the computational scheme. On the numerical analysis front, higher order Lagrange and hierarchical Legendre basis functions have been employed to solve the monolithic problem accurately [47] [28]. Due to similar spatial description of electrical and mechanical variables, additional shear locking has been experienced [9], which has been rectified by utilising higher order bases as well as reduced integration.

From studies on the nature of electric potential distribution across the area directions, it is concluded that the inclusion of quadratic term affects the overall piezoelectric beam behaviour significantly, in that one additional material parameter from piezoelectric tensor is accessed which changes the nature of coupling.

Static, modal and dynamic analyses have been performed for a series of single-layer energy harvesters under various loading scenarios. Since the electrostatic part does not contribute to the mass of the system, hence the computed eigenmodes associated with the mechanical beam and the piezoelectric beam show resemblance and the shift in eigenfrequencies has been identified as negligible for lower frequencies. This is due to the fact that piezoelectric and dielectric constants are orders of magnitude smaller than the mechanical ones.

Crucial to the problems of energy harvesting is the mechanically driven nature of electromechanical coupling. The decomposition of stress resultants into mechanical and electrical contributions, suggests that the mechanical contribution is way more pronounced in these problems. Opposite observations should hold for actuation problems. The maximum instantaneous electric power harvested from the fibre under bending excitations has been in the range of 960μWatt and for the fibre undergoing torsional vibration as 0.065μWatt, which is certainly because the dominant modes of the fibre were bending related.

The results obtained with isotropic and anisotropic formulations indicate that for PZT-5H the coupling is unaffected by the choice of formulation, in that only elastic modulus is replaced with C_{33} with shear modulus having remained the same. Similar observation should also hold for other classes of transerve isotropic piezoelectric materials, for which the change in the results will depend on the difference between these elastic properties.

Appropriate error norms namely L^2, H^1 and energy, have been computed and convergence studies with different basis functions and different numerical integration schemes have been carried out. Equally spaced Lagrange bases show end oscillation which is due to ill-conditioning of the underlying Vandermonde matrix associated with them [28]. Lagrange basis functions with Gauss-Lobatto-Legendre points are robust on the other hand, but require more computational effort as their zeroth points are not explicitly known. Legendre bases show the best convergence, however they are not associated with any node inside the element domain.

Numerical integration with Gauss and Gauss-Lobatto quadrature both yield similar results, although Gauss-Lobatto scheme uses two extra hat functions which can be seen as extra computation, however they can be computed only once for mass and stiffness matrices, with the advantage of mass matrix being diagonal but rank-1 deficient; as opposed to Gauss quadrature using which needs different Gauss points and weights for mass and stiffness.

On its entirety, the formulation, finite element implementation and analytical solutions for three dimensional linear piezoelectric beams outlined in this work are fundamentally novel, with the advantage of retaining as much of the physics of continuum piezoelectricity as Timoshenko model allows, in that there is no assumption on the electrostatic part of the problem. The limitations of the approach are exactly the ones described by Hjelmstad [24] for linear three-dimensional beams, which are essentially associated with dimensional reduction, i.e. loss of Poisson's ratio, no warping of cross section and the equations of continuum elasticity and electrostatics having been averaged out over the cross section.

A.1 Appendices

1.1. Appendix 1

1.1.1. Third Order Tensors

This section is devoted to matrix computations involving third order tensors, which are extensively used in the analysis of three-dimensional piezoelectric beams formulated in the earlier sections. Third order tensors and their idealisation as matrices are discussed with a view to give the reader an idea of various simplified computing techniques. Third order tensors can be represented geometrically by a cube, with slices (planes) in three dimensions i.e. $x_1 - x_2$, $x_1 - x_3$ and $x_2 - x_3$. We will use the term slice for planes and matrices arising from the geometrical representation of third order tensors [8]. Fig. 48 follows this argument.

$$\mathcal{A} = \begin{bmatrix} A_{111} & A_{211} & A_{311} \\ A_{122} & A_{222} & A_{322} \\ A_{133} & A_{211} & A_{333} \\ A_{123} & A_{211} & A_{323} \\ A_{113} & A_{213} & A_{313} \\ A_{112} & A_{212} & A_{312} \\ A_{132} & A_{232} & A_{332} \\ A_{131} & A_{231} & A_{331} \\ A_{121} & A_{221} & A_{321} \end{bmatrix}$$

$$A_{1jk} = \begin{bmatrix} A_{111} & A_{112} & A_{113} \\ A_{121} & A_{122} & A_{123} \\ A_{131} & A_{132} & A_{133} \end{bmatrix}$$
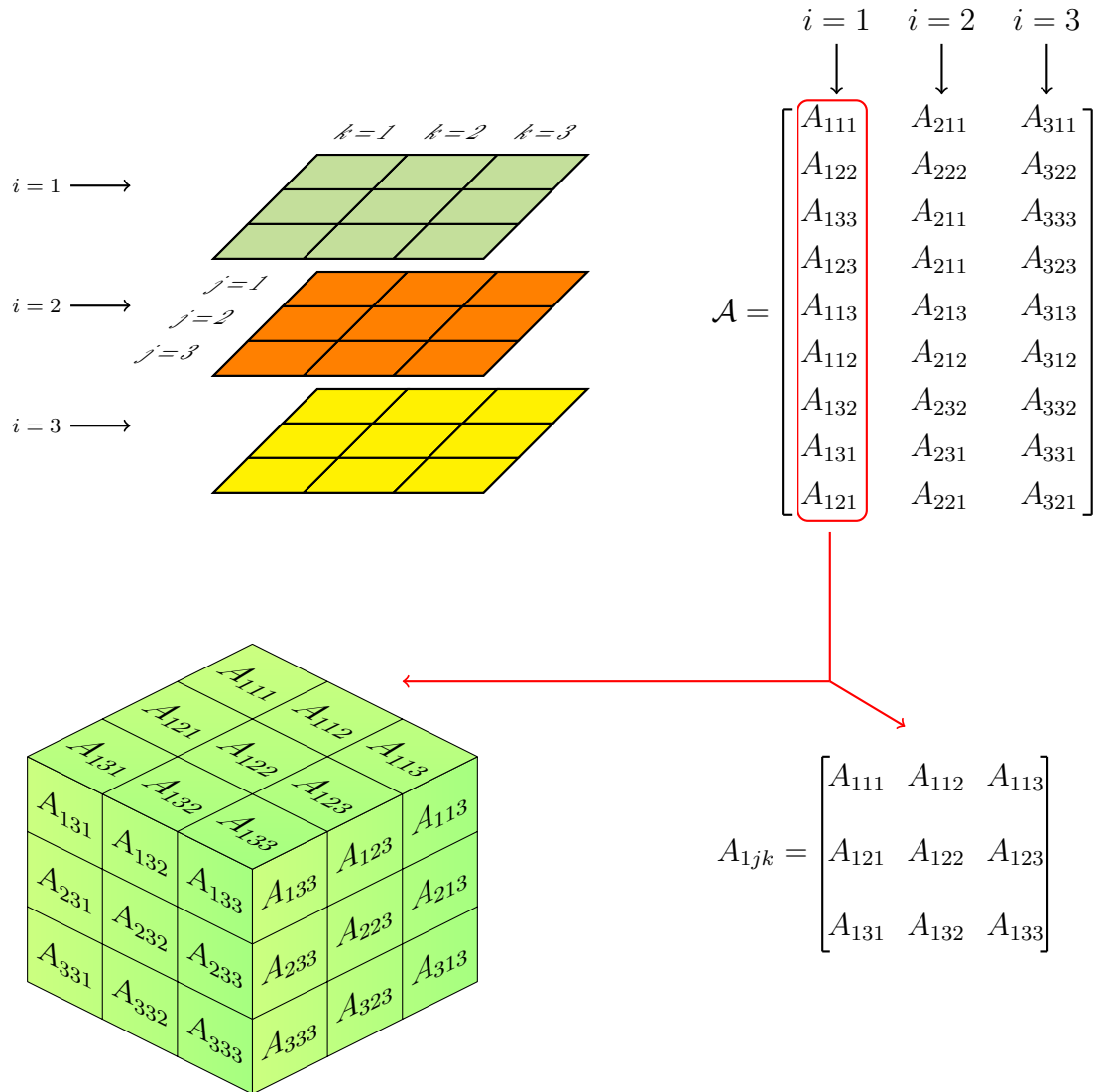
Figure 48: Geometrical Representation of 3$^{\text{rd}}$ Order Tensors

1.1.2.   Pre & Post Multiplication with Vectors

The main goal here is to show how change in indicial notation can lead to pre- and post-multiplication of tensors and their various transpose forms. Most problems encountered in formulating three-dimensional piezoelectric beams, involve manipulating third order tensors and their products with vectors and second order tensors in such a way that the final result remains the same. To this end, we show how third order tensors applied to low order tensors in general can give the same result in the explicit matrix form. To understand this, let us evaluate some tensor multiplications involving vectors, second order tensors and third order tensors. By definition third order tensors can be seen as linear operators which once applied to vectors yield second order tensors.

$$\mathcal{A}\vec{b} = \mathcal{A}_{ijk}b_k(\vec{e}_i \otimes \vec{e}_j) \tag{A.1.1}$$

As evident from the indices, the right hand side of (A.1.1) is a second order tensor. In fact, each horizontal slice of tensor $\mathcal{A}$ is multiplied with vector $\vec{b}$ to yield three vectors which can be arranged as the rows of a 3×3 matrix. Since $\mathcal{A}_{1jk}$, $\mathcal{A}_{2jk}$ and $\mathcal{A}_{3jk}$ are the first, second and third horizontal slices, respectively [See Fig. 48], we have,

$$\mathcal{A}_{1jk}b_k = \begin{bmatrix} A_{111} & A_{112} & A_{113} \\ A_{121} & A_{122} & A_{123} \\ A_{131} & A_{132} & A_{133} \end{bmatrix} \begin{Bmatrix} b_1 \\ b_2 \\ b_3 \end{Bmatrix} = \begin{Bmatrix} c_1 \\ c_2 \\ c_3 \end{Bmatrix}$$

$$\mathcal{A}_{2jk}b_k = \begin{bmatrix} A_{211} & A_{212} & A_{213} \\ A_{221} & A_{222} & A_{223} \\ A_{231} & A_{232} & A_{233} \end{bmatrix} \begin{Bmatrix} b_1 \\ b_2 \\ b_3 \end{Bmatrix} = \begin{Bmatrix} d_1 \\ d_2 \\ d_3 \end{Bmatrix}$$

$$\mathcal{A}_{3jk}b_k = \begin{bmatrix} A_{311} & A_{312} & A_{313} \\ A_{321} & A_{322} & A_{323} \\ A_{331} & A_{332} & A_{333} \end{bmatrix} \begin{Bmatrix} b_1 \\ b_2 \\ b_3 \end{Bmatrix} = \begin{Bmatrix} f_1 \\ f_2 \\ f_3 \end{Bmatrix}$$
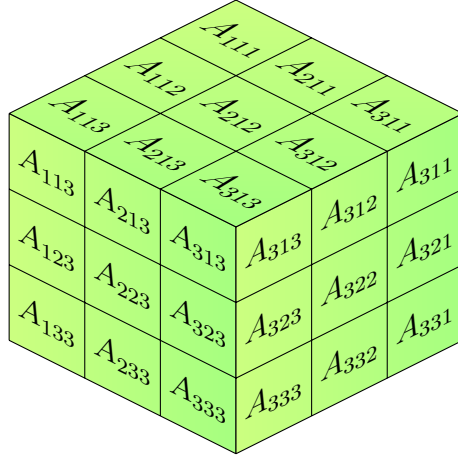
and thus.

$$\mathcal{A}_{ijk}b_k = \begin{bmatrix} c_1 & c_2 & c_3 \\ d_1 & d_2 & d_3 \\ f_1 & f_2 & f_3 \end{bmatrix}$$

Our aim here is in showing a simple way of carrying out these computations. If we were to compute the product of vector $\vec{b}$ and $\mathcal{A}$, proceeding from (A.1.1), we have,

$$\mathcal{A}\vec{b} = \mathcal{A}_{ijk}b_k(\vec{e}_i \otimes \vec{e}_j) = b_k\mathcal{A}_{kij}(\vec{e}_i \otimes \vec{e}_j) = \vec{b}\mathcal{A}^{T^\star} \tag{A.1.2}$$

where by $(\cdot)^{T^\star}$ of a third order tensor $\mathcal{A}$ in (A.1.2), we imply an even permutation of indices such that the two latter indices are not interchanged and only the last index is shifted to the first position. In Fig. 48, this is equivalent to placing each horizontal slice from $x_2 - x_3$ plane, vertically as a $x_1 - x_3$ slice. Fig. 49 shows the transpose of tensor $\mathcal{A}$.

Figure 49: $T^\star$ Transpose of a 3$^{\text{rd}}$ Order Tensor

Looking at Fig. 49, the matrix representation of $\mathcal{A}^{T^\star}$ can be written as.

$$\mathcal{A}^{T^\star} = \begin{bmatrix} A_{111} & A_{121} & A_{131} \\ A_{212} & A_{222} & A_{232} \\ A_{313} & A_{323} & A_{333} \\ A_{312} & A_{322} & A_{332} \\ A_{311} & A_{321} & A_{331} \\ A_{211} & A_{221} & A_{231} \\ A_{213} & A_{223} & A_{233} \\ A_{113} & A_{123} & A_{133} \\ A_{112} & A_{122} & A_{132} \end{bmatrix}$$

In the above expression for $\mathcal{A}^{T^\star}$, we have purposely not transposed the matrix itself i.e. the matrix is still in 9×3 format and not 3×9. If we now look at each column of this matrix we identify that the last index is shifted to the first position. This tempts us to see how (A.1.2) holds in the explicit form. To this end, we can write,

$$b_k \mathcal{A}_{kj1} = \begin{bmatrix} A_{111} & A_{112} & A_{113} \\ A_{121} & A_{122} & A_{123} \\ A_{131} & A_{132} & A_{133} \end{bmatrix} \begin{Bmatrix} b_1 \\ b_2 \\ b_3 \end{Bmatrix} = \begin{Bmatrix} c_1 \\ c_2 \\ c_3 \end{Bmatrix}$$

$$b_k \mathcal{A}_{kj2} = \begin{bmatrix} A_{211} & A_{212} & A_{213} \\ A_{221} & A_{222} & A_{223} \\ A_{231} & A_{232} & A_{233} \end{bmatrix} \begin{Bmatrix} b_1 \\ b_2 \\ b_3 \end{Bmatrix} = \begin{Bmatrix} d_1 \\ d_2 \\ d_3 \end{Bmatrix}$$

$$b_k \mathcal{A}_{kj3} = \begin{bmatrix} A_{311} & A_{312} & A_{313} \\ A_{321} & A_{322} & A_{323} \\ A_{331} & A_{332} & A_{333} \end{bmatrix} \begin{Bmatrix} b_1 \\ b_2 \\ b_3 \end{Bmatrix} = \begin{Bmatrix} f_1 \\ f_2 \\ f_3 \end{Bmatrix}$$

and thus.

$$b_k \mathcal{A}_{kij} = \vec{b} \mathcal{A}^{T^\star} = \begin{bmatrix} c_1 & c_2 & c_3 \\ d_1 & d_2 & d_3 \\ f_1 & f_2 & f_3 \end{bmatrix}$$

It is interesting to note that nothing has changed in the explicit form, apart from the fact that we are now post-multiplying vector $\vec{b}$ with each $x_1 - x_3$ slice of $\mathcal{A}$ instead of $x_2 - x_3$ slice, to get the same result. Note that while its straightforward to do such manipulation in the explicit form, the indicial form may lead us to some confusion. However, one should note that same question can arise with second order tensor, in that in the indicial form $\boldsymbol{A}_{ij}b_j$ and $b_j\boldsymbol{A}_{ji}$ are not the same, if we treat $\boldsymbol{A}_{ij}$ and $\boldsymbol{A}_{ji}$ as two different tensors. To show this, since a summation convention is employed, we have.

$$\boldsymbol{A}_{ij}b_j \ \vec{e}_i = (A_{11}b_1 + A_{12}b_2 + A_{13}b_3) \ \vec{e}_1 \qquad b_j\boldsymbol{A}_{ij} \ \vec{e}_i = (A_{11}b_1 + A_{21}b_2 + A_{31}b_3)\vec{e}_1$$
$$+ (A_{21}b_1 + A_{22}b_2 + A_{23}b_3) \ \vec{e}_2 \qquad\qquad + (A_{12}b_1 + A_{22}b_2 + A_{32}b_3)\vec{e}_2$$
$$+ (A_{31}b_1 + A_{32}b_2 + A_{33}b_3) \ \vec{e}_3 \qquad\qquad + (A_{13}b_1 + A_{23}b_2 + A_{33}b_3)\vec{e}_3$$

This rather discrepancy is due to our treatment of $\boldsymbol{A}_{ji}$ as a separate tensor and not as the transpose of $\boldsymbol{A}_{ij}$, otherwise certainly, their product with the same vector will yield the same result. Now, the same is true for what we have presented on third order tensors i.e. we treat $\mathcal{A}_{kj1}$, $\mathcal{A}_{kj2}$ and $\mathcal{A}_{kj3}$ as resulting slices, after the transpose operation is executed. This is illustrated in Fig. 50.
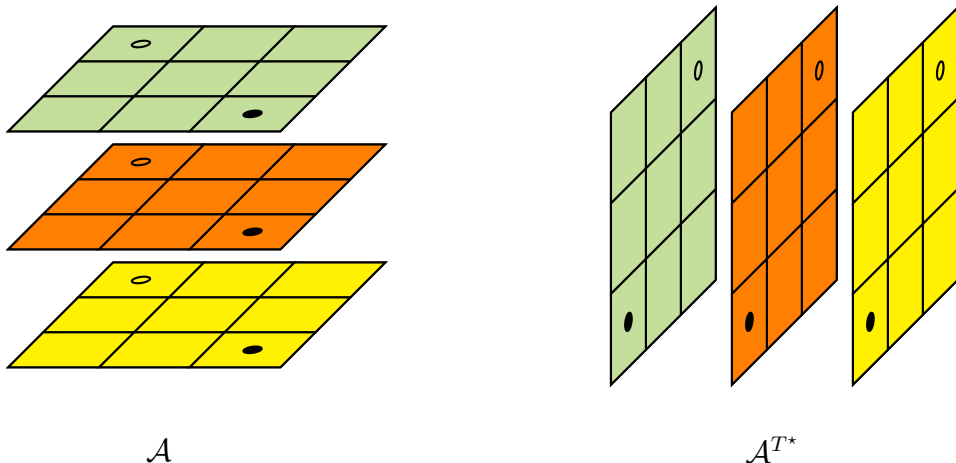
Figure 50: $T^\star$ Transpose of $\mathcal{A}$

1.1.3. Double Contraction with a Second Order Tensor

Consider the double contraction of a third order tensor with a second order tensor.

$$\mathcal{A} : \boldsymbol{B} = \mathcal{A}_{ijk}B_{jk} \ \vec{e}_i \tag{A.1.3}$$

Equation (A.1.3) is equivalent to double contracting each horizontal slice of $\mathcal{A}$ with $\boldsymbol{B}$. This is a straightforward algebra, however to show this with the matrix form of third order tensor we proceed this way.

$$
\mathcal{A} : \boldsymbol{B} =
\begin{bmatrix}
A_{111} & A_{211} & A_{311} \\
A_{122} & A_{222} & A_{322} \\
A_{133} & A_{233} & A_{333} \\
A_{123} & A_{223} & A_{323} \\
A_{113} & A_{213} & A_{313} \\
A_{112} & A_{212} & A_{312} \\
A_{132} & A_{232} & A_{332} \\
A_{131} & A_{231} & A_{331} \\
A_{121} & A_{221} & A_{321}
\end{bmatrix}
:
\begin{bmatrix}
B_{11} & B_{12} & B_{13} \\
B_{21} & B_{22} & B_{23} \\
B_{31} & B_{32} & B_{33}
\end{bmatrix}
$$

$$
=
\begin{bmatrix}
\begin{bmatrix}
A_{111} & A_{112} & A_{113} \\
A_{121} & A_{122} & A_{123} \\
A_{131} & A_{132} & A_{133}
\end{bmatrix}
:
\begin{bmatrix}
B_{11} & B_{12} & B_{13} \\
B_{21} & B_{22} & B_{23} \\
B_{31} & B_{32} & B_{33}
\end{bmatrix} \\[2em]
\begin{bmatrix}
A_{211} & A_{212} & A_{213} \\
A_{221} & A_{222} & A_{223} \\
A_{231} & A_{232} & A_{233}
\end{bmatrix}
:
\begin{bmatrix}
B_{11} & B_{12} & B_{13} \\
B_{21} & B_{22} & B_{23} \\
B_{31} & B_{32} & B_{33}
\end{bmatrix} \\[2em]
\begin{bmatrix}
A_{311} & A_{312} & A_{313} \\
A_{21} & A_{322} & A_{323} \\
A_{31} & A_{332} & A_{333}
\end{bmatrix}
:
\begin{bmatrix}
B_{11} & B_{12} & B_{13} \\
B_{21} & B_{22} & B_{23} \\
B_{31} & B_{32} & B_{33}
\end{bmatrix}
\end{bmatrix}
$$

Now to evaluate $\boldsymbol{B} : \mathcal{A}$ we do double contraction of each $x_1 - x_3$ slice of $\mathcal{A}$ with $\boldsymbol{B}$ which certainly gives us the same result.

$$
\mathcal{A} : \boldsymbol{B} = \mathcal{A}_{ijk} B_{jk} \ \vec{e}_i = B_{jk} \mathcal{A}_{jki} \ \vec{e}_i = \boldsymbol{B} : \mathcal{A}^{T^\star} \tag{A.1.4}
$$

$$
\boldsymbol{B} : \mathcal{A}^{T^\star} =
\begin{bmatrix}
B_{11} & B_{12} & B_{13} \\
B_{21} & B_{22} & B_{23} \\
B_{31} & B_{32} & B_{33}
\end{bmatrix}
:
\begin{bmatrix}
A_{111} & A_{121} & A_{131} \\
A_{212} & A_{222} & A_{232} \\
A_{313} & A_{323} & A_{333} \\
A_{312} & A_{322} & A_{332} \\
A_{311} & A_{321} & A_{331} \\
A_{211} & A_{221} & A_{231} \\
A_{213} & A_{223} & A_{233} \\
A_{113} & A_{123} & A_{133} \\
A_{112} & A_{122} & A_{132}
\end{bmatrix}
$$

$$
=
\begin{bmatrix}
\begin{bmatrix}
B_{11} & B_{12} & B_{13} \\
B_{21} & B_{22} & B_{23} \\
B_{31} & B_{32} & B_{33}
\end{bmatrix}
:
\begin{bmatrix}
A_{111} & A_{112} & A_{113} \\
A_{121} & A_{122} & A_{123} \\
A_{131} & A_{132} & A_{133}
\end{bmatrix} \\[2em]
\begin{bmatrix}
B_{11} & B_{12} & B_{13} \\
B_{21} & B_{22} & B_{23} \\
B_{31} & B_{32} & B_{33}
\end{bmatrix}
:
\begin{bmatrix}
A_{211} & A_{212} & A_{213} \\
A_{221} & A_{222} & A_{223} \\
A_{231} & A_{232} & A_{233}
\end{bmatrix} \\[2em]
\begin{bmatrix}
B_{11} & B_{12} & B_{13} \\
B_{21} & B_{22} & B_{23} \\
B_{31} & B_{32} & B_{33}
\end{bmatrix}
:
\begin{bmatrix}
A_{311} & A_{312} & A_{313} \\
A_{21} & A_{322} & A_{323} \\
A_{31} & A_{332} & A_{333}
\end{bmatrix}
\end{bmatrix}
$$

1.1.4. Transpose & Symmetry of Third Order Tensor

As was discussed earlier the $\mathcal{A}^{T^\star}$ was in fact a change in each slice i.e. an even permutation of indices. The transpose of a third order tensor, however, is normally when there is an odd number of permutation, which in the indicial form can be written as.

$$\mathcal{A} = \mathcal{A}_{ijk} \; \vec{e}_i \otimes \vec{e}_j \otimes \vec{e}_k \qquad (A.1.5)$$

$$\mathcal{A}^T = \mathcal{A}_{ijk} \; \vec{e}_i \otimes \vec{e}_k \otimes \vec{e}_j \qquad (A.1.6)$$

Hence, the transpose can be written as $\mathcal{A}_{ikj}$. If $\mathcal{A}_{ijk} = \mathcal{A}_{ikj}$, then $\mathcal{A}$ is a symmetric third order tensor. Note that there are two other possibilities for introducing symmetry.The piezoelectric tensor $\mathcal{P}$ is a symmetric tensor, in that $\mathcal{P}_{ijk} = \mathcal{P}_{ikj}$. In a geometrical representation, a symmetric third order tensor can be shown as a cube cut diagonally.
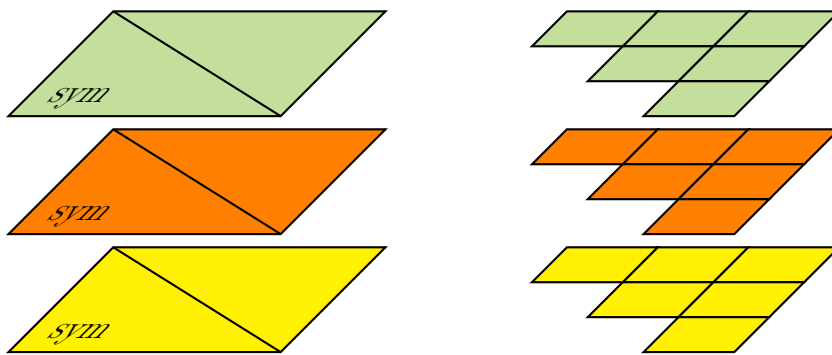

Figure 51: Geometrical Representation of Symmetry and Transpose of Thrid Order Tensors

As shown in Fig. 51 each matrix in the horizontal slice is symmetric and in terms of storage we can only store the upper half of each of these matrices.

1.1.5. Double Contraction of Two Third Order Tensors

Consider two third order tensors now.

$$\mathcal{A} : \mathcal{P} = \mathcal{A}_{ijk}\mathcal{P}_{jkl} \; \vec{e}_i \otimes \vec{e}_l \qquad (A.1.7)$$

From (A.1.7) it can be observed that by double contracting two third order tensors, we in fact perform a double contraction between each $x_2 - x_3$ slice of $\mathcal{A}$ and $x_1 - x_3$ slice of $\mathcal{P}$. Now if were to compute $\mathcal{P} : \mathcal{A}$, that would mean performing double contraction between each $x_2 - x_3$ slice of $\mathcal{P}$ and $x_1 - x_3$ slice of $\mathcal{A}$. But if our aim is in obtaining the same result from both multiplication then we can proceed as.

$$\mathcal{A} : \mathcal{P} = \mathcal{A}_{ijk}\mathcal{P}_{jkl} \; \vec{e}_i \otimes \vec{e}_l = \mathcal{P}_{ljk}\mathcal{A}_{jki} \; \vec{e}_i \otimes \vec{e}_l = \mathcal{P}^{T^\star} : \mathcal{A}^{T^\star} \qquad (A.1.8)$$

Note that, while we have already dealt with $\mathcal{A}_{jki}$ as the $T^\star$ transpose of $\mathcal{A}$, denoting $\mathcal{P}_{ljk}$ as $\mathcal{P}^{T^\star}$ may look a bit inconsistent. In fact $\mathcal{P}_{ljk}$ is exactly the opposite of $T^\star$, in that, it transforms each $x_1 - x_3$ slice of $\mathcal{P}$ to a horizontal $x_2 - x_3$ slice. But as in second order tensors, transpose and inverse of transpose imply the same thing and hence, we stick with our notation.

$$\mathcal{A} : \mathcal{P} = \begin{bmatrix} A_{111} & A_{211} & A_{311} \\ A_{122} & A_{222} & A_{322} \\ A_{133} & A_{233} & A_{333} \\ A_{123} & A_{223} & A_{323} \\ A_{113} & A_{213} & A_{313} \\ A_{112} & A_{212} & A_{312} \\ A_{132} & A_{232} & A_{332} \\ A_{131} & A_{231} & A_{331} \\ A_{121} & A_{221} & A_{321} \end{bmatrix} : \begin{bmatrix} P_{111} & P_{211} & P_{311} \\ P_{122} & P_{222} & P_{322} \\ P_{133} & P_{233} & P_{333} \\ P_{123} & P_{223} & P_{323} \\ P_{113} & P_{213} & P_{313} \\ P_{112} & P_{212} & P_{312} \\ P_{132} & P_{232} & P_{332} \\ P_{131} & P_{231} & P_{331} \\ P_{121} & P_{221} & P_{321} \end{bmatrix}$$

$$= \begin{bmatrix} A_{1jk}P_{jk1} & A_{1jk}P_{jk2} & A_{1jk}P_{jk3} \\ A_{2jk}P_{jk1} & A_{2jk}P_{jk2} & A_{2jk}P_{jk3} \\ A_{3jk}P_{jk1} & A_{3jk}P_{jk2} & A_{3jk}P_{jk3} \end{bmatrix}$$

1.1.6. Piezoelectric Three-Dimensional Beam Tensors

The piezoelectric 3$^{\text{rd}}$ order beam tensors discussed in stress resultant section are given in the following. Note that we strictly obey the rules presented in the earlier section of this appendix, for generating 3$^{\text{rd}}$ order tensors, in that in the following, each horizontal slice of 3$^{\text{rd}}$ order tensor is represented by a column in the matrix form.

$$
\mathcal{A}_1^e = \begin{bmatrix} 0 & 0 & A \\ 0 & 0 & A \\ 0 & 0 & A \\ 0 & 0 & 0 \\ 0 & 0 & 0 \\ 0 & 0 & 0 \\ 0 & 0 & 0 \\ 0 & 0 & 0 \\ 0 & 0 & 0 \end{bmatrix}
\quad
\mathcal{S}_1^e = \begin{bmatrix} 0 & 0 & 0 \\ 0 & 0 & 0 \\ 0 & 0 & 0 \\ 0 & 0 & 0 \\ 0 & 0 & 0 \\ 0 & 0 & 0 \\ 0 & 0 & S_2 \\ 0 & 0 & S_1 \\ 0 & 0 & 0 \end{bmatrix}
\quad
\mathcal{S}_2^e = \begin{bmatrix} 0 & 0 & S_1 \\ 0 & 0 & S_2 \\ 0 & 0 & 0 \\ 0 & 0 & 0 \\ 0 & 0 & 0 \\ 0 & 0 & 0 \\ 0 & 0 & 0 \\ 0 & 0 & 0 \\ 0 & 0 & 0 \end{bmatrix}
\quad
\mathcal{I}_1^e = \begin{bmatrix} 0 & 0 & 0 \\ 0 & 0 & 0 \\ 0 & 0 & 0 \\ 0 & 0 & 0 \\ 0 & 0 & 0 \\ 0 & 0 & 0 \\ 0 & 0 & \frac{1}{2}I_{22} \\ 0 & 0 & \frac{1}{2}I_{11} \\ 0 & 0 & 0 \end{bmatrix}
$$

The third order tensor $\mathcal{C}$ required for computing second stress resultant (moments) has the explicit form

$$
\mathcal{C} = [\vec{p}\times]\mathcal{P} = \begin{bmatrix}
x_2 P_{131} & x_2 P_{231} & x_2 P_{331} \\
-x_1 P_{132} & -x_1 P_{232} & -x_1 P_{332} \\
-x_2 P_{113} + x_1 P_{123} & -x_2 P_{213} + x_1 P_{223} & -x_2 P_{313} + x_1 P_{323} \\
-x_1 P_{133} & -x_1 P_{233} & -x_1 P_{333} \\
x_2 P_{133} & x_2 P_{233} & x_2 P_{333} \\
x_2 P_{132} & x_2 P_{232} & x_2 P_{332} \\
-x_2 P_{112} + x_1 P_{122} & -x_2 P_{212} + x_1 P_{222} & -x_2 P_{312} + x_1 P_{322} \\
-x_2 P_{111} + x_1 P_{121} & -x_2 P_{211} + x_1 P_{221} & -x_2 P_{311} + x_1 P_{321} \\
-x_1 P_{131} & -x_1 P_{231} & -x_1 P_{331}
\end{bmatrix}
$$

The second order tensors related to pure mechanical kinematics are,

$$
\mathbf{A}^m = \begin{bmatrix} \mu A k_s & 0 & 0 \\ & \mu A k_s & 0 \\ sym & & (2\mu+\lambda)A \end{bmatrix}
\qquad
\mathbf{S}^m = \begin{bmatrix} 0 & 0 & -\mu S_2 \\ 0 & 0 & \mu S_1 \\ (2\mu+\lambda)S_2 & -(2\mu+\lambda)S_1 & 0 \end{bmatrix}
$$

$$
\mathbf{I}^m = \begin{bmatrix} (2\mu+\lambda)I_{22} & -(2\mu+\lambda)I_{12} & 0 \\ & (2\mu+\lambda)I_{11} & 0 \\ sym & & \mu J \end{bmatrix}
$$

and the explicit form of tensors arising in the dynamics of the three-dimensional beams are.

$$
\mathbf{A}_D = \begin{bmatrix} \rho A & 0 & 0 \\ & \rho A & 0 \\ sym & & \rho A \end{bmatrix}
\quad
\mathbf{S}_D = \begin{bmatrix} 0 & 0 & -\rho S_2 \\ 0 & 0 & \rho S_1 \\ \rho S_2 & -\rho S_1 & 0 \end{bmatrix}
\quad
\mathbf{I}_D = \begin{bmatrix} \rho I_{22} & -\rho I_{12} & 0 \\ & \rho I_{11} & 0 \\ sym & & \rho J \end{bmatrix}
$$

The tensors related to electrical kinematics (dielectric tensors) are.

$$
\mathbf{A}_2^e = A \begin{bmatrix} \epsilon_{11} & \epsilon_{12} & \epsilon_{13} \\ \epsilon_{21} & \epsilon_{22} & \epsilon_{13} \\ \epsilon_{31} & \epsilon_{32} & \epsilon_{33} \end{bmatrix}
\quad
\mathbf{S}_4^e = \begin{bmatrix} \epsilon_{13}S_1 & \epsilon_{13}S_2 & 0 \\ \epsilon_{23}S_1 & \epsilon_{23}S_2 & 0 \\ \epsilon_{33}S_1 & \epsilon_{33}S_2 & 0 \end{bmatrix}
\quad
\mathbf{S}_5^e = \begin{bmatrix} \epsilon_{11}S_1 & \epsilon_{12}S_2 & 0 \\ \epsilon_{21}S_1 & \epsilon_{22}S_2 & 0 \\ \epsilon_{31}S_1 & \epsilon_{32}S_2 & 0 \end{bmatrix}
$$

$$\mathbf{I}_4^e = \frac{1}{2}\begin{bmatrix} \epsilon_{13}I_{11} & \epsilon_{13}I_{22} & 0 \\ \epsilon_{23}I_{11} & \epsilon_{23}I_{22} & 0 \\ \epsilon_{33}I_{11} & \epsilon_{33}I_{22} & 0 \end{bmatrix} \quad \mathbf{I}_5^e = \begin{bmatrix} \epsilon_{33}I_{11} & \epsilon_{33}I_{12} & 0 \\ \epsilon_{33}I_{21} & \epsilon_{33}I_{22} & 0 \\ 0 & 0 & 0 \end{bmatrix} \quad \mathbf{I}_6^e = \begin{bmatrix} \epsilon_{31}I_{11} & \epsilon_{32}I_{12} & 0 \\ \epsilon_{31}I_{21} & \epsilon_{32}I_{22} & 0 \\ 0 & 0 & 0 \end{bmatrix}$$

$$\mathbf{I}_7^e = \begin{bmatrix} \epsilon_{11}I_{11} & \epsilon_{12}I_{12} & 0 \\ \epsilon_{21}I_{21} & \epsilon_{22}I_{22} & 0 \\ 0 & 0 & 0 \end{bmatrix} \quad \mathbf{G}_2^e = \frac{1}{2}\begin{bmatrix} \epsilon_{33}G_{111} & \epsilon_{33}G_{112} & 0 \\ \epsilon_{33}G_{221} & \epsilon_{33}G_{222} & 0 \\ 0 & 0 & 0 \end{bmatrix} \quad \mathbf{G}_3^e = \frac{1}{2}\begin{bmatrix} \epsilon_{13}G_{111} & \epsilon_{13}G_{112} & 0 \\ \epsilon_{23}G_{221} & \epsilon_{23}G_{222} & 0 \\ 0 & 0 & 0 \end{bmatrix}$$

$$\mathbf{J}^e = \frac{1}{4}\begin{bmatrix} \epsilon_{33}J_{1111} & \epsilon_{33}J_{1122} & 0 \\ \epsilon_{33}J_{2211} & \epsilon_{33}J_{2222} & 0 \\ 0 & 0 & 0 \end{bmatrix}$$

The second order tensors related to coupled piezoelectric kinematics are.

$$\mathbf{S}_3^e = \begin{bmatrix} P_{133}S_2 & P_{233}S_2 & P_{333}S_2 \\ -P_{133}S_1 & -P_{233}S_1 & -P_{333}S_1 \\ P_{123}S_1 - P_{113}S_2 & P_{223}S_1 - P_{213}S_2 & P_{323}S_1 - P_{313}S_2 \end{bmatrix}$$

$$\mathbf{I}_2^e = \begin{bmatrix} P_{333}I_{21} & P_{333}I_{22} & 0 \\ -P_{333}I_{11} & -P_{333}I_{12} & 0 \\ P_{323}I_{11} - P_{313}I_{12} & P_{323}I_{21} - P_{313}I_{22} & 0 \end{bmatrix}$$

$$\mathbf{I}_3^e = \begin{bmatrix} P_{133}I_{21} & P_{233}I_{22} & 0 \\ -P_{133}I_{11} & -P_{233}I_{12} & 0 \\ P_{123}I_{11} - P_{113}I_{12} & P_{223}I_{21} - P_{213}I_{22} & 0 \end{bmatrix}$$

$$\mathbf{G}_1^e = \frac{1}{2}\begin{bmatrix} P_{333}G_{112} & P_{333}G_{222} & 0 \\ -P_{333}G_{111} & -P_{333}G_{221} & 0 \\ P_{323}G_{111} - P_{313}G_{112} & P_{323}G_{221} - P_{313}G_{222} & 0 \end{bmatrix}$$

The second order tensor counterparts of some of the third order tensors used in the variational formulation of the problem are listed in the following.

$$\mathbf{A}_1^e = \mathcal{P}^{T^\star} : \mathcal{A}_1^e = A\begin{bmatrix} P_{113} & P_{213} & P_{313} \\ P_{123} & P_{223} & P_{323} \\ P_{133} & P_{233} & P_{333} \end{bmatrix} \quad \mathbf{A}_3^e = \mathcal{P}^{T^\star} : \mathcal{A}_3^e = A\begin{bmatrix} P_{113} & P_{123} & P_{133} \\ P_{213} & P_{223} & P_{233} \\ P_{313} & P_{323} & P_{333} \end{bmatrix}$$

$$\mathbf{S}_1^e = \mathcal{P}^{T^\star} : \mathcal{S}_1^e = \begin{bmatrix} P_{313}S_1 & P_{313}S_2 & 0 \\ P_{323}S_1 & P_{323}S_2 & 0 \\ P_{333}S_1 & P_{333}S_2 & 0 \end{bmatrix} \quad \mathbf{S}_2^e = \mathcal{P}^{T^\star} : \mathcal{S}_2^e = \begin{bmatrix} P_{113}S_1 & P_{213}S_2 & 0 \\ P_{123}S_1 & P_{223}S_2 & 0 \\ P_{133}S_1 & P_{233}S_2 & 0 \end{bmatrix}$$

$$\mathbf{I}_1^e = \mathcal{P}^{T^\star} : \mathcal{I}_1^e = \frac{1}{2}\begin{bmatrix} P_{313}I_{11} & P_{313}I_{22} & 0 \\ P_{323}I_{11} & P_{323}I_{22} & 0 \\ P_{333}I_{11} & P_{333}I_{22} & 0 \end{bmatrix}$$

1.1.7. Anistropic Case

$$\mathbf{A} = A \begin{bmatrix} C_{55} & C_{45} & C_{35} \\ & C_{44} & C_{34} \\ sym & & C_{33} \end{bmatrix} \qquad \mathbf{S} = \begin{bmatrix} C_{35}S_2 & -C_{35}S_1 & C_{45}S_1 - C_{55}S_2 \\ C_{34}S_2 & -C_{34}S_1 & C_{44}S_1 - C_{45}S_2 \\ C_{33}S_2 & -C_{33}S_1 & C_{34}S_1 - C_{35}S_2 \end{bmatrix}$$

$$\mathbf{I} = \begin{bmatrix} C_{33}I_{22} & -C_{33}I_{12} & C_{34}I_{12} - C_{35}I_{22} \\ & C_{33}I_{11} & -C_{34}I_{11} + C_{35}I_{21} \\ sym & & C_{44}I_{11} - 2C_{45}I_{12} + C_{55}I_{22} \end{bmatrix}$$

1.1.8. The More Familiar Voigt Notation of Solid Mechanics

In solid mechanics literature its common to write the strains and stresses in Voigt form. Following such a notation eases out the process of multiplication and specially the double contractions involving higher order tensor. This way we will have to modify our tensor, since so far we have strictly followed the appropriate rules of multiplications. The piezoelectric three-dimensional beam tensors given in the earlier section should be written in a format that a normal matrix product with the piezoelectric tensor $\mathcal{P}$ should suffice. Knowing that the double contraction of two third order tensor implies multiplying each horizontal $x_2 - x_3$ slice of the first one with the vertical $x_1 - x_3$ slice of the second one, we write the corresponding beam tensors in such a matrix format that each column represents a vertical $x_1 - x_3$ slice. This way a double contraction with piezoelectric tensor can be achieved with the common matrix multiplication.

$$\mathcal{A}_1^e = \begin{bmatrix} 0 & 0 & 0 \\ 0 & 0 & 0 \\ 0 & 0 & A \\ 0 & 0 & 0 \\ 0 & 0 & 0 \\ 0 & 0 & 0 \\ 0 & A & 0 \\ A & 0 & 0 \\ 0 & 0 & 0 \end{bmatrix} \quad \mathcal{S}_1^e = \begin{bmatrix} 0 & 0 & 0 \\ 0 & 0 & 0 \\ S_1 & S_2 & 0 \\ 0 & 0 & 0 \\ 0 & 0 & 0 \\ 0 & 0 & 0 \\ 0 & 0 & 0 \\ 0 & 0 & 0 \\ 0 & 0 & 0 \end{bmatrix} \quad \mathcal{S}_2^e = \begin{bmatrix} 0 & 0 & 0 \\ 0 & 0 & 0 \\ 0 & 0 & 0 \\ 0 & 0 & 0 \\ 0 & 0 & 0 \\ 0 & S_2 & 0 \\ S_1 & 0 & 0 \\ 0 & 0 & 0 \end{bmatrix} \quad \mathcal{I}_1^e = \begin{bmatrix} 0 & 0 & 0 \\ 0 & 0 & 0 \\ \frac{1}{2}I_{11} & \frac{1}{2}I_{22} & 0 \\ 0 & 0 & 0 \\ 0 & 0 & 0 \\ 0 & 0 & 0 \\ 0 & 0 & 0 \\ 0 & 0 & 0 \\ 0 & 0 & 0 \end{bmatrix}$$

1.2. Appendix 2

1.2.1. Explicit Forms of Three-Dimensional Beam Tensors

The linearised strain tensor $\boldsymbol{\varepsilon}$ in equation (2.3) has the following explicit form.

$$\boldsymbol{\varepsilon} = \frac{1}{2} \begin{bmatrix} 0 & 0 & \frac{dw_1}{dx_3} - \theta_2 - x_2\frac{d\theta_3}{dx_3} \\ & 0 & \frac{dw_2}{dx_3} + \theta_1 + x_1\frac{d\theta_3}{dx_3} \\ sym & & 2(\frac{dw_3}{dx_3} + x_2\frac{d\theta_1}{dx_3} - x_1\frac{d\theta_2}{dx_3}) \end{bmatrix} \tag{A.2.9}$$

Observe that $\varepsilon_{\alpha\beta} = 0$, where $\alpha, \beta = 1, 2$, which means there is no deformation in the cross sectional plane of the beam; the basic kinematic assumption in beams. For the case of planar beams stricted to $x_1 - x_3$ plane, $w_2 = 0$, $\theta_1 = 0$ and $\theta_3 = 0$, and the strain tensor takes the form.

$$\boldsymbol{\varepsilon} = \frac{1}{2} \begin{bmatrix} 0 & 0 & \frac{dw_1}{dx_3} - \theta_2 \\ & 0 & 0 \\ sym & & 2(\frac{dw_3}{dx_3} - x_1\frac{d\theta_2}{dx_3}) \end{bmatrix} \tag{A.2.10}$$

Further if we simplify our notation according for comparison with the common 2D Timoshenko beam, by denoting $x_3 = x$, $x_1 = z$, $w_1 = w$, $\theta_2 = \theta$ and $w_3 = u$, the non-zero strain terms become,

$$\begin{Bmatrix} \varepsilon_{13} \\ \varepsilon_{31} \\ \varepsilon_{33} \end{Bmatrix} = \begin{bmatrix} \frac{1}{2}(\frac{dw}{dx} - \theta) \\ \frac{1}{2}(\frac{dw}{dx} - \theta) \\ \frac{du}{dx} - z\frac{d\theta}{dx} \end{bmatrix} \tag{A.2.11}$$

which are exactly the strain terms in Timoshenko beam model. The explicit form of the traction vector $\vec{t}_{e_3}$ is.

$$\vec{t}_{e_3} = \begin{bmatrix} \mu(\frac{dw_1}{dx_3} - \theta_2 - x_2\frac{d\theta_3}{dx_3}) \\ \mu(\frac{dw_2}{dx_3} + \theta_1 + x_1\frac{d\theta_3}{dx_3}) \\ (2\mu + \lambda)(\frac{dw_3}{dx_3} + x_2\frac{d\theta_1}{dx_3} - x_1\frac{d\theta_2}{dx_3}) \end{bmatrix} \tag{A.2.12}$$

Similarly, the explicit form of equations stress resultants are.

$$\vec{Q} = \begin{Bmatrix} Q_1 \\ Q_2 \\ Q_3 \end{Bmatrix} = \begin{bmatrix} \mu A k_s(\frac{dw_1}{dx_3} - \theta_2) \\ \mu A k_s(\frac{dw}{dx_3} + \theta_1) \\ (2\mu + \lambda)A\frac{dw_3}{dx_3} \end{bmatrix} \tag{A.2.13}$$

The three traction forces of (A.2.13) correspond to the shear forces in $x_1 - x_3$ plane and $x_1 - x_2$ plane and the axial force normal to the cross sectional plane, respectively. One can think of (A.2.13) as the three forces in three directions at a particular node of a three-dimensional beam. Similarly, the explicit form of moment resultant becomes.

$$\vec{M} = \begin{Bmatrix} M_1 \\ M_2 \\ M_3 \end{Bmatrix} = \begin{bmatrix} (2\mu + \lambda)I_{22}\frac{d\theta_2}{dx_3} \\ (2\mu + \lambda)I_{11}\frac{d\theta_1}{dx_3} \\ \mu J\frac{d\theta_3}{dx_3} \end{bmatrix} \tag{A.2.14}$$

The three moment resultants of (A.2.14) correspond to the bending moment about x_2 axis and x_1 axis and the torsion or twisting moment of the cross section about x_3 or the beam axis itself. One can think of (A.2.14) as the three moments about three directions at a particular node of a three-dimensional beam. Equations (A.2.13) and (A.2.14) are of particular importance in finite element post-processing for moment and shear force recovery, where their values at Gauss points are interpolated.

1.3. Appendix 3

1.3.1. The Euler-Bernoulli Beam Model - EBB

Focusing our attention to the more familiar plane stress formulation for planar beams, the displacement field of EBB can be described as,

$$u_3 = u(x) - z\frac{\partial w(x)}{\partial x} \tag{A.3.15}$$

$$u_2 = 0 \tag{A.3.16}$$

$$u_1 = w(x) \tag{A.3.17}$$

where as before x_3 is the axial direction. The corresponding strain field is now obtained by taking gradient of the displacement field.

$$\varepsilon_{ij} = \nabla^s u = \frac{1}{2}(\frac{\partial u_i}{\partial x_j} + \frac{\partial u_j}{\partial x_i}) \tag{A.3.18}$$

$$\varepsilon_{33} = \frac{\partial u}{\partial x} - z\frac{\partial^2 w}{\partial x^2}; \qquad \varepsilon_{\alpha\beta} = 0; \qquad \varepsilon_{3\alpha} = 0 \tag{A.3.19}$$

Using above relations we can obtain the internal virtual work of EBB,

$$\delta W_{int} = \int_l \int_A \delta\varepsilon_{33} E \varepsilon_{33} \; \mathrm{d}A\mathrm{d}x = \int_l \int_A (\frac{\partial \delta u}{\partial x} - z\frac{\partial^2 \delta w}{\partial x^2})E(\frac{\partial u}{\partial x} - z\frac{\partial^2 w}{\partial x^2}) \; \mathrm{d}A\mathrm{d}x$$

$$= \int_l \int_A E(\frac{\partial \delta u}{\partial x}\frac{\partial u}{\partial x} + z^2\frac{\partial^2 \delta w}{\partial x^2}\frac{\partial^2 w}{\partial x^2}) \; \mathrm{d}A\mathrm{d}x \tag{A.3.20}$$

where E is the elastic modulus. Equation above can be written in a more consistent way as,

$$\delta U = \int_l \begin{bmatrix} \frac{\partial \delta u}{\partial x} \\ \frac{\partial^2 \delta w}{\partial x^2} \end{bmatrix}^T \mathbf{D} \begin{bmatrix} \frac{\partial u}{\partial x} \\ \frac{\partial^2 w}{\partial x^2} \end{bmatrix} \mathrm{d}x \tag{A.3.21}$$

where $\mathbf{D}$ is.

$$\mathbf{D} = \int_A \begin{pmatrix} E & 0 \\ 0 & Ez^2 \end{pmatrix} \mathrm{d}A \tag{A.3.22}$$

The finite element equations can be easily established from (A.3.20) by choosing linear Lagrangian basis function for axial terms and Hermite cubic basis functions for bending terms.

1.3.2. The Timoshenko Beam Model - TB

Unlike the Euler-Bernoulli beam model, the Timoshenko beam model also takes shear deformation into account. The displacement field of TB can be described as.

$$u_3 = u(x) - z\beta(x) \tag{A.3.23}$$

$$u_2 = 0 \tag{A.3.24}$$

$$u_1 = w(x) \tag{A.3.25}$$

This kinematical assumption is shown in Fig. 3. Note that β is taken as the rotation in this appendix and should not be confused with electric potential gradient. Taking gradient of the displacement field we obtain the two non-zero strains.

$$\varepsilon_{33} = \frac{\partial u}{\partial x} - z\frac{\partial \beta}{\partial x}; \tag{A.3.26}$$

$$\varepsilon_{31} = \varepsilon_{13} = \frac{1}{2}(\frac{\partial w}{\partial x} - \beta) = \frac{1}{2}\gamma; \tag{A.3.27}$$

$$\varepsilon_{\alpha\beta} = \varepsilon_{32} = \varepsilon_{23} = 0 \tag{A.3.28}$$

Using (A.3.26 - A.3.28) the virtual work of Timoshenko beam can be described as.

$$\begin{aligned}
\delta W_{int} &= \int_l \int_A \left(\delta\varepsilon_{33}E\varepsilon_{33} + \delta\varepsilon_{31}(2\mu)\varepsilon_{31} + \delta\varepsilon_{13}(2\mu)\varepsilon_{13} \right) \, \mathrm{d}A\mathrm{d}x \\
&= \int_l \int_A \left(\delta\varepsilon_{33}E\varepsilon_{33} + 4\delta\varepsilon_{31}\mu\varepsilon_{31} \right) \, \mathrm{d}A\mathrm{d}x = \int_l \int_A \left(\delta\varepsilon_{33}E\varepsilon_{33} + 4\frac{1}{2}\delta\gamma\mu\frac{1}{2}\gamma \right) \, \mathrm{d}A\mathrm{d}x \\
&= \int_l \int_A (\frac{\partial\delta u}{\partial x} - z\frac{\partial\delta\beta}{\partial x})E(\frac{\partial u}{\partial x} - z\frac{\partial\beta}{\partial x}) + (\frac{\partial\delta w}{\partial x} - \delta\beta)\mu(\frac{\partial w}{\partial x} - \beta) \, \mathrm{d}A\mathrm{d}x \\
&= \int_l \int_A E(\frac{\partial\delta u}{\partial x}\frac{\partial u}{\partial x} + z^2\frac{\partial\delta\beta}{\partial x}\frac{\partial\beta}{\partial x}) + (\frac{\partial\delta w}{\partial x} - \delta\beta)\mu(\frac{\partial w}{\partial x} - \beta) \, \mathrm{d}A\mathrm{d}x \tag{A.3.29}
\end{aligned}$$

The finite element equations can be easily established from (A.3.29) by choosing equal Lagrangian basis functions for all variables. Its is important to point out that if there is an external moment $\overline{m}$ applied on the structure, this will be evaluated by $\overline{m}\vec{N}^T|_{\Gamma_m}$, since rotations are interpolated with the same basis functions as translations in the C^0 and corresponding higher order approaches - cf. elementary books on FEM [18] [25].

1.3.3. The Dynamic Problem

In this section the dynamics of EBB and TB are dealt with. We start by finding analytical frequencies of both the models for two simple geometries and then compare them with the numerical results. To this end, the mass matrices of both EBB and TB models are first derived from Hamilton's prinicple outlined in chapter 3. which is.

$$\frac{\mathrm{d}}{\mathrm{d}t}\frac{\partial\mathcal{L}}{\partial\vec{\dot{u}}} = \frac{\mathrm{d}}{\mathrm{d}t}\frac{\partial\mathcal{K}}{\partial\vec{\dot{u}}} = \frac{\mathrm{d}}{\mathrm{d}t}\int_{\Omega_t}\frac{1}{2}\rho\,\vec{\dot{u}}\cdot\vec{\dot{u}}\,\mathrm{d}V$$

$$= \frac{\mathrm{d}}{\mathrm{d}t}\int_{\Omega_t}\rho\vec{\dot{u}}\,\mathrm{d}V = \int_{\Omega_t}\rho\frac{\mathrm{d}^2\vec{u}}{\mathrm{d}t^2}\,\mathrm{d}V = \int_{\Omega_t}\rho\frac{D^2\vec{u}}{Dt^2}\,\mathrm{d}V \qquad (A.3.30)$$

Substituting the displacement vector field from (A.3.15 - A.3.17) and dropping the axial term, we obtain.

$$\delta W_{iner} = \int_l\left(\rho I\frac{\partial w}{\partial x}\frac{\partial\delta w}{\partial x} + \rho Aw\delta w\right)\mathrm{d}x \qquad (A.3.31)$$

Using finite element discretisation, the total mass matrix can now obtained. In (A.3.31) the first term of the integrand gives rise to rotational mass matrix and the second term of the integrand to translational mass matrix. For Timoshenko beam, we substitute the displacement field (A.3.23-A.3.25) in (A.3.30) and obtain.

$$\delta W_{iner} = \int_l\left(\rho I\beta\delta\beta + \rho Aw\delta w\right)\mathrm{d}x \qquad (A.3.32)$$

In (A.3.32) the first term of the integrand gives rise to rotational mass matrix and the second term to translational mass matrix. Expressions (A.3.31) and (A.3.32) can be derived from the more generic dynamic equilibrium equations i.e.

$$\mathrm{div}\boldsymbol{\sigma} + \vec{b} = \rho\frac{D^2\vec{u}}{Dt^2} \qquad (A.3.33)$$

in which case separation of variables on right hand side would yield the exact work expressions for virtual inertial forces, but factored with ω^2, where ω is the angular frequency and its emergence is due to the separation of variables in time and space. Thus the dynamic equilibrium equations (dropping the axial terms as well as the virtual work of external forces at the moment) are given by; For EBB,

$$\delta W_{iner} + \delta W_{int} = \omega^2\int_l\left(\rho I\frac{dw}{dx}\frac{d\delta w}{dx} + \rho Aw\delta w\right)\mathrm{d}x - \int_l\left(EI\frac{d^2\delta w}{dx^2}\frac{d^2w}{dx^2}\right)\mathrm{d}x \qquad (A.3.34)$$

and for TB,

$$\delta W_{iner} + \delta W_{int} = \omega^2\int_l\left(\rho I\beta\delta\beta + \rho Aw\delta w\right)\mathrm{d}x$$

$$- \int_l\left(EI\frac{d\delta\beta}{dx}\frac{d\beta}{dx} + (\frac{d\delta w}{dx} - \delta\beta)\mu Ak_s(\frac{dw}{dx} - \beta)\right)\mathrm{d}x \qquad (A.3.35)$$

The partial derivatives in (A.3.34) and (A.3.35) are replaced with full derivatives since equations are no longer time dependent; although similar observation holds for (?? - A.3.32) but

we have kept them like that for the purpse of illustration. The Euler-Lagrange equations can now be extracted from (A.3.34) and (A.3.35) for the two models, respectively. This can be achieved by working from weak form to strong form of the problems. For the particular case of EBB it is straightforward to show the equivalent form of (A.3.34) as,

$$\delta W_{iner} + \delta W_{int} = \int_l \delta w \left[\omega^2 \left(\rho A w - \rho I \frac{d^2 w}{dx^2} \right) - EI \frac{d^4 w}{dx^4} \right] dx \tag{A.3.36}$$

from which the governing differential equation turns out.

$$\omega^2 \left(\rho A w - \rho I \frac{d^2 w}{dx^2} \right) - EI \frac{d^4 w}{dx^4} = 0 \tag{A.3.37}$$

Noting that ω^2 is a consequence of separation of variables and corresponds to twice differentiation with respect to time, as well as adding the contribution of external forces [from $\int_l \delta w q(x,t) dx$], we obtain the fourth order differential equation governing dynamics of EBB.

$$-\left(\rho A \frac{\partial^2 w}{\partial t^2} - \rho I \frac{\partial^4 w}{\partial t^2 \partial x^2} \right) - EI \frac{\partial^4 w}{\partial x^4} = 0 \tag{A.3.38}$$

$$\Rightarrow \ \rho A \frac{\partial^2 w}{\partial t^2} - \rho I \frac{\partial^4 w}{\partial t^2 \partial x^2} + EI \frac{\partial^4 w}{\partial x^4} = q(x,t) \quad \text{on} \ \ \Omega \times \mathrm{T} \tag{A.3.39}$$

Equation (A.3.39) is the differential equation governing dynamics of EBB. When working from weak to strong form some boundary terms appear, which essentially correspond to the boundary conditions of (A.3.39). Considering ω^2 as the second time derivative, for (A.3.39) boundary conditions turn out to be.

$$\delta w \left(-\rho I \frac{\partial^3 w}{\partial t^2 \partial x} + EI \frac{\partial^3 w}{\partial x^3} \right) \bigg|_{\Gamma_s + \Gamma_w} - \frac{\partial \delta w}{\partial x} \left(EI \frac{\partial^2 w}{\partial x^2} \right) \bigg|_{\Gamma_m + \Gamma_\theta} \tag{A.3.40}$$

The terms inside the brackets are the specified shear force and specified moment boundary conditions, respectively, and the two other boundary conditions arise from the terms outside the brackets which are specified translation and specified rotation, respectively. These boundary conditions coupled with initital conditions can be conveniently written as.

$$w = \overline{w} \ \ \text{on} \ \ \Gamma_w \tag{A.3.41}$$

$$\frac{\partial w}{\partial x} = \overline{\theta} \ \ \text{on} \ \ \Gamma_\theta \tag{A.3.42}$$

$$-\rho I \frac{\partial^3 w}{\partial t^2 \partial x} + EI \frac{\partial^3 w}{\partial x^3} = \overline{s} \ \ \text{on} \ \ \Gamma_s \tag{A.3.43}$$

$$-EI \frac{\partial^2 w}{\partial x^2} = \overline{m} \ \ \text{on} \ \Gamma_m \tag{A.3.44}$$

$$\vec{u}(0,t) = \vec{u}_0; \quad \dot{\vec{u}}(0,t) = \dot{\vec{u}}_0 \tag{A.3.45}$$

For TB model, we can similarly find the Euler-Lagrange equations from (A.3.35),

$$\delta W_{iner} + \delta W_{int} = \int_l \left\{ \left[\omega^2 \rho I \beta + EI \frac{d^2 \beta}{dx^2} + \mu A k_s (\frac{dw}{dx} - \beta) \right] \delta \beta \right.$$

$$\left. + \left[\omega^2 \rho A w + \frac{dw}{dx} \left(\mu A k_s (\frac{dw}{dx} - \beta) \right) \right] \delta w \right\} dx \tag{A.3.46}$$

whence,

$$\omega^2 \rho I \beta + EI\frac{d^2\beta}{dx^2} + \mu Ak_s(\frac{dw}{dx} - \beta) = 0 \tag{A.3.47}$$

$$\omega^2 \rho Aw + \frac{d}{dx}\left(\mu Ak_s(\frac{dw}{dx} - \beta)\right) = 0 \tag{A.3.48}$$

Above set of equations are suitable for eigenvalue/model analysis. The fully dynamic equilibrium equations of TB can now be written as,

$$\rho I\frac{\partial^2\beta}{\partial t^2} = EI\frac{\partial^2\beta}{\partial x^2} + \mu Ak_s(\frac{\partial w}{\partial x} - \beta) \quad \text{on} \ \ \Omega \times T \tag{A.3.49}$$

$$\rho A\frac{\partial^2 w}{\partial t^2} - q(x,t) = \frac{\partial}{\partial x}\left(\mu Ak_s(\frac{\partial w}{\partial x} - \beta)\right) \quad \text{on} \ \ \Omega \times T \tag{A.3.50}$$

which are exactly the equations reported in Reddy [43]. The boundary conditions arising in the process are,

$$\delta w\left(\mu Ak_s(\frac{\partial w}{\partial x} - \beta)\right)\Big|_{\Gamma_s + \Gamma_w} + \delta\beta\left(EI\frac{\partial\beta}{\partial x}\right)\Big|_{\Gamma_m + \Gamma_\theta} \tag{A.3.51}$$

the terms inside the brackets are the specified shear force and specified moment boundary conditions, respectively, and the two other boundary conditions arise from the terms outside the brackets which are specified translation and specified rotations respectively. These boundary conditions coupled with initital conditions can be conveniently written as.

$$w = \overline{w} \ \ \text{on} \ \ \Gamma_w \tag{A.3.52}$$

$$\beta = \overline{\theta} \ \ \text{on} \ \ \Gamma_\theta \tag{A.3.53}$$

$$\mu Ak_s(\frac{\partial w}{\partial x} - \beta) = \overline{s} \ \ \text{on} \ \ \Gamma_s \tag{A.3.54}$$

$$EI\frac{\partial\beta}{\partial x} = \overline{m} \ \ \text{on} \ \Gamma_m \tag{A.3.55}$$

$$\vec{u}(0,t) = \vec{u}_0; \ \ \ \dot{\vec{u}}(0,t) = \dot{\vec{u}}_0 \tag{A.3.56}$$

As pointed out at the end of previous section that, applied moments are dealt with differently in EBB and TB finite element formulations. From (A.3.40) and (A.3.51) one can clearly make out, why in the evaluation of applied moments we use $\overline{m}(\frac{\partial \vec{N}^T}{\partial x})|_{\Gamma_m}$ for EBB and $\overline{m}\vec{N}^T|_{\Gamma_m}$, for TB model. Under linear elastic isotropic and homogenous cross section assumptions, equations (A.3.49) and (A.3.50) can be coupled to give one fourth order differential equation.

$$EI\frac{\partial^4 w}{\partial x^4} + \rho A\frac{\partial^2 w}{\partial t^2} - (\rho I + \frac{\rho EI}{\mu k_s})\frac{\partial^4 w}{\partial x^2 \partial t^2} + \frac{\rho^2 I}{\mu k_s}\frac{\partial^4 w}{\partial t^4} = q + \frac{\rho I}{\mu Ak_s}\frac{\partial^2 q}{\partial t^2} - \frac{EI}{\mu Ak_s}\frac{\partial^2 q}{\partial x^2} \tag{A.3.57}$$

The derivation is straightforward and can be achieved from (A.3.49) and (A.3.50) by eliminating rotation terms. Dropping the external force term, the separation of variables into space and time leads to,

$$EI\frac{d^4 w}{dx^4} + \omega^2(\rho I + \frac{\rho EI}{\mu k_s})\frac{d^2 w}{dx^2} + \omega^4\frac{\rho^2 I}{\mu k_s}w - \omega^2 \rho Aw = 0 \quad \text{on} \ \ \Omega = [0, L] \tag{A.3.58}$$

The above form is more suitable for modal analysis.

96

1.3.4. Modal Analysis with Rotary Inertia Neglected

In this section modal analysis of both EBB and TB models is presented. Analytical solutions for simply supported and cantilever beams are derived with and without rotary inertia consideration. When rotary inertial is neglected both EBB model and TB model yield the same expression,

$$EI\frac{d^4w}{dx^4} - \omega^2\rho Aw = 0 \tag{A.3.59}$$

which can be verified from A.3.37 and A.3.58 by dropping the rotary inertia terms. In (A.3.59) w is just a function of x. To solve this homogenous ordinary differential equation, the characteristic equation has to be found which in this case is,

$$\lambda^4 - a^4 = 0 \tag{A.3.60}$$

where $a = \sqrt[4]{\omega^2\rho AL^4/EI}$. The four roots of this equation are distinct and are.

$$\lambda = a \qquad\qquad\qquad \lambda = ia \tag{A.3.61}$$
$$\lambda = -a \qquad\qquad\qquad \lambda = -ia \tag{A.3.62}$$

The complete solution of (A.3.59) comprises of only the homogenous solution which for two distinct real and two distinct imaginary roots takes the form [Noting that for each distinct real root λ_i we add $c_i e^{\lambda_i x}$ and for each distinct complex root $p \pm iq$ we add $e^{px}(c_1\cos(qx) + c_2\sin(qx))$].

$$w(x) = c_1 e^{ax/L} + c_2 e^{-ax/L} + c_3\cos(ax/L) + c_4\sin(ax/L) \tag{A.3.63}$$

This is the complete generic solution of (A.3.59). Depending on the boundary conditions, the coefficients can be determined. For simply supported beam, we have.

$$w(0) = 0 \qquad\qquad\qquad w(L) = 0 \tag{A.3.64}$$
$$w''(0) = 0 \qquad\qquad\qquad w''(L) = 0 \tag{A.3.65}$$

Imposing the above four boundary conditions yields the following system of equations.

$$\begin{bmatrix} 1 & 1 & 1 & 0 \\ 1 & 1 & -1 & 0 \\ e^a & e^{-a} & \cos(a) & \sin(a) \\ e^a & e^{-a} & -\cos(a) & -\sin(a) \end{bmatrix} \begin{Bmatrix} c_1 \\ c_2 \\ c_3 \\ c_4 \end{Bmatrix} = \begin{Bmatrix} 0 \\ 0 \\ 0 \\ 0 \end{Bmatrix} \tag{A.3.66}$$

The above sytem of equations has a trivial solution. To get the non-trivial solution, the determinant of the matrix should be zero, which consequently leads to.

$$8\sin(a)\sinh(a) = 0 \tag{A.3.67}$$

whose solution is

$$a = n\pi \implies \sqrt[4]{\frac{\omega^2\rho AL^4}{EI}} = n\pi \Rightarrow \omega = \frac{n^2\pi^2}{L^2}\sqrt{\frac{EI}{\rho A}} \tag{A.3.68}$$

The first four fundamental frequencies are listed below.

$$w_n = \frac{1}{L^2}\sqrt{\frac{EI}{\rho A}} \begin{Bmatrix} 9.8696 \\ 39.4784 \\ 88.8264 \\ 157.9137 \\ \cdot \\ \cdot \end{Bmatrix} \tag{A.3.69}$$

For cantilever beam the following boundary conditions have to be imposed.

$$w(0) = 0 \qquad\qquad\qquad w''(L) = 0 \tag{A.3.70}$$

$$w'(0) = 0 \qquad\qquad\qquad w'''(L) = 0 \tag{A.3.71}$$

That is transverse displacement and rotation are zero at fixed end and moment and shear force are zero at the free end. Imposing boundary conditions yield.

$$
\begin{bmatrix}
1 & 1 & 1 & 0 \\
1 & -1 & 0 & 1 \\
e^a & e^{-a} & -\cos(a) & -\sin(a) \\
e^a & -e^{-a} & \sin(a) & -\cos(a)
\end{bmatrix}
\begin{Bmatrix}
c_1 \\ c_2 \\ c_3 \\ c_4
\end{Bmatrix}
=
\begin{Bmatrix}
0 \\ 0 \\ 0 \\ 0
\end{Bmatrix}
\tag{A.3.72}
$$

The above sytem of equations has a trivial solution. To get the non-trivial solution, the determinant of the matrix should be zero, which consequently leads to,

$$\cos(a)\cosh(a) = -1 \tag{A.3.73}$$

whose roots can be found using an iterative procedure like Newton-Raphson. For convenience, the first four fundamental frequencies of cantilever beam are listed below.

$$
w_n = \frac{1}{L^2}\sqrt{\frac{EI}{\rho A}}
\begin{Bmatrix}
3.5160 \\
22.0345 \\
61.6972 \\
120.9019 \\
. \\
.
\end{Bmatrix}
\tag{A.3.74}
$$

Equations A.3.69 and A.3.74 represent the exact frequencies of both EBB and TB model for simply supported and cantilever beams, respectively.

1.3.5. Rotary Inertia Included

When rotary inertia is included the eigenvalues and eigenmodes are different for EBB and TB models. We start with finding exact frequencies of EBB model, for simply supported and cantilever beams. From (A.3.37) we have,

$$EI\frac{d^4 w}{dx^4} + \omega^2 \rho I \frac{d^2 w}{dx^2} - \omega^2 \rho A w = 0 \tag{A.3.75}$$

and the characteristic equation becomes,

$$\lambda^4 + b\lambda^2 - a = 0 \tag{A.3.76}$$

where $b = \frac{\rho L^2}{E}\omega^2$ and $a = \frac{\rho A L^4}{EI}\omega^2$. Since both a and b are real and positive, one can show that the characteristic equation has two distinct real and two distinct imaginary roots, so the complete solution of (A.3.75) becomes,

$$w(x) = c_1 e^{m_1 x/L} + c_2 e^{-m_1 x/L} + c_3 \cos(m_2 x/L) + c_4 \sin(m_2 x/L) \tag{A.3.77}$$

where $\pm m_1$ are the real roots and $\pm i m_2$ are the complex roots of (A.3.76). For simply supported beam, after imposing the boundary conditions (A.3.64 - A.3.65), and finding the determinant we obtain a similar equation to that. of (A.3.67)

$$8\sin(m_2)\sinh(m_1) = 0 \tag{A.3.78}$$

Substituting for $m_2 = \sqrt{b/2 + 1/2\sqrt{b^2 + 4a}}$, as well as a and b we obtain the natural frequencies of simply supported EBB with rotary inertia included as.

$$w_n = \frac{n^2\pi^2}{L}\sqrt{\frac{EI}{(\rho A L^2 + \rho I n^2 \pi^2)}} \tag{A.3.79}$$

It is clear that when rotary inertia term is neglected A.3.79 reduces to A.3.68. For convenience once again four natural frequencies of simply supported EBB with rotary inertia is listed as factor of $\frac{1}{L^2}\sqrt{EI/\rho A}$.

$$w_n = \frac{1}{L^2}\sqrt{\frac{EI}{\rho A}} \begin{Bmatrix} 9.8692 \\ 39.4719 \\ 88.7936 \\ 157.8099 \\ . \\ . \end{Bmatrix} \tag{A.3.80}$$

We can observe that rotary inertia decreases natural frequencies of the system. For cantilever EBB, after imposing boundary conditions (A.3.70 - A.3.71) and finding the determinant we obtain.

$$\cos(m_1)\cosh(m_2) = -1 \tag{A.3.81}$$

Unlike A.3.78 closed form solution of (A.3.81) is not as trivial, especially that it involves both $m1$ and $m2$ [Note that in A.3.78 we only solve for $\sin(m2) = 0$ since $\sinh(m1) = 0$ gives the trivial solution]. It turns out that, this issue has been the subject of much debate in the literature [37] [49]. For the case of Timoshenko with rotary inertia included, one solves the for the roots of a characteristic equation similar to (A.3.76), with coefficients $a = (\omega^4\rho^2 I/\mu k_s - \omega^2\rho A)L^4/EI$ and $b = (\rho I + \rho EI/\mu k_s)\omega^2 L^2/EI$. Its clear from these coefficients that for Timoshenko beam, the differential equation (A.3.58) does not have a generic homogeneous solution because of the unknown nature of $b^2 - 4a$. Depending on geometrical and material properties, two solutions exist in general. Elegant analytical solutions for natural frequencies of simply supported and cantilever TB are given in [49]. Going deeper into this issue would defeat the purpose of this appendix and what has been presented so far generally suffices, however for the sake of comparison with numerical results presented later, the exact frequencies for $L/h = 100$ are listed below. For cantilever EBB with rotary inertia the first four exact fundamental frequencies are,

$$w_n = \frac{1}{L^2}\sqrt{\frac{EI}{\rho A}} \begin{Bmatrix} 3.5158 \\ 22.0315 \\ 61.6774 \\ 120.8300 \\ . \\ . \end{Bmatrix} \tag{A.3.82}$$

and for TB model including rotary inertia the first four exact natural frequencies for simply supported and cantilever configurations are,

$$
w_n^{SS} = \frac{1}{L^2}\sqrt{\frac{EI}{\rho A}}\begin{Bmatrix} 9.8682 \\ 39.4564 \\ 88.7149 \\ 157.5619 \\ . \\ . \end{Bmatrix} \;\; ; \;\; w_n^{C} = \frac{1}{L^2}\sqrt{\frac{EI}{\rho A}}\begin{Bmatrix} 3.5158 \\ 22.0244 \\ 61.6298 \\ 120.6580 \\ . \\ . \end{Bmatrix} \tag{A.3.83}
$$

respectively.

Some plots of h, p and hp refinement for eigen frequencies of simply supported and cantilever timoshenko beams are shown in the following.
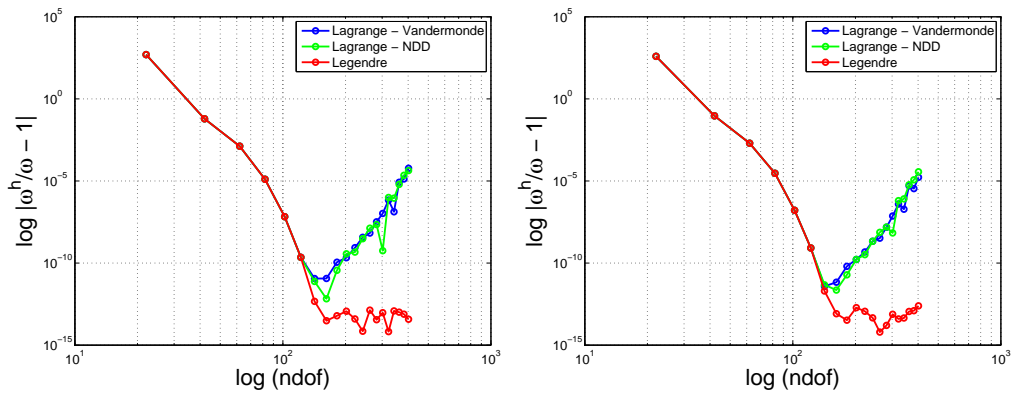

Figure 52: Comparative Convergence with Various Basis Functions; L - SSB, R - CB
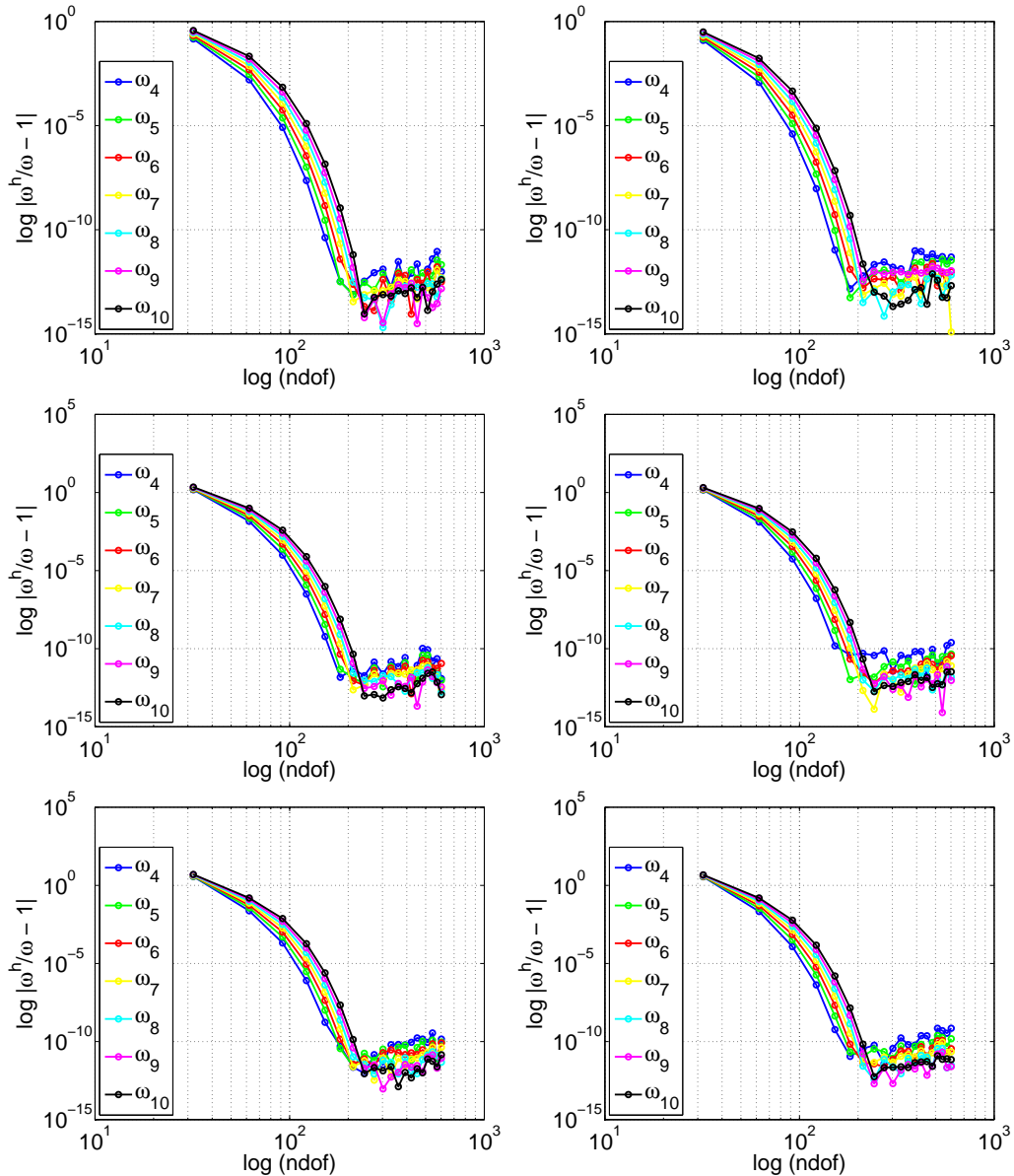
Figure 53: Convergence of 4th-10th Frequencies; T - $L/h = 10$, M - $L/h = 50$, B - $L/h = 100$, L - SSB, R - CB
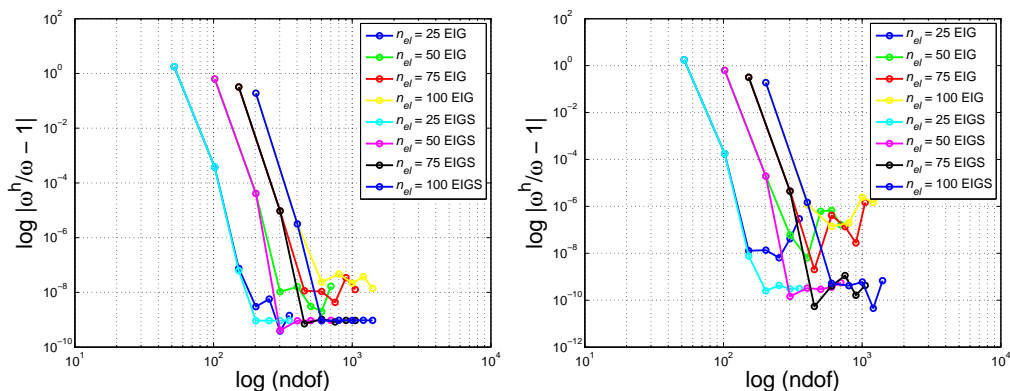

Figure 54: Convergence of 1st Frequency with hp-refinement; L - SSB, R - CB

101
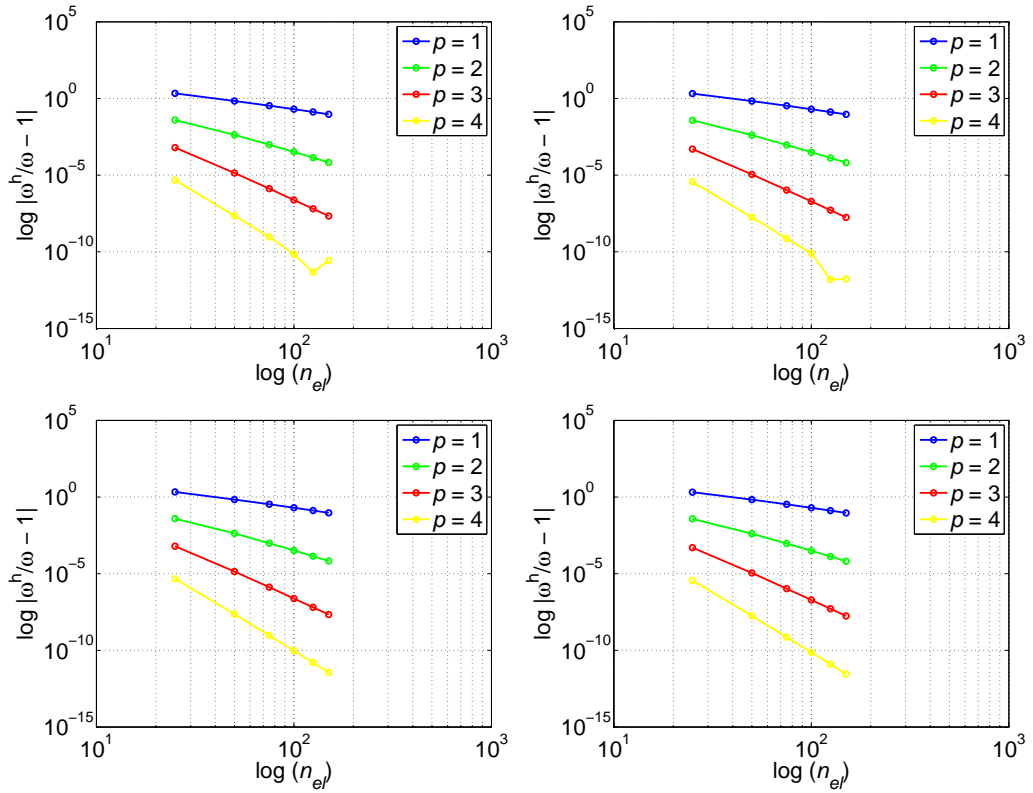
Figure 55: Convergence of 1st Frequency with h-refinement; L - SSB, R - CB
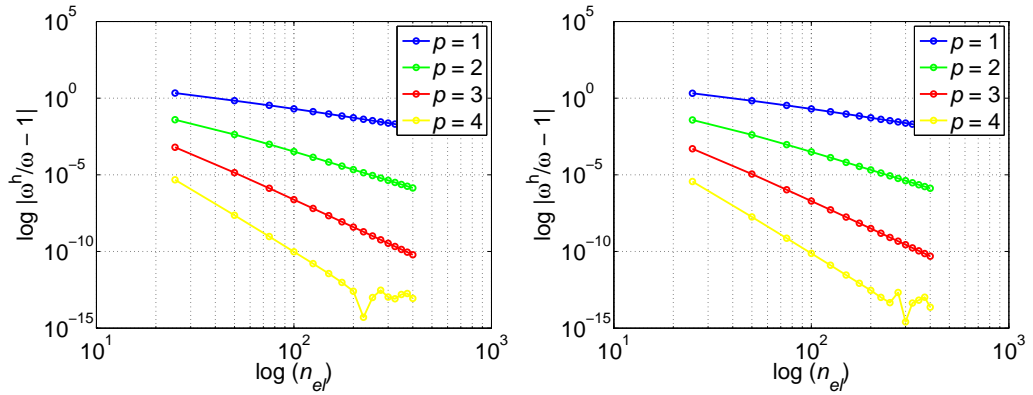
Figure 56: Convergence of 1st Frequency with hp-refinement; L - SSB, R - CB

In light of the above discussion, this section is concluded.

1.4. Appendix 4

1.4.1. Direct Time Integration Algorithms

In this section some important direct time integration algorithms are discussed with their relative advantages and disadvantages over each other. The structure of this Appendix heavily borrows that of Bathe [3]. Damping is neglected throughout the analysis, however its inclusion is straightforward.

1.4.2. The Central Difference Method

Consider the equations of motion, in general

$$\boldsymbol{M}\vec{\ddot{u}} + \boldsymbol{K}\vec{u} = \vec{F} \tag{A.4.84}$$

Using the central difference method to approximate first and second time derivatives we have.

$$\vec{\dot{u}}_i = \frac{\vec{u}_{i+1} - \vec{u}_{i-1}}{2\Delta t} \tag{A.4.85}$$

$$\vec{\ddot{u}}_i = \frac{\vec{u}_{i+1} - 2\vec{u}_i + \vec{u}_{i-1}}{\Delta t^2} \tag{A.4.86}$$

Substituting above in the earlier equation gives.

$$\boldsymbol{M}(\frac{\vec{u}_{i+1} - 2\vec{u}_i + \vec{u}_{i-1}}{\Delta t^2}) + \boldsymbol{K}\vec{u}_i = \vec{F}_i \tag{A.4.87}$$

$$\boldsymbol{M}\vec{u}_{i+1} = \Delta t^2 \vec{F}_i + (2\boldsymbol{M} - \Delta t^2 \boldsymbol{K})\vec{u}_i - \boldsymbol{M}\vec{u}_{i-1} \tag{A.4.88}$$

The above system of equations has to be solved for every time step. To compute $\vec{u}_{i-1}$ we can make use of the two aforementioned central difference equations i.e.

$$\vec{u}_{i-1} = \vec{u}_i - \Delta t\vec{\dot{u}}_i + \frac{\Delta t^2}{2}\vec{\ddot{u}}_i \tag{A.4.89}$$

Note that in dynamic analysis of structures initial nodal acceleration vector is usually computed from initial nodal displacement vector and initial nodal force vector by sovling the motion equation, i.e.

$$\boldsymbol{M}\vec{\ddot{u}}_0 = \vec{F}_0 - \boldsymbol{K}\vec{u}_0 \tag{A.4.90}$$

The entire procedure can be effectively summarised as:

---

1. Build Stiffness $\boldsymbol{K}$ and Mass $\boldsymbol{M}$ Matrices.

2. Initiate nodal displacements $\vec{u}_0$, nodal velocities $\vec{\dot{u}}_0$ and nodal forces vectors $\vec{F}_0$.

3. Choose time step size Δt and number of time steps *nstep*.

4. Compute initial nodal acceleration: $\boldsymbol{M}\vec{\ddot{u}}_0 = \vec{F}_0 - \boldsymbol{K}\vec{u}_0$

5. Compute displacement at time t_{-1}: $\vec{u}_{-1} = \vec{u}_0 - \Delta t\vec{\dot{u}}_0 + \frac{\Delta t^2}{2}\vec{\ddot{u}}_0$

6. For each time step compute the nodal quantities

   (a) Nodal displacements: $\boldsymbol{M}\vec{u}_{i+1} = \Delta t^2 \vec{F}_i + (2\boldsymbol{M} - \Delta t^2 \boldsymbol{K})\vec{u}_i - \boldsymbol{M}\vec{u}_{i-1}$

   (b) Nodal velocities: $\dot{\vec{u}}_{i+1} = \frac{1}{2\Delta t}((\vec{u}_{i+1} + \vec{u}_i)$

   (c) Nodal accelerations: $\ddot{\vec{u}}_{i+1} = \frac{1}{\Delta t^2}(\vec{u}_{i+1} - 2\vec{u}_i + \vec{u}_{i-1})$

Central difference method is explicit, second order accurate and requires extremely small time step size.

1.4.3. The Houbolt Method

The following finite difference expansions are employed in Houbolts method.

$$\ddot{\vec{u}}_{i+1} = \frac{1}{\Delta t^2}(2\vec{u}_{i+1} - 5\vec{u}_i + 4\vec{u}_{i-1} - \vec{u}_{i-2}) \tag{A.4.91}$$

$$\dot{\vec{u}}_{i+1} = \frac{1}{6\Delta t}(11\vec{u}_{i+1} - 18\vec{u}_i + 9\vec{u}_{i-1} - 2\vec{u}_{i-2}) \tag{A.4.92}$$

which are two backward formulas with error of order $O(\Delta t)^2$, for acceleration and velocity in terms of displacement. The step-by-step procedure for Houbolt method is given in the following. Note that Houbolt method needs special starting procedure, such as using central difference:

---

1. Build Stiffness $\boldsymbol{K}$ and Mass $\boldsymbol{M}$ Matrices.

2. Initiate nodal displacements $\vec{u}_0$, nodal velocities $\dot{\vec{u}}_0$ and nodal forces vectors $\vec{F}_0$.

3. Choose time step size Δt and number of time steps *nstep*.

4. Compute initial nodal acceleration: $\boldsymbol{M}\ddot{\vec{u}}_0 = \vec{F}_0 - \boldsymbol{K}\vec{u}_0$

5. Compute displacement at time t_{-1}: $\vec{u}_{-1} = \vec{u}_0 - \Delta t \dot{\vec{u}}_0 + \frac{\Delta t^2}{2}\ddot{\vec{u}}_0$

6. Special starting procedure, central difference method:

   (a) Nodal displacements: $\boldsymbol{M}\vec{u}_1 = \Delta t^2 \vec{F}_0 + (2\boldsymbol{M} - \Delta t^2 \boldsymbol{K})\vec{u}_0 - \boldsymbol{M}\vec{u}_{-1}$

   (b) Nodal velocities: $\dot{\vec{u}}_1 = \frac{1}{2\Delta t}((\vec{u}_1 + \vec{u}_0)$

   (c) Nodal accelerations: $\ddot{\vec{u}}_1 = \frac{1}{\Delta t^2}(\vec{u}_1 - 2\vec{u}_0 + \vec{u}_{-1})$

7. For each time step compute the nodal quantities

   (a) Nodal displacements: $(2\boldsymbol{M} + \Delta t^2 \boldsymbol{K})\vec{u}_{i+1} = \Delta t^2 \vec{F}_{i+1} + \boldsymbol{M}(5\vec{u}_i - 4\vec{u}_{i-1} + \vec{u}_{i-2})$

   (b) Nodal velocities: $\dot{\vec{u}}_{i+1} = \frac{1}{6\Delta t}(11\vec{u}_{i+1} - 18\vec{u}_i + 9\vec{u}_{i-1} - 2\vec{u}_{i-2})$

   (c) Nodal accelerations: $\ddot{\vec{u}}_{i+1} = \frac{1}{\Delta t^2}(2\vec{u}_{i+1} - 5\vec{u}_i + 4\vec{u}_{i-1} - \vec{u}_{i-2})$

Houbolt method is an implicit technique with second order accuracy, conditional stability and the time step size is not restricted to numerical stability of the technique as in central difference method. However it introduces a lagre amplitude decay and period elongation compared to other methods.

1.4.4. The Wilson θ Method

The implementation procedure for Wilson θ is briefly summarised in the following:

---

1. Build Stiffness $\boldsymbol{K}$ and Mass $\boldsymbol{M}$ Matrices.

2. Initiate nodal displacements $\vec{u}_0$, nodal velocities $\dot{\vec{u}}_0$ and nodal forces vectors $\vec{F}_0$.

3. Choose time step size Δt and number of time steps $nstep$.

4. Compute initial nodal acceleration: $\boldsymbol{M}\ddot{\vec{u}}_0 = \vec{F}_0 - \boldsymbol{K}\vec{u}_0$

5. For each time step compute the nodal quantities

   (a) Nodal displacements at time $t + \theta\Delta t$:

   $$(\tfrac{6}{\theta^2\Delta t^2}\boldsymbol{M} + \boldsymbol{K})\vec{u}_{i+\theta} = (1-\theta)\vec{F}_i + \theta\vec{F}_{i+1} + \tfrac{6}{\theta^2\Delta t^2}\boldsymbol{M}\vec{u}_i + \tfrac{6}{\theta\Delta t}\boldsymbol{M}\dot{\vec{u}}_i + 2\boldsymbol{M}\ddot{\vec{u}}_i$$

   (b) Nodal accelerations at time $t + \Delta t$: $\quad \ddot{\vec{u}}_{i+1} = \tfrac{6}{\theta^3\Delta t^2}(\vec{u}_{i+\theta} - \vec{u}_i) - \tfrac{6}{\theta^2\Delta t}\dot{\vec{u}}_i + (1 - \tfrac{3}{\theta})\ddot{\vec{u}}_i$

   (c) Nodal velocities at time $t + \Delta t$: $\quad \dot{\vec{u}}_{i+1} = \dot{\vec{u}}_i + \tfrac{\Delta t}{2}(\ddot{\vec{u}}_{i+1} + \ddot{\vec{u}}_i)$

   (d) Nodal displacements at time $t + \Delta t$: $\vec{u}_{i+1} = \vec{u}_i + \Delta t\dot{\vec{u}}_i + \tfrac{\Delta t^2}{6}(\ddot{\vec{u}}_{i+1} + 2\ddot{\vec{u}}_i)$

Wilson θ method is an implicit technique with second order accuracy. The method is unconditionaly stable for $\theta \geq 1.37$.

1.4.5. The Newmark's Method

The Newmark's method is a two parameter single step integrator which uses the following approximation.

$$\dot{\vec{u}}_{i+1} = \dot{\vec{u}}_i + \Delta t\left[(1-\delta)\ddot{\vec{u}}_i + \delta\ddot{\vec{u}}_{i+1}\right] \tag{A.4.93}$$

$$\vec{u}_{i+1} = \vec{u}_i + \Delta t\dot{\vec{u}}_i + \Delta t^2\left[(\frac{1}{2} - \gamma)\ddot{\vec{u}}_i + \gamma\ddot{\vec{u}}_{i+1}\right] \tag{A.4.94}$$

If $\delta = \frac{1}{2}$ and $\gamma = \frac{1}{6}$ the method reduces to linear acceleration method (this corresponds to $\theta = 1$ in Wilson's method), if $\delta = \frac{1}{2}$ and $\gamma = \frac{1}{4}$ the method reduces to trapazoidal/average

acceleration method, if $\delta = \frac{1}{2}$ and $\gamma = \frac{1}{12}$ the method reduces to Fox-Goodwin scheme and if $\delta = \frac{1}{2}$ and $\gamma = 0$ the method reduces to central difference method. The implementation procedure for Newmark's method is briefly summarised in the following:

1. Build Stiffness $\boldsymbol{K}$ and Mass $\boldsymbol{M}$ Matrices.

2. Initiate nodal displacements $\vec{u}_0$, nodal velocities $\dot{\vec{u}}_0$ and nodal forces vectors $\vec{F}_0$

3. Choose time step size Δt, number of time steps $nstep$ and integration parameters δ and γ

4. Compute initial nodal acceleration: $\boldsymbol{M}\ddot{\vec{u}}_0 = \vec{F}_0 - \boldsymbol{K}\vec{u}_0$

5. For each time step compute the nodal quantities

   (a) Nodal displacements : $(\frac{1}{\Delta t^2 \gamma}\boldsymbol{M} + \boldsymbol{K})\vec{u}_{i+1} = \vec{F}_{i+1} + \frac{1}{\Delta t^2 \gamma}\boldsymbol{M}\vec{u}_i + \frac{1}{\Delta t \gamma}\boldsymbol{M}\dot{\vec{u}}_i + (\frac{1}{2\gamma} - 1)\boldsymbol{M}\ddot{\vec{u}}_i$

   (b) Nodal accelerations : $\ddot{\vec{u}}_{i+1} = \frac{1}{\Delta t^2 \gamma}(\vec{u}_{i+1} - \vec{u}_i) - \frac{1}{\Delta t \gamma}\dot{\vec{u}}_i + (1 - \frac{1}{2\gamma})\ddot{\vec{u}}_i$

   (c) Nodal velocities : $\dot{\vec{u}}_{i+1} = \dot{\vec{u}}_i + \Delta t\left[\delta\ddot{\vec{u}}_{i+1} + (1-\delta)\ddot{\vec{u}}_i\right]$

Newmark's method is second order accurate and unconditionally stable for $\delta \geq 0.5$ and $\gamma \geq 0.25(0.5 + \delta)^2$ Notice that unlike in the central difference and Houbolt methods in the two latter schemes displacements, velocitites and accelerations are coupled.

1.4.6. The Hilbert-Hughes-Taylor-α Method

The Hilbert-Hughes-Taylor-α or simply α-method is a three parameter single step integration technique which allows for energy dissipation [23]. The method uses the two equations of Newmark together with.

$$\boldsymbol{M}\ddot{\vec{u}}_{i+1} + (1+\alpha)\boldsymbol{K}\vec{u}_{i+1} - \alpha\boldsymbol{K}\vec{u}_i = (1+\alpha)\vec{F}_{i+1} - \alpha\vec{F}_i \qquad (A.4.95)$$

The parameter values are normally choosen in the range $-\frac{1}{3} \leq \alpha \leq 0$; $\gamma = 0.25(1-\alpha)^2$; and $\delta = \frac{1}{2} - \alpha$. By setting $\alpha = 0$ Newmark's method is recovered. The implementation procedure for the method is briefly summarised in the following:

1. Build Stiffness $\boldsymbol{K}$ and Mass $\boldsymbol{M}$ Matrices.

2. Initiate nodal displacements $\vec{u}_0$, nodal velocities $\dot{\vec{u}}_0$ and nodal forces vectors $\vec{F}_0$

3. Choose Δt, $nstep$, α, δ and γ.

4. Compute initial nodal acceleration: $\boldsymbol{M}\ddot{\vec{u}}_0 = \vec{F}_0 - \boldsymbol{K}\vec{u}_0$

5. For each time step compute the nodal quantities

(a) Nodal displacements :

$$\left[\frac{1}{\Delta t^2 \gamma}\boldsymbol{M} + (1+\alpha)\boldsymbol{K}\right]\vec{u}_{i+1} =$$

$$(1+\alpha)\vec{F}_{i+1} - \alpha\vec{F}_i + \left[\frac{1}{\Delta t^2 \gamma}\boldsymbol{M} + \alpha\boldsymbol{K}\right]\vec{u}_i + \frac{1}{\Delta t\gamma}\boldsymbol{M}\dot{\vec{u}}_i + (\frac{1}{2\gamma} - 1)\boldsymbol{M}\ddot{\vec{u}}_i$$

(b) Nodal accelerations : $\ddot{\vec{u}}_{i+1} = \frac{1}{\Delta t^2 \gamma}(\vec{u}_{i+1} - \vec{u}_i) - \frac{1}{\Delta t\gamma}\dot{\vec{u}}_i + (1 - \frac{1}{2\gamma})\ddot{\vec{u}}_i$

(c) Nodal velocities : $\dot{\vec{u}}_{i+1} = \dot{\vec{u}}_i + \Delta t\left[\delta\ddot{\vec{u}}_{i+1} + (1-\delta)\ddot{\vec{u}}_i\right]$

1.4.7. The Generalised-α Method

The Generalised-α method is 4 parameter single step integration technique which allows for energy dissipation [10]. The method uses the two equations of Newmark's together with the following equations.

$$\boldsymbol{M}\ddot{\vec{u}}_{i+1-\alpha_m} + \boldsymbol{K}\vec{u}_{i+1-\alpha_f} = \vec{F}_{i+1-\alpha_f} \qquad (A.4.96)$$

$$\vec{u}_{i+1-\alpha_f} = (1-\alpha_f)\vec{u}_{i+1} + \alpha_f\vec{u}_i \qquad (A.4.97)$$

$$\dot{\vec{u}}_{i+1-\alpha_f} = (1-\alpha_f)\dot{\vec{u}}_{i+1} + \alpha_f\dot{\vec{u}}_i \qquad (A.4.98)$$

$$\ddot{\vec{u}}_{i+1-\alpha_m} = (1-\alpha_m)\ddot{\vec{u}}_{i+1} + \alpha_m\ddot{\vec{u}}_i \qquad (A.4.99)$$

$$\vec{F}_{i+1-\alpha_f} = (1-\alpha_f)\vec{F}_{i+1} + \alpha_f\vec{F}_i \qquad (A.4.100)$$

The values for these parameters are normally chosen based on the spectral radius i.e. absolute value of maximum eigenvalue of the matrix $\boldsymbol{A}$ such that $\vec{X}^{n+1} = \boldsymbol{A}\vec{X}^n$, where $\vec{X}$ can be the vector of any unknown quantity (i.e. displacements, velocities, accelerations) and the superscripts n and $n+1$ denote the two subsequent time steps. For an scheme to be stable, the spectral radius ρ should be at most equal unity i.e $\rho \leq 1$. Based on spectral radius ρ, the 4 integration parameters are given as, $\alpha_f = \rho/(\rho+1)$, $\alpha_m = (2\rho-1)/(\rho+1)$, $\delta = 0.5 + (\alpha_f - \alpha_m)$, and $\gamma \geq 0.25 + 0.5(\alpha_f - \alpha_m)$. By setting $\alpha_f = \alpha_m = 0$ Newmark's method is recovered. If only $\alpha_m = 0$ the scheme reduces to HHT-α scheme. The method is unconditionally stable for $\alpha_m \leq \alpha_f \leq 0.5$ and $\gamma \geq 0.25 + 0.5(\alpha_f - \alpha_m)$. The implementation procedure for the method is briefly summarised in the following:

1. Build Stiffness $\boldsymbol{K}$ and Mass $\boldsymbol{M}$ Matrices.

2. Initiate nodal displacements $\vec{u}_0$, nodal velocities $\dot{\vec{u}}_0$ and nodal forces vectors $\vec{F}_0$

3. Choose Δt, $nstep$, α_f, α_m, δ and γ.

4. Compute initial nodal acceleration: $\boldsymbol{M}\ddot{\vec{u}}_0 = \vec{F}_0 - \boldsymbol{K}\vec{u}_0$

5. For each time step compute the nodal quantities

(a) Nodal displacements :

$$\left[\frac{(1-\alpha_m)}{\Delta t^2\gamma}\boldsymbol{M} + (1-\alpha_f)\boldsymbol{K}\right]\vec{u}_{i+1} = (1-\alpha_f)\vec{F}_{i+1} + \alpha_f\vec{F}_i + \left[\frac{(1-\alpha_m)}{\Delta t^2\gamma}\boldsymbol{M} - \alpha_f\boldsymbol{K}\right]\vec{u}_i +$$
$$\frac{(1-\alpha_m)}{\Delta t\gamma}\boldsymbol{M}\dot{\vec{u}}_i + \left[(1-\alpha_m)(\frac{1}{2\gamma}-1) - \alpha_m\right]\boldsymbol{M}\ddot{\vec{u}}_i$$

(b) Nodal accelerations : $\quad \ddot{\vec{u}}_{i+1} = \frac{1}{\Delta t^2\gamma}(\vec{u}_{i+1} - \vec{u}_i) - \frac{1}{\Delta t\gamma}\dot{\vec{u}}_i + (1 - \frac{1}{2\gamma})\ddot{\vec{u}}_i$

(c) Nodal velocities : $\quad \dot{\vec{u}}_{i+1} = \dot{\vec{u}}_i + \Delta t\left[\delta\ddot{\vec{u}}_{i+1} + (1-\delta)\ddot{\vec{u}}_i\right]$

We are now prepared to examine the various aspects of dynamic analysis including the choice of dynamic integrators, reduced/full integration and the choice of basis functions. In what immediately follows the generalised-α integrator is employed, with material properties as $E = 1e06; \mu = 5e-05; a, b = 1; L = 100; k_s = 5/6$ and ρ is changed for parametric study. The cantilever TB beam is subjected to a transverse sinusoidal excitation and all the plots presented correspond to transverse displacement of the free end. For the present study consistent mass matrices are used throughout. From Fig. 57 it can be observed that when full integration is performed all basis functions give the same results as expected.
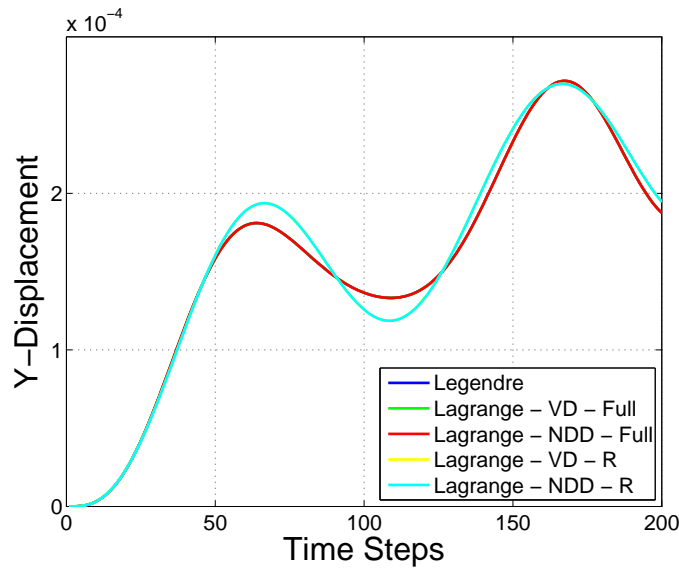

Figure 57: Choice of Bases

Next the choice of full/reduced integration is presented for Lagrangian basis functions. Fig. 58 follows this argument.

108
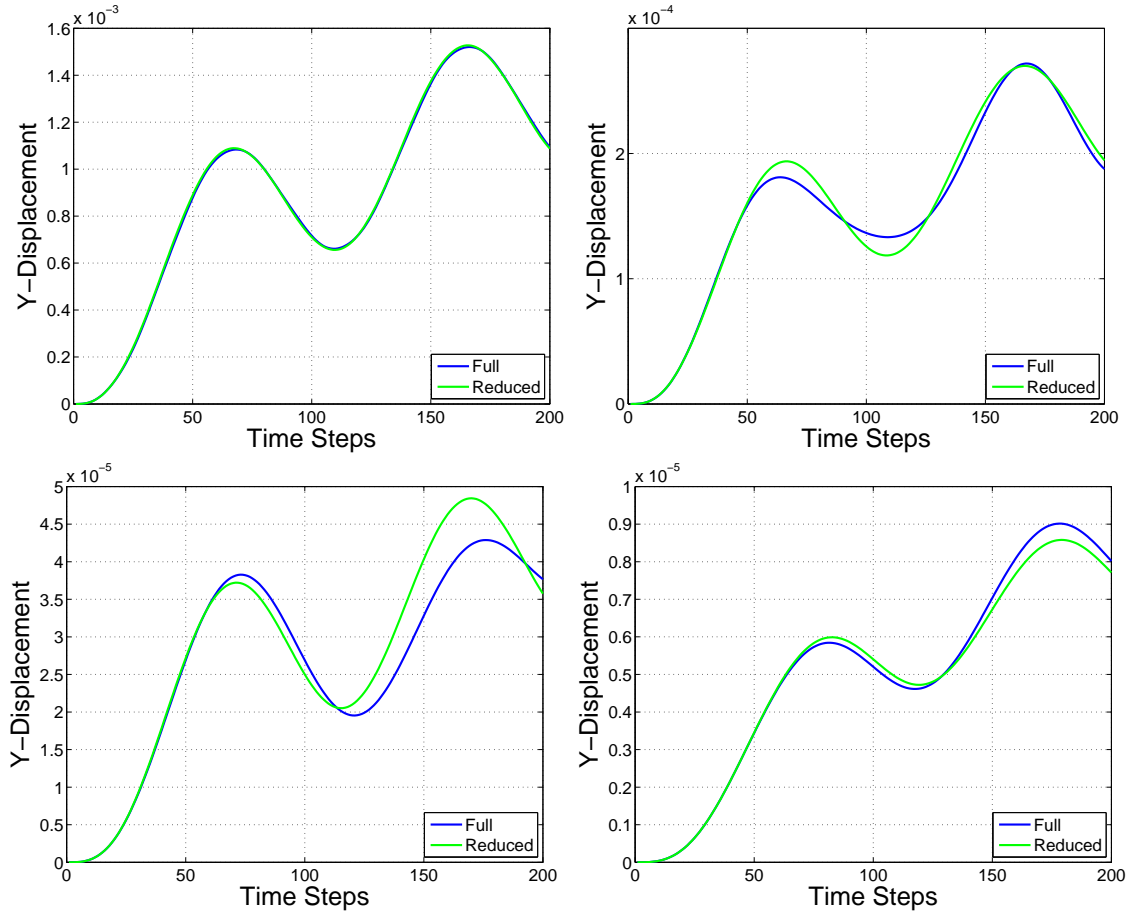
Figure 58: LT - $\rho = 10$, RT - $\rho = 1000$, LB - $\rho = 1000$, RB - $\rho = 10000$

It is time to investigate the performance of dynamic integrators. A comparison is made in Fig. 60.
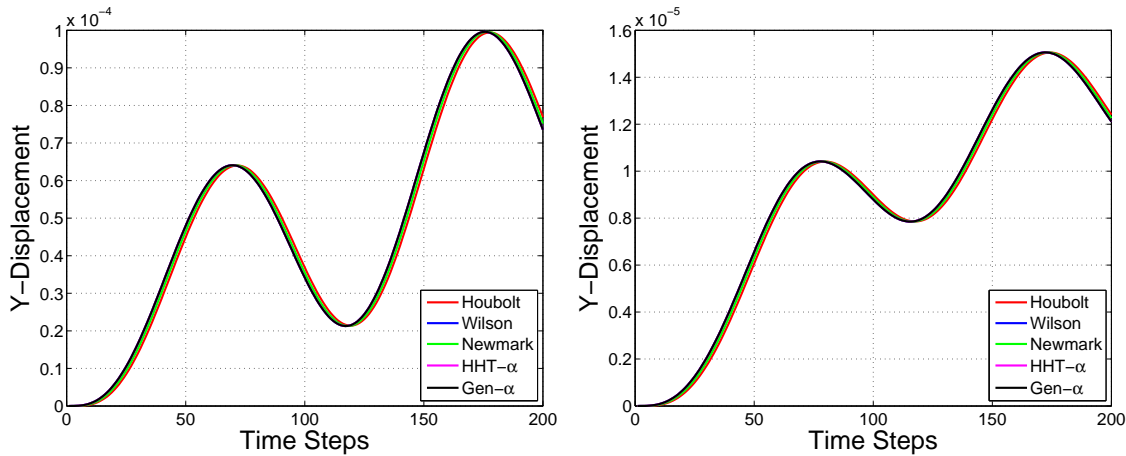
Figure 59: L - $\rho = 500$, R - $\rho = 5000$

It can be verified that Houbolt method has the largest period elongation and frequency decay. Some oscillatory nature of the schemes are shown in Fig. 60.
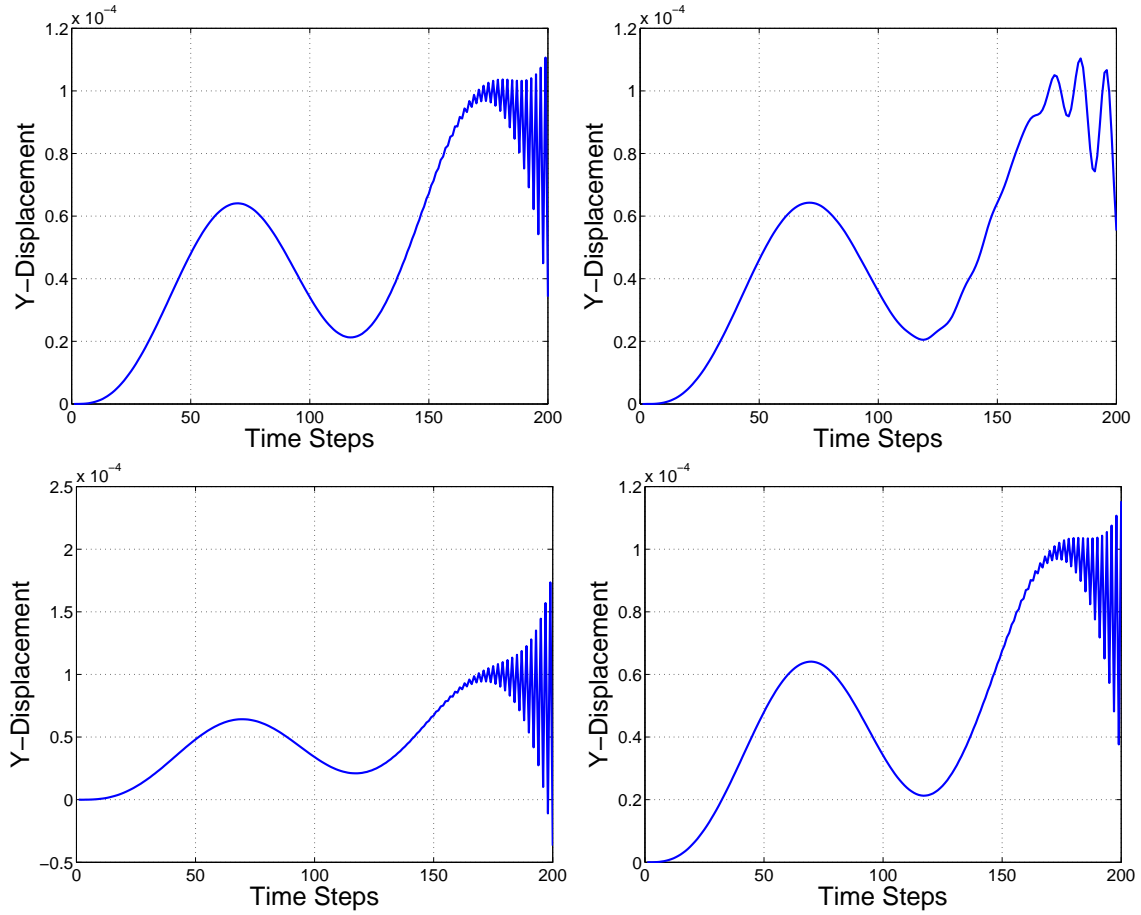
Figure 60: Cross-check for Conditional Stability of the schemes; LT - Wilson $\theta = 0.475 < 0.5$, RT - Newmark $\delta = 0.1 < 0.5$, LB - HHT $\alpha = -1.5 < -1/3$, RB - Generalised Alpha $\lambda_r = 1.03 > 1$

With these observation we conclude this section.

1.5. Appendix 5

1.5.1. Constructing Basis Functions

The Lagrangian basis functions are built using three approaches namely, using Vandermonde matrices, using their recurring formula of Newton Divided Differences and using Bjorck-Pererya [6]. To show this, consider the quadratic polynomial.

$$f(\xi) = a_0 + a_1\xi + a_2\xi^2 \tag{A.5.101}$$

In one-dimension finite element (A.5.101) can be used to built quadratic Lagrangian shape functions.

$$\xi = -1 \qquad \xi = 0 \qquad \xi = 1$$

Knowing that the first shape function is unity at $\xi = -1$ and zero on the other nodes we obtain the following matrix.

$$\begin{bmatrix} 1 & -1 & 1 \\ 1 & 0 & 0 \\ 1 & 1 & 1 \end{bmatrix} \begin{Bmatrix} a_0 \\ a_1 \\ a_2 \end{Bmatrix} = \begin{Bmatrix} 1 \\ 0 \\ 0 \end{Bmatrix} \tag{A.5.102}$$

A more generic form of this matrix can be written as.

$$\begin{bmatrix} 1 & -1 & 1 & -1 & \dots & (-1)^n \\ 1 & \xi_2 & \xi_2^2 & \xi_2^3 & \dots & \xi_2^n \\ 1 & \xi_3 & \xi_3^2 & \xi_3^3 & \dots & \xi_3^n \\ 1 & \xi_4 & \xi_4^2 & \xi_4^3 & \dots & \xi_4^n \\ & & \dots & & & \\ 1 & 1 & 1 & 1 & \dots & 1 \end{bmatrix} \begin{Bmatrix} a_0 \\ a_1 \\ a_2 \\ a_3 \\ \dots \\ a_n \end{Bmatrix} = \begin{Bmatrix} 1 \\ 0 \\ 0 \\ 0 \\ \dots \\ 0 \end{Bmatrix} \tag{A.5.103}$$

The remaining shape functions can be found by only changing the right hand side vector. The derivatives of any order can be found by knowing the coefficients. For instance the first derivative is $[a_1 + 2a_2\xi + 3a_3\xi^2 + 4a_4\xi^3 + \dots + na_n\xi^{n-1}]$.

Building the shape functions in this fashion has the disadvantage of susceptiblity to numerical errors which arises from an ill-conditioned Vandermonde-type matrix. Fig. 61 shows the logarthmic plot of reverse condition number vs. polynomial degree. The reverse condition number RCOND is a LAPACK reverse condition number estimator in the 1-norm.
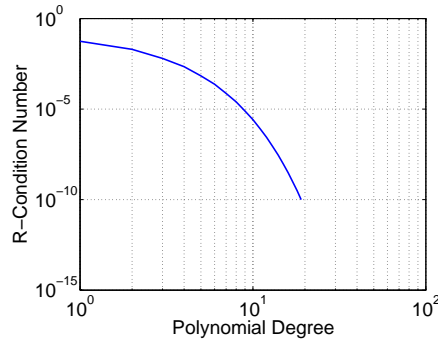
Figure 61: Reverse Condition Number vs. Polynomial Degree

Another way of generating Lagrange shape functions is to use there generic formula, based on Newton Divided Differences. This formula reads.

$$N_i = \frac{(\xi - \xi_1)(\xi - \xi_2)(\xi - \xi_3)....(\xi - \xi_{i-1}).....(\xi - \xi_{i+1})(\xi - \xi_{i+2})....(\xi - \xi_n)}{(\xi_i - \xi_1)(\xi_i - \xi_2)(\xi_i - \xi_3)....(\xi_i - \xi_{i-1}).....(\xi_i - \xi_{i+1})(\xi_i - \xi_{i+2})....(\xi_i - \xi_n)} \quad \text{(A.5.104)}$$

Higher order Legendre polynomials are less susceptible to accumulating errors and computationally more demanding compared to Lagrangian ones. In a *hp*-finite element context they are constructed in a hierarchical fashion, and they may or may not be attached to the interior nodes. A normalisation is needed to transform Legendre polynomials to Legendre basis functions [47]. The Recursive formula for constructing higher order Legendre polynomials is given by,

$$(n + 1)P_{n+1}(\zeta) = (2n + 1)\zeta P_n(\zeta) - nP_{n-1}(\zeta) \quad \text{(A.5.105)}$$

with the first two polynomials being 1 and ζ. The following normalisation is employed for obtaining the required basis functions.

$$N_n(\zeta) = \frac{P_n(\zeta) - P_{n-2}(\zeta)}{\sqrt{2(2n - 1)}} \quad \text{(A.5.106)}$$

In one dimension these basis functions are used for the interior nodes of the elements and as a continuity requirement they all have to vanish at the element boundaries [-1,+1]. The shape functions corresponding to the two exterior nodes are always the linear basis functions,

$$N_{-1} = \frac{1}{2}(1 - \zeta) \qquad N_{+1} = \frac{1}{2}(1 + \zeta)$$

and the shape fucntions corresponding to interior nodes are Legendre ones. The first few of them are listed here,

$$N_i^2 = \frac{3}{2\sqrt{6}}(\zeta^2 - 1), \qquad N_i^3 = \frac{5}{2\sqrt{10}}\zeta(\zeta^2 - 1)$$

$$N_i^4 = \frac{7}{8\sqrt{14}}(5\zeta^4 - 6\zeta^2 + 1), \qquad N_i^5 = \frac{9}{8\sqrt{18}}(7\zeta^5 - 10\zeta^3 + 3\zeta)$$

where for convenience a single subscript i is used to represent the interior nodes. In the following these polynomials and their corresponding shape functions are plotted.
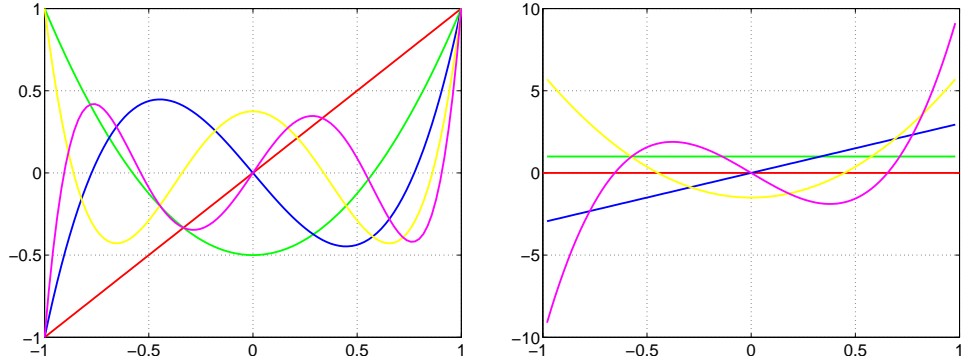
Figure 62: Right - Legendre Polynomials, Left - Derivatives of Legendre Polynomials
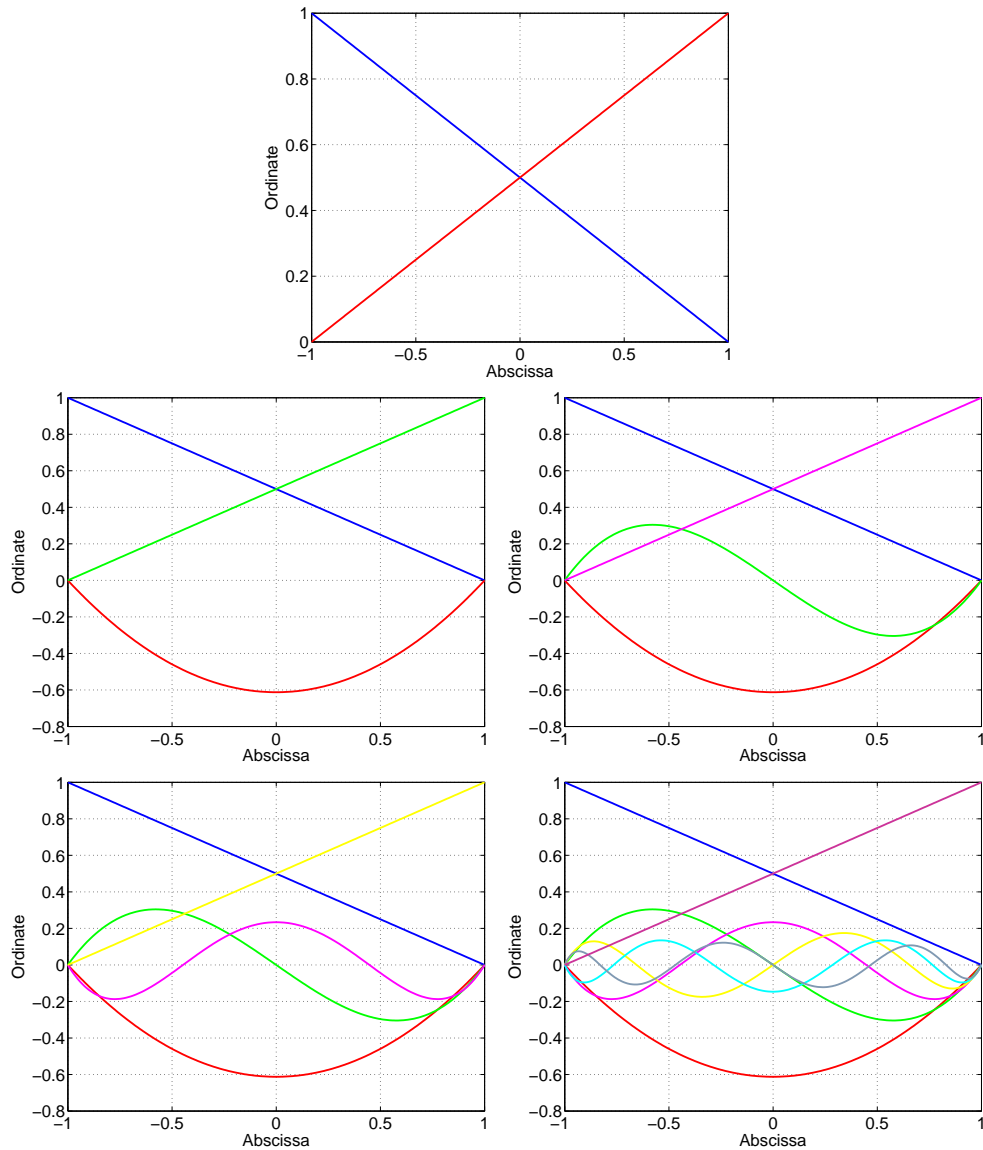
Figure 63: Legendre Shape Functions

113

1.5.2. Lagrangian Bases with Gauss-Lobbato-Legendre Points

As observed in the section on modal analysis, the Lagrangian bases with equi-spaced points are numerically not stable. In this section we focus on constructing Lagrangian shape functions with Gauss-Lobbato-Legendre points which yield comparatively well-conditioned matrices which are imune from end oscillations [28]. To find the Gauss-Lobbato points, first we need to construct Jacobi polynomials. This is achieved by using the recurrence relationship.

$$P_0^{\alpha,\beta}(\zeta) = 1 \tag{A.5.107}$$

$$P_1^{\alpha,\beta} = \frac{1}{2}\big[\alpha - \beta + (\alpha + \beta + 2)\zeta\big] \tag{A.5.108}$$

$$P_{n+1}^{\alpha,\beta} = \frac{\big[(a_n^2 + a_n^3\zeta)P_n^{\alpha,\beta} - a_n^4 P_{n-1}^{\alpha,\beta}\big]}{a_n^1} \tag{A.5.109}$$

where

$$a_n^1 = 2(n+1)(n+\alpha+\beta+1)(2n+\alpha+\beta) \tag{A.5.110}$$
$$a_n^2 = (2n+\alpha+\beta+1)(\alpha^2-\beta^2) \tag{A.5.111}$$
$$a_n^3 = (2n+\alpha+\beta)(2n+\alpha+\beta+1)(2n+\alpha+\beta+2) \tag{A.5.112}$$
$$a_n^4 = 2(n+\alpha)(n+\beta)(2n+\alpha+\beta+2) \tag{A.5.113}$$

The derivative of these polynomials can be evaluated by.

$$\frac{d}{d\zeta}P_n^{\alpha,\beta}(\zeta) = \frac{1}{2}(\alpha+\beta+n+1)P_{n-1}^{\alpha+1,\beta+1}(\zeta) \tag{A.5.114}$$

Since Legendre polynomials correspond to the case $\alpha = \beta = 0$, (i.e. $L_P(\zeta) = P_n^{0,0}$), we can compute Legendre polynomials and their derivatives. The next step is to find the roots of $(1 - \zeta^2)L_P'(\zeta)$ as Gauss-Lobatto points are the roots of these polynomials. This can be achieved by using a Newton-Raphson method with polynomial deflation. Once Gauss-Lobatto points are determined the corresponding weights (necessary for integration only) are computed as.

$$w_i^n = \frac{2}{n(n-1)[P_{n-1}]^2} \tag{A.5.115}$$

Knowing Gauss-Lobatto points one can generate shape functions employing either Vandermonde matrix approach or by product of monomial basis. Both approaches are followed here. It should be noted that compared to its equi-spaced counterpart Vandermonde matrix built with Gauss-Lobatto points are more well-conditioned. Fig. 64 shows the condition number of both Vandermonde matrices.
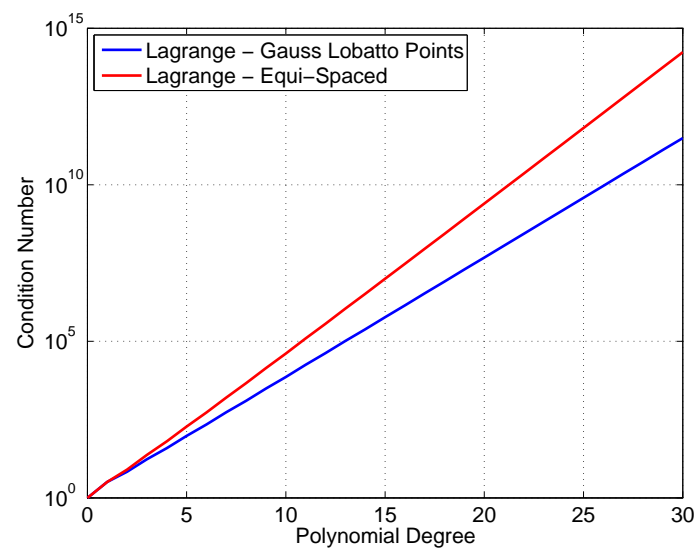
Figure 64: Condition Number vs. Polynomial Degree
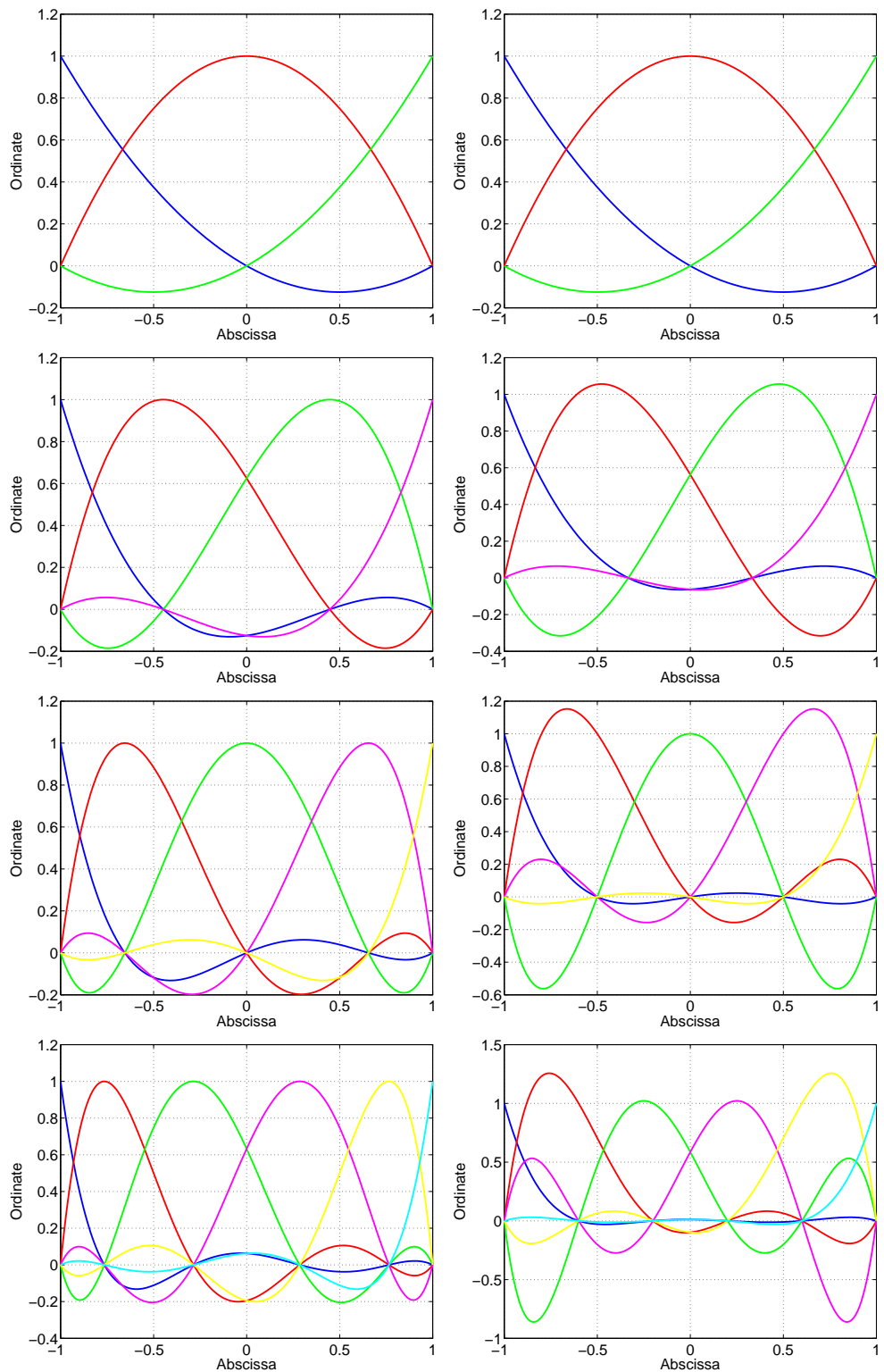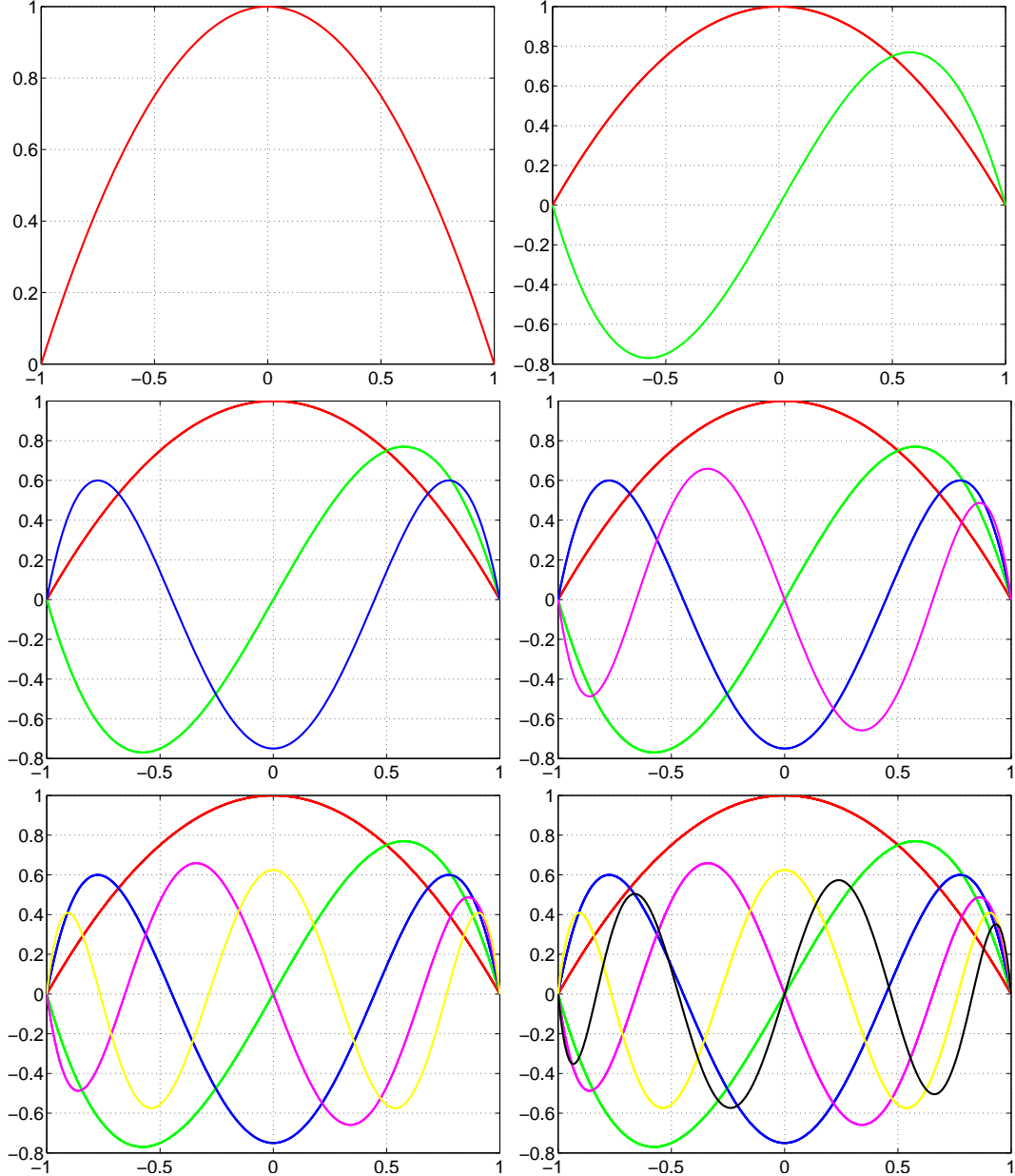
Figure 65: Lagrange Shape Functions, Left - Gauss-Lobatto, Right - Equally-Spaced

As it can be observed Lagrange shape functions with equi-spaced points show end oscillation. This oscillation is not present in case of Lagrange basis with Gauss-Lobatto points. The Gauss-Lobatto points are in fact the zeros of $(1 - \zeta^2)L'_P(\zeta)$. For a better illustration, these polynomials are plotted in the following.

Figure 66: Plots of $(1 - \zeta^2)L'_P(\zeta)$

An important feature of Lagrangian shape functions with GLL points is that they yield diagonal mass matrix if the number of Gauss-Lobatto points is the same as the underlying interpolation functions. This diagonal mass matrix is however underintegrated to generate a lumped mass matrix, so it comes with the drawback of normal mass lumping. For the case when quadratic basis functions are employed the corresponding integration scheme is in fact the Simpson's 1/3 rule, as the 3-point Gauss-Lobatto weights are 1/3, 4/3 and 1/3. Fig. 67 shows p-refinement on two different frequencies of CB and SSB models computed through modal analysis with both consistent and diagonal mass matrix.
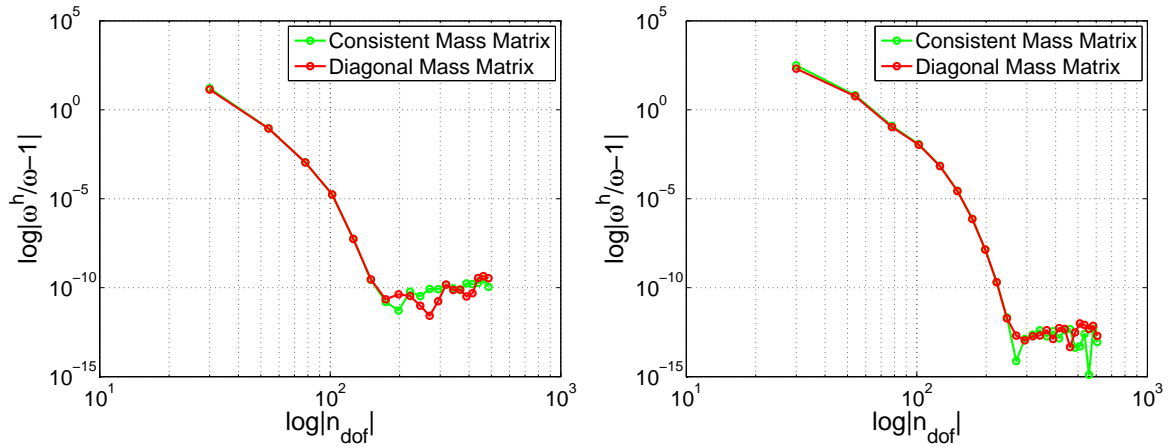

Figure 67: Choice of Mass Matrix for Gauss-Lobatto-Legendre Lagrange Basis Functions, Left - CB [2nd Frequency], Right - SSB [5th Frequency]

And the following plot is from full dynamic analysis (without static condensation) of cantilever beam subjected to a harmonic load. The analysis is performed with HHT-α scheme using a sufficiently fine mesh (50 elements) and the cubic Lagrangian-GLL interpolation functions to have avoided numerical errors originating from sources other than the one(s) related to the choice of mass matrix. However it should be noted that a sufficiently fine mesh also implies that diagonal and consistent mass matrices will yield almost similar results. In general, the behaviour of different mass matrices depend on material and geometric properties and especially to a good extent on the density of the matrial used. ρ is taken as 500 for this analysis.
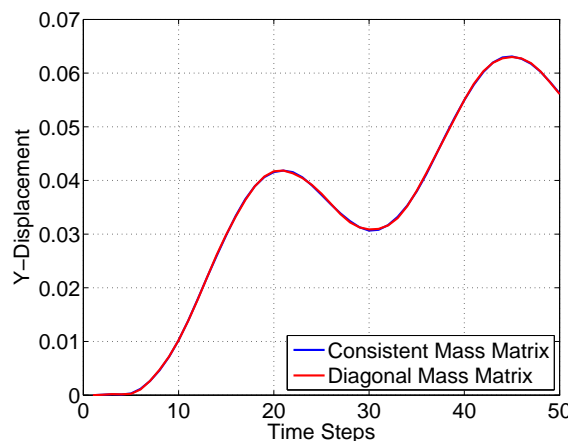

Figure 68: Choice of Mass Matrix for Gauss-Lobatto-Legendre Lagrange Basis Functions

Bibliography

[1] ABDELKEFI, A., NAJAR, F., H., N. A., AND AYED, S. B. An energy harvester using piezoelectric cantilever beams undergoing coupled bending-torsion vibrations. *Smart Materials and Structures 20*, 11 (2011), 115007.

[2] ANTON, S. R., AND SODANO, H. A. A review of power harvesting using piezoelectric materials (2003-2006). *Smart Materials and Structures 16*, 3 (2007), R1.

[3] BATHE, K. J. *Finite Element Procedures*. Prentice Hall Inc., New York, 1996.

[4] BENJEDDOU, A. Advances in piezoelectric finite element modeling of adaptive structural elements: a survey. *Computers and Structures 76*, 1-3 (2000), 347–363.

[5] BENJEDDOU, A., TRINIDADE, M. A., AND OHAYON, R. A unified beam finite element model for extension and shear piezoelectric actuation mechanisms. *Intelligent Material Systems and Structures 8*, 12 (1997), 1012–1025.

[6] BJÖRCK, A., AND PEREYRA, V. Solution of Vandermonde system of equations. *Mathematics of Computation 24*, 122 (1970).

[7] BOWEN, C. R., NELSON, L. J., STEVENS, R., CAIN, M. G., AND STEWART, M. Optimisation of interdigitated electrodes for piezoelectric actuators and active fibre composites. *Journal of Electroceramics 16*, 4 (2006), 263–269.

[8] BRAMAN, K. Third-order tensors as linear operators on a space of matrices. *Linear Algebra and its Applications 433*, 7 (2008), 1241–1253.

[9] BUTZ, A., KLINKEL, S., AND WAGNER, W. A geometrically and materially nonlinear piezoelectric three-dimensional-beam finite element formulation including warping effects. *International Journal for Numerical Methods in Engineering 76*, 5 (2008), 601–635.

[10] CHUNG, J., AND HUBERT, G. M. A time integration algorithm for structural dynamics with improved numerical dissipation: The generalized-alpha method. *ASME Journal of Applied Mechanics 60* (1993), 371–375.

[11] DAS, R. Batteryless infrared remote control from Arveni, November 2009.

[12] DUTOIT, N. E., WARDLE, B. L., AND KIM, S. G. Design considerations for MEMS-scale piezoelectric mechanical vibration energy harvesters. *Integrated Ferroelectrics 16* (2005), 121–160.

[13] ERTURK, A. *Electromechanical Modeling of Piezoelectric Energy Harvesters*. PhD thesis, Virginia Polytechnic Institute and State University, 2009.

[14] ERTURK, A., AND INMAN, D. J. Issues in mathematical modeling of piezoelectric energy harvesters. *Smart Materials and Structures 17* (2008), 065016.

[15] ERTURK, A., AND INMAN, D. J. On mechanical modeling of cantilevered piezoelectric vibration energy harvesters. *Journal of Intelligent Material Systems and Structures 19*, 11 (2008), 1311–1325.

[16] ERTURK, A., AND INMAN, D. J. *Piezoelectric Energy Harvesting*, first ed. John Wiley & Sons Inc., Chichester, England, 2011.

[17] ERTURK, A., RENNO, J. M., AND INMAN, D. J. Modeling of piezoelectric energy harvesting from an L-shaped beam-mass structure with an application to UAVs. *Journal of Intelligent Material Systems and Structures 20* (2009), 529–544.

[18] FISH, J., AND BELYTSCHKO, T. *A First Course in Finite Elements*. John Wiley & Sons Inc., Chichester, England, 2002.

[19] GANAPATHI, M., PATEL, B. P., AND TOURATIER, M. Refined finite element for piezoelectric laminated composite beams. *Smart Materials and Structures 13*, 4 (2004), N57.

[20] GRANSTROM, J., FEENSTRA, J., SODANO, H. A., AND FARINHOLT, K. Energy harvesting from a backpack instrumented with piezoelectric shoulder straps. *Smart Materials and Structures 16*, 5 (2007), 1810.

[21] GUILLOT, F. M., BECKHAM, H. W., AND LEISEN, J. Hollow piezoelectric ceramic fibers for energy harvesting fabrics. *Journal of Engineered Fibers and Fabrics 8*, 1 (2013), 75–81.

[22] HENRY, A. S., PARK, G., AND DANIEL, J. I. Estimation of electric charge output for piezoelectric energy harvesting. *Strain 40*, 2 (2004), 49–58.

[23] HILBER, H. M., HUGHES, T. J. R., AND TAYLOR, R. L. Improved numerical dissipation for time integration algorithms in structural dynamics. *Earthquake Engineering and Structural Dynamics 5* (1977), 282–292.

[24] HJELMSTAD, K. D. *Fundamentals of Structural Mechanics*. International series in civil engineering and engineering mechanics. Springer Inc., 2005.

[25] HUGHES, T. J. R. *The Finite Element Method: Linear Static and Dynamic Finite Element Analysis*. Prentice Hall Inc., Englewood Cliffs, New Jersey, 1987.

[26] JEON, Y. B., SOOD, R., H., J. J., AND KIM, S. G. MEMS power generator with transverse mode thin film PZT. *Sensors and Actuators 122*, 1 (2005), 16–22.

[27] KANT, A., AND GUPTA, A. A finite element model for a higher-order shear-deformable beam theory. *Journal of Sound and Vibration 125*, 2 (1988), 193–202.

[28] KARNIADAKIS, G. E., AND SHERWIN, S. J. *Spectral/hp Element Methods for CFD*. Oxford University Press, Oxford, England, 1999.

[29] KLINKEL, S., LEGNER, D., AND WAGNER, W. Advanced finite element formulations for modeling thin piezoelectric structures. *PAMM: Proceedings in Applied Mathematics and Mechanics 11* (2011), 31–34.

[30] KLINKEL, S., AND WAGNER, W. A piezoelectric solid shell element based on a mixed variational formulation for geometrically linear and nonlinear applications. *Computers and Structures 86*, 1-2 (2007), 38–46.

[31] KOK, S. L., WHITE, N. M., AND HARRIS, N. R. Free-standing thick-film piezoelectric device. *Electronics Letters 44*, 4 (2008), 280–281.

[32] KOK, S. L., WHITE, N. M., AND HARRIS, N. R. A free-standing, thick-film piezoelectric energy harvester. *Proceedings of IEEE Sensors* (19-20 October 2008).

[33] KOK, S. L., WHITE, N. M., AND HARRIS, N. R. Free-standing thick-film piezoelectric multimorph cantilevers for energy harvesting. *IEEE International Ultrasonics Symposium* (20-23 September 2008).

[34] KOK, S. L., WHITE, N. M., AND HARRIS, N. R. Fabrication and characterization of free-standing thick-film piezoelectric cantilevers for energy harvesting. *Measurement in Science and Technology 20*, 12 (2009), 124010.

[35] KOUTSAWA, Y., GAETANO, G., AND BELOUETTAR, S. Hierarchical FEM modelling of piezo-electric beam structures. *Composite Structures 95* (2013), 705–718.

[36] KUSHNIR, U., AND RABINOVITCH, O. Nonlinear ferro-electro-elastic beam theory. *International Journal of Solids and Structures 46*, 11-12 (2009), 2397–2406.

[37] MANEVICH, A., AND KOAKOWSKI, Z. Free and forced vibrations of Timoshenko beam made of viscoelastic material. *Jounral of Theoretical and Applied Mechanics 49*, 1 (2011), 3–16.

[38] MARSDEN, J. E., AND HUGHES, T. J. R. *Mathematical Foundations of Elasticity*. Prentice-Hall Inc., Englewood Cliffs, New Jersey, 1983.

[39] MATEU, L., AND MOLL, F. Optimum piezoelectric bending beam structures for energy harvesting using shoe inserts. *Journal of Intelligent Material Systems and Structures 16*, 10 (2005), 835–845.

[40] PEARCE, D. H., HOOLEY, A., AND W., B. T. On piezoelectric super-helix actuators. *Sensors and Actuators A: Physical 100*, 2-3 (2002), 281–286.

[41] PIEFORT, V. *Finite Element Modelling of Piezoelectric Active Structures*. PhD thesis, Universitè Libre de Bruxelles, 2001.

[42] REDDY, J. N. *Energy Principles and Variational Methods in Applied Mechanics*, second ed. John Wiley & Sons, Chichester, England, 2002.

[43] REDDY, J. N. *An Introduction to the Finite Element Method*, third ed. McGraw-Hill, New York, 2006.

[44] ROUNDY, S., AND WRIGHT, P. K. A piezoelectric vibration based generator for wireless electronics. *Smart Materials and Structures 13*, 5 (2004), 1131–1142.

[45] SHENCK, N. Energy scavenging with shoe-mounted piezoelectrics. *Micro, IEEE 21*, 3 (2001), 30–42.

[46] SODANO, H. A., LLOYD, J., AND INMAN, D. J. An experimental comparison between several active composite actuators for power generation. *Smart Materials and Structures 15*, 5 (2006), 1211.

[47] SZABÓ, B., AND BABUŠKA, I. *Finite Element Analysis*. John Wiley and Sons Inc., New York, 1991.

[48] TABESH, A., AND FRÉCHETTE, L. G. An improved small-deflection electromechanical model for piezoelectric bending beam actuators and energy harvesters. *Journal of Micromechanics and Microengineering 18* (2008), 104009.

[49] WANG, C. M., ZHANG, Y. Y., AND Q., H. X. Vibration of nonlocal Timoshenko beams. *Nanotechnology 18* (2007), 105401.

[50] YANG, J. *Special Topics in the Theory of Piezoelectricity*. Springer Inc., Dordrecht, Heidelberg, London, New York, 2009.

ABSTRACT

Piezoelectric materials find myriad of industrial application for energy harvesting purposes. These piezoelectric energy harvesters are essentially designed with beam and membrane type configurations. The thesis presents a continuum mechanics based formulation and finite element descritisation of three dimensional piezoelectric beams. Starting from the Lagrangian of the piezoelectric system, using Hamilton's principle, the variational statement and Euler-Lagrange equations are derived. The postulated linear mechanical kinematics and quadratic electric potential variables are embedded in the linearised functional in a seamless fashion, to obtain the governing equations of three-dimensional beam model. Higher order nodal - *Lagrange* and modal - *Legendre* basis functions are employed to resolve the coupled problem accurately. Appropriate error norms are computed to have ensured accuracy of the method.